CYTOSKELETON, DEFINING THE FUNC

OF GRANCALCIN

PING XU

A thesis submitted to the University of London for the degree
Doctor of Philosophy

Department of Medicine
University College London

2006

ProQuest LLC
789 East Eisenhower Parkway
P.O. Box 1346
Ann Arbor, MI 48106-1346

To

Bochun Xu and Minghua Zhong

ABSTRACT

The cytoskeleton plays an essential role in neutrophil adhesion, chemotaxis, and phagocytosis, however, the composition and regulation of function of the neutrophil cytoskeleton are still poorly understood. To elucidate some of these questions, we analysed the proteome of the cytosolic, membrane and phagosome skeleton. Using proteomic approach, we identified 138 proteins associated with the neutrophil cytoskeleton, among them 72 proteins in the cytosol, 39 in the membrane and 26 associated with the phagosome skeleton. Some of the newly reported proteins associating with the cytoskeleton encompass n-acetylglucosamine kinase, phosphoglycerate mutase 1, prohibitin, ficolin-1 (M-ficolin, ficolin A), phosphogluconate dehydrogenase, glucosidase, transketolase, major vault protein, valosin-containing protein, aldehyde dehydrogenase and LCRP8. Furthermore, we report for the first time that filamin, grancalcin, L-plastin and IQGAP1 are associated with the phagosome skeleton in neutrophils. Our mass spectrometric analysis also suggested the previously unknown post-translational modification of grancalcin, a protein of unknown function. By using a high-speed co-sedimentation assay, we found that grancalcin directly binds to F-actin with a dissociation constant of 2.5×10^{-6}M and a stoichiometric ratio of 1.1:1. Furthermore, the identification of F-actin as a novel binding partner of grancalcin, indicates a novel mechanism for the association of this protein with cytoskeleton that is potentially relevant for actin dynamics. This study constitutes the broadest investigation to date of the neutrophil cytoskeletal proteome and identifies a series of proteins not previously reported to be associated with this subcellular compartment.

The work based on grancalcin deficient mice suggested it has defects in adhesion and spreading on fibronectin-coated surface and this could be due to the reduced expression of surface integrins $\alpha_4\beta_1$ and $\alpha_5\beta_1$ in the grancalcin-deficient mice.

Taken together, our results suggested that grancalcin could be a protein linking the integrins and cytoskeleton.

CONTENTS

FIGURES

TABLES

ABBREVIATIONS

ATP	Adenosine triphosphate
BSA	Bovine serum albumin
cDNA	Complementary deoxyribonucleic acid
CGD	Chronic granulomatous disease
CHCA	α-cyano-4-hydroxycinnamic acid
CR	Complement receptor
C-termianl	Carboxyl terminal
DAPI	4'6-diamidino-2-phenylindole
DTT	Dithiothreitol
DMSO	Dimethyl sulphoxide
ECL	Enhanced chemiluminescence
E.coli	Escherichia coli
EDTA	Ethylene diamine tetra-acetic acid
ESI	Electrospray ionization
F-actin	Filamentous actin
FAD	Flavin adenine dinucleotide
FCA	Freund's complete adjuvant
FCS	Foetal calf serum
FcR	Fc receptor
FIA	Freund's incomplete adjuvant
FITC	Fluorescein isothiocyanate
fMLP	N-formyl-L-methionyl-L-leucyl-phenylalanine
G-actin	Globular actin
GEF	Guanine-nucleotide exchange factor

GTP	Guanosine 5'-triphosphate
GST	Glutathione S-transferase
IEF	Isoelectric focusing
IgG	Immunoglobulin G
IPTG	Isoprophyl-β-D-thiogalactopyranoside
Kb	kilobase
MALDI-TOF	Matrix assisted laser desorption ionisation-time of flight
MS	Mass spectrometer
M/Z	mass to charge ratio
MTOC	Microtubule-organizing center
NADPH oxidase	Nicotinamide adenine dinucleotide phosphate oxidase
NCBI	National Center for Biotechnology Information
NES	Nuclear export signal domain
PBS	Phosphate buffered saline
PCR	Polymerase chain reaction
PE	Phycoerythrin
Phox	Phagocytic oxidase
PKC	Protein kinase C
PMA	12-phorbol myristate 13-acetate
PMSF	Phenylmethylsulfonyl fluoride
ppm	parts per million
PRS	Proline rich sequence/polyproline motif
PX domain	Phox domain
SDS-PAGE	Sodium dodecyl sulphate polyacrylamide gel electrophoresis
SH3 domain	Src homology domain 3
SOD	Superoxide dismutase

TBS	Tris buffered saline
TCA	Trichloro-acetic acid
TLCK	N-alpha-p-tosyl-L-lysine chloro methyl ketone
TPR	Tetratripeptide repeat domain
Tris	Tris-(hydroxymethyl)-aminomethane

CHAPTER 1

INTRODUCTION

1.1 NEUTROPHIL AND HOST DEFENCE

Neutrophils are the most numerous of the white blood cells (40-65%), and are essential for the killing of bacteria and fungi. The number of neutrophils increases dramatically after infection. Their half-life in the circulation is short (8-20 hours), but they can survive up to several days in the tissues (Deinard et al., 1975).

The development of mature neutrophils in the bone marrow occurs via the differentiation of multipotential stem cells into progenitor cells that are committed to neutrophilic lineages. These stem cells differentiate into myeloid lineages. The earliest identifiable cells of the neutrophil lineage are the myoblasts, which are capable of proliferation. Myoblasts then differentiate into promyelocytes, which are characterised by the acquisition of large numbers of peroxidase-containing granules. Promyelocytes then differentiate into myelocytes, which are mature and are released into the circulation as neutrophils. The whole differentiation process is controlled by acquisition of specific growth / differentiation factor receptors at different stages of development. At last, neutrophils are produced in the bone marrow at a very high rate of around 80 million per minute (Chikkappa et al., 1976; Boggs et al., 1977; Collins et al., 1978; Edwards, 1994).

Neutrophils are crucial in the acute phase of inflammation, whereas macrophages and lymphocytes are dominant in the chronic phase (Oort et al., 1977). Unlike lymphocytes, neutrophils do not show any inherent specificity for antigens, they recognize microbial targets labelled by antibodies or complement (Walford et al., 1965; Gale et al., 1975). They also release their granule content of antimicrobial substances to the exterior. The proper function of neutrophils is critical for host defence, but uncontrolled events can lead to chronic

inflammation (Faist and Kim, 1998; Fossati et al., 2001). The regulation of neutrophil function is therefore critical in order to achieve the killing of pathogens without inducing tissue injury (Klebanoff et al., 1975).

The actin-myosin contractile system is important to perform these key functions in polymorphonuclear leukocytes. The cytoskeletal distribution in neutrophil can be observed clearly in transmission electron microscopy. Actin filaments were observed enriching at the leading lamellipodia, running parallel to the cortical membrane and surrounding the membrane of the phagocytic vacuole (Ryder et al., 1982; Nakata and Hirokawa 1992; Valerius etal., 1981; Grogan et al., 1997). Thus the distribution of neutrophil cytoskeleton can be divided into three main structures: cytosol, membrane and phagosome.

Cytoskeletal proteins of neutrophil cytosol are distributed between three main pools: an assembled cytoskeleton that is insoluble and sediments when centrifuged at low speed; a labile pool of polymerised proteins that are released from detergent solubilised cells but consist of assemblies of proteins that are large enough to pellet fairly rapidly at high centrifugal force; and a pool of soluble proteins which remain in the high speed supernatant cytosol (Hinshaw et al., 1993).

A prerequisite for directed migration is the acquisition of a polarized morphology. Cellular polarization and motility require that separate regions of the cell adopt different properties to carry out specialized functions. Co-labelling detergent resistant membranes (DRM)s and F-actin revealed a correlation between DRM distribution and F-actin remodelling, suggesting that plasma membrane organization may orient signalling events that control cytoskeletal rearrangements and, consequently, cell polarity (Seveau et al., 2001).

Phagocytosis of opsonized particles by neutrophils involves highly localized alterations in the actin cytoskeleton that result in the formation of prominent pseudopodia and the phagocytic cup (Robinson et al., 2002). At the same time, the swelling of phagosome requires this cytoskeletal structure to resolve. The formation of the phagocytic vacuole is a

highly localised event, in which the membrane-bound cytoskeleton plays an important role (Grogan et al., 1997).

But how the cytosol high-speed pellet is composed, how the polarised structure at the membrane are organized, and how the cytoskeletal structure around the phagosome is evolved, are largely unknown. The purpose of this thesis is to apply a proteomic approach to conduct the first comprehensive research of cytoskeletal proteins in all three compartments, to thus provide the basis for understanding the mechanisms underlying the regulation of cytoskeleton in human neutrophils.

1.2. THE NADPH OXIDASE

The 'extra respiration of phagocytosis', which indicated the activity of the NADPH oxidase during phagocytosis of bacteria by canine neutrophils, was first observed by Baldridge and Gerard (Baldridge and Gerard, 1933). In 1959, Sbarra and Karnovsky found that this added oxygen consumption was entirely resistant to conventional inhibitors of mitochondrial function, thus raising the question of the mechanism and its purpose during phagocytosis (Sbarra and Karnovsky, 1959). Later it was found that the oxygen is required for neutrophils to kill bacteria, as killing was less efficient in anaerobic conditions, even though both the phagocytosis and degranulation were normal (Selvaraj and Sbarra, 1966; Mandell, 1974). The oxygen is consumed by the NADPH oxidase which produces a respiratory burst. The physiological importance of the respiratory burst was emphasized in the syndrome of chronic granulomatous disease (CGD), an inherited immunodeficiency syndrome characterised by the absence of NADPH oxidase activity and increased susceptibility to bacterial and fungal infections (Reviewed in Thrasher et al., 1994).

Hattori and Shinagawa subsequently found cytochrome b_{558} in leukocytes that could be reduced by NADH and NADPH under anaerobic conditions, thus suggesting that NADPH oxidase is in fact cytochrome b_{558} (Hattori et al., 1961; Shinagawa et al., 1966). In 1978 Segal

et al discovered the cytochrome b_{558} was in the phagocytic vacuole of human neutrophils. Cytochrome b_{558} has distinct spectrum at 429nm and 560nm. These two peaks were observed when neutrophils were incubated with latex particles, which results in phagocytic vacuole formation, but they were not observed when the cells were stimulated with PMA, in which phagocytic vacuoles were not formed. By comparing the dithionite difference spectra and carbon monoxide difference spectra of whole cell homogenates, phagocytic vacuoles and myeloperoxidase, the spectra of the phagocytic vacuoles produced distinct peaks at 429 nm and 560nm, which were also present in the whole cell homogenate fraction. The CO difference spectra produced a small peak at 420nm in the whole cell homogenate, which indicated the binding of CO by the cytochrome b, whereas it was not present in myeloperoxidase fraction. Thus the authors concluded that cytochrome b_{558} was in the vacuoles. The characteristic spectrum of cytochrome b was also deficient in some of the X-linked CGD patients and thus cytochrome b_{558} was identified as a terminal electron-transporting component of the NADPH-oxidase at the phagocytic vacuole (Segal et al., 1978). Oxidase components include flavocytochrome b_{558}, an integral membrane heterodimer comprised of $gp91^{phox}$ and $p22^{phox}$ (Harper et al., 1985; Parkos et al., 1987), and cytosolic proteins, $p47^{phox}$, $p67^{phox}$ (Segal et al., 1985; Tanaka et al., 1993; Teahan et al., 1990; Pilloud-Dagher and Vignais, 1991), $p40^{phox}$ (Wientjes et al., 1993) and Rac1 (Abo and Pick, 1991; Abo et al., 1991) or Rac2 (Knaus et al., 1991), depending on the species and type of phagocytic cell. Upon activation, $p40^{phox}$, $p47^{phox}$ and $p67^{phox}$ translocate to the membrane, thereby activating the NADPH oxidase (Fig 1) (Rotrosen et al., 1990).

1.2.1. Phosphorylation of oxidase components

The phosphorylation of the subunits of NADPH oxidase has essential role in the activation of the enzyme. $p40^{phox}$, $p47^{phox}$, $p67^{phox}$ and cytochrome b can be phosphorylated. Serine phosphorylation sites: S303, 304, 320, 328, 345, 348, 359, 370 and 379, at the C-

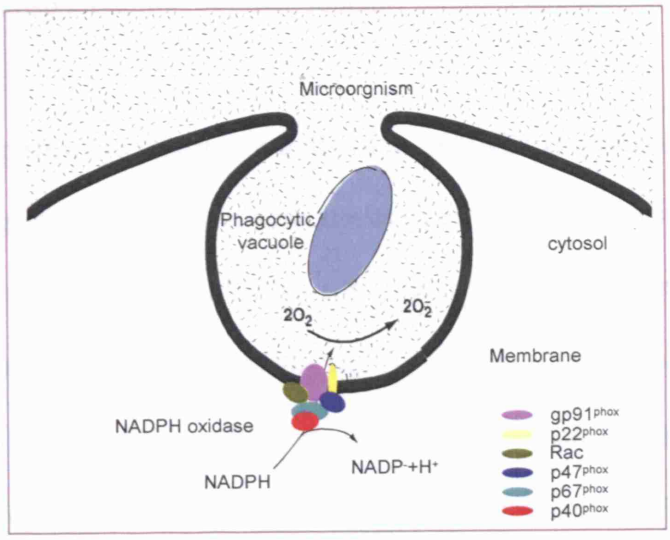

Fig 1. The NADPH oxidase located in the wall of the phagocytic vacuole.
It pumps electrons from NADPH into the vacuole to form superoxide (Segal et al., 1999).

terminus have been identified in $p47^{phox}$. Kinases such as ERK, p38, PAK-1, PAK-2 and PKC are able to phosphorylate this protein at multiple sites (El Benna et al., 1994a, b and c; Ding et al., 1995, 1996; Knaus et al., 1995; Prigmore et al., 1995; Waite et al., 1997). $p67^{phox}$ can be phosphorylated at its threonine residue (T233) and serine residues in PKC-dependent and PKC-independent manner (El-Benna et al., 1999). $p40^{phox}$ can be phosphorylated on serine 315 and threonine 154 (Bouin et al., 1998). While the contribution of phosphorylation of $p47^{phox}$ to the activation of NADPH oxidase activation is established, the biological significance of the phosphorylation of other subunits remains unclear.

1.2.2. Signalling pathways leading to activation of NADPH oxidase

The binding of a ligand to a membrane receptor leads to activation of one or several signalling pathways. For example, fMLP receptor induces the activation of heterotrimeric G-proteins, which in turn activate phospholipase C, whereas Fcγ receptors activate tyrosine kinases leading to tyrosine phosphorylation of downstream signalling proteins. The downstream pathways of different receptors overlap considerably. fMLP and Fcγ receptors both activate phospholipase C, PI-3 kinase and tyrosine kinases (Simon et al., 1991; Katz et al., 1992; Lee et al., 1992; Jiang et al., 1996; Offermanns and Simon, 1996).

PI-3 kinase can regulate a number of signalling processes including the activation of protein kinase B, phosphoinositide-dependent kinase, small GTP-binding proteins such as ras and rac, and finally phospholipase D, which is involved in the activation of $p47^{phox}$ (Baggiolini et al., 1978).

Phospholipase C activation leads to formation of membrane diacylglycerol, activating PKC, which then activates NADPH oxidase. The effect of PKC on NADPH oxidase can be mediated by direct phosphorylation of NADPH oxidase components such as $p47^{phox}$, or maybe mediated through phospholipase D, or microtubule-associated kinases such as ERK and p38 (Rhee and Bae, 1997).

The distal effects of serpentine, β-adrenergic and Fcγ receptor activation include activation of rac, proline-directed kinases and phopholipase D. Rac can directly activate NADPH oxidase, its upstream factors include exchange factors like vav, which can be triggered by the activation of PI-3 kinase, PI-3,4,5-P3 (Parker, 1995; Klarlund et al., 1997). Rac can also activate NADPH oxidase indirectly, through activation of protein kinases such as PAK-1 and PAK-2, which then phosphorylate $p47^{phox}$ (Knaus et al., 1995).

$p47^{phox}$ is phosphorylated by various activated kinases as mentioned above. It activates NADPH oxidase directly (Bey et al., 2004).

1.3 CHRONIC GRANULOMATOUS DISEASE

The proper function of NADPH oxidase is vital for neutrophil function and its defect can cause disease. CGD is a syndrome of deficiency of the immune response to bacteria and fungi caused by the defective NADPH oxidase of neutrophils and monocytes. It is characterized by severe recurrent bacterial and fungal infections (Quie et al., 1993; Janeway et al., 1954; Landing et al., 1957; Holmes et al., 1967). The oxidase comprises an electron transport chain in the membrane of the phagocytic vacuole, which is activated by cytosolic proteins. Defects of the some of the NADPH oxidase components may be complete or incomplete, where incomplete the syndrome is called the variant CGD (Dinauer et al., 1990; Leto et al., 1990; Mendelsohn et al., 1983; Marsh et al., 1981).

The diagnosis of CGD is confirmed by the reduced or absent respiratory burst in phagocytic cells. The diagnostic tests for CGD include superoxide production assay, western blotting, which identifies missing proteins, and genotyping, which characterizes DNA mutations.

According to genetic defects, chronic granulomatous disease can be classified as X-linked cytochrome b_{558} negative CGD when the abnormality lies in the $gp91^{phox}$ protein, accounting for about 60-70% of cases in CGD. The most common lesions in this type are

missense mutations or deletions in genomic DNA (Rabbani et al., 1993; Curnutte et al., 1993). In this case, the protein level of $gp91^{phox}$ is reduced or not detectable. The autosomal recessive, cytochrome b negative form is deficient in $p22^{phox}$. The expression of $p22^{phox}$ is restricted to cells that also express $gp91^{phox}$, as interactions of these proteins is necessary for their stability (Yu et al., 1997). The autosomal recessive, cytochrome b positive form of CGD relates to the defect when $p47^{phox}$ or $p67^{phox}$ are abnormal (Rodaway et al., 1990). A single deletion in $p47^{phox}$ accounts for majority of these cases, about 25% (Casimir et al., 1992; Teahan et al., 1987). So far, no abnormality in $p40^{phox}$ has been described (Massenet et al., 2005).

1.4. MECHANISM OF MICROBIAL KILLING WITHIN THE PHAGOCYTIC VACUOLE

NADPH oxidase pumps large amounts of electrons into the lumen of a phagocytic vacuole. These electrons combine with oxygen, thus forming superoxide. This process is important for bacterial killing, as it is impaired under anaerobic conditions, and in CGD where the oxidase is defective. Taken together, these findings have led to a conclusion that killing of ingested microorganisms is a result of direct toxicity of reactive oxygen species (ROS) and resulting myeloperoxidase-catalysed halogenation (Klebanoff, 1975).

According to this paradigm, the lack of proteases should not influence the killing ability of neutrophils. However, Belaaouaj et al. found that mice deficient in neutrophil elastase (NE) were more susceptible to *E.coli* sepsis since NE was capable of degrading outer membrane protein A, localized at the surface of Gram-negative bacteria (Belaaouaj et al., 1998 and 2000). Later, Segal et al. found that bacteria (*Staphylococcus*) and fungi (*Candida albicans*) were not killed by neutrophils from neutrophil elastase- and cathepsin G- deficient mice despite the production of normal amounts of superoxide and normal levels of iodination (Reeves et al., 2002). Segal et al. therefore proposed a new mechanism of killing. The

generation of negative charged reactive oxygen species by NADPH oxidase causes charge imbalance across the vacuole. To compensate that, positively charged potassium ions are pumped into the vacuole, which causes an increase in the pH. The consequently increased ionic strength in the phagosome releases the protease enzymes from the anionic sulphated proteoglycan granule matrix to kill bacteria and fungi (Reeves et al., 2002). Later, they demonstrated the existence of a large-conductance Ca^{2+} -activated K^{+} channel (BKca) in human neutrophils and microbial killing and digestion was abolished when BKca channel was blocked with iberotoxin (Ahluwalia et al., 2004). Electrons pumped into the lumen of a phagosome by NADPH oxidase generate a charge across the membrane, which must be compensated if electron transport is to continue. The efflux of chloride ions from the phagosome results in charge compensaton and activation of hydrolytic enzymes. Therefore the main role of electrons pumped by the NADPH oxidase is to drive the efflux of chloride ions (Ahluwalia, unpublished data). This novel insight has significant implications. It is important for the understanding of the pathogenesis of CGD because it means that we should examine the interplay between the granule proteins and NADPH oxidase, in order to understand microbial killing. This is also important because there is likely to exist a group of patients in whom the NADPH oxidase system functions normally but the defect lies in the proteases, either in their packaging or activity (Reeves et al., 2002).

1.5. CYTOSKELETON IN NEUTROPHIL FUNCTION

1.5.1. The neutrophil cytoskeleton

The cytoskeleton of eukaryotic cells is composed of three major protein families that form filamentous structures running throughout the cell, ie actin microfilamentous structures consisting of different actin isoforms and their associated proteins, microtubules made of α- and β-tubulin and associated proteins, and intermediate filaments, molecular motors and signal transduction proteins.

The neutrophil is one of the most efficient vertebrate motile cells. The signalling of the motility responses finds its climax in the polymerization of F-actin, which results in overall rearrangement of cellular cytoskeleton, chemotaxis, phagocytosis and therefore microbial killing by neutrophils (Zhelev et al., 2002; Howard et al., 1994). Recent advances in the understanding of the mechanism of F-actin polymerization have shown that the small GTPases cdc42, Rac2, and RhoA, play a critical role in motility. The bound integrin receptors may also contribute to the signalling of motility via tyrosine kinase phosphorylation of guanine nucleotide exchange factors and other regulatory proteins (Zhelev et al., 2002).

The key function of the microtubule is to transport cargos inside the cell. A microtubule end has three different properties: the alternative structures, the transition regulation by GTP hydrolysis cycle and the distinct target for the binding of microtubule associated proteins. These characteristics enable the microtubule to switch between growing and shrinkage, thus it is capable of coping with the dynamic functions involved in cellular movement (Howard and Hyman et al., 2003).

Intermediate filament proteins have been considered as structural support proteins for a long time. But recently the knowledge about this coiled coil protein has been improved, in conjunction with identification of mutations in this family of proteins that leads to genetic human diseases (Kreplak et al., 2004). The biological roles of that intermediate filaments play in the various physiological processes have been determined.

The main interest in this field is to understand the regulated assembly of cytoskeletal polymers, such as actin, microtubules and intermediate filaments and their associated proteins and motors, and the exact mechanism of their participation in different motility cellular functions. This introduction will discuss the three main cytoskeleton components, actin microfilaments, microtubules and intermediate filaments, then focus on the actin microfilamentous cytoskeleton, which plays an important role in the control of transmigration, chemotaxis, and phagocytosis in neutrophils.

1.5.2. Actin microfilaments

The engine that drives neutrophil motility is the actin cytoskeleton (Cicchetti et al., 2002). Actin is a major protein of the microfilaments in eukaryotic cells. It can be divided into three categories: α-, β- and γ- isoforms, according to their isoelectric points. Monomeric (G-) actin has a molecular mass of nearly 43KDa (Dos Remedios et al., 2003). G-actin can be assembled to form filamentous (F-) actin. F-actin is arranged as a polarised structure of G-actin subunits. One end is called the pointed end and the other is called the barbed end according to the direction of the arrowheads observed when binding of the myosin heads to the filament in the electromicroscopy (Pollard and Borisy, 2003).

1.5.2.1. Actin polymerization

A slow initial association of G-actin to form unstable dimers leads to the formation of a stable trimer, followed by the elongation phase during which actin monomers are quickly added. Each subunit binds one molecule of nucleotide, generally ATP, and a divalent cation, generally Ca^{2+} or Mg^{2+}, which are important for stability (Carraway et al., 1992). Low pH (around 5-6), moderate ionic strength, ATP, magnesium and physiological temperature favour polymer formation, while filaments dissociate if ATP or γ-phosphate of ATP dissociate (Carraway et al., 1992).

The concentration of G-actin in equilibrium with actin filaments (F-actin) is referred to as the critical concentration. Actin filaments are in a continuous state of assembly and disassembly. At the critical concentration actin filaments assemble and dissassemble at the same rate so the filament length is unchanged. The actin filament will assemble when G-actin concentration is higher than the critical concentration, while they will dissemble if it is below the critical concentration. The critical concentration at the pointed end is 12-15 fold higher than at the barbed end under physiological conditions (Wegner et al., 1983). This difference

may contribute to the unidirectional growth of the actin filament at the barbed end (Fig 2). For Mg-ATP actin, the critical concentration is lower at the barbed end than at the pointed end. So at steady state, the concentration of Mg-ATP actin is above the critical concentration at the barbed end and below that at the pointed end. Hydrolysis of ATP from polymerised actin and dissociation of the γ phosphate appear to be the indication of the age of the filament and trigger its dissociation (Pollard and Borisy et al., 2003; Carlier et al., 1988). ATP hydrolysis is fast and irreversible but phosphate dissociation is much slower. ADP-actin dissociates faster from the barbed end than ATP-actin, but they both dissociate slowly at the pointed end. These properties of actin filaments lead to a net flux of G-actin monomers from the pointed to the barbed end of the filament. This process is known as 'treadmilling', which provides a possible mechanism for cell motility *in vivo* (Pollard and Borisy, 2003).

1.5.2.2. Actin-binding proteins

Actin binds a number of proteins collectively called actin-binding proteins (ABPs). So far 162 distinct actin-binding proteins are known and among them at least 12 are membrane-associated proteins. Some of these ABPs are essential whereas the others may serve a regulatory role (reviewed by Dos Remedios et al., 2003). The functions of actin binding proteins can be divided as follows:

(1) actin monomer binding protein to maintain of the pool of actin monomers with a purpose of prevention of G-actin polymerization (e.g. profilin and thymosin β4); (2) actin depolymerising protein to depolymerise F- to G-actin (e.g. cofilin and profilin); (3) filament capping proteins to cap at the pointed end (e.g. tropomodulin) and at the barbed end (e.g. Cap Z; Annexin II); (4) severing proteins to shorten the average length of F-actin by cutting it into two to generate more barbed ends (e.g. gelsolin and cofilin); (5) cross-linking proteins contain at least two binding sites for F-actin to promote the bundle formation (e.g. actinin); (6)

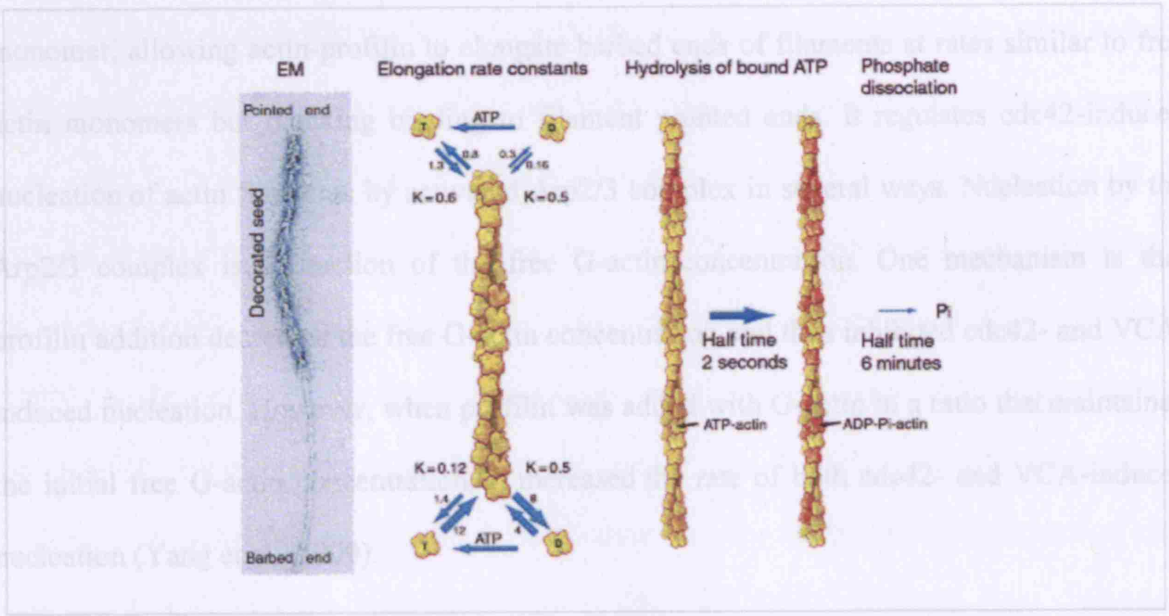

Figure 2. Actin filament elongation, ATP hydrolysis, and phosphate dissociation. The EM shows that the actin filament is decorated with myosin heads at the pointed end. The equilibrium constants are higher at the barbed end than that at the pointed end so provide the biochemical basis for treadmilling. Hydrolysis of ATP bound to each subunit is fast, but dissociation of the gamma phosphate is very slow (Courtesy of Pollard, 2003).

branching (e.g. Arp2/3 complex); (7) side binding proteins to stabilise its structure (e.g. tropomyosin) (reviewed by Dos Remedios et al., 2003).

Profilin is an ATP-actin monomer binding protein. Profilin inhibits spontaneous nucleation of actin filaments (Pollard et al., 2003). It also serves as the nucleotide exchange factor for actin, catalysing exchange of ADP for ATP and returning subunits to the ATP-actin-profilin pool, ready for another cycle of assembly. It binds the barbed end of an actin monomer, allowing actin-profilin to elongate barbed ends of filaments at rates similar to free actin monomers but blocking binding to filament pointed ends. It regulates cdc42-induced nucleation of actin filaments by activated Arp2/3 complex in several ways. Nucleation by the Arp2/3 complex is a function of the free G-actin concentration. One mechanism is that profilin addition decreases the free G-actin concentration and thus inhibited cdc42- and VCA-induced nucleation. However, when profilin was added with G-actin in a ratio that maintained the initial free G-actin concentration, it increased the rate of both cdc42- and VCA-induced nucleation (Yang et al., 2000).

Cofilin and profilin are significantly expressed in human neutrophils. Cofilin is an actin depolymerisation factor. Fifty percent of the cofilin in the resting state was phosphorylated. Dephosphorylation of cofilin quickly occurred after activation by fMLP, PKC, or the calcium ionophore A23187 (Okada et al., 1996; Zhan et al., 2003; Heyworth et al., 1997). In neutrophils stimulated with fMLP, a pronounced activation of Rac was observed, which coincides with a massive dephosphorylation of cofilin (Heyworth et al., 1997). Whether LIMK phosphorylates cofilin in neutrophils is controversial. Results have suggested that activated (GTP-bound) Rac mediates actin reorganization, in part, by stimulating LIMK 1, which in turn catalyzes the phosphorylation/inactivation of cofilin, which is then unable to bind and depolymerise F-actin (Zhan et al., 2003), but other studies suggest that this is only observed in cell types other than neutrophils (Stanyon et al., 1999).

Recent studies found that the mechanism of dephosphorylation of cofilin can be both PKC-dependent and independent, with the latter pathway predominating in fMLP-stimulated cells. These pathways may also contain calmodulin and a type 2C and/or novel phosphatase (Heyworth et al., 1997; Zhan et al., 2003). In addition to their role in recycling actin subunits during steady state movement, ADF/cofilins may also help to initiate protrusions by severing filaments to generate barbed ends for elongation (Zebda et al., 2000).

Apart from chemotaxis, the biological function of cofilin in neutrophils has also been suggested in NADPH oxidase activation and phagocytosis. In human neutrophils undergoing phagocytosis of opsonized *Candida albicans*, cofilin was found to undergo rapid association with the developing phagosomes (Zhan et al., 2003). Immunofluorescence studies revealed that cytosol cofilin of resting neutrophils underwent rapid translocation to the F-actin-rich, ruffled membranes upon stimulation, where large amounts of hydrogen peroxide, a product of the $O_2^{\cdot}/H_2O_2^{\cdot}$ generating activity of stimulated neutrophils (NADPH oxidase), was present. Cofilin is therefore well placed to participate in the continual polymerization and depolymerization of F-actin that is thought to give rise to the oscillatory pattern of H_2O_2 production observed under certain conditions (Heyworth et al., 1997).

Together with profilin (and thymosin-β4 in higher eukaryotes), ADF/cofilin and capping of barbed ends allow cells to maintain a high concentration of unpolymerized actin far from equilibrium. This pool sustains high rates of filament elongation at the steady state and is available to add extensively to barbed ends when they become available. Thus, to a large extent, regulation of polymerization reduces to regulation of the availability of free barbed ends (Pollard et al., 2003).

The polymerization of actin provides the force of protrusion in non-muscle cells as illustrated in Fig 3, which is called the dendritic-nucleation model for protrusion of lamellipodia. It refers to the thin layer of cytoplasm (~0.2μm thick) that protrudes at the front

of the spreading and migrating cell and parallel to the substrate, also termed the 'leading edge' (Pollard, 2003; Fig 3). This model in general describes the mechanism of membrane protrusion. The actin polymerisation can be turned on by a variety of extracellular stimuli. These in turn activate the GTPase and PIP_2. GTPases activate the Wiskott-Aldrich Syndrome Protein (WASP) and related proteins. The downstream target for the WASP is Arp2/3 complex. The main function of Arp2/3 is to create the branching points by nucleating the assembly of filaments. The new filament forms an angle with the old filament of 70°. According to 'elastic Brownian ratchet' model put forward by Mogilner and Oster to explain the protrusive force of lamellipodia, the actin filament is constantly bending like a spring because of the thermal energy. The filament growth velocity will be maximal when the filament at a particular orientation angles with the direction of the movement (Mogilner and Oster, 1996). This angle is half the branching angle (35°) as determined by Maly and Borisy. Filaments subtend a roughly 55° angle with the front edge of the cell in a nearly square-lattice structure (Maly and Borisy, 2001) (Fig 4). New filament formation needs a large amount of ATP-actin. The new filaments grow very quickly and this growth pushes the membrane forward. The capping protein can terminate this elongation. Actin-depolymerizing factor (ADF)/cofilin severs and depolymerises the aged filament, so ADP-actin can be released and recycled. Profilin catalyses the exchange of ADP for ATP and profilin-bound ATP-actin can reenter the cycle to form new filaments (Pollard et al., 2003).

1.5.2.3. The Wiskott-Aldrich syndrome protein family and its activation

The Wiskott-Aldrich syndrome protein (WASP) family consists of five members in mammals: WASP, neuronal WASP (N-WASP), and three suppressors of cAMP receptor (SCAR) isoforms (Caron et al., 2002). Scar protein was originally isolated from Dictyostelium (Bear et al., 1998). Three human Scar homologues (Scar 1-3) are also known as WASP-family verprolin-homologous proteins (WAVE1-WAVE3) (Miki et al., 1998). All

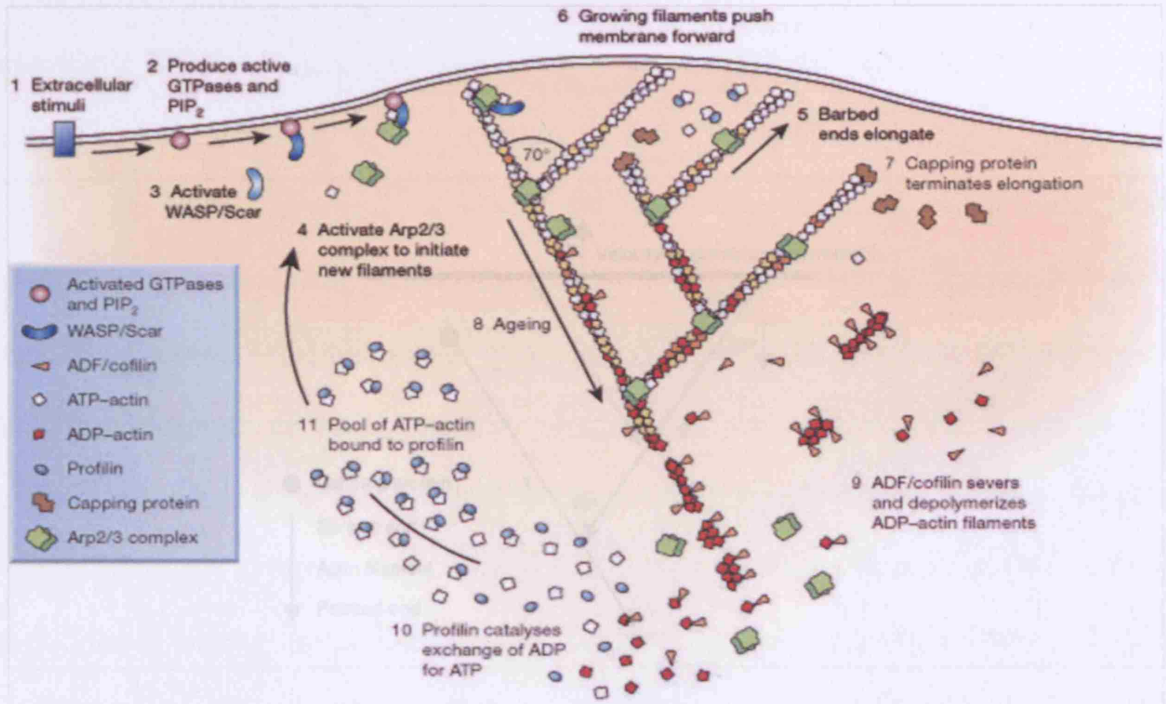

Fig 3. The dendritic-nucleation model for protrusion of lamellipodia.

Extracellular stimuli (1) activate signalling pathways that lead to GTPases (2). These then activate Wiskott-Aldrich syndrome protein (WASP) and related proteins (3), which in turn activates Arp2/3 complex. Arp2/3 complex initiates a new filament forming a branch on the side of the existing filament (4). Each new filament grows rapidly (5), fed by a high concentration of profilin-bound actin stored in the cytoplasm, and this pushes the plasma membrane forward (6). Capping protein binds to the growing ends, terminating elongation (7). Filaments age by hydrolysis of ATP bound to each actin subunit followed by dissociation of the γ-phosphate (8,9). Profilin reenters the cycle at this point, promoting dissociation of ADP and binding of ATP to dissociated subunits (10). ATP-actin binds to profilin, refilling the pool of subunits available for assembly (11). (Courtesy of Pollard, 2003)

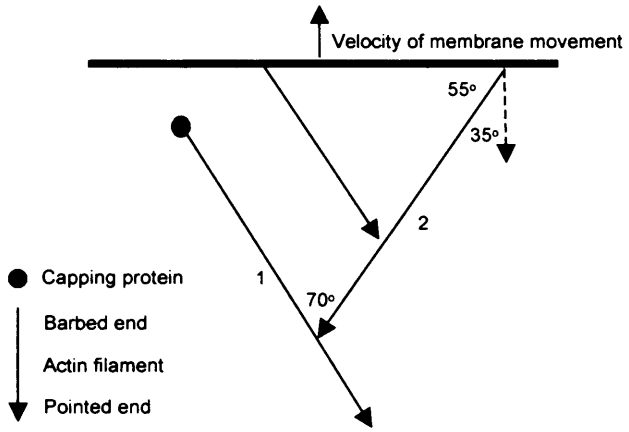

Fig 4. Organizational unit of actin network at the leading edge.
Near the leading edge (heavy line), actin filaments are nucleated by arp2/3 complex. The angle between mother (1) and daughter (2) filament are determined as 70°. The elongation of the filament is terminated by capping protein. Orientation of a filament is characterized by its incidence angle with the leading edge as 35°, while the new filament subtend a 55° with the leading edge (Maly et al., 2001; Mogilner et al., 1996).

members display a very similar organisation at their C-terminal half with a proline-rich region (PRO) domain followed by a WH2 domain, also called Verprolin homology domain (V), a central region (C) and an acidic region. The N-terminus of WASP and N-WASP contains WH1 domain, lysine-rich basic region (BR) domain and GTPase-binding domain (GBD), whereas in SCARs' N-terminus is replaced by SH domain and basic region (Caron et al., 2002).

The ectopic expression of WASP and N-WASP in the cell does not lead to major changes in cell morphology suggesting that these two proteins are predominantly inactive, thus favoring the autoinhibition hypothesis. This is supported by two facts: first, the isolated VCA module binds the GBD region *in vitro*; second, the molecular linker between GBD domain and C-region maintains WASP and N-WASP in an autoinhibition state so the acidic regions are unable to bind to Arp2/3 complex. Upon the activation by profilin, Grb2 and other SH3-domain binding proteins, cdc42 and phosphatidylinositol 4,5-bisphosphate (PIP_2), the autoinhibition is released. The mechanism of this release is explained by the fact that cdc42 bound to the GBD region induces a conformational change rendering this region unable to bind to the C-domain. So the VCA region is unmasked (Caron et al., 2002) (Fig 5).

The autoinhibition mechanism is unlikely to exist in the WAVE subgroup of proteins because some of the members of this family are fully active in actin polymerisation *in vitro* (Machesky et al., 1997). The activation of each WAVE protein seems unique. The mechanism of the activation of WAVE1 has been described recently. Through the interaction with Nap125, PIR121, Abi2 and HSPC300, WAVE1 is unable to stimulate actin polymerisation because it is in a repressed condition. Following the activation, Rac2 forms a complex with Nap-PIR-Abi2, thus releasing the inhibition and allowing HSPC-WAVE1 complex to bind to Arp2/3 complex through its VCA domain and activate the actin nucleation (Eden et al., 2002). Active Rac can bind to IRSp53, a downstream factor of Rac GTPase, then binding to

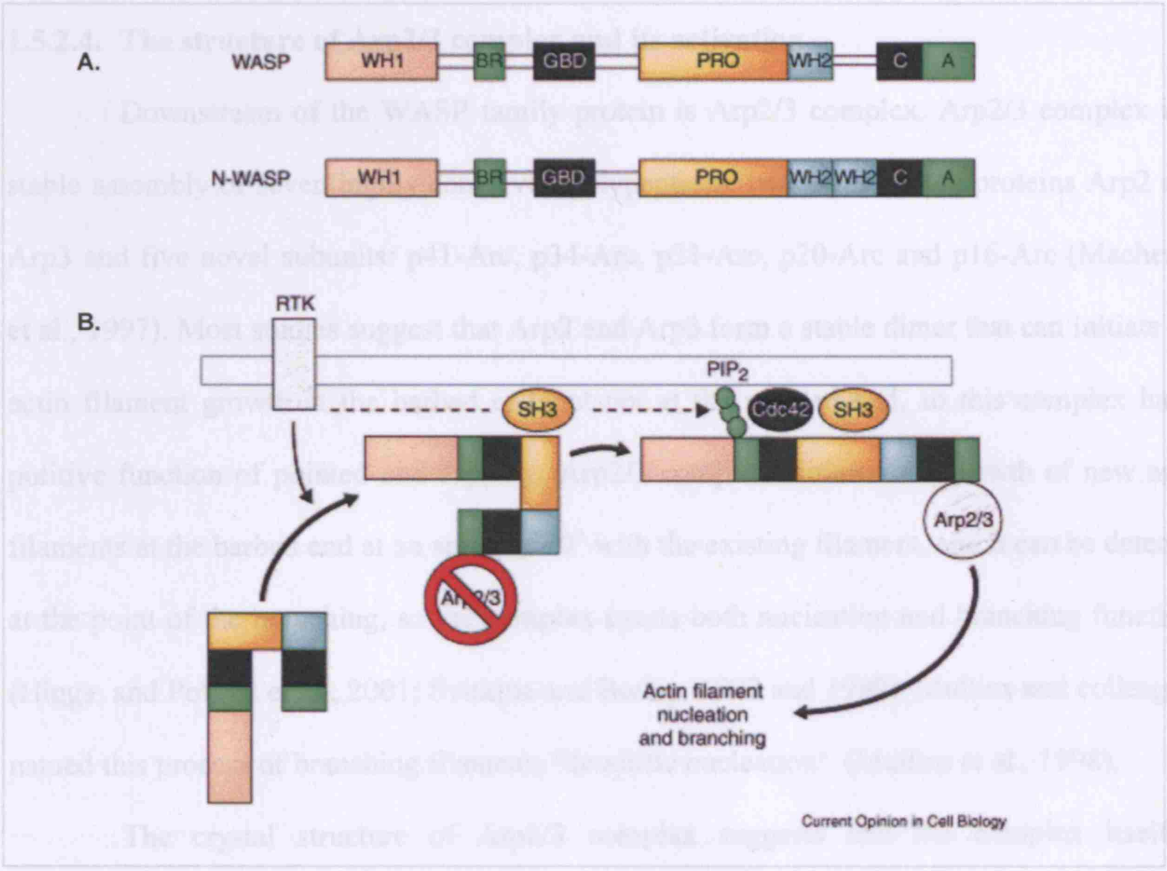

Fig 5. Structures of WASP family proteins and the activation of WASP.
(A) Domain structure of WASP and N-WASP. The proline-rich region (PRO) is followed by a WH2 (also called V for verprolin-homology) domain, a central (C) region and an acidic (A) domain. The domains that are able to interact have the same colour. (B) model for receptor-mediated recruitment and activation of WASP. Activation of a tyrosine kinase-coupled receptor (RTK; e.g. TCR) elicits the recruitment of WASP, SH3-containing proteins, cdc42–GTP, and Arp2/3 complex in the vicinity of the activated receptor. Upon cooperative interaction with PIP_2 and active GTP-bound cdc42, WASP is released from autoinhibition and can activate actin nucleation from the bound Arp2/3 complex (Caron et al., 2002).

WAVE2 and activating it (Miki et al., 2000). The activation mechanism of WAVE3 is unknown.

1.5.2.4. The structure of Arp2/3 complex and its activation

Downstream of the WASP family protein is Arp2/3 complex. Arp2/3 complex is a stable assembly of seven highly conserved polypeptides, two actin-related proteins Arp2 and Arp3 and five novel subunits: p41-Arc, p34-Arc, p21-Arc, p20-Arc and p16-Arc (Machesky et al., 1997). Most studies suggest that Arp2 and Arp3 form a stable dimer that can initiate the actin filament growth at the barbed end but not at the pointed end, so this complex has a putitive function of pointed end capping. Arp2/3 complex initiates the growth of new actin filaments at the barbed end at an angle of 70^{o} with the existing filament, and it can be detected at the point of the branching, so the complex exerts both nucleation and branching functions (Higgs and Pollard et al., 2001; Svitkina and Borisy, 1997 and 1999). Mullins and colleagues named this process of branching filaments 'dendritic nucleation' (Mullins et al., 1998).

The crystal structure of Arp2/3 complex suggests that the complex itself is intrinsically inactive (Robinson et al., 2001), so its activation needs external stimuli. VCA-domain at the C-terminus of WASP and Scar proteins is sufficient to bind both actin and Arp2/3 complex, and stimulate nucleation of actin polymerisation by Arp2/3 complex (Machesky et al., 1997; Rohatgi et al., 1999 and Winter et al., 1999). The Arp2/3 complex subunit(s) that bind(s) VCA-domain of WASP and Scar are not very clear. Two WH2 motifs in N-WASP are able to enhance the Arp2/3 complex nucleation efficiency and might be able to increase its binding to actin filaments (Yamaguchi et al., 2000). Their ability to activate the Arp2/3 complex appears similar, but the rates of nucleation among the three are quite different, N-WASP exerting the highest activity (Wiesner et al., 2003).

Arp2/3 complex can be activated by ActA, a surface protein of Listeria (Welch et al., 1998). The binding domain located at residues 31-170 of the ActA is similar to the

WASP/Scar VCA domain (Zalevsky et al., 2001). Fungal myosin can also bind to Arp2/3 complex since its C-terminal sequence resembles the C and A domain of WASP and Scar (Lechler et al., 2000). The activation of cortactin to Arp2/3 complex's nucleation activity is mediated through its N-terminal acidic motif, which is similar to other activators (Weed et al., 2000). Furthermore, cortactin stabilizes branches formed by Arp2/3 complex and may serve to prolong the lifetime of dendritic networks (Weaver et al., 2001).

Other activators of Arp2/3 include Abp1 and Pan1. Abp1 is an actin-binding protein first identified in *Saccharomyces cerevisiae* (Drubin et al., 1990). Activation of Arp2/3 complex by Pan1 is exerted by two different mechanisms. One is through its nucleation promoting factors (NPF). NPFs stimulate Arp2/3 complex nucleation activity by strengthening its association with the sides of filaments, thereby stabilizing the filament created by Arp2/3. Another is mediated by its actin depolymerising factor homology (ADFH) domain since the mutation at this region abolishes the Arp2/3 complex activation, but the precise mechanism of the activation is unknown (Quintero- Monzon et al., 2005). Pan1 is an endocytic protein. It contains an acidic stretch with a carboxy-terminal tryptophan residue, which is similar to motifs found in all known Arp2/3 activators. The region containing Eps15 homologous domain and acidic stretch is able to activate Arp2/3 complex (Duncan et al., 2001).

1.5.3. Microtubules

Compared with most vertebrate cells, neutrophils polarize, move, and turn more rapidly, over time scales of 30–90 sec rather than minutes or hours (Xu et al., 2005). But the roles of the microtubule network in neutrophils in these processes are not clear. Microtubules are polymers of tubulin. These are hollow cylindrical polymer structures, consisting of 13 protofilaments of tubulin arranged into a cylinder. They are assembled by the polymerisation of α-β dimers of tubulin and several microtubule-associated proteins (MAPs). Microtubules

also exert polarity: each microtubule has a plus and a minus end. The fast growing end is called the 'plus' end and is terminated by the β subunit of tubulin and the other end is called the 'minus' end and capped by the α subunit. Plus ends of microtubules usually point to the extremities of the cell (Howard and Hyman et al., 2003).

During polymerisation of tubulin, the plus end switches between two states: slow growth and rapid shrinkage (Mitchison et al., 1984). This distinct physiological behaviour of the microtubules is referred to as dynamic instability (Kinoshita et al., 2002). The conversion from growing to shrinkage is called catastrophe, and from shrinkage to growing is called rescue. These processes are a result of the addition or loss of subunits from the ends of microtubules (Kinoshita et al., 2002). Polymerization and depolymerization are mediated by the GTP hydrolysis cycle. Polymerization is driven by the high affinity of the tubulin-GTP dimer towards the end of the microtubule. The minus end usually lacks the GTP cap, unless hydrolysis and/or Pi release is slow compared to subunit addition. The plus end generally has a GTP cap, but the loss of this cap, by nucleotide exchange, dissociation of end dimers, or donation of the GDP to the β subunit, results in depolymerization. This model is in agreement with a more dynamic plus end and a less motile minus end and it provides an explanation for dynamic instability (Howard and Hyman, 2003).

Once the microtubules assemble, they provide the track for the organelles and chromosomes to move along. This is achieved by the interaction of microtubules with motor proteins such as kinesin and dynein. They move along the sides of microtubules. Kinesin is a microtubule activated ATPase with processivity, which enables it to take greater than 100 steps along a microtubule without detaching and diffusing away. And that makes kinesin a highly efficient cargo transporter because other motor proteins, such as myosin or dynein do not share this processivity (Howard et al., 1997).

The role of microtubule-associated proteins in regulation of the end of the microtubules is still not clear, but recent studies of CLIP-170 are beginning to shed light onto this process. CLIP-170 is a plus-end-binding protein and serves as a linker between membranes and microtubules (Perez et al., 1999). These studies have suggested that CLIP-170 binds to the growing end of the microtubules and rescues them near the cell cortex (Komarova et al., 2002; Brunner et al., 2000). At that part of the cell, microtubules continuously alternate between the two states to adapt to the requirement of rapid cell shape change at the periphery. The N-terminus of CLIP-170 has also been found to form a complex with IQGAP1 by binding to its distal C-terminus. IQGAP1 is a scaffolding protein which transducts signals through diverse pathways, involving mediating signalling by Rho family GTPases and calmodulin, regulating E-cadherin and beta-catenin function and organizing microtubules (Briggs et al., 2003). Fukata et al reported that at the leading edge of the Vero fibroblast, CLIP-170 binds to Rac-IQGAP1 and cdc42-IQGAP1 and then dissociates from the microtubules, thus leading to microtubule shrinkage. This finding has significant implications, because for a long time CLIP-170 has been speculated to have a receptor at the membrane. This finding integrates the microtubules and actin cytoskeleton, linking microtubules to special cortical region for cell polarization (Fukata et al., 2002).

1.5.4. Intermediate filaments

Another important element in the cytoskeleton to provide mechanical strength to cells and tissues is intermediate filaments (IFs). They are named because the size of the filaments they form is between large microtubules (25nm) and actin microfilaments (5nm). In contrast to microtubules and microfilaments, intermediate filaments are not controlled by nucleotide hydrolysis. They are highly charged, extended α-helical molecules forming dimeric proteins from fibrous coiled-coil. IFs have non-polar structures (Parry et al., 1995;

Miller et al., 1993). They can resist extraction with non-ionic detergents and high concentrations of salt, except urea (Kreplak et al., 2004).

On the basis of sequence homology, IFs can be divided into five classes: type I comprises acidic keratins, type II constitutes the basic keratins, type III includes vimentin, desmin, GFAP, and peripherin, type IV encompasses the neurofilament triplet proteins NF-L, NF-M, NF-H together with α-internexin and syncoilin, and type V represents A- and B-type nuclear lamins (Kreplak et al., 2004).

The most obvious function of IFs is to provide mechanical strength to cells and tissues (Reviewed by Quinlan et al., 1999). IFs also integrate with actin and microtubule cytoskeletal proteins and their motors, namely through interactions with kinesin, dynein and myosin Va to directionally move organelles and motor cargoes (Styers et al., 2005; Ameen et al., 2001; Toivola et al., 2004; Salas et al., 1997).

1.5.5. Cytoskeleton and NADPH oxidase

The cytoskeleton is vital for neutrophil function. Circumstantial evidence suggests the role of actin filaments in the regulation of NADPH oxidase (Nauseef et al., 1991; Allen et al., 1999; Wientjes et al., 1997). The evidence for the association of $p40^{phox}$ with cytoskeleton was mainly because of its presence in the detergent-soluble and detergent-insoluble fractions when resting neutrophils were lysed in Triton X-100 or octyl glucoside buffer (El Benna et al., 1999), its colocalization with filamentous actin by immunofluorescence confocal microscopy (El Benna et al., 1999), and its binding to N-terminal part of moesin through its PX domain in a phosphoinositide-dependent manner (Wientjes et al., 2001). Unlike $p47^{phox}$, the association of $p40^{phox}$ with the cytoskeleton was not induced by the PMA-stimulation. It has been suggested that its association with the cytoskeleton was via $p67^{phox}$. There are distinct states of $p40^{phox}$ that can be manipulated with Triton X-100 (Tsunawaki et al., 2000), but direct interactions between cytoskeleton proteins and NADPH oxidase components have

been shown recently. Coronin, an actin-binding protein, has been shown to attach to the C-terminal half of $p40^{phox}$, a binding partner of $p67^{phox}$. Also, both coronin and $p40^{phox}$ accumulate at the membrane of the phagocytic vacuole. Interestingly, rearrangement of F-actin in cells from patients lacking $p47^{phox}$ or $p67^{phox}$ was diminished, suggesting that phox proteins may also participate in reorganization of cytoskeleton (Grogan et al., 1997). Further, the small GTP-binding protein rac2 is involved in actin modulation and is also implicated in oxidase activation (Abo et al 1991; Hall et al., 1992; DeLeo et al., 1996; Knaus et al., 1991 &1992; Leusen et al., 1996; El Benna et al., 1994).

Apart from those mentioned above, NADPH oxidase components have also been reported to interact with other cytoskeletal proteins. Evidence from immunoprecipitation experiments has shown that the oxidase components $p47^{phox}$ and $p67^{phox}$ associates with cofilin (Suzuki et al., 1995). Ruffle catalyst WAVE-1 and suppressor of cAMP receptors have been identified as binding partners of $p47^{phox}$. Following stimulation of endothelial cells with VEGF, $p47^{phox}$ associates with WAVE-1 as well as Rac1 and PAK1, proteins involved in both ruffle formation and oxidase activation (Wu et al., 2003), thus supporting the functional interdependence between the cytoskeleton and NADPH oxidase.

1.5.6. Neutrophil transmigration and cytoskeleton

The leukocyte recruitment to sites of inflammation is a highly regulated cascade of events: rolling of endothelial cells of blood vessels and sequential transmigration through endothelium and extravascular tissue components. Transient and dynamic interactions with the extracellular matrix are established during this process involving adhesion and detachment. At the front of the cell, the plasma membrane extends forward and adheres to the substratum, while in a coordinated manner, the back of the cell contracts and detaches from the substratum (Bretscher, 1996; Lauffenburger and Horwitz, 1996; Mitchison and Cramer,

1996). These processes need tightly regulated linkage between integrin receptors, cytoskeleton and external cues. It has been proposed that Rac 1, L-plastin, talin, vinculin and tyrosine kinase FAK^{125} are among the cytoskeletal proteins that are actively linked to integrin intracellular domains (Rush and Izard et al., 2004; Gustavsson et al., 2004; Anderson and Ferriera, 2004; Palazzo et al., 2004). In the activated state, talin and vinculin bind to other regulators of the cytoskeleton, including paxillin, α-actinin and vinexin, as well as to F-actin, and the latter interaction effectively joins the 'bridge' linking integrin receptors with the actin cytoskeleton (Critchley, 2000).

1.5.7. Neutrophil chemotaxis and cytoskeleton

The movement of neutrophils *in vivo* is directed by chemotactic signals. Potent chemoattractants include complement factor C5a, arachidonic acid metabolites such as leukotriene B_4 (LTB_4), platelet-activating factor (PAF), various cytokines like interleukin-8 (IL-8) and bacteria-derived N-formyl peptides (Elferink and VanUffelen, 1996). In order to migrate in the direction of a concentration gradient of an activating agent, a neutrophil needs to sense direction, polarize its cytoskeleton towards the origin of the signal and then chemotax. Upon binding of a chemoattractant to a neutrophil cell-surface receptor, a series of events is triggered resulting in forward movement, which is driven by extending the leading edge (lamellipod or pseudopod) through localized polymerization of F actin.

The best-studied chemotactic receptor in neutrophils is the fMLP receptor. Receptor-ligand interaction results in activation of heterotrimeric G-proteins and their downstream effectors PLC and PI-3 kinase. At least two main pathways to actin polymerization lie downstream from this receptor (Glogauer et al., 2000). One leads from cdc42 to *de novo* actin nucleation through Arp2/3 complex. The Arp2/3 complex localizes to regions of active actin polymerization in neutrophils (Machesky et al., 1997). The other pathway involves a Rac dependent mechanism, which contributes to elongation from existing

actin filament barbed ends generated through uncapping or severing (Evangelista et al., 2003; Wallar et al., 2003). Neutrophils from mice deficient in Rac2 display defects in chemotaxis and polarization (Roberts et al., 1999). Several lines of evidence suggest the importance of gelsolin as downstream target of Rac in neutrophils. Gelsolin-deficient mice have increased expression of Rac, probably due to a compensation mechanism (Azuma et al., 1998). GTP-Rac stimulates the removal of gelsolin from the end of the actin filaments in neutrophil extracts (Arcaro et al., 1998). The recent discovery of P-Rex1, a G protein βγ and phosphatidylinositol (3,4,5) triphosphate (PIP_3)-dependent guanine-nucleotide exchange factor GEF for Rac, suggests that chemoattractants may regulate Rac via P-Rex1 (Welch et al., 2002). Another signaling mechanism by which Gβγ directly interacts with PAK1 and activates cdc42 through PAK1-associated PIXα has also been identified (Li et al., 2003), revealing an essential role for this particular pathway in chemotaxis. Many participating molecules have been described in recent years, but little is known about the pathway upstream of Rho family GTPases (Li et al., 2003).

1.5.8. Phagocytosis and cytoskeleton

When neutrophils reach the site of inflammation or injury, phagocytosis takes place. Phagocytosis, the process by which cells engulf and digest bacteria and other foreign bodies, is essential in innate immunity. Metchnikoff first observed the importance of phagocytosis as a host defence mechanism in 1891 (Metchnikoff, 1968). Enormous progress has been made since that time towards the understanding of this process. Phagocytosis can be triggered by two alternative mechanisms: one is mediated by the activation of complement receptors and another is through Fcγ receptors (FcγR) (Kaplan, 1977). Other receptors involved in phagocytosis include scavenger receptors, lectin and mannose receptors co-operating in detection of bacteria by macrophages. Plasma proteins, fibronectin and vitronectin can non-specifically opsonize pathogens or cell debris. The uptake process in monocytes is primarily

mediated through fibronectin receptor $\alpha_5\beta_1$ and vitronectin receptor $\alpha_v\beta_3$ (Blystone et al., 1994 and 1999).

Complement-opsonised particles tend to sink into the cells, whereas IgG-coated beads are more actively engulfed by the lamellipodia, which project from the cell surface. It has been indicated from these ultrastructral studies that mechanisms involved in these two processes are different (Allen and Aderem, 1996).

Even though the precise signaling pathways linking ligated phagocytic receptors to actin polymerization are not fully understood, it is known that Rho GTPases are critical in controlling the cytoskeletal rearrangements during phagocytosis (Caron and Hall, 1998; Massol et al., 1998). In macrophages, internalization of IgG coated particles is mediated by co-ordinated actions of cdc42 and Rac1. Cdc42 and Rac1 are small GTPases involved in different steps of phagocytosis. Cdc42 is activated after FcγRII ligation, and this results in activation of a Rac-Rho cascade and the concomitant association of all three GTPases with the phagosome (Caron et al., 1998; Ridley et al., 1992; Nobes et al., 1995). Cdc42 controls the pseudopod emission while Rac1 is responsible for phagosome closure, at least in the case of FcεRI-mediated phagocytosis (Massol et al., 1998; Castellerno et al., 2001). The function of RhoA in FcR-mediated phagocytosis is still not clear.

In contrast, phagocytosis through Complement Receptor 3 (CR3) is dependent on Rho family members, particularly Rho A (Allen and Aderem, 1996; Caron and Hall, 1998), and neither cdc42 nor Rac1 are required for this process (Caron and Hall, 1998). Recently, it has been found that Rho-associated kinase and myosin II are required for phagocytic cup formation for CR3- but not for FcγR-mediated phagocytosis, and that myosin II is required for later stages of phagosome formation (Olazabal et al., 2002). Rho GTPases are likely to have several downstream effectors. WASP/N-WASP and Scar/WAVE family of proteins are the main regulators of actin polymerization downstream of cdc42 and Rac. The macrophages from Wiskott-Aldrich syndrome patients exert a deficient uptake of IgG-opsonized particles,

suggesting the important role of WASP protein in FcR-mediated phagocytosis (Blanchoin et al., 2000). Activation of the WASP family of proteins activates downstream proteins and recruits them to the phagosomes (May et al., 2000). The Arp2/3 recruitment and activation can account for *de novo* actin nucleation and branching of pre- existing filaments.

Severing and capping activities can also participate in remodelling of the actin skeleton. For example, gelsolin, a calcium-dependent actin severing and capping protein, has been suggested to be specific for IgG-mediated phagocytosis, but not complement-mediated phagocytosis. In gelsolin-deficient neutrophils, the attachment and ingestion of IgG-coated yeast are abolished, while several steps in phagosome processing, namely the formation of an actin ring around the phagosome, translocation of granules and activation of the NADPH oxidase are all normal in gelsolin-deficient neutrophils (Serrander et al., 2000). Furthermore, neutrophils lacking L-plastin, the F-actin crosslink protein, are deficient in the killing of *S.aureus* in *vivo* and *in vitro*, despite normal phagocytosis, demonstrating the importance of cytoskeletal proteins in immunopathogenesis (Chen et al., 2003). A growing number of mice deficient in particular cytoskeletal proteins, are helping to reveal the precise functions of these proteins.

Studies of the involvement of the cytoskeleton in phagocytic vacuole physiology in neutrophils remain sparse. The phagocytic vacuole is constrained by a surrounding meshwork of cytoskeletal proteins, such as vinculin and paxillin, in order to control the extent of its swelling during phagocytosis (Reeves et al., 2002). GTPase cdc42, its inhibitory subunit Rho-GDI, γ-Pak and cofilin have been reported to rapidly associate with the developing phagosomes (Robinson and Badwey, 2002). However, the molecular mechanisms governing the integration of these signalling molecules into a coherent cytoskeletal response remain largely unknown. Thus the analysis of the composition of the actin cytoskeleton, microtubule network and intermediate filaments are of crucial importance.

Standard techniques for determining the subcellular location of actin polymerization, through incorporation of fluorescently labelled actin by microinjection or permeabilization, have proven difficult or impossible to use when studying primary neutrophils. Overexpression of recombinant proteins in neutrophils would be a powerful tool to analyze the dynamics of the cytoskeleton in neutrophils during phagocytosis. However, neutrophils are not suitable for this technique because they are short-lived terminally differentiated cells and almost impossible to transfect (Weiner et al., 1999). Thus, immunohistochemical examination of the cytoskeleton remains to be the main technique employed to monitor the distribution of proteins that regulate the cytoskeleton in neutrophils undergoing phagocytosis.

1.5.9. Disorders of the neutrophil cytoskeleton

The cytoskeleton is involved in cell locomotion, cell shape maintainance and cell signalling (Fuchs et al., 1998). Abnormalities in actin cytoskeleton and associated proteins, microtubules and associated proteins, intermediate filaments and molecular motors, are known to lead to various diseases (Ramaekers and Bosman, 2004). So far, the association of keratin mutations with genetic skin fragility disorders due to decreased physical resilience of epithelial cells constitutes one of the most striking examples of cytoskeleton disorders (Lane et al., 2004; Zatloukal et al., 2004; Owens et al., 2004). Mutations in α-actin, α- and β-tropomyosin, troponin-T, nebulin, and microtubule associated protein tau, have been linked to various diseases (Chaponnier et al., 2004; Rottner et al., 2004; Cairns et al., 2004).

Wiskott-Aldrich Syndrome (WAS) is a severe X-linked primary immunodeficiency with thrombocytopenia, small platelets, eczema, recurrent infections, autoimmune disorders and potential hematopoietic malignancies. Around 300 mutations have been found in the Wiskott-Aldrich Syndrome (WAS) gene. These mutations in the first 3 exons are associated with X-linked thrombocytopenia or attenuated WAS, while mutations elsewhere are associated with a variable phenotype (Sullivan et al., 1999; Dupuis-Girod et al., 2003; Burns

et al., 2004). Mutations are most frequent at the EVH1 domain of the WAS gene and often result in the disturbed interaction between EVH1 and WASP interacting proteins (WIP). WIP is a widely expressed protein that stabilizes actin filaments and regulates actin polymerization, in a vaccinia-based actin motility system, to the immunological synapses after T-cell-receptor ligation (Sasahara et al., 2002; Moreau et al., 2000), or in the induction of filopodia (Burns et al., 2004). The consequence of this disturbance is in WASP-mediated actin polymerisation, in particular spatial localization of WASP activity. In WAS patients, the defect results in abnormal platelet production and T-cell dysfunction (Burns et al., 2004). The impact of loss of WASP function in human neutrophils has not been fully elucidated. Although a portion of WAS patients suffer from recurrent infections classically attributed to neutrophil dysfunction (Burns et al., 2004), and the patient's neutrophils and monocytes responded poorly to chemoattractants (Capsoni et al., 1986), but the direct correlation between WASP defect and neutrophil function has not been established in humans.

The following group of diseases are not strictly classified as neutrophil cytoskeletal diseases. More correctly, these diseases show disorder of cytoskeletal arrangement, but the defects rely on the proteins that are indirectly associated with the cytoskeleton.

Leukocyte adhesion deficiency (LAD) is an immunodeficiency with defects in adhesion and recruitment of leukocytes or platelets to the blood vessel wall, which therefore result in severe bacterial infections, impaired wound healing, or a tendency towards severe bleeding in patients. The molecular lesions in LAD I and II are found in the β_2 integrins (Jamal T et al., 1998) or GDP-fucose (Wild et al., 2002) respectively, whereas in LAD III, a clear biochemical defect in the activation of Rap1 is shown (Etzioni et al., 2004). Rap1 is a GTPase important in the dissociation of Rap-1 associating molecule RAPL from microtubules and thus is a key element in the inside-out and outside-in (ligand-induced) signalling underlying integrin activation by cytokines. In this case, both chemokines and cytokines were

unable to activate Rap1 leading to severe adhesive defects analyzed *in vitro* (Fujita et al., 2005; Tamada et al. 2004).

Glycogen storage disease (GSD) 1b is a metabolic disorder characterized by a deficiency of glucose 6-phosphate transporter and neutrophil alterations, which are reduced in number and functionally impaired. A recent study has shown the correlation of submembrane and cytoskeletal changes in actin, focal adhesion kinase (FAK) and gelsolin associated with this disease (Lesma et al., 2005), although the precise mechanism has not been fully elucidated.

The basic structure of neutrophil contains cytosol, membrane and granules. The azurophilic granules, specific granules, gelatinase granules as well as secretory vesicles, differ in their size, density, protein content, and tendency for exocytosis, and they reflect the stage of granulocytic differentiation at which they are formed (Gullberg et al., 1999). The granule proteins play important roles in the immuno-defense mechanism. The abnormalities in several granule proteins form the basis of the following disorders of neutrophil function.

Neutrophil-specific granule deficiency (SGD) is a rare congenital disorder, characterized by atypical bi-lobed nuclei. SGD neutrophils lack expression of all secondary and tertiary granule proteins, and possess defects in chemotaxis, disaggregation, receptor up-regulation, and bactericidal activity, resulting in frequent and severe bacterial infections. The molecular defect of this disease lies in the homozygous mutation in the CCAAT/enhancer binding protein-epsilon (C/EBP epsilon) gene. The mutant C/EBP epsilon in protein is localized in the cytoplasm rather than the nucleus and is unable to activate transcription (Gombart et al., 2001). A microarray study comparing the gene expression differences between C/EBP epsilon deficient mice and wild type has revealed the major changes in the expression of genes, which are involved in cytoskeletal organization and other biological events (Gombart et al., 2005).

Chediak-Higashi Syndrome (CHS) is a rare and fatal autosomal recessive disorder that characterised clinically by abnormalities of pigmentation, blood clotting, and neurologic function (Barak et al., 1987; Spritz et al., 1998). Morphologically the lesion is characterised by the presence of 'giant' clustered lysosomes near the nucleus, which exhibit both azurophilic and specific granular markers. The pathogenesis of the disease was thought to be the impaired microtubule assembly and function. However, some recent studies have questioned this cytoskeletal membrane interface model, and it is suggested to be rather a secondary manifestation of CHS (Barak et al., 1987). The study conducted by Peron and colleagues has also suggested that the defective gene product is not an altered microtubular element involved in lysosomal movement. Lysosome morphology in macrophages is maintained by microtubules and microtubule-based motors, such as kinesin. Macrophages from beige mice (a murine homolog of Chediak-Higashi Syndrome) were able to display the same changes as occurred in the wild type when both of them were subjected to the lowering of cytoplasmic pH or by adding phorbol esters, which induce dramatic changes in lysosome morphology. These results indicate that lysosomes in Chediak cells are capable of interacting with the microtubule-based motor system (Perou et al., 1993).

The neutrophil granule protein elastase has been reported to be associated with bullous pemphigoid, an inflammatory blistering disorder associated with autoantibodies directed against two components of hemidesmosomes, BP180 and BP230. Neutrophil elastase has been implicated in subepidermal blister formation via proteolytic degradation of BP180 (Verraes et al., 2001), but elastase defects do not account for the pathogenesis of this disease.

Elucidation of the underlying mechanisms causing these diseases will bring insight into the functionality of the cytoskeleton and eventually contribute to the development of efficient therapeutics.

1.6. THE FUNCTION OF GRANCALCIN

Phagocytosis is important for the killing of micro-organism. As mentioned before, the phagocytic cells contain NADPH oxidase which catalyses the reduction of molecular oxygen to superoxide and toxic oxygen species (Babior et al., 1987; Segal et al., 1989). A defect in this enzyme will cause chronic granulomatous disease. The cytosolic components of NADPH oxidase translocate to the membrane. In an attempt to identify other NADPH oxidase components, antibodies to neutrophil membranes after PMA stimulation have been used to detect all cytosolic proteins that translocate to the membrane. A novel calcium-binding protein named grancalcin has thus been identified in the Segal's laboratory (Boyhan et al., 1992). It is highly expressed at the membrane and granules of the neutrophils in a calcium dependent manner (Lollike et al., 1995). L-plastin has been identified as a binding partner of grancalcin (Lollike et al., 1995), but the clear interaction between grancalcin and cytoskeleton has not been fully elucidated.

1.6.1. Molecular structure of the penta-EF-hand proteins

Grancalcin belongs to penta-EF-hand family (PEF) of proteins that are composed of five repetitive Ca^{2+} binding EF-hand motifs. In addition to the structural similarities in the EF-hand regions, the PEF family members share several other common features: 1) dimerization through unpaired C-terminal EF5s, 2) contain N termini of varying length and sequence but all are rich in glycine and hydrophobic residues, which may be responsible for association with phospholipids, 3) Ca^{2+} dependent translocation to membranes (Maki and Kitaura, 2002).

Members of the penta-EF-hand family proteins comprise calpain, sorcin, grancalcin, ALG-2, peflin and YG25-yeast (Boyhan et al., 1992). So far, these proteins have shown diverse functions. For example, calpain exhibits protease activity (Kitaura et al., 2001), and participates in a variety of biological processes, such as remodelling of cytoskeletal/membrane attachments, modulation of different signal transduction pathways and apoptosis (Kitaura et al., 2001; Goll et al., 2003). Sorcin binds to and regulates the cardiac

ryanodine calcium channel (Meyers et al., 1995; Lokuta et al., 1997), while ALG-2 plays a role in apoptosis (Krebs et al., 2002). The function of grancalcin is still unknown.

1.6.2. The phenotype of grancalcin deficient mice

To determine the physiological role of grancalcin *in vivo*, Dr. Jurgen Roes generated the grancalcin (Gca)-deficient mice by inactivating the gene encoding grancalcin in the mouse (accession: NW-000176) (Roes et al., 2003). The targeting vector for inactivation of the mouse Gca gene was constructed by insertion of a loxP-flanked neomycin resistance gene into a PstI site in exon 4, disrupting the second EF-hand motif near the N-terminus (Figure 6). The functional studies of these grancalcin-deficient mice have shown that 100% of the wild type suffered lethal endotoxic shock while 40% of the mutants survived a low-dose of LPS (Roes, et al., 2003). On the basis of this result it was concluded that grancalcin has a role in the immune response. The exact mechanism of this action of grancalcin has remained unknown (Roes, et al., 2003).

1.6.3. Interaction of grancalcin with calpain, L-plastin, sorcin and YopM protein

Recent protein interaction studies have started to uncover the functions of proteins belonging to this penta-EF-hand family. The interactions of grancalcin with sorcin, YopM and p65/L-plastin have been characterised (Hansen et al., 2003, Lollike et al., 2001).

The alignment of grancalcin and calpain sequences shows that these two proteins have 36% identity. Calpain was found in the focal adhesions and was able to cleave the proteins involved in focal adhesion, such as integrin receptors, focal adhesion kinase and talin due to its cysteine protease activity. By using a calpain inhibitor, both β_1 and β_3 integrin-mediated cell migration are reduced (Huttenlocher et al., 1997). By inhibition of calpain, the rate at which the rear of the cell detaches from the extracellular matrix is reduced. Since association between integrin and cytoskeletal at the rear of the cell dissociates when the cell

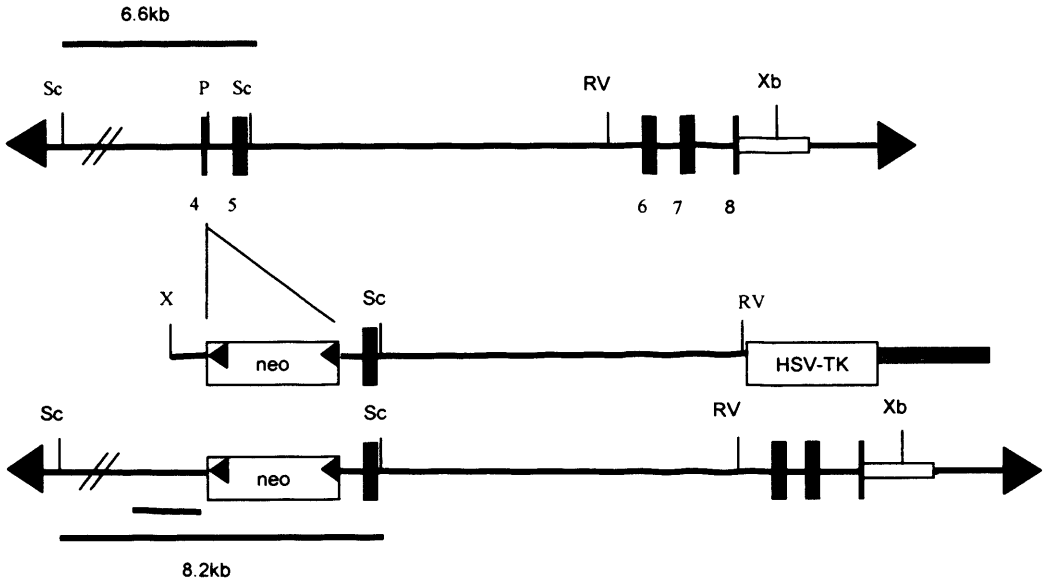

Fig 6. The structure of grancalcin gene locus (top), the insertion of the neo cassette (middle) and the homologous recombination (bottom) are illustrated.
The insertion of the neo gene disrupts the EF2. Open boxes indicate neo and hepes simplex virus thymidine kinase (HSV-TK) genes;Sc,ScaI; P, PstI; RV, EcoRV; Xb, XbaI; X, XhoI (Roes et al., 2003)

migrates, this finding suggests that calpain may serve as a linking protein between integrin receptor and the cytoskeleton (Huttenlocher et al., 1997). Dewitt et al have shown that in cells overexpressing calpain, the abundancy of β_2 integrin is increased at the phagocytic cup. After calpain inhibition, the binding and formation of a phagocytic cup were not altered, but the phagocytosis was impaired. β_2 integrin expression at the phagocytic cup was reduced. Calpain has also been shown to accelerate integrin-mediated phagocytosis by releasing integrin molecules from the initial contact site (Dewitt et al., 2002).

Sorcin is a protein initially identified in multidrug-resistance cells and is thought to contribute to their drug resistance (Suarez et al., 2004). In common with other penta-EF-hand proteins, sorcin translocates from the cytosol to membranes when it binds calcium. Grancalcin heterodimerizes with sorcin. This interaction has been revealed by a yeast two-hybrid study, a glutathione S-transferase pull-down assay and immunoprecipitation (Hansen et al., 2003). However, the physiological relevance of this interaction is not yet clear.

Recently, a plague virulence protein YopM has also been found to directly bind to grancalcin. YopM is a *Yersina* outer membrane protein found in plague infection. YopM may be used to displace the platelet glycoprotein GPIbα binding to the coagulation factor thrombin. The influx of PMN and monocytes into the tissue can be induced by a variety of chemotactic substances and thrombin is among the most potent of these. It could be that the major virulence-promoting effect of YopM is in muting the inflammatory response (Leung et al., 1990). Whether this interaction between grancalcin and YopM has *in vivo* significance for the virulence function of YopM is currently under investigation (personal communication with Prof. Sue Straley).

Grancalcin has been shown to associate with the cytoskeleton (Lollike et al., 2001; Liu et al., 2004). L-plastin, a leukocyte-specific actin bundling protein was found to interact with grancalcin in the absence of calcium through the use of affinity chromatography. No direct binding assay of grancalcin and L-plastin was performed to prove this interaction

(Lollike, et al., 2001). Immunohistochemical studies have previously demonstrated the translocation of grancalcin to the actin cytoskeleton in macrophages upon treatment with bacterial lipopolysaccharide (Liu et al., 2004) thus implicating its role in cytoskeletal function of these cells. It is thought that cytoskeletal localization of grancalcin results from binding to the actin-bundling protein L-plastin (Lollike et al. 2001). Like other plastin isoforms and fimbrin, L-plastin is a mosaic protein containing two EF-hands, one calmodulin-binding domain and two actin-binding domains (Zu et al., 1990). L-plastin is mostly involved in the cross-linking of F-actin fibers. L-plastin is phosphorylated after activation of neutrophils and this event leads to integrin activation and increased adhesion (Jones et al., 1998). The release of grancalcin in the presence of calcium from its binding partner L-plastin, which can cross-link F-actin may suggest its function in cell adhesion. L-plastin also associates with the intermediate filament protein vimentin at adhesion sites and regulates neutrophil integrin function (Chen, et al., 2003; Correia, et al., 1999).

1.6.4. The structure of grancalcin in the presence and absence of calcium

Like other PEF proteins, grancalcin is a cytosolic protein that can reversibly associate with cell membranes at physiological Ca^{2+} concentrations (Zamparelli et al., 1997). Such translocation can be mediated by two mechanisms: exposure of hydrophobic amino acid sequences of the molecule or by a myristoyl switch mechanism, when a covalently bound fatty acid becomes exposed after binding of calcium thus directing the protein to the membrane (Zozulya et al., 1992; Lollike et al., 2001). Grancalcin is highly soluble in metal-free form, but precipitates when the concentration of calcium in solution rises above 100 μM (Liu et al., 2004).

The X-ray crystallographic studies of grancalcin in the apo state at 1.9A resolution and at 2.5A resolution in a partially Ca^{2+}-bound state has been determined, demonstrating one Ca^{2+} ion per grancalcin dimer. Only rather small conformational changes have been observed

in grancalcin upon binding of Ca^{2+}. Out of five EF hands, only EF1 and EF3 have the ability to bind calcium. EF5 pairs with a similar C-terminal EF-hand from another monomer to form a dimer. How these Ca^{2+} induced changes contribute to the regulation of grancalcin activity remains unclear (Jia et al., 2000).

1.7. THE PRINCIPAL OF PROTEOMICS AND THE APPLICATION OF FUNCTIONAL PROTEOMICS IN NEUTROPHIL STUDIES

1.7.1. The definition of proteomics

Proteomics is defined as the large-scale analysis of the function of genes in a living system, including the description of co- and post-translationally modified proteins and altered spliced variants. This includes their covalent and non-covalent associations, spatial and temporal distributions within the cells, and their changes induced by extracellular or intracellular stimuli (Pandey et al., 2000; Guerrera et al., 2005).

The proteomics studies are composed of following steps: protein purification, gel imaging, spot digestion, database searching and analysis.

In order to understand the biological function of a cell or an organelle, it is important to analyse its protein composition. Therefore the protein purification can be done by cell prefractionation. To reduce the complexity of the protein mixture, two procedures are used to fractionate the cells: organelle isolation and chromatography. By using different centrifugal forces, it is possible to isolate different organelles in a relatively pure form, followed by two-dimensional electrophoresis. Chromatographic methods used to fractionate proteins include size-exclusion, anion-exchange, cation-exchange and reversed-phase chromatography, affinity chromatography. Combination of the above approaches is called multidimensional chromatography. Pre-fractionation of protein samples results in enrichment of the low-abundance proteins (Righetti et al., 2005; Mann et al., 2001).

The purified protein samples are then dissolved in urea buffer and are ready for separation on a gel. Two-dimensional electrophoresis is composed of two steps. The proteins are first separated by isoelectric focusing according to their isoelectric points, and then separated according to their molecular mass. The resulting 2D gel can be analysed by image analysis software. Melanie and BioImage software have been developed to carry out the batch mode analysis for spot detection, quantification, fitting and modelling, background subtraction, image alignment and comparison of different gels (Quadroni et al., 1999).

After image analysis, the protein spots can be picked manually or automatically and prior to protein digestion. The procedures including reduction, alkalytion and digestion can be completed in a fully automated system to avoid sample contamination, such as the Progest system. Automation of the sample handling at this stage, besides increasing throughput, is also important in order to avoid contamination with keratin. Usually the enzyme used for protein digestion is trypsin, which is known to cleave proteins specifically after a lysine or arginine residue.

Mass spectra of the tryptic digests can be obtained by using an Autoflex MALDI-TOF mass spectrometer (Bruker Daltonics, Billerica, MA), calibrated with a mixture of known peptides. If the spectra are collected automatically, Xmass software under "fuzzy logic" control can be used (Bruker Daltonik GmbH, 2001). This software under 'fuzzy logic' control and membership function can be used to decide the required change of laser power depending on the ion peak intensity and resolution of MS data acquisition. 'Fuzzy logic' presents a non-binary system of quantification and reasoning. In MALDI, the fuzzy logic rule for laser irradiance can be described as: IF ion intensity is very low THEN change laser irradiance accordingly. Taking the change of ion intensity and peak resolution as an example, if the decision process is done by a human operator, the intensity rules can be changed according to very low, low, average, high intensity and very high intensity five degrees. And the fluence change can be adjusted accordingly into large positive, small positive, none, small

negative and large negative. But in the fuzzy logic, the qualifiers of this five-shot spectrum are overlapping and the fluence change membership functions are overlapping as well. The input variable resolution has only low and high definition. Once the ion intensity is above the threshold level, a down-regulation of the laser influence immediately occurs thus enabling the laser fluence to be kept at the optimal level without major fluctuations (Jensen et al., 1997). The spectra can be internally calibrated using trypsin autolysis peaks, thereafter the baseline was subtracted and monoisotopic mass data extracted. The data can be subsequently analysed using Bruker Biotools software in conjunction with the Mascot search engine using the NCBI database.

The analysis of the mass spectra data will be discussed in detail in 1.7.3.

1.7.2. The principles of mass spectrometry

The main tool for the identification and analysis of proteins in proteomics is mass spectrometry. In general it works by separating and measuring the masses of ionised particles in a high vaccum. A mass spectrometer consists of an ion source where a beam of gaseous ions is formed from a sample, a mass analyser that separates the ions according to their mass-charge-ratio (m/z), and a detector that delivers a mass spectrum.

Matrix-assisted laser desorption/ionisation (MALDI-TOF) and electrospray ionisation (ESI) are two major ionisation approaches in mass spectrometric protein identification.

In MALDI-TOF, microlitre quantities of liquid sample are applied to a stainless steel or gold-plated target, and crystallised together with the matrix solution. When the laser irradiates the sample, the matrix vaporises, carrying the sample with it, helping to ionise the sample. The ions are then accelerated by the electric field and hit by the detector. All ions receive the same amount of kinetic energy, so the velocity is proportional to their mass. The mass of sample ions can therefore be determined by measuring the time it takes them to reach

the detector. Linear and reflector are two modes of MALDI-TOF analysis. Due to the inaccuracies which occur during the ion formation process, not all the ions are desorbed and ionised at the same time and place, the consequence of which is that ions with identical mass may not reach the detector at the same time in the linear mode. The mass peak is therefore broader and the resolution is poorer. This problem is solved by a reflector, which works like an ion mirror. Ions with the same mass-to-charge ratio but with a higher kinetic energy penetrate deeper (Fig 7A) (Wilkins et al., 1997).

Electrospray ionisation mass spectrometry (ESI-MS) is another powerful method frequently used in proteomic analysis. It generates ions from samples in liquid and measures their mass in quadrupole, ion trap or in MALDI-TOF mass spectrometers. Samples for electrospray need to be free of salt and detergent, because the presence of salt inhibits the vaporation process and therefore inhibits the electro-ionization process. In order to obtain high-quality electrospray mass data, the salt concentration should be lower than 500 μM (Siuzdak et al., 1996). The sample is introduced through a very fine capillary needle under high voltage, thus producing a mist of small solvent droplets of protein with high electrical charge. Then the molecules are transferred into the mass spectrometer for analysis. A quadrupole mass spectrometer has four parallel-arranged metal rods (quadrupole) and the force of an electrical field composed of a direct current voltage and a superimposed radio-frequency potential. Depending on the voltages applied, it only allows definite ions oscillating on a stable track, so a quadrupole mass spectrometer in general works as a mass filter. The molecules can be fragmented by collision at the second quandrupole and the masses produced by fragmentation, called daughter masses, can be analysed in the third mass spectrometer. The principle of this technique is illustrated in Fig 7B (Wilkins et al., 1997). It is frequently used if there is more than one match from MALDI, for analysis of post-translational modifications or for the sequencing of peptides.

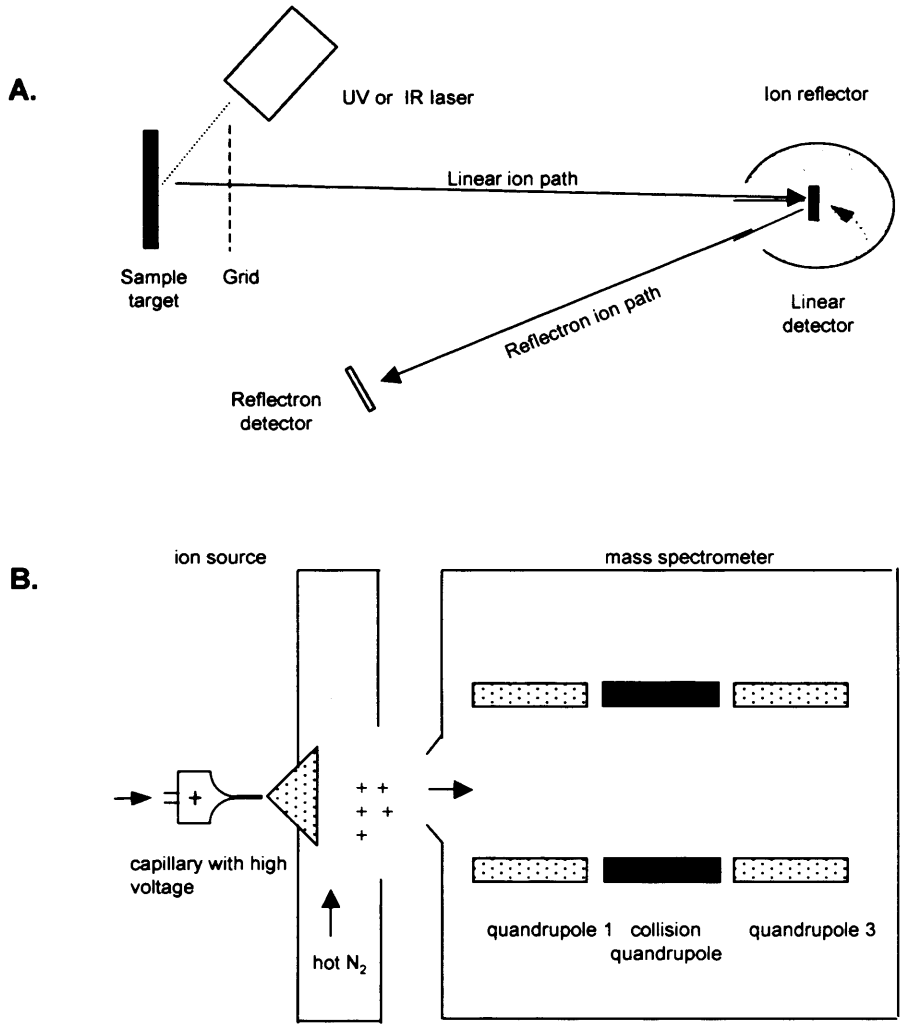

Fig 7. The principle of mass spectrometry.
(A) Schematic diagram of a MALDI mass spectrometer. The laser irradiates the matrix-embedded sample and creates molecular ions accelerated by the electric field. The time of flight is measured by the reflectron and /or the linear detector. (B) Schematic diagram of ESI-MS. In this case a triple quadrupole mass spectrometer equipped with electrospray ion source. The sample is introduced through a very fine capillary to which a high voltage is applied. There it forms a mist of small solvent droplets of high electrical charge, containing protein. It is thought that with the aid of hot nitrogen gas, the evaporation of the solvent causes the droplets to shrink and the charge density to increase. This brings the positive ions together and eventually the force of repulsion between them is strong enough to cause the ions to leave the droplet. They then enter the mass spectrometer. Masses of molecules can be measured by the first quadrupole. Alternatively the molecules can be fragmented by collision with an inert gas at the second quadrupole and the mass of fragmentation products be measured in the third. (Courtesy of Wilkins and Gooley, 1997)

1.7.3. The application of mass spectrometry

1.7.3.1. Protein identification

In MALDI, the acquired mass spectra are compared against the protein databases consisting of mammalian proteins using a probability-based method. Several databases now store theoretical protease digests of all known proteins. Trypsin is known to cleave proteins specifically after a lysine or arginine residue. Matching the spectrum of masses obtained by mass spectrometry with the existing database, which contains the theoretical masses digested with the enzymes such as trypsin, is known as 'mass fingerprinting' (Mann et al., 1993). From this a list of possible matches is provided by the database with a score indicating the probability of identification.

In ESI-MS, complete interpretation of the spectra is not necessary. One approach is to cleave the protein by sequence specific enzymatic digestion, measure the resulting peptides by mass spectrometry and search the sequence database for the proteins that match the peptide. Another strategy is to search for obvious sequence tags. A fragmentation spectrum usually contains a short, easily identifiable series of sequence ions, which yields a partial sequence. This partial sequence divides the peptide into three parts, regions 1, 2, and 3- characterized by the added mass m1 of region 1, the partial sequence of region 2, and the added mass m3 of region 3. The construct, m1 partial sequence m3, is called "peptide sequence tag", and is highly specific for the peptide. The 'peptide sequence tag', a short string of amino acid mass differences deduced from the fragment spectrum, combined with the parent peptide ion mass determined by regular MS spectrum and the distance in mass units to the N- and C-termini of the peptide, is in most cases sufficiently specific to identify a protein (Mann and Wilm 1994). The advantage of this method is that no prior enzymatic or chemical degradation is required.

1.7.3.2. Peptide sequencing

Both MALDI and collision induced dissociation (CID) can fragment peptides in different ways to determine peptide sequence. Peptides can be fragmented within mass spectrometers using post-source-decay (PSD) in MALDI or CID techniques in a variety of mass spectrometers, such as ESI machines or tandem mass spectrometry. In all methods, the objective is to produce spectra containing a series of peptide peaks differing by the mass of amino acid residues, thus allowing stretches of peptide sequence to be deduced.

In MALDI, the ions accelerate within the source. The area between accelerator and detector is called drift region. The process of metastable decomposition occurs during ion out of the ion source and in the field free region of the mass spectrometer. Thus this method is called post-source-decay (PSD). PSD ions formed in the drift region continue the flight with the same velocity as the original ion and are therefore in principle not separately detectable using a linear TOF. But reflector mass spectrometer can separate precursor and metastable decay ions exploiting the difference in their kinetic energy. In order to view the whole composite mass spectrum of the metastable decay ions, a series of reflector steps are needed. Most metastable decompositions occur along the peptide chain. By comparing the precursor and metastable decay ions, partial fragments of the peptide sequence can be obtained.

By contrast with MALDI-PSD fragmentation, CID is robust and general, frequently producing a series of B or Y ions from which sequence can be deduced. When collided with atoms of inert gas, the starting peptide is fragmented. When the spectrometer in used in 'positive-ion mode', the sample is introduced into an acidic solution, so ionisation involves the addition of H^+ to all fragments. Fragmentation at the peptide bonds will produce B series ions if the peptide positive charge remains at the peptide N-terminus. This fragmentation can occur at three different positions, each of which is sequenced, designated as types a_n, b_n and c_n. Alternatively it will produce Y series ions if the charge remains at the peptide C-terminus and fragments are called x_n, y_n and z_n. Only the charged portion of the peptide will be detected after fragmentation. Y and B ions are most usful for sequencing peptides. When ions are

generated which include neither terminus, they are termed internal fragments (Wilkins et al., 1997).

Tandem mass spectrometry (MS/MS) has high accuracy of mass measurement. Because it is prone to formation of multiple charged molecules, it enables the analysis of large molecules with an instrument having a relatively small mass range. The disadvantage is that the sample needs to be very pure.

1.7.3.3. Post-translational modifications

MALDI can be used to predict the post-translational modifications such as phosphorylation, because an addition in the mass of a peptide of 80 Da implies the presence of one phosphate group. For defining the exact localization of post-translational modifications, ESI and tandem mass spectrometry need to be used. Phosphopeptides can be retrieved from the LC-MS/MS data, either by searching a database of MS/MS spectra and allowing the presence of a phosphorus on any serine, threonine, or tyrosine residues, or by treating the samples with phosphatases and filtering out ions that show loss of a fragment corresponding to the mass of the phosphorous (Wilkins et al., 1997).

1.7.4. Quantitative proteomics

In mass spectrometry the intensity of the signal can not easily be correlated with the amount of analyte present in the sample (Mann et al., 2001). But in many cases, quantitative analysis is needed in drug discovery or analysis of signalling pathways. Thus, metabolic labelling with stable isotopic amino acids in cell culture (SILAC) or isotopic affinity coded tagging (ICAT) has been applied to differentially label proteins in stimulated versus unstimulated cells. The principle of these methods is the incorporation of a stable isotope into one of the two experimental groups to be compared.

In SILAC, unstimulated cells are grown in normal arginine-containing medium, whereas stimulated cells are grown in [^{13}C] arginine-containing medium, labeling all proteins with 6Da heavier amino acid. The two samples are mixed, proteins are digested with trypsin and the resulting peptides are analysed by mass spectrometer. The MS measurement readily differentiates between peptides originating from the two pools because incorporation of a high abundance of ^{13}C shifts the mass of any given peptide upwards, which leads to a pair of peaks from each peptide (Blagoev et al., 2003; Guerrera et al., 2005). The SILAC method has been extended to allow simultaneous quantitation of three differently labelled cell populations (Blagoev et al., 2003).

Recently there has been a significant breakthrough in gel-free quantitative proteomics approaches by chemical labelling. Vandekerckhove and colleagues at Ugent University in Belgium developed a peptide isolation procedure based on diagonal electrophoresis and diagonal chromatography—called combined fractional diagonal chromatography (COFRADIC). This technique has been used to isolate N-terminal peptides. Since every protein only has one N-terminus, it is only represented by one peptide. In this method, free amino groups in proteins are first blocked by acetylation while cysteines are alkylated with iodoacetamide. After trypsin digestion and a primary run of reverse-phase chromatographic fractionation, all peptides are treated with 2,4,6-trinitrobenzenesulfonic acid (TNBS). Only internal peptides react with TNBS to form trinitrophenyl-peptides (TNP), whereas blocked N-terminal peptides are not affected. TNP-peptides display a strong shift in the second run and therefore segregate from the unaltered peptides. N-terminal peptides can be collected and then analysed by liquid-chromatography (LC)-MS/MS (Gevaert et al., 2003). Alternatively, if the different peptides after trypsin digestion from different samples are labelled with O^{16} or O^{18}, COFRADIC can be used to distinguish changes between two different samples (Gevaert, 2002). Currently the application of this method in extraction of phosphorylated peptides is under investigation. *In vitro* labelling is extremely useful if applied

to primary cells, like neutrophils, because it overcomes the current limit of stable isotopic amino acids in cell culture (SILAC), which is only available for cultured cells (Blagoev et al., 2003).

The quantitative mass spectrometry often used in clinical research is surface-enhanced laser desorption ionisation-time of flight (SELDI-TOF). It is a modified MALDI technique utilizing stainless steel or aluminum-based supports, or chips, engineered with chemical or biological bait surfaces. Solubilized tissue or body fluids are directly applied to these surfaces, where proteins with affinities to the bait surface bind. After washing off the non-specific binding, the bound proteins are laser desorbed and ionized for MS analysis. Masses of proteins ranging from 1000 Da to greater than 300 kDa can be calculated based on time-of-flight. As mixtures of proteins are analyzed within different samples, a unique sample fingerprint or signature will result for each sample tested. Consequently, patterns of masses rather than actual protein identifications are produced by SELDI analysis. These mass spectral patterns are used to differentiate patient samples from one another, such as diseased from normal. Thus, this technique is frequently used in clinical investigations to analyse differential biomarker expression. While protein fingerprints can be analyzed for differential biomarker expression, this technology is currently unable to specifically identify proteins within a sample using MS. However, coupling this technology with tandem mass spectrometers, will enable amino acid sequencing and subsequent protein identification (Merrick et al., 2003).

1.7.5. Proteomic studies in neutrophils

Despite its importance in early immune defence, the cytoskeleton associated with the membrane and phagosome in neutrophils is still largely uncharacterised, due to the fact that these cells are refractory to genetic manipulation by either transfection or microinjection (Weiner et al., 1999). Also, the molecules and mechanisms coordinating various steps involved in phagolysosome biogenesis are still mostly unknown. A significant part of our

ignorance originates from the fact that few of the phagosome proteins are currently known or studied, despite the presence of hundreds of proteins in this compartment. Most of our knowledge regarding the molecular mechanisms of phagocytosis has been derived from studies in macrophages. Desjardins et al analyzed the proteome of the phagosome in macrophages. In order to differentiate proteins exposed to the cytoplasmic side of the phagosome, from luminal proteins, intact phagosomes were treated with pronase. This protease degraded the proteins exposed on the cytoplasmic side of the phagosomes (Garin et al., 2001).

A proteomic analysis of neutrophil soluble granule proteins has identified 286 proteins on three granule subsets (Lominadze et al., 2005). Initially, when whole granule fractions were subjected to 2D electrophoresis, gels were dominated by large amount of luminal proteins such as lactoferrin and lipocalin and very few cytoskeletal proteins were revealed. Consequently, alkaline sodium carbonate lysis was used to separate membrane and luminal proteins, and ammonium sulphate precipitation of Triton X-100 insoluble proteins was applied to fractionation of the granule subset. Thus the granule membrane, specific granule and gelatinase granule proteins have been mapped. Overall, it provides a basis for understanding the role of granule exocytosis in neutrophil biology, which is involved of a variety of receptors, cytoskeletal membrane anchors, channels, transporters, GTPases, structural proteins, adaptors, kinases, phosphatases, luminal and host defense proteins, and proteins involved in membrane traffic and fusion (Boussa et al., 2000; Lominadze et al., 2005).

Piubelli and colleagues have produced a two-dimensional map of rat neutrophils thereby identifying 52 major proteins by utilizing both MALDI-TOF and electrospray quadrupole (Q)-TOF mass spectrometry (Piubelli et al., 2002). The proteomic analysis of a detergent-resistant membrane skeleton from bovine neutrophil plasma membrane provided the proteomic profile of the cholesterol-rich membrane fractions. On the basis of the results

obtained it was concluded that this fraction represents a membrane skeleton-associated subset of leukocyte signalling proteins (Nebl et al., 2002). A proteomic study of bovine neutrophils identified over 250 proteins using one-dimensional electrophoresis followed by reverse-phase chromatography in line with electrospray tandem mass spectrometry. This study provided an overview of the total proteome of bovine neutrophils (Lippolis et al., 2005).

Two-dimensional electrophoresis with tandem mass spectrometry has also been used to investigate mechanisms of maturation of neutrophils at the molecular level in a mouse promyelocytic cell line model (MPRO). These cells derive from murine bone marrow and are developmentally arrested at the promyelocytic stage due to the presence of a dominant-negative retinoic acid receptor. They morphologically differentiate to mature neutrophils in the presence of supraphysiological concentration of retinoic acid at 10mM and granulocyte/macrophage colony-stimulating factor (GM-CSF). GM-CSF induces the maturation of cells from the promyelocytic stage to neutrophils. Since it was observed that GM-CSF-induced neutrophil differentiation of uninfected cells requires physiological concentrations of retinoic acid, the differentiation block exhibited by the dominant negative retinoic acid receptor is probably due to inability of these cells to respond to the physiological concentration of retinoic acid present in the medium. However, this block can be overcome by supraphysiological concentration of retinoic acid (Lawson et al., 1998; Tsai et al., 1993; Lian et al., 2001). Comparing the protein patterns and mRNA expression at different time points after induction, this study resulted in identification of 29 new differentiation-associated proteins. This study provides the most comprehensive list of factors involved in neutrophil maturation, including 12 functional categories such as cytoskeletal proteins, metabolic-related molecules, signaling -related proteins, possible transcription factors, cytokines and others (Lian et al., 2001 and 2002).

A frequently used technique in proteomic clinical studies is surface-enhanced laser desorption-ionization-time of flight (SELDI-TOF) mass spectrometry, as described in the

previous section. Its main application is to identify biological markers (Buhimschi et al., 2005; Bannenberg et al., 2005; Albrethsen et al., 2005; Gronborg et al., 2004), quantitatively characterize the alterations in the expression of proteins that are secreted during the acute inflammatory response (Jayaraman et al., 2005), chemotaxis (Rane et al., 2005) and chronic inflammation (Sepper et al., 2004).

The other focus of neutrophil proteomic studies has been the identification of the changes in neutrophil proteome induced by their activation with bacterial lipopolysaccharide (LPS). Fessler and colleagues have found the up-regulation of 100 distinct genes among the 900 genes tested, including cytokines and chemokines, signaling molecules, and regulators of transcription after LPS stimulation. Some of these changes can be attenuated by inhibition of p38 MAPK. Thus the role of p38 was demonstrated in regulation of neutrophil transcripts and proteins following LPS exposure, and proteomic analysis yielded a list of up-regulated modulators of inflammation, signaling molecules, and cytoskeletal proteins (Fessler et al., 2002).

There are tens to hundreds of proteins involved in actin turnover in motile cells while only a small number of those are essential for protrusion. One of the major aims of current proteomic experiments is discovering novel proteins, which conventional biochemical, and molecular methods have not been able to find. The global analysis of cytoskeletal proteins is expected to provide a detailed knowledge of the cytoskeleton function in locomotion, degranulation and phagocytosis of neutrophils.

We hypothesise that a proteomic study of human neutrophil cytoskeleton at different subcellular compartments will provide the insight into the composition of the cytoskeleton in neutrophils. Proteins, which associate with a specific location, are likely to be found in this study, and thus provide a better understanding of that protein in that specific location. As cytosol and membrane are major compartments within the cell and the vacuole is the most dynamic structure produced upon phagocytosis. In order to analyse which protein presents in

the resting states of cytosol and membrane transmigrates to the phagocytic vacuole, we chose to examine the protein composition of cytoskeleton in these compartments (Fig 8).

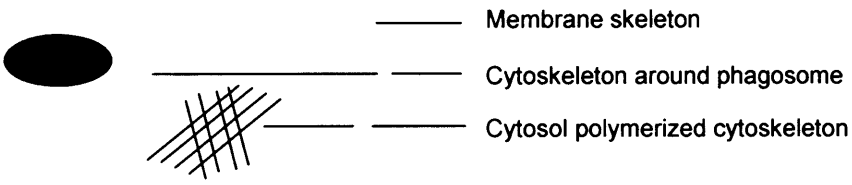

Fig 8. The diagram of the analysis of neutrophil cytoskeleton.
The cytoskeleton will be analysed in three compartments: cytosol polymerized structure, membrane skeleton and cytoskeleton around phagosome.

1.8. AIMS

The aims of the thesis were to analyse the composition of the neutrophil cytoskeleton, to investigate the possibility of the direct binding of grancalcin to actin filaments, and to define the function of the cytoskeleton-associated protein grancalcin.

CHAPTER 2

MATERIALS AND METHODS

2.1. MATERIALS

All chemicals were purchased from Sigma Chemical Co (Poole, UK) unless otherwise noted. Thioglycollate was purchased from MERCK (MERCK, Darmstadt, Germany). Immobilized pH gradient (IPG) buffers and strips were purchased from Amersham (Amersham Bioscience, Chalfont, UK). Non-muscle actin was purchased from Cytoskeleton Inc. (Denver, CO).

FITC-conjugated rat anti mouse CD49d (PS/2), FITC-conjugated rat anti mouse F4/80 (CI:A3-1), FITC (mouse absorbed) $F(ab')_2$ goat anti rat IgG (star 69) and PE-conjugated goat anti mouse IgG2b were purchased from Serotec Ltd (Oxford, UK). FITC labelled anti-mouse secondary antibody was purchased from Jackson Laboratory (Maine 04609, USA). Rat anti mouse integrin $\alpha_5\beta_1$ monoclonal antibody was from Chemicon International (Temecula, USA). R-Phycoerythrin (R-PE)-conjugated rat anti-mouse Ly-6G and Ly-6C (Gr-1) monoclonal antibody was purchased from BD Biosciences Pharmingen (Oxford, UK). Anti MyC (9E) monoclonal antibody was obtained from Santa Cruz (Santa Cruz, CA) and FITC-labelled donkey anti-mouse secondary antibody was from Jackson Laboratory (Bar Harbor, ME). Mouse anti-IQGAP1 monoclonal antibody was from Transduction Laboratory (Lexington, KY40511). Rabbit anti-Valosin-containing protein polyclonal antibody was from Dr. N. K. Tonks (Cold Spring Harbor Laboratory, Cold Spring Harbor, NY). The hybridoma cell lines produced antibodies against mouse integrin β_1 and β_2 were from Dr. S. Broad (Cancer Research UK, Lincoln's Inn Fields Laboratories, London, United Kingdom). Antiserum to grancalcin raised in Prof. Segal's laboratory (Teahan et al., 1992). Briefly, grancalcin (100μg in 20mM Tris/HCl, pH7.3) was emulsified in equal volume

of Freund's complete adjuvant (FCA) and injected subcutaneously into rabbits. The rabbits were boosted with 40μg and 10μg of proteins in Freund's incomplete adjuvant (FIA) at 3 weeks and 5 weeks later respectively. High-titration antisera were present by day 45.

2.1. Concentrations and storage conditions of protease inhibitors

	Stock conc.	Working conc.
DIFP	1M in isopropanol	1 mM
TLCK	10mg/ml in ddH_2O	10μg/ml
Pepstatin A	10mg/ml in ethanol	10μg/ml
Leupeptin	10mg/ml in ddH_2O	10μg/ml
PMSF	2mM in ethanol	2μM

DIFP was added directly to cell pellets as it is hydrolysed in aqueous solutions and penetrates into cells.

2.2. CELL BIOLOGY

2.2.1. Preparation of neutrophils

Neutrophils were isolated from freshly drawn heparinised blood from healthy donors, buffy coats (anti-coagulated blood depleted of plasma), or buffy coat residues (buffy coat depleted of platelets) (North London blood service). The method was as described by Segal and Jones (Segal and Jones, 1980). Buffy coats or buffy coat residues were diluted 1:1 with 0.9% saline; 10% dextran dissolved in saline (0.9% NaCl) was added to the blood to give a final concentration of 1%. The mixture was allowed to settle in a tall, narrow measuring cylinder for 45 minutes at room temperature to sediment erythrocytes. The upper plasma layer containing leukocytes was then layered over a cushion of $1/10^{th}$ of the volume of Lymphoprep (Nycomed) and centrifuged at 900x g for 10min at room temperature (RT) in a bench top AllegraTM 6R centrifuge with swing-out buckets. The supernatant was discarded and the erythrocytes in the pellet at the bottom of the tube were lysed by resuspending the cells in

water for a few seconds after which the tonicity was restored by adding an equal volume of 2 x saline (1.8% NaCl). Neutrophils (95% pure as assessed by Giemsa staining) were finally pelleted by centrifugation at 500x g for 3min at RT. The cells were resuspended in phosphate-buffered saline containing 5mM glucose and counted using a microscope haemocytometer.

2.2.2. Preparation of postnuclear supernatant (PNS)

Neutrophil lysate was prepared by sonication or homogenised using a Dounce homogenizer. In brief, 1mM DIFP (final concentration) was added to the cell pellet and incubated for 10min. Cells were then resuspended in break buffer (10mM KCl, 3mM NaCl, 4mM $MgCl_2$, 10mM Pipes, pH7.2) containing protease inhibitors (100μg/ml TLCK, 100μg/ml Pepstatin A, 100μg/ml Leupeptin and 20μM PMSF). Cells were either sonicated with Soniprep 150 (MSE, Sanyo, Japan) by 3x5 second bursts at 15 amplitude microns on ice or homogenised in a 15ml tight fitting Dounce homogeniser with 100-150 strokes, and centrifugated at 400x g for 15min at 4°C. The postnuclear supernatant, was collected and the pellet containing unbroken cells and nuclei was discarded.

2.2.3. Preparation of neutrophil cytoskeletal fractions

2.2.3.1. Neutrophil cytosol high-speed pellet

Purified neutrophils ($1x10^9$) were disrupted by nitrogen cavitation in break buffer (10 mM KCl, 3 mM NaCl, 4 mM $MgCl_2$, 10 mM PIPES, pH 7.2) containing protease inhibitors: Leupeptin 10 μg/ml, pepstatin 10 μg/ml, tosyl-lysine-chloromethyl ketone 10 μg/ml and 2 μM Phenylmethylsulfonyl fluoride (PMSF). Postnuclear supernatant (PNS) was prepared by centrifugation at 400x g for 10 minutes at 4°C. The PNS was layered over a discontinuous gradient of 15%, 34% and 55% sucrose (w/w) and centrifuged at 100,000x g for 20 minutes at 4°C. Under these conditions membranes settle at the interface of 15%-34% sucrose while

granules accumulate at the interface of 34%-55% sucrose. The membrane fraction was used for the isolation of membrane skeleton as explained below, while the granules were discarded. The cytosol above 15% sucrose was recentrifuged at 420,000x g for 30 minutes to obtain a high-speed pellet.

2.2.3.2. Triton-insoluble membrane

Membrane was prepared from the postnuclear supernatant as described in 2.2.3.2. The interface between 15%-34% sucrose was collected and centrifuged at 250,000x g for 30 minutes at 4°C. The pellet was extracted by Triton in 2ml of 1% Triton, 25mM HEPES, 10mM EGTA and 2mM $MgCl_2$, pH6.8. After 15 minutes incubation on ice, the extract was layered over 1ml of extraction buffer containing 6% sucrose and centrifuged at 250,000x g for 30 min in a Beckman ultracentrifuge. The Triton insoluble fractions of the membrane were recovered from the pellet.

2.2.3.3. Detergent insoluble phagocytic vacuolar proteins

Unlike most approaches relying on the isolation of organelles based on their intrinsic density, isolation of latex bead–containing phagosomes is facilitated by the low buoyant density of latex. Thus, phagosomes are floated in a region of the sucrose gradient where other cellular organelles are not detected. Previous morphological and biochemical analysis of latex bead phagosome preparations indicated the virtual absence of contamination by mitochondria, Golgi vesicles, endosomes, and the plasma membrane (Segal et al., 1980; Garin et al., 2001). The experimental procedure is as described (Segal et al., 1980). Briefly, The latex beads (0.81μm) were coated with IgG by incubating 1.0 ml of the particles with 0.2 ml of IgG in 0.1M Tricine buffer with pH 8.5 at 37°C for 30 mins. The beads were then centrifuged at 8000x g for 2 min and washed three times with PBS and resuspended in PBS at the desired concentration. The neutrophil suspension ($2x10^8$/ml) was rapidly stirred with a magnetic

stirring rod in a thermostatically controlled (37°C) chamber above an oxygen electrode, and allowed to equilibrate for 2 min. Latex beads were mixed with neutrophils at a bead: cell ratio of 100:1. After 4 min incubation, phagocytosis was stopped by adding 5 volumes of ice-cold PBS to the suspension. The mixture was centrifuged at 75x g for 10min at 4°C, and the pellet then suspended in 10ml of 11.2% (w/w) sucrose in break buffer (10mM KCl, 3mM NaCl, 4mM $MgCl_2$, 10mM PIPES and protease inhibitors 1mM DIFP, 10μg/ml leupeptin, 10μg/ml pepstatin A, 2μM PMSF and 10μg/ml TLCK) and centrifuged again at 75x g for 10 min at 4°C. The pellet was resuspended in 10ml of 11.2% sucrose in break buffer and homogenized in a 15ml Dounce homogenizer (Scientific Laboratory Suppliers, Nottingham NG11 7EP) with a tight-fitting pestle. After 100-150 strokes, the cell lysate was centrifuged at 1,000rpm for 10 min at 4°C. 5 ml of postnuclear supernatant was then mixed with 12 ml of 60% sucrose and placed at the base of a 50ml Sorvall centrifuge tube, overlaid with 20ml of 33% and then 5.0ml of 11.2% sucrose, and centrifuged at 18,000x g for 20min at 4°C in a Sorvall RC5B centrifuge with an SS34 angle rotor. Phagocytic vacuoles at the interface between the 11.2% and 33% sucrose were collected and diluted with ice-cold break buffer to maintain a concentration of 11.2%. The vacuoles were then pelleted by centrifugating for 30 min at 12,700x g at 4°C. The pellet was resuspended in 20% sucrose and sonicated gently for three times and for three seconds each to break, and the vacuoles laid under 11.2% (w/w) sucrose and centrifuged at 125,000x g for 20 min at 4°C. The pellet was extracted with break buffer containing 1% Triton for 15 min and pelleted again at 415,000x g for 30 min at 4°C. All the solutions contained 1mM EDTA and 5u/ml heparin with protease inhibitors.

The schematic illustration of the extraction procedures of neutrophil cytoskeleton as described above is in Fig 9.

2.2.4. Induction of sterile peritonitis and isolation of murine neutrophils

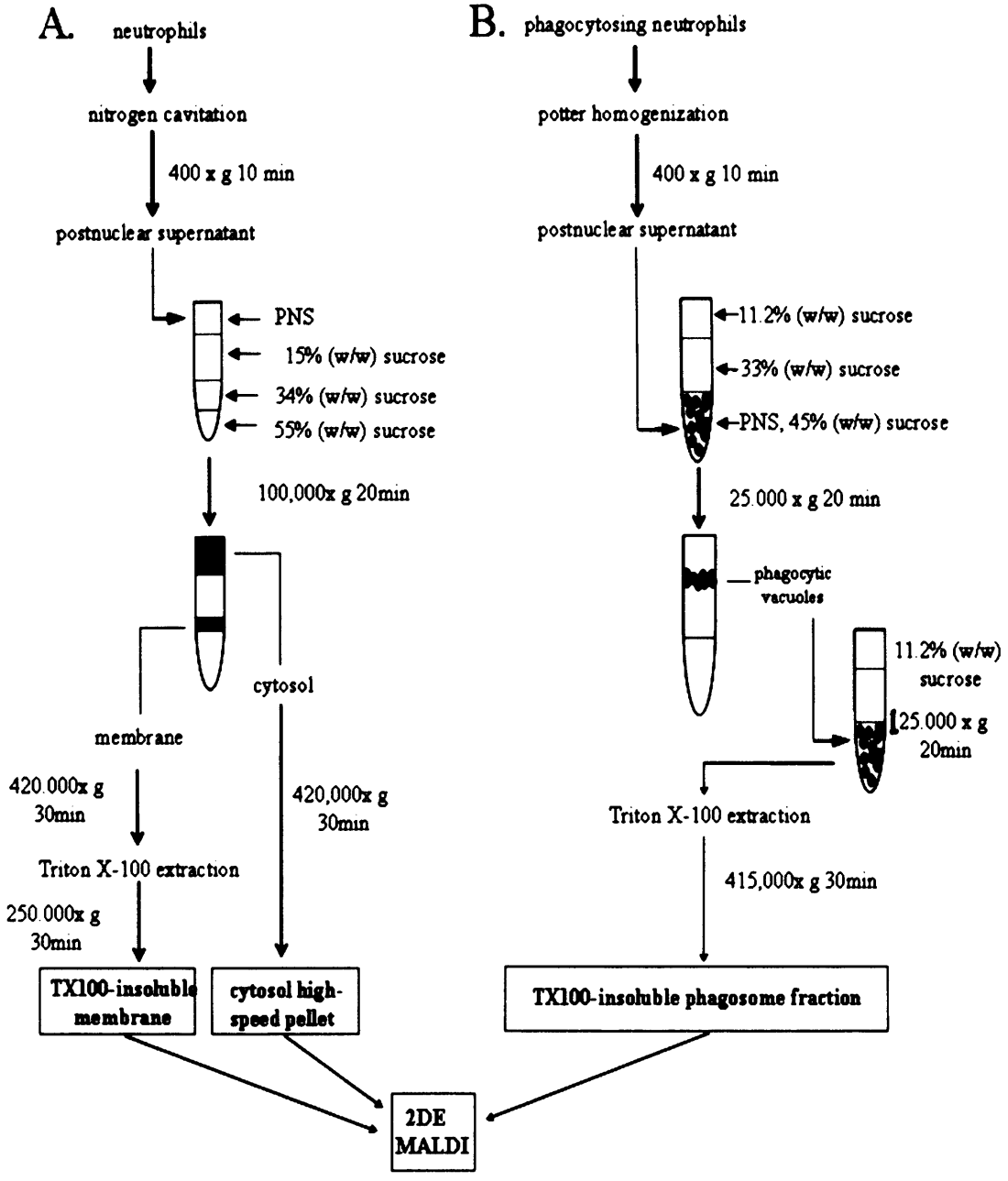

Fig 9. The schematic illustration of the extraction of neutrophil cytoskeleton fractions from cytosol high speed pellet, Triton X-100 insoluble membrane and Triton X-100 insoluble phagosome.

Cells were disrupted either by nitrogen cavitation or Dounce homogenization. Subcellular fractions were then separated on sucrose gradients and centrifugation as illustrated.

Three percent thioglycollate broth solution was boiled to reduce the amount of oxygen dissolved, and autoclaved. It was injected intraperitoneally at 0.7ml/20g of body weight. Animals were sacrificed by CO_2 asphyxiation, and peritoneal exudate cells were recovered by peritoneal lavage with 5 ml of PBS with 5μg/ml heparin at different time points.

The lavages were centrifuged and resuspended in 1ml of PBS, and laid on top of 55% and 60% Percoll in PBS. Cells were then centrifuged at 1,250x g for 20min. The neutrophils localised to the interphase between 55% and 60% Percoll. Neutrophils were collected and washed with PBS. Cells were then resuspended in 1ml of PBS and counted.

Bone marrow neutrophils (BMNs) were obtained by density gradient centrifugation using a modification of previously described techniques (Kim et al., 2001; Lowell et al., 1996). Briefly, BMNs were isolated from the femurs and tibiae by flushing them with 3ml PBS supplemented with 5.5mM glucose and 5μg/ml heparin using a 22-gauge needle. Cells were pelleted by centrifugation at 300x g for 10minutes. Contaminating erythrocytes were removed by suspending the BM cells in red blood cell lysing buffer for 2 min at room temperature and washed with PBS.

2.2.5. Measurement of oxygen consumption and superoxide production

Oxygen consumption was measured with a Clark oxygen electrode (Dual digital model 200, Rank Brothers Ltd, Cambridge, UK). For reference, 1ml of H_2O was added to a rapidly stirred, thermostatically controlled (37°C) chamber above the electrode, warmed up for 2 min, then several granules of sodium dithionite were added to reduce all the oxygen in the solution. The correlation of O_2 was taken as 220nmol O_2/ml H_2O. To measure NADPH oxidase activity, 1 ml of neutrophils at density of $2x10^7$ cells/ml was stimulated with $1x10^9$ IgG opsonised *Staphylococcus aureus*. The sample chamber was closed immediately and the measurement was recorded.

Production of superoxide by $1x10^6$ neutrophils was measured by superoxide dismutase (SOD) inhibitable reduction of cytochrome C after stimulation with PMA or A23157 using a Shimadzu UV-3000 dual beam spectrophotometer at 37°C (Metcalf et al., 1986). The neutrophils were added to both the reference and test cuvettes with cytochrome C in PBS with Ca^{2+} and Mg^{2+}, SOD was then added only to the reference cuvette. After the stimulatants were added, superoxide production was measured by the changing absorbance of cytochrome C at 550nm taking absorption coefficient at $21.1mM^{-1}cm^{-1}$ (Van Gelder & Slater, 1962).

2.2.6. Phagocytosis assay

Neutrophils from peritoneal lavages of wild type and the grancalcin deficient mice were purified as described before. Fluorescein isothiocyanate (FITC) was used to attach a fluorescent label via the amino group to bacteria (labelled according to manufacturer's instructions). *S.aureus* were heat-killed at 70°C for ten minutes and resuspended in 0.1 M sodium carbonate buffer, pH 9.0. For each 1 ml of protein solution, continuously stirred 50µl of 1 mg/ml FITC in anhydrous DMSO was added. After the required amount of FITC solution has been added, the reaction was incubated in the dark for an hour at 37°C. The unbound FITC was separated from the conjugated by extensive washing in PBS. Labelled *S.aureus* were then incubated with 5µg/ml fibronectin for an hour at 37°C and washed with PBS. Fibronectin-*S.aureus* were then added to the neutrophil suspension at a 37°C via stirred chamber at a ratio of 10:1. Aliquots were taken from the chamber at time point 0, 2min, 4min, 8min and 16min and put into ice-cold 4% paraformaldehyde in PBS to stop the reaction and fix the sample. The samples were then analysed using a FACScalibur flow cytometer (Becton Dickinson, Franklin Lakes, NJ, U.S.A).

2.2.7. Adhesion assay

200μl of vitronectin (Promega) at a concentration of 10μg/ml and fibronectin at a concentration of 5μg/ml were added to the glass coverslip of MeTek dishes and left at 4°C overnight or 2hr at RT. Collagen, laminin and fibrinogen slides were purchased from Sigma. After coating, the dishes were washed 3 times with PBS. 200μl of neutrophils at a density of $2x10^6$/ml were put onto the matrix coated dishes, slides or coverslips and incubated at 37°C for 30min. After incubation, the dishes were washed 3 times with 37°C PBS and fixed with warm 3.7% formaldehyde in PBS. Images were taken from at least ten random chosed fields for each sample by a light microscopy (40x).

2.2.8. Immunofluorescence

Neutrophils were fixed with warm 3.7% formaldehyde (37°C) in cytoskeletal buffer (5mM KCl, 137mM NaCl, 4mM $NaHCO_3$, 0.4mM KH_2PO_4, 1.1mM Na_2HPO_4, 2mM $MgCl_2$, 5mM PIPES pH7.2, 2mM EGTA, 5.5mM Glucose, pH6.0-6.1) at 37°C for 5min. After fixation, cells were extracted with 0.5% Triton X-100 in cytoskeletal buffer at room temperature for 20min and then blocked with 0.1M glycine in cytoskeletal buffer for 10min. After blocking, cells were rapidly washed 5 times with Tris buffered saline (TBS) (20mM Tris pH 8.0, 150mM NaCl), and incubated with TBS containing 1% BSA, 1% FCS, 0.5μM Alex 488-Phalloidin or TRITC-Phalloidin for 20min at RT. Phalloidin binds stoichiometrically to actin subunits in filaments, stabilizing them against conditions that would normally depolymerize them, especially below their critical concentration (Carraway et al., 1992). After F-actin staining, cells were washed 5 times with TBS for 5min each.

After TRITC-phalloidin staining in transiently transfected COS-7 cells, anti-MyC monoclonal antibody at concentration of 1:100 (Santa Cruz) was added and incubated at RT for 1hr and washed 5 times with TBS containing 1%BSA. After washing, the cells were

incubated with FITC labelled anti-mouse secondary antibody at 1:50 (Jackson Laboratory) at RT for 1hr.

For nucleus staining, cells were stained with 0.5μg/ml of 4'6-diamidino-2-phenylindole (DAPI) for 10 min at room temperature in the dark.

For staining of grancalcin, the antibody against human grancalcin was diluted to 1:50 in TBS containing 1% BSA and incubated at RT for 1hr. After cells were washed 5 times for 5 min each with TBS containing 1% BSA. Cells were then incubated with FITC labelled donkey anti-rabbit (1:50) in TBS containing 1% BSA at RT for 1hr and washed with TBS.

The slides were mounted with TBS containing 50% glycerol, 0.02% sodium cyanide, 6g/l N-propyl gallate.

Images were taken on a BioRad fluorescence confocal microscope using 40x, 60x or 100x objectives, and processed using Photoshop.

2.2.9. Electron microscopy

5 x10^8 *S. aureus* was opsonised with 0.2mg murine IgG at 37°C for an hour and washed three times with PBS. To assess the morphology and degranulation difference between neutrophils from wild type and grancalcin-deficient mice, 5x10^7 cells from bone marrow were mixed with 5x10^8 IgG-opsonized *S.aureus* in a stirred chamber at 37°C. Aliquots were taken at 0, 40 seconds, 90 seconds and 4 minutes into a fixative containing 1.5% glutaraldehyde, 0.1% picric acid in sodium cacodylate buffer (0.1M, pH7.2). They were postfixed in osmium tetroxide, dehydrated in ethanol and embedded in araldite. Sections were applied to the copper grids, contrast-stained with uranyl acetate and lead citrate and viewed at a maginification of x 16,000. In order to measure degranulation, the electron-microscopy negatives were projected through a microfilm reader. The profiles were traced and measured on prints using a digitising tablet connected to a computer running SigmaScan software (Jandel Scientific, Corte Masera, CA) for quantitative measurement. Only the volumes of

neutrophils that were judged to have been sectioned in the region of maximum width were measured and the numbers of granules were counted.

2.2.10. Flow cytometry

To measure the granulocyte population in the peritoneal cavity, the peritoneal lavages were stained with Gr-1 (Ly-6G) and F4/80 antibody. Stained cell populations were analysed with a FACScan flow cytometer (Becton Dickinson, Inc., Mountain view, Calif.).

To measure the surface integrin expression on granulocytes, granulocytes from the peritoneal lavage ($2x10^5$) were incubated for 10 minutes at room temperature in 5% mouse serum and then incubated in FACSwash (TBS/0.2% BSA) containing primary antibodies at the desired concentrations. After an hour at room temperature, the cells were washed three times and resuspended in FACSwash buffer (TBS, 0.2% BSA and 0.01% Sodium Azide) containing FITC-conjugated goat anti-rat IgG at a dilution of 1:50. After an hour at room temperature, the cells were again washed, resuspended in 100ul FACSwash buffer and analyzed using a FACSCalibur (Becton Dickinson) with CellProquest software.

2.3 PROTEIN BIOCHEMISTRY

2.3.1. Protein precipitation

2.3.1.1. TCA-ether precipitation

10% TCA was added to protein samples and kept on ice for an hour. The samples were then centrifuged at 18,000x g for 10 min. The pellet was washed once with 10% TCA for 10 min on ice. The pellet was resuspended in ice-cold ether/ethanol (1:1, v/v) and mixed for 30 minutes at room temperature with agitation and spun again at 18,000x g for 5 min. The ether/ethanol wash was repeated once and the pellet was dried on the bench for no longer than 5 min. The pellet was then resuspended in the urea buffer containing 8M urea, 2M

thiourea, 4% CHAPS, 1% Triton, 65mM DTT, 10mM Tris base, 0.8% Ampholyte and protease inhibitors.

2.3.1.2. TCA-acetone precipitation

Protein samples were precipitated by adding ice-cold 60% TCA to make the final concentration 10%. Samples were mixed and incubated on ice for 30 minutes and spun for 10 minutes at 15,000x g at 4°C. The protein pellet was washed once with ice-cold 10% TCA and 4 times with ice-cold 80% acetone and then resuspended in the urea sample buffer as 2.3.1.1.

2.3.1.3. Acetone precipitation

Three volumes (minimum) of acetone at –20°C were added to the samples and incubated at –20°C from 2 hours to overnight, then spun at 15,000x g for 10min in a microfuge at 4°C. The pellet was air-dried and resuspended in the appropriate volume of urea sample buffer as 2.3.1.1.

2.3.2. Protein concentration assays

2.3.2.1. Reducing agent compatible (RC) detergent compatible (DC) assay

The protein concentration of samples in SDS sample buffer was measured by RC DC assay (Bio-Rad) following the manufacturer's instructions. It is based on the Lowry assay but has been modified to be compatible with reducing agents as well as detergents. The protein concentration was obtained from a standard curve using BSA which was made up with the same buffer as the protein sample. 3-5 dilutions of protein standard from 0.2mg/ml to 1.5mg/ml were prepared. 125µl RC reagent I and II were added to the standard and protein samples and centrifuged at 15,000x g for 3-5 minutes at room temperature. The supernatant was drained completely from the tube. Reagent A' which was composed of DC reagent S and DC reagent A was added to each microfuge tube, vortexed and centrifuged. Finally, DC

reagent B was added to each tube and incubated for 15 minutes. The absorbance was read at 750nm.

2.3.2.2. Modified Bradford assay—compatible with IEF buffer

The protein concentration of samples in IEF buffer was measured using the modified Bradford assay to make it more linear and more compatible with the detergent (Ramagli et al., 1999; Zor et al., 1996). In this assay, HCl at 0.2N was used to dilute IEF buffer. Various concentrations of BSA and protein samples were then diluted in this buffer. The ratio of OD at 595_{nm} and 450_{nm} was measured and the protein concentration was calculated from the BSA standard curve.

2.3.3. Electrophoresis of proteins

2.3.3.1. One dimensional polyacrylamide gel electrophoresis

Sodium dodecyl sulphate polyacrylamide gel electrophoresis (SDS/PAGE) was carried out using standard Laemmli methods, with 30% (w/v) acrylamide/ 0.8% (w/v) bisacrylamide solution (Protogel, National Diagnostics) at a final concentration of 8.0-15.0% acrylamide, depending on protein size and required resolution. Hoefer Mighty Small II apparatus was used for electrophoresis at ~25mA per gel. Molecular weight standards were from Bio-Rad or Pharmacia and gels were stained with Commassie-blue R-250.

2.3.3.2. Two dimensional polyacrylamide gel electrophoresis (2D-PAGE)

2.3.3.2. 1st dimension: Isoelectric focusing (IEF)

Table 3.1. Focusing programme for 13cm IEF strips (A) and 7cm IEF strips (B)

A

Step	Voltage	Volthours(Vh)	Gradient type
1	30	330	Step-n-hold
2	3000	1500	Step-n-hold
3	4000	4000	Step-n-hold
4	6000	60000	Step-n-hold

B

Step	Voltage	Volthours(Vh)	Gradient type
1	30	360	Step-n-hold
2	250	113	Step-n-hold
3	500	188	Gradient
4	500	500	Step-n-hold
5	1000	750	Gradient
6	1000	2000	Step-n-hold
7	3500	6750	Gradient
8	3500	50750	Step-n-hold

7cm or 13cm isoelectrofocusing strips (IPG) pH range 3-10NL (increased resolution between pH 5-7, 4-7 or 5-8 were used). The strips were rehydrated with the sample in rehydration buffer (8M urea, 2M thiourea, 4% CHAPS, 1% Triton X-100) overnight, and covered with mineral oil to prevent the sample from drying. After rehydration, isoelectric focusing was performed in Ettan IPGphor isoelectric focusing system (Amersham Biosciences UK). Time and voltage protocols for isoelectric focusing in the IPGphor system are given in table 3.1. After the first dimension, the IPG strips were either kept at –70°C or used immediately for the second dimension.

2.3.3.2. 2nd dimension: SDS-PAGE

After the first dimension, the IPG strips were rinsed with electrophoresis buffer and the excess buffer was drained on a piece of filter paper. The strips were then first equilibrated with 2% DTT in equilibration buffer (50mM Tris-HCl, pH8.8, 6M Urea, 30% (v/v) Glycerol, 2% (w/v) SDS, 0.002% (w/v) Bromophenol blue) for 20 min and then 4.5% iodoacetamide in equilibration buffer for another 20 min. After a brief wash in electrophoresis buffer, the edges of the strips were cut and the strips were placed on top of a polyacrylamide gel. Molecular weight markers were loaded onto a piece of filter paper and placed onto the acidic region of the IPG strip above the polyacrylamide gel. The plastic back of the strip was pushed and adhered to the glass plate. The strip and the markers were overlayed with 0.5% agarose in

stacking buffer with a trace of bromophenol blue. Electrophoresis was run at a constant voltage of 200V for approximately 5 hours or 40V overnight at 20°C. The gel was then stained with silver (detailed procedure in 2.3.5).

2.3.4. Western blotting

Western blotting was performed using a semidry blotter for 1 hour at 1.4mA/cm^2 using reinforced nitrocellulose membrane (Amersham). Membranes were stained with Ponceau (0.5% Ponceau in 3% TCA solution, Sigma) and destained with ddH_2O. Non-specific binding was blocked with 5% milk powder and/or 1% BSA in TBS/0.05% Tween for an hour at room temperature. Membranes were then probed with different primary antibodies diluted in blocking buffer either for one hour at room temperature, or 4°C overnight. After four washes in TBS/Tween for 15 minutes each, the membranes were incubated with horseradish peroxidase-conjugated secondary antibody diluted in blocking buffer for an hour at room temperature. After four washes with TBS/TWEEN at 15 minutes intervals, the blots were developed using an enhanced chemiluminescence method (ECL plus, Amersham).

2.3.5. Silver staining of polyacrylamide gels

The procedure was as described by Shevchenko (Shevchenko et al., 1996). The gel was fixed in 50% methanol and 12% acetic acid for at least 2 hours, and then washed with 50% methanol three times at 20 min intervals. After sensitisation with 0.02% sodium thiosulfate for 1 min and a brief wash with deionized water, the gel was treated with 0.1% silver nitrate for 20 min and again briefly washed in deionized water. The gel was then developed with 3% sodium carbonate, 0.0002% sodium thiosulfate and 0.0093% formaldehyde. When the protein spots developed a dark brown colour, the gel was rinsed twice in distilled water. The development of the stain was stopped by immersing the gels in

12% acetic acid and 50% methanol for 10 min. The gel was washed in 50% methanol and stored in 5% methanol and 4% glycerol.

2.3.6. In-gel tryptic protein digestion

For one-dimension SDS-PAGE Commassie stained gels, the protein bands of interest were cut out of the gel, destained with 40% ethanol in 50mM NH_4HCO_3 overnight and cut into 1mm cubes. The gel pieces were then soaked in 20ul of 25mM NH_4HCO_3 for 15 minutes and this step was then repeated for a further 15 minutes or until the pH reached 7-8. The buffer was removed and 25ul of acetonitrile was added for 10 minutes, and this step was repeated until the pieces of gel turned white and clumped together. The gel cubes were dried in a Speedvac (Savant, TeleChem International, Inc, Sunnyvale, CA USA) for a few minutes, then 2.5-5ul of trypsin gold (mass spectrometry grade) at a concentration of 40ng/ul in 50mM NH_4HCO_3 was added. After approximately 15min, when the liquid was absorbed by the gel pieces, 10-15ul of 50mM NH_4HCO_3 with 10% Acetonitrile was added to cover them. The digests were then incubated at 30°C overnight.

For silver stained gels, protein spots were excised from the gel, and processed automatically by Progest (Genomic Solutions, Huntingdon, United Kingdom). Briefly, gel pieces were soaked in 50 mM NH_4HCO_3 and dehydrated with acetonitrile, then reduced by 10 mM DTT and alkylated with 100 mM iodoacetamide. Dried gel pieces were rehydrated with 3 µl of 30 ng/µl solution of sequencing grade porcine trypsin (Promega) in 50mM NH_4HCO_3 buffer for 15 minutes. An additional 9 µl of 50 mM NH_4HCO_3 was added thereafter and digestion was carried out at 30°C overnight.

2.3.7. Mass spectrometry

2.3.7.1. Matrix-assisted Laser Desorption Ionization-Time of flight mass spectrometry (MALDI-TOF MS) Analysis

0.5µl of the tryptic digest was applied to the target plate and allowed to air-dry, then 0.5 µl of a saturated solution of α-cyano-4-hydroxycinnamic acid in 33% acetonitrile and 0.1% TFA (v/v) was overlaid. In the case of low abundant proteins, the tryptic digest was concentrated by Zip tip as instructed by the manufacturer (Millipore, Gloucestershire, UK) ZipTip® pipette tip is a 10 µl pipette tip with a bed of chromatography media fixed at its end. It is intended for concentrating and purifying peptide, protein or oligonucleotide samples. 100% TFA was added to the protein digestion to the final concentration of 0.1-1.0%. The ZipTip was preweted with wetting solution containing 100% acetonitrile and equilibrated with 0.1%TFA in distilled water. Samples were aspirated to the tip. The tip was washed with 0.1% TFA in distilled water and eluted in a solution containing 0.1% TFA and 50% acetonitrile in 4ul.

Mass spectra of the tryptic digests were obtained by using an Autoflex MALDI-TOF mass spectrometer (Bruker Daltonics, Billerica, MA) and calibrated with a mixture of seven known peptides: human argiotensin I and II, adrenocorticotropic hormone, glu-fibrinopeptide B, rennin substrate tetradecapeptide, ACTH and insulin β chain.

After a mass list of peptides was obtained for each protein digest, the peptide mass fingerprint was processed using four different search engines (Mascot at *www.matrixscience.com*, MS-Fit at *http://prospector.ucsf.edu/ucsfhtml3.4/msfit.html*, Pepident at *www.expasy.ch/tools/pepident.html* and ProFound at *www.prowl.rockefeller.edu/cgi-bin/ProFound)* and analysed by comparing against two separate databases (National Centre for Biotechnology Information 'NCBI' and SwissProt). Peptide mass fingerprinting used the assumption that peptides are monoisotopic, oxidized at methionine residues, and carbamidomethylated at cysteine residues (Castegna et al., 2002).

Additional criteria were considered to positively identify a protein from its tryptic peptide mass fingerprint. The most important was the coverage of the full-length protein and number of matched peptides. When the coverage exceeded 20%, it was considered to be

sufficient unless there were some obvious conflicts such as discrepancies between the experimental molecular weight and that of the identified protein. Between 15% and 20% of coverage, the identification was only considered valid if confirmed by three different search engines: Mascot, PepIdent and MS-Fit. The minimal requirement for the number of peptides matched was five. The mass accuracy of our analysis was usually set at 100ppm. The probability of a match being correct is calculated using the MS data subtracting the background information.

2.3.7.2. Automatic mass spectrum collection

If the spectra were collected automatically, Xmass software under "fuzzy logic" control was used (Bruker Daltonik GmbH, 2001). The maximum of consecutive rejected trials before moving on to the next sample was 30, the criteria used was that the signal to noise ratio was at least 3 within the m/z range 800-3000. Bruker's Xtof 5.1.1 software was used to process the spectra. The spectra were internally calibrated using trypsin autolysis peaks 842.509, 1045.564 and 2211.104, thereafter the baseline was subtracted and monoisotopic mass data extracted. The data were subsequently analysed using Bruker Biotools software in conjunction with the Mascot search engine using the NCBI database. The tolerance for errors was 50 ppm, the number of allowed missed cleavages was 1, oxidation of methionine allowed as a variable modification and cysteines modified with Iodoacetamide. The sample was classified as "certain" if significant ($p<0.05$) and unique, "uncertain" if significant but not unique and "Undefined" if not significant. All samples defined as "uncertain" or "undefined" were recollected and analysed manually.

2.3.8. Actin binding assay

2.3.8.1. Expression and purification of recombinant Grancalcin

Recombinant grancalcin was expressed by using pGEX-2T vector (GST gene fusion system) (2.4.5.). GST-fusion protein binds to glutathione Sepharose and can be eluted by the reduced form of glutathione. pGEX-2T-grancalcin was transformed into BL21 and plated onto a LB agar plate containing 100 μg/ml of ampicillin. The plate was incubated at 37°C overnight. A single clone was picked and inoculated into 50ml of LB containing 100 μg/ml of ampicillin at 37°C overnight with vigorous shaking. The overnight cultures were diluted to 4 L of defined media containing 3.5g/L K_2HPO_4, 5g/L KH_2PO_4, 3.5g/L $(NH_4)_2HPO_4$, 10g/L Yeast extract, 10g/L glucose, 0.5g/L $MgSO_4.6H_2O$ and 100ug/ml ampicillin. The culture was left to grow at 37°C until O.D.600 =0.6~1 (2-3hrs), protein expression was then induced by adding IPTG (Calbiochem) to give a final concentration of 0.5mM and incubated at 30°C for an additional 5 hrs. Cells were harvested by centrifugation at 2,500 x g for 15 min and kept at -20°C until further use.

To purify recombinant grancalcin, bacteria from a 1L culture were resuspended in 20ml of 50mM Tris, pH8.0, 150mM NaCl and lysed by adding 20ml of 50mM Tris, pH 8.0, 150mM NaCl, 2mg/ml of lysozyme at 4°C for 45min. The cell lysate was homogenized in a Dounce homogenizer with ten strokes and then centrifuged at 28,500x g for 30min, and the supernatant was carefully removed and incubated with 1ml of glutathione-Sepharose beads (50% slurry, pre-equilibrated with 5 beads volumes of TBS, pH8.0) at 4°C for 30min. The beads were washed with 50mM Tris, pH8.0, 150mM NaCl. Grancalcin was eluted with 10mM reduced form of glutathione in 100mM Tris, pH8.0, 150mM NaCl. Eluates were collected and dialysed against 10mM Tris, pH 8.0, 50mM NaCl and 1mM EDTA overnight. 10μl of the sample was taken for SDS-PAGE analysis.

2.3.8.2. High speed and low speed co-sedimentation

Ultracentrifuge tubes and microcentrifuge tubes were siliconized with 1ml Sigmacote (SIGMA) for 1 min. The solution was then removed. The tubes were dried in a flow hood for an hour. The tubes were then washed three times with ddH_2O and dried. Non-muscle actin (1mg, Cytoskeleton) was reconstituted in 100µl water at 4°C for 1hr, and diluted to 2.5mg/ml with G-buffer (5mM Tris, pH 8.0, 0.2mM $CaCl_2$, 0.2mM ATP, 0.5mM DTT) and dialysed against G-buffer overnight. Grancalcin was dialysed against 10mM Tris, pH8.0, 100mM NaCl and 1mM EDTA overnight. After dialysis, proteins were cleaned by centrifugation at 375,000x g for 20min. Protein concentration was measured using a Spectrophotometer (GST E_{280}=52 $mM^{-1}cm^{-1}$, GST-grancalcin E_{280}=78 $mM^{-1}cm^{-1}$, Actin E_{290}=27 $mM^{-1}cm^{-1}$).

F-actin was polymerised by adding $1/10^{th}$ of the volume of 10x F-buffer (20mM $MgCl_2$, 1M NaCl, 10mM EGTA or 0.2mM $CaCl_2$) to 30µM G-actin and kept at RT for 2hr. 5µM of F-actin was then mixed with 5µM grancalcin or 5µM of GST in siliconised tubes and incubated at RT for 30min. After incubation, the samples were split into two, and centrifuged at 375,000x g for 20min or 15,000x g for 5min at RT respectively. After centrifugation, the supernatant was carefully removed and 12.5 µl 5x sample buffer was added. The tubes were rinsed with F-buffer. After the wash, 62.5 µl of hot 1x sample buffer was added to the tubes to dissolve the pellet. Samples were then heated at 95°C for 5min, 10 µl of each sample were resolved by SDS-PAGE. To determine the stoichiometric binding curve of grancalcin and F-actin, 5µM of F-actin was then mixed with different concentrations of grancalcin and high-speed and low-speed co-sedimentation assays performed.

2.4. MOLECULAR BIOLOGY

2.4.1. Agarose gel electrophoresis

DNA separation was performed by agarose gel electrophoresis using gels containing 0.8-1.2% agarose depending on the DNA size, 1x TAE and 0.5 µg/ml ethidium bromide.

Mini-sub® Cell GT (Bio-Rad) was used for electrophoresis, using 1x TAE as running buffer and operated at ~5-10 mA/cm. DNA markers were from Promega and DNA bands were visulised on a transilluminator (Syngene).

2.4.2. Restriction enzyme digestion:

DNA 2μg was mixed in a reaction mixture containing 1x reaction buffer, 10u of restriction enzymes (Promega), BSA and ddH_2O to give a final volume of 20μl. The mixture was incubated at the desired temperature for 4hrs. The DNA was then separated by agarose gel electrophoresis.

2.4.3. DNA recovery from agarose gel:

Restriction enzyme digested plasmid was separated by agarose gel electrophoresis. The band of the correct size was cut out of the gel and weighed. The DNA was extracted from the agarose using QIAEXquick kit followed the protocol provided by the manufacturer (QIAGEN). The purified DNA was ethanol precipitated on dry ice for 2hrs and pelleted by centrifugation at 13,000 x g for 1 min. The pellet was washed in 70% ethanol and air-dried. The DNA was then resuspended in appropriate volume of ddH_2O. 1ul of DNA was taken for agarose gel electrophoresis and roughly quantified by comparing the intensity of the band with molecular weight standards in SmartLadder (Eurogentec, Hampshire, UK) on the same gel.

2.4.4. Ligation:

Standard DNA ligation was performed in 10ul volume containing 1x ligation buffer, 200ng vector, 3u ligase (3u/ml Promega) and appropriate amount of insert DNA to give a molar ratio of insert DNA: vector of 3:1, and incubated at 16°C overnight.

2.4.5. Transformation:

Two constructs (pGEX2T-grancalcin and pRKMyC-grancalcin) were using the following procedure. 1-10ul of ligation mixture was mixed with 100ul of XL 1-blue competent cells on ice for 30min, heat shocked at 42°C for 45 sec and cooled on ice for 2 min. 1ml of LB medium was added to the mixture and left shaking at 37°C for an hour. Cells were then collected by centrifugation at 6,000x g for 5 min. Excess medium was removed leaving 200µl in the tubes to resuspend the cells in, and they were then plated onto LB agar with ampicillin. The plates were incubated at 37°C overnight.

2.4.6. Positive colony identification:

To identify the positive colonies, ten colonies were inoculated into 10ml of LB broth and grown at 37°C overnight. Plasmid purified from the overnight culture was then digested with appropriate restriction enzymes and positive colonies were recognised by the inserts of the correct size on 1% agarose gel.

2.4.7. Plasmid preparation:

Plasmid mini-preparation or midi-preparation was performed using 10ml or 100ml of overnight cultures and Wizard® plus SV minipreps or midipreps DNA purification system (Promega) according to the protocol provided by the manufacturer (Promega).

2.4.8. Transient transfection of pRKMyC-grancalcin into COS-7 cells:

The COS-7 cells were trypsinized and seeded on to the Metek dish and left at 37°C overnight. 4ul of pRKMyC-grancalcin at 0.6ug/ul was mixed with 100ul of opti-MEM. 4ul of Lipofectamine-200 (Invitrogen) was mixed with 100ul opti-MEM and incubated at RT for 5 minutes. The DNA and Lipofectamine were then mixed at RT for 20 minutes. The cells on the

coverslips were washed with 1ml opti-MEM twice. 0.8ml opti-MEM was added to the coverslip with 0.2ml of mixture of the DNA and Lipofectamine. The cells were incubated at 37°C for 5 hours and checked every two hours for viability. After 5 hours of transfection, the medium was replaced with DMEM supplemented with 10% serum and incubated at 37°C overnight.

2.4.9. Genotyping

For genotyping the grancalcin-deficient mice, genomic DNA was extracted from the tail tips by using a DNA extraction kit II (QIAGEN Ltd, Doncaster, UK) as instructed by the manufacturers. This kit uses advanced silica-gel-membrane technology for rapid and efficient purification of total cellular DNA without organic extraction or ethanol precipitation. Tail tips around 1.0cm in length were cut and digested in 500µl PK buffer, which contains proteinase K to digest proteins and release DNA at 56°C. The lysate was then loaded onto the DNeasy Mini Spin Column. After brief centrifugation, DNA is selectively bound to the DNeasy membrane as contaminants pass through. Remaining contaminants and enzyme inhibitors are removed in the wash steps and DNA is then eluted in water. DNA concentration was measured at A_{260}.

Concentration of DNA sample = 50µg/ml x A_{260} x dilution factor.

The ratio of the reading at 260nm and 280nm provides an estimate of the purity of DNA with respect to contaminants that absorb UV, such as protein. The schematic diagram of the areas that I am going to amplify up is illustrated in Fig 10. Three primers were designed to detect differences in the sequences of the wild type and grancalcin deficient mice in the exon 4. The primer sequences were:

m285': GCA CAT TTC ACC TAC CCC GAG TC,

NEO: 363r TGC GTG CAA TCC ATC TTG TTC AAT GG

R3a: CCA ACA TGG CAA TCA TAA TTC TGC.

PCR with primers m285' and R3a generate a product of 600bp in the wild type allele whereas m285' and neo 363r will result in a 1000bp product reflecting the insertion of neomycin resistence gene in the exon 4 in the deficient mice. PCR was performed with 3μl of extracted DNA in a final volume of 50μl containing PCR primers at a concentration of 20pmoles, 0.2mM dNTPs, 2mM $MgCl_2$, and 3μl DNA polymerase in 1x reaction buffer. After the initial denaturation at 95°C for 10min, 38 cycles were performed with denaturation at 94°C for 30 seconds, annealing at 65°C for 30 seconds, and elongation at 74°C for 60 seconds. PCR products were separated in 1% agarose gel in TAE buffer in the presence of Ethidium Bromide. Bands were visulized under UV light and photographed with Bio-Rad chemidoc (Bio-Rad).

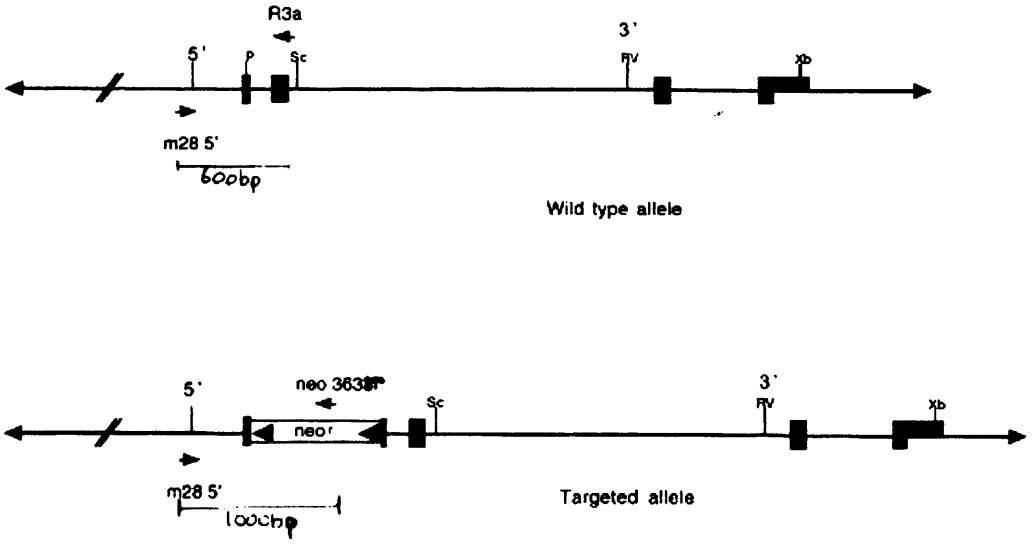

Fig 10. The schematic illustration of the design of the primers used to differentiate in the sequences of the wild type and grancalcin deficient mice in the exon 4. Primers m285' and R3a will generate a 600bp product in the wild type, and m285' and neo363r will produce a 1000bp product in the targeted allele.

CHAPTER 3

RESULTS

3.1. PROTEOMIC ANALYSIS OF THE CYTOSKELETON IN HUMAN NEUTROPHILS

3.1.1. Analysis neutrophil cytosol high speed pellet in one-dimensional electrophoresis

Interactions between cytoskeletal proteins are resistant to disruption by non-ionic detergents, such as Triton X-100 and octyl glucoside, permitting the isolation of the cytoskeleton. Therefore, the standard approach for the isolation of the cytoskeleton is by the use of 1% Triton X-100, since most of the cytoskeletal proteins are found in the Triton X-100-insoluble fraction (Sawada et al., 2002). The problem with this approach in neutrophils is that very abundant proteins in the granules that are not associated with the cytoskeleton, are also insoluble in Triton X-100.

In order to analyse the assembled cytoskeleton structure in neutrophil cytosol, the neutrophil cytosol high-speed pellet was extracted. On comparison with the cytosol after cytosol high-speed pellet extraction on a 1D gel, we found that their patterns were different (Fig 11).

By employing MALDI-TOF MS, twenty-five proteins were identified from cytosol high-speed pellet. They were high abundant cytoskeletal proteins, such as actin and associated protein α-actinin, heat shock protein, actin, subunits of Arp2/3 complex, 14-3-3 ε, cofilin, and microtubule and associated protein β-tubulin. Other proteins like molecular motors, such as myosin heavy chain and light chain, proteins involved in ubiquitin-proteosome degradation and S-100 calcium binding protein A8 and A9 were also found (Fig 12). Fig 13 illustrates the mass spectrum of the tryptic digest of IQGAP1 from neutrophil cytosol high-speed pellet. At the same time, a group of metabolic enzymes and proteins involved in ubiquitin-proteasome degradations was mainly found in the cytosol. Although the enrichment of cytoskeletal

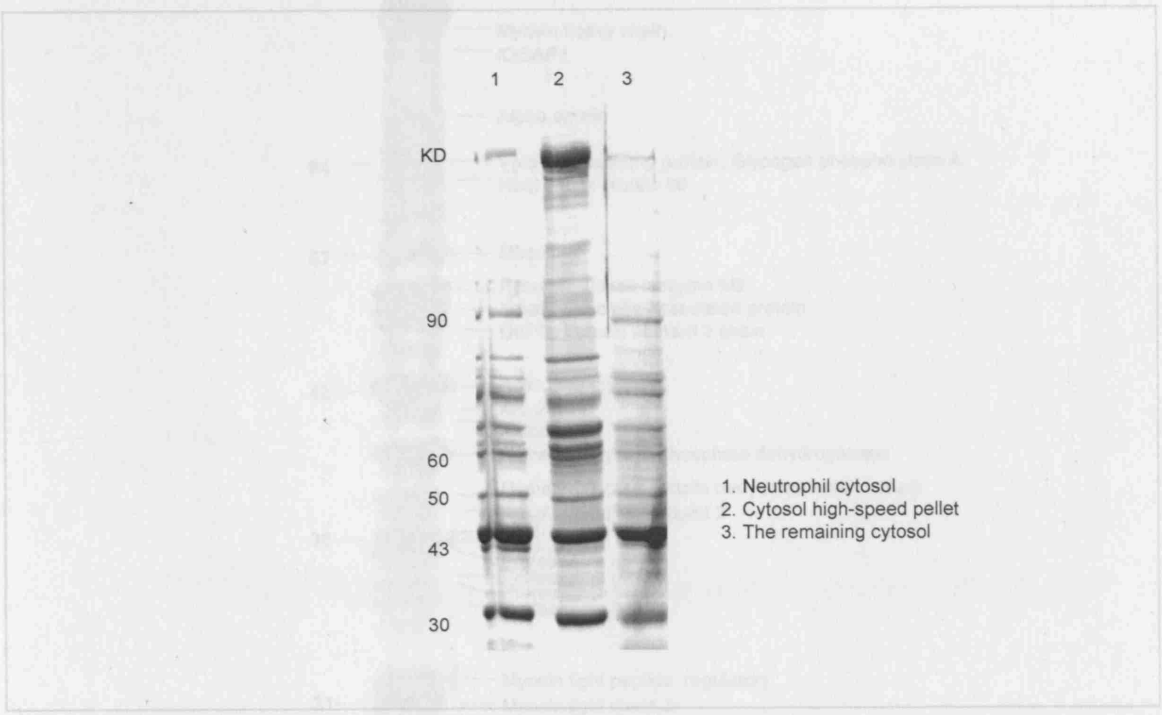

Fig 11. The neutrophil cytosol high-speed pellet and the remaining cytosol depleted of cytosol high-speed pellet showed different patterns.
The neutrophil cytosol, cytosol high-speed pellet and the remaining supernatant were extracted and analysed by SDS-PAGE. They displayed the different patterns on 1D gel. The samples were loaded as follows: 1.neutrophil cytosol; 2. cytosol high-speed pellet; 3. the remaining cytosol depleted of cytosol high-speed pellet. Typical results of at least three separate experiments are shown.

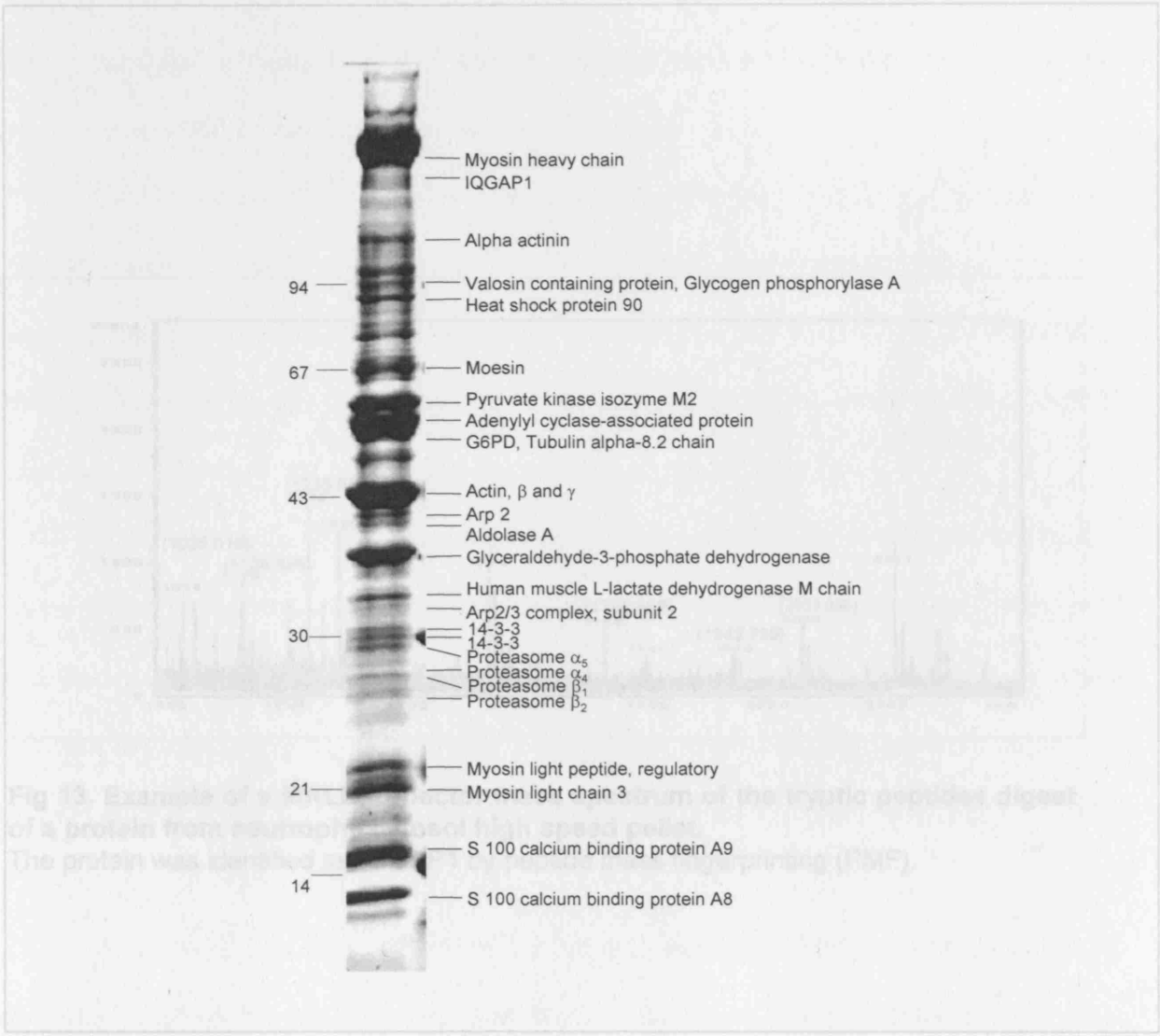

Fig 12. One dimensional electrophoresis of proteins from cytosol high-speed pellet.
Proteins from cytosol high-speed pellet (right) were separated by SDS-PAGE and stained with Commassie blue. Proteins were identified by MALDI-TOF mass spectrometry.

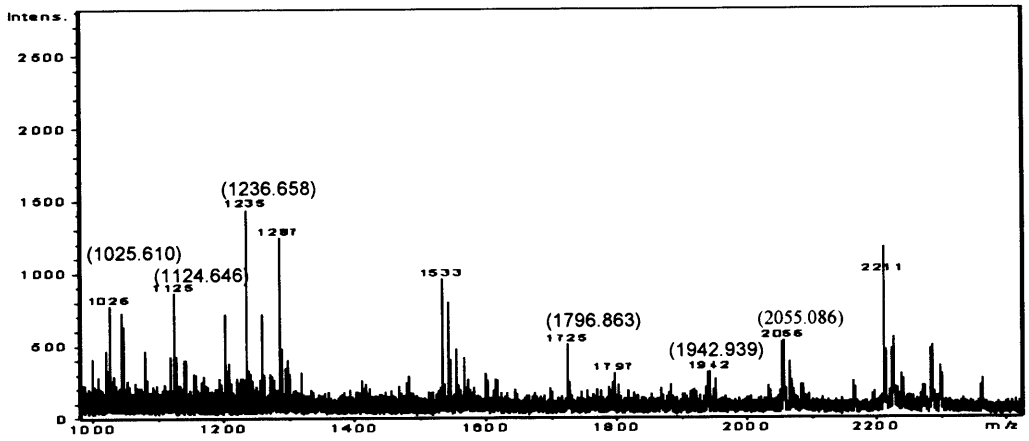

Fig 13. Example of a MALDI reflector mass spectrum of the tryptic peptides digest of a protein from neutrophil cytosol high speed pellet.
The protein was identified as IQGAP1 by peptide mass fingerprinting (PMF).

proteins in the cytosol high-speed pellet enabled the first identification of IQGAP1 in human neutrophils, we concluded that two-dimensional electrophoresis should be applied to enable the identification of more cytoskeletal proteins at different locations.

3.1.2. Analysis of cytoskeletal fractions from different cell compartments of the neutrophil by two-dimensional electrophoresis

Cell fractionation was employed here in order to extract cytoskeletal proteins with minimal contamination by the proteins unrelated to the cytoskeleton. A reduction of the sample's complexity to suborganellar level also facilitated the identification of low abundance proteins. The resulting protein patterns of cytosol high-speed pellet, Triton X-100 insoluble membrane and Triton X-100 insoluble phagosomes are shown in Fig 14-16.

On 2-D gels of the three different subcellular compartments, attempts have been made to analyse all the protein spots that were visible on the gel. Totally 138 proteins were identified, 72 from the cytosol high-speed pellet, 39 from the detergent-resistant plasma membrane and 26 from the detergent-resistant phagosome. The patterns were consistently observed in three different sample preparations. Detailed information on the proteins identified is given in Table 1-3.

As shown in Table 1, the identified proteins have been grouped into a number of categories based on the previous functional studies. Many known cytoskeletal proteins were identified, but some of them have not been previously identified in the human neutrophils, or their subcellular distribution are not clear. Proteins with other known functions, but of unknown/uncertain function in the cytoskeleton, and proteins without established cellular functions were also observed. Only a few of these latter proteins have previously been observed in the neutrophil cytoskeleton, where their function has not been defined. Consideration of the possible cytoskeletal function of these proteins is in the discussion.Overall, six proteins were present in all three cytoskeletal compartments, which

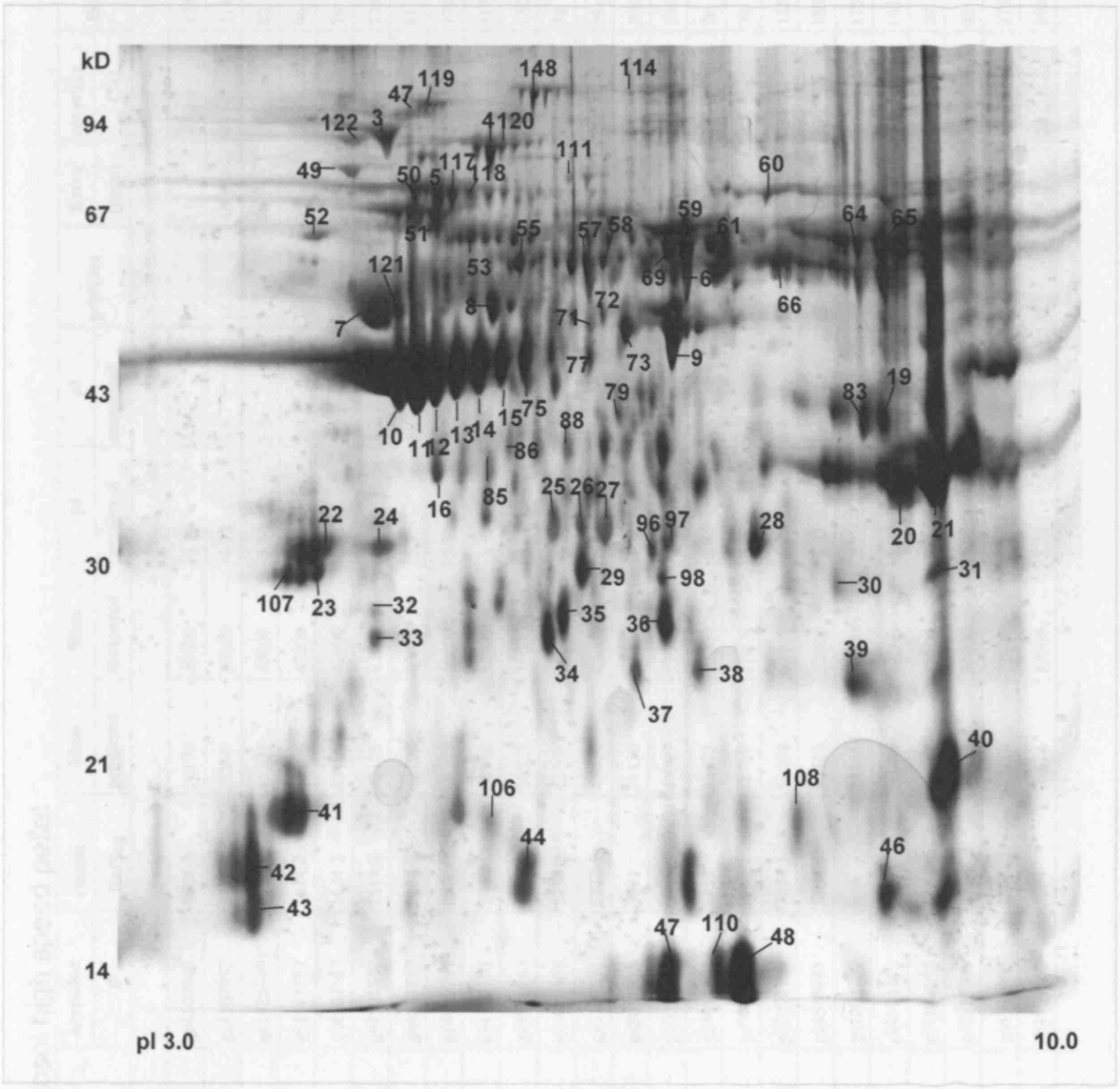

Fig 14. Representative 2-D map of neutrophil cytosol high-speed pellet.
Cytosolic cytoskeletal fraction was extracted and subjected to 2-DE, followed by silver staining. IEF (pH 3-10) nonlinear gradient was in the horizontal direction and 11% SDS-PAGE was in the vertical direction. Proteins identified by MALDI-TOF mass spectrometry are summarised in Table 1.

Table 1. Proteins identified in neutrophil cytosol high speed pellet

Protein	Gene	Accession gi	closest RefSeq	Mass predicted	Mass measured	pI predicted	pI measured	peptides	Error (ppm)	coverage (%)	Score	spot #	PMID
1.Actin and associated proteins													
14-3-3 b	YWHAB	gi|4507949	3404.3	28179	30000	4.76	4.55	12	11	43	135	22	N/A
14-3-3 e	YWHAZ	gi|4507953	3406.2	27899	30000	4.73	4.6	11	48	44	118	23	12551948
Actin b	ACTB1	gi|14250401	N/A	41321	43000	5.56	5.9	7	90	25	82	15	12663865
Actin g	ACTG1	gi|4501887	1614.2	42108	43000	5.31	5.4	7	45	23	96	13	12663865
Actin g	ACTG1	gi|4501887	1614.2	42108	43000	5.31	5.3	8	21	26	74	12	12663865
Actin g	ACTG1	gi|4501887	1614.2	42108	43000	5.31	5.2	11	26	33	124	11	12663865
Actin g	ACTG1	gi|4501887	1614.2	42108	43000	5.31	5.1	11	21	33	91	10	12663865
a- actinin	ACTN1	gi|4639781	N/A	103480	100000	5.22	7.1	16	26	20	170	47	2351691
Annexin I	ANXA1	gi|4502101	700.1	38918	38000	6.57	6.35	10	27	40	117	88	9187254
Annexin III	ANXA3	gi|4826643	5139.1	36524	36000	5.63	5.8	12	23	42	132	85	15260827
ARP1	ACTR1A	gi|5031569	5736.2	42701	48000	6.19	6.5	7	13	21	78	77	15157458
ARP 2	ACTR2	gi|5131571	5722.1	45030	45000	6.3	6	6	38	20	94	75	10322212
ARP 2/3 (subunit 2)	ARPC2	gi|5031599	5731	34430	34000	6.84	6	5	30	21	100	55	10322212
ARP 3	ACTR3	gi|5031573	5721.3	47797	52000	5.61	5.8	17	21	30	136	8	10322212
Cap Z	CAZ1	gi|3453597	6135	33073	32000	5.45	5.4	4	119	24	76	16	12660160
Cofilin 1	CFL1	gi|5031635	5507.2	18719	21000	8.22	9	5	6	40	76	40	14598374
Coronin 1A	CORO1A	gi|5902134	7074.1	51678	67000	6.25	6.4	18	18	38	185	111	10461187
*eEF 1 g	EEF1G	gi|4503481	1404.3	50429	52000	6.25	6.6	13	17	27	185	72	N/A
Filamin	FLN	gi|1203969	N/A	283460	250000	5.7	N/A	39	29	18	175	+1D	7929100
Gelsolin	GSN	gi|4504165	177.3	86043	87000	5.9	5.9	13	17	17	141	4	12663865
Gelsolin	GSN	gi|4504165	177.3	86043	87000	5.9	5.9	13	21	17	79	120	12663865
*Grancalcin	GCA	gi|6912388	12198.2	24223	30000	5.02	5	10	117	34	80	32	N/A
L-plastin	LCP1	gi|4504965	2298	70814	72000	5.29	5.7	25	17	40	273	118	12525560
L-plastin	LCP1	gi|4504965	2298	70814	72000	5.29	5.6	32	19	54	394	117	12525560

Table 1. Continued,

Protein	Gene	Accession gi	closest RefSeq	Mass predicted	Mass measured	pI predicted	pI measured	peptides	Error (ppm)	coverage (%)	Score	spot #	PMID
Moesin	MSN	gi|4505257	2444.1	67892	85000	6.08	5.1	26	26	43	223	3	15147559
Profilin 1	1AWH-A	gi|3891601	N/A	15014	16000	8.46	8.55	12	23	75	157	46	9360613
S100 protein, A8	S100A8	gi|21614544	2964.3	10870	12000	6.5	7.4	5	12	44	78	110	9920411
S100 protein, A8	S100A8	gi|21614544	2964.3	10870	12000	6.5	7.7	8	18	57	125	48	9920411
S100 protein, A8	S100A8	gi|21614544	2964.3	10870	12000	6.5	7	6	16	46	109	47	9920411
S100 protein, A9	S100A9	gi|4506773	N/A	13280	16000	5.7	6	6	9	53	83	44	9920411
S100 protein, A9	S100A9	gi|4506773	N/A	13280	18000	5.7	5.8	8	47	78	111	106	9920411
Cytoskeletal tropomyosin	N/A	gi|37424	N/A	28185	28000	4.81	4.8	6	57	26	81	107	14722123
Vinculin	VCL	gi|24657579	N/A	117234	110000	5.83	7.1	26	29	28	244	148	14702644
2.Molecular chaperones													
Bip protein	HSPA5	gi|6470150	N/A	71002	70000	5.23	5.45	12	41	25	129	5	8797085
*Chaperonin containing TCP 1,subunit 6A	CCT6A	gi|4502643	1762	58444	60000	6.23	5.45	8	43	18	120	51	11532003
Chaperonin containing TCP 1, subunit 2	CCT2	gi|5453603	6431	58444	60000	6.01	6.5	24	19	49	278	57	11532003
Heat shock cognate protein	HSPA8	gi|24234686	153201.1	53598	70000	5.62	5.2	14	21	33	154	50	8404847
Heat shock protein 90	HSPCA	gi|123678	N/A	85020	92000	4.94	5.33	14	17	22	111	122	12522269
*T complex protein 1	CCT1	gi|14755380	30752	60819	60000	5.8	6.85	13	22	23	109	58	10079067
bTubulin	TUBB	gi|18088719	N/A	50096	52000	4.75	5	22	16	43	128	7	12700769
3.Intermediate filaments and associated proteins													
Vimentin	VIM	gi|4507895	3380.1	53710	50000	5.06	5.1	24	23	55	254	121	14676269
4.Molecular motors and associated proteins													
Myosin light chain alkali	MLY6	gi|17986258	21019.2	17090	16000	4.56	4.2	9	27	52	101	42	2304459
Myosin light chain alkali	MLY6	gi|17986258	21019.2	17090	16000	4.56	4.2	10	12	58	139	43	2304460
Myosin, heavy polypeptide 9	MYH9	gi|12667788	2473.2	227646	220000	5.5	5	23	24	14	141	ID	14706930
Myosin regulatory light chain	MRCL3	gi|5453740	6471.1	19500	19000	4.67	4.5	6	5	35	94	41	3839239
5.Energy and metabolic enzymes													
Adenylyl cyclase-associated protein	CAP1	gi|5453595	6367	51926	62000	8.07	8	12	13	30	107	66	10391948
Aldolase A	1ALD	gi|229674	N/A	39720	39000	8.39	8.55	7	53	23	70	19	9244396

Table 1. Continued,

Protein	Gene	Accession gi	closest RefSeq	Mass predicted	Mass measured	pI predicted	pI measured	peptides	Error (ppm)	coverage (%)	Score	spot #	PMID
Aldolase A	1ALD	gi|229674	N/A	39720	39000	8.39	8.55	12	7	29	117	83	9244396
Catalase	CAT	gi|455701 4	1752.1	59947	60000	6.9	7.1	21	24	42	212	6	15206463
Catalase	CAT	gi|455701 4	1752.1	59947	60000	6.9	7.2	12	23	29	140	59	15206463
Catalase	CAT	gi|455701 4	1752.1	59947	60000	6.9	7.5	9	14	24	114	61	15206463
Catalase	CAT	gi|455701 4	1752.1	59947	60000	6.9	7	11	75	26	66	69	15206463
Enolase 1	ENO1	gi|4503571	1428.2	47481	49000	7.01	7.1	16	18	43	163	9	2553125
Enolase	ENO1	gi|4503571	1428.2	47481	49000	7.01	7.1	17	20	42	171	73	2553125
GAPDH	GAPD	gi|7669492	2046.2	36201	35000	8.57	8.8	14	24	46	141	20	9568479
GAPDH	GAPD	gi|7669492	2046.2	36201	35000	8.57	8.9	16	19	51	143	21	9568479
Glucosidase II	KIAA0088	gi|2274968	N/A	107289	102000	5.71	6.66	17	37	22	165	ID	15234963
Leukotriene A4 hydrolase	LTA4H	gi|4505029	895.1	69868	70000	5.8	5	18	12	32	178	49	11175901
*N-acetylglucosamine kinase	NAGK	gi|24638065	N/A	37694	38000	5.81	5.9	9	22	29	78	86	10824116
*Phosphoglycerate mutase 1	PGAM1	gi|4505753	2629.2	28900	30000	6.67	6.9	5	40	28	64	96	2553125
Phosphogluconate dehydrogenase	PGD	gi|12653201	N/A	53619	51000	6.8	6.4	18	22	43	150	71	15128828
Procollagen-proline, 2-oxoglutarate 4-dioxygenase	P4HB	gi|20070125	918.2	57480	60000	4.76	4.6	19	15	35	215	52	14985345
Protein disulfide-isomerase	N/A	gi|7437388	N/A	57160	50000	5.98	6.9	14	13	24	139	73	9826346
Pyruvate kinase	N/A	gi|478822	N/A	58470	60000	7.96	8.2	16	19	30	146	65	2553125
Transketolase	tk	gi|388891	N/A	68528	68000	7.89	7.8	8	23	16	84	60	7679932
Vacuolar ATP synthase catalytic subunit A	ATP6V1A	gi|22096378	N/A	68677	70000	5.35	5.2	15	25	28	136	123	12598655
6.Signal transduction molecules													
*IQGAP 1	IQGAP 1	gi|4506787	3870.2	189761	180000	6.08	N/A	24	63	18	107	+ID	8798539
Rab GDP-dissociation inhibitor, beta	GDI2	gi|6598323	1494.2	51087	55000	6.11	8.3	14	44	32	96	64	10512627
Rac-Rho GDI complex, chain B	ARHGDIB	gi|1835002	1175.1	23031	27000	6.1	5	6	25	25	60	33	11513579
7.Proteins involved in ubiquitin-proteasome degradation													
*Major vault protein	MVP	gi|19913410	17458.2	99551	105000	5.34	5.3	13	28	17	98	119	9331335
Proteosome, a1	PSMA1	gi|4506179	2786.2	29822	31000	6.15	6.4	9	11	34	76	26	12424373

Table 1. Continued,

Protein	Gene	Accession gi	closest RefSeq	Mass predicted	Mass measured	pI predicted	pI measured	peptides	Error (ppm)	coverage (%)	Score	spot #	PMID
Proteosome, a1	PSMA1	gi|4506179	2786.2	29822	31000	6.15	6.2	6	10	42	67	25	12424373
Proteosome, a1	PSMA1	gi|4506179	2786.2	29822	31000	6.15	6.6	9	11	34	76	27	12424373
Proteasome, a2	PSMA2	gi|4506181	2787.3	25996	27000	6.92	7	9	19	47	97	36	12424373
Proteasome, a3	PSMA3	gi|296736	152132.1	25078	29000	5.58	5.1	7	40	31	102	24	12424373
Proteasome, a4	PSMA4	gi|4506185	2789.3	29750	30000	7.57	7.1	5	22	21	69	97	12424373
Proteasome, a4	PSMA4	gi|4506185	2789.3	29750	30000	7.57	7.6	7	5	21	87	28	12424373
Proteasome, a6	PSMA6	gi|8394076	17283.2	27840	30000	6.3	6.5	10	76	39	130	29	12424373
Proteasome, a7	PSMA7	gi|4092058	2792.2	28057	28500	8.6	8.9	11	23	52	145	31	12424373
Proteasome, b1	PSMB1	gi|12653473	N/A	26674	24000	8.27	8.3	14	25	50	123	39	12424373
Proteasome, b2	PSMB2	gi|4506195	2794.3	22993	24000	6.51	6.8	8	14	38	144	37	12424373
Proteasome, b2	PSMB2	gi|4506195	2794.3	22993	24000	6.51	7.2	8	52	38	134	38	12424373
Proteasome, b3	PSMB3	gi|22538465	2795.2	23219	25000	6.14	6.25	9	8	42	93	34	12424373
Proteasome, b4	PSMB4	gi|631345	2796	25950	25000	5.7	6.4	5	44	25	64	57	12424373
Proteasome activator 1	PSME1	gi|5453990	6263.2	28880	28000	5.8	6.3	11	87	44	68	35	12424373
Proteasome LMP2.s	LMP-2	gi|2118154	2800	22420	22000	4.9	4.6	6	32	33	70	59	12424373
*Valosin containing protein	VCP	gi|6005942	6005942	89950	90000	5.14	5.1	14/27	28	21	133	3	10364224
8.Others													
Chain A of constant regulatory domain of human Pp2a	N/A	gi|4558258	N/A	65934	60000	5	5.7	12	49	18	117	53	9989501
Cyclophilin A complexed with Dipeptide Gly-Pro	5CYH-A	gi|1633054	N/A	18098	18000	7.82	8	5	41	43	93	108	8652512
aldehyde dehydrogenase	N/A	gi|23503239	153329.2	86086	90000	6.35	6.8	15	15	20	178	114	N/A
PTK9L protein tyrosine kinase 9-like	PTK9L	gi|6005846	7284.3	39751	41000	6.37	6.7	8	19	33	85	79	10406962

Table 1. The proteins identified from cytosol high-speed pellet.

a) Only proteins identified in two out of three experiments are listed .

b) The sequence coverage represents the percentage of coverage of the whole sequence by tryptic peptides detected by MALDI-TOF MS.

c) Significance scores were obtained from Mascot.

d) Spot numbers are indicated in Fig. 14. Spots marked +WB were identified by western blot and presented on Fig. 16, while spots marked +1D were identified by one-dimensional SDS-PAGE (not shown).

e) PMID, denotes the Medline reference describing the function of each protein.

* Proteins previously not known to associate with cytoskeleton.

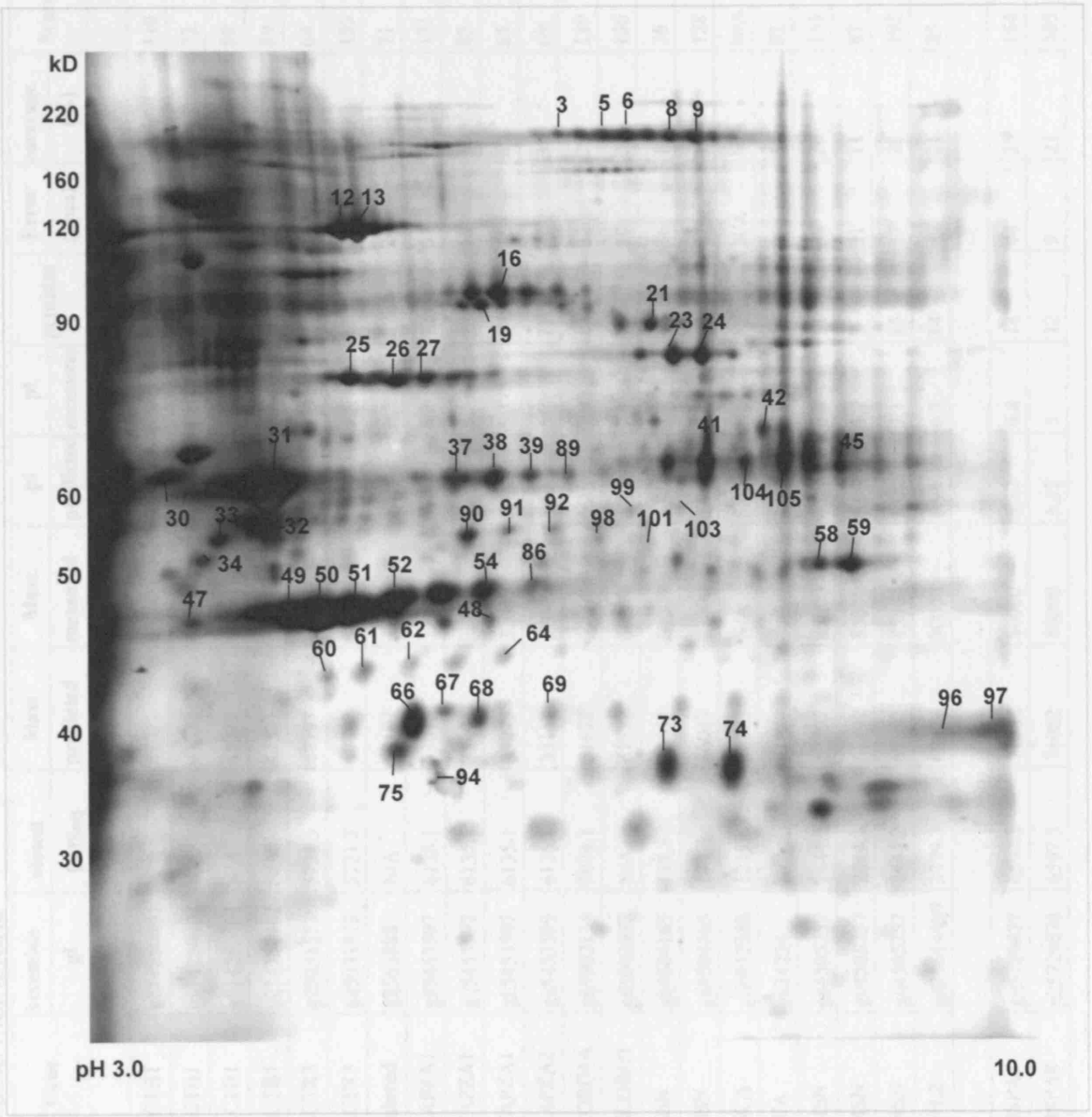

Fig 15. 2-DE separation pattern of the Triton X-100 insoluble cytoskeletal preparation from neutrophil membrane.
The conditions were the same as for figure 14. IEF (pH 3-10) nonlinear gradient was in the horizontal direction and 8% SDS-PAGE was in the vertical direction. Proteins spots identified by MALDI-TOF mass spectrometry are numbered and summarised in Table 2.

Table 2. Proteins identified in Triton-insoluble membrane

Protein	Gene	Accession gi	closest RefSeq	Mass predicted	Mass measured	pI predicted	pI measured	peptides	Error (ppm)	coverage (%)	Score	spot #	PMID
1.Actin and associated proteins													
Actin b	ACTB1	gi|14250401	N/A	41321	43000	5.56	5.8	13	45	33	110	54	12663865
Actin b	ACTB1	gi|14250401	N/A	41321	43000	5.56	4.8	6	N/A	N/A	72	51	12663865
Actin b	ACTB1	gi|14250401	N/A	41321	43000	5.56	4.5	7	60	22	89	50	12663865
Actin b	ACTB1	gi|14250401	N/A	41321	43000	5.56	4.3	7	6	21	89	49	12663865
ARP 3	ACTR3	gi|5031573	5721.3	47797	52000	5.61	5.8	7	24	19	64	92	10322212
ARP 3	ACTR3	gi|5031573	5721.3	47797	52000	5.61	5.8	13	32	33	139	91	10322213
b-centractin	pubmed	gi|563888	N/A	37187	45000	6.19	6.3	5	24	17	71	86	15157458
Cap Z, ?1	CAPZA1	gi|5453597	6135.1	33073	32000	5.45	5.2	12	61	57	131	66	12660160
Cap Z, ?1	CAPZA1	gi|5453597	6135.1	33073	32000	5.45	5.5	9	15	40	85	67	12660161
Cap Z, ?1	CAPZA1	gi|5453597	6135.1	33073	32000	5.45	5.3	9	15	40	85	75	12660162
Cap Z, ?2	CAPZA2	gi|5453599	6136.1	33157	37000	5.57	6.2	7	34	38	69	69	8120062
Coronin 1A	CORO1A	gi|5902134	7074.1	51678	67000	6.25	7.9	17	22	29	119	45	10461187
Coronin like protein	HCORO1	gi|1002923	N/A	51722	60000	6.12	7.1	12	29	22	136	41	8380174
Gelsolin	GSN	gi|4504165	177.3	86043	87000	5.9	5.8	12	36	15	76	16	12663865
Gelsolin	GSN	gi|4504165	177.3	86043	87000	5.9	5.8	13	17	17	128	19	12663866
*Grancalcin	GCA	gi|6912388	12198.2	24223	N/A	5.02	N/A	N/A	N/A	N/A	N/A	32	N/A
Laminin-binding protein	N/A	gi|34234	N/A	31888	40000	4.84	3.8	12	18	52	82	47	12950264
Moesin	MSN	gi|4505257	2444.2	67892	85000	6.08	6.8	11	38	20	133	23	15147559
Moesin	MSN	gi|4505257	2444.2	67892	85000	6.08	6.7	7	21	11	87	22	15147560
Moesin	MSN	gi|4505257	2444.2	67892	85000	6.08	7.1	15	37	28	192	24	15147561
Villin 2	VIL2	gi|21614499	3379.3	69484	90000	5.94	6.8	14	49	21	85	21	1563281
2.Molecular chaperones													
Heat shock 70kDa protein 8 isoform 1	HSPA8	gi|5729877	6597.3	71082	80000	5.37	4.8	14	44	25	154	25	14612456
Heat shock 70kDa protein 8 isoform 1	HSPA8	gi|5729878	6597.3	71082	80000	5.37	5	12	9	21	105	27	14612457

Table 2. Continued,

Protein	Gene	Accession gi	closest RefSeq	Mass predicted	Mass measured	pI predicte	pI measur	peptide	Error (ppm)	coverage (%)	Score	spot #	PMID
3.Intermediate filaments and associated proteins													
Keratin 10, cytoskeletal	KRT10	gi|71528	N/A	59740	59000	5.2	4.2	10	21	15	95	32	15274135
Keratin 10, cytoskeletal	KRT10	gi|18588130	49972.4	59740	59000	5.2	6.4	11	22	16	77	39	15274136
Vimentin	VIM	gi|2119204	N/A	53676	60000	5.06	4.1	23	25	47	223	33	14676269
Vimentin	VIM	gi|2119204	N/A	53676	60000	5.06	4.6	30	18	68	215	31	14676270
4.Molecular motor and associated proteins													
Myosin, heavy polypeptide 9	MYH9	gi|12667788	2473.3	227646	180000	5.5	4	39	19	24	224	10	14706930
5.Energy and metabolic enzymes													
Carbonic anhydrase IV	N/A	Gi|2554743	N/A	30532	38000	6.4	7.8	12	33	43	116	74	9054574
GAPDH	GAPD	gi|31645	N/A	36201	35000	8.57	9	6	43	19	76	96	9568479
GAPDH	GAPD	gi|31646	N/A	36201	35000	8.57	9.3	9	43	30	80	97	9568480
Glutamate dehydrogenase	glud1	gi|20151189	N/A	56315	60000	6.71	7.1	8	11	17	87	104	12125925
Glutamate dehydrogenase	glud1	gi|20151189	N/A	56315	60000	6.71	7.3	8	12	18	73	105	12125926
glycogen phosphorylase	PYGL	gi|3170407	N/A	97461	100000	6.31	7.8	13	48	18	141	11	10677363
Protein disulfide-isomerase	N/A	gi|7437388	N/A	57160	50000	5.98	5.8	8	22	15	64	37	9826346
Protein disulfide-isomerase	N/A	gi|7437388	N/A	57160	50000	5.98	6	10	37	20	80	38	9826347
Protein disulfide-isomerase	N/A	gi|7437388	N/A	57160	50000	5.98	6.3	10	37	20	80	89	9826348
6.Signal transduction molecules													
Ficolin 1	FCN1	gi|5510127	2003.2	34830	35000	6.7	6.9	12	62	28	117	73	8947836
Flotillin	FLOT	gi|5114049	N/A	47531	52000	7.04	7.9	24	12	44	150	58	15128873
Flotillin 1	FLOT1	gi|5031699	5803.2	47554	52000	7.08	8	25	29	51	206	59	15128874
G protein, alpha inhibiting unit	N/A	gi|45044041	2070	40995	40000	5.34	4.6	13	16	43	136	60	15196565
G protein, alpha inhibiting unit	N/A	gi|45044041	2070	40995	40000	5.34	5.3	13	16	43	136	62	15196566
Gi alpha-2 chain	LUCA16.1	gi|4218034	N/A	22314	42000	5.3	6.09	6	41	37	71	64	12153986
G protein, beta 2	Gnb2	gi|13937391	10312.3	38061	35000	5.6	5.8	9	23	32	97	94	12887916
G protein, beta 2	Gnb2	gi|13937391	10312.3	38061	37000	5.6	5.8	7	27	22	77	68	12887917
*Hpast (EHD1)	HPAST	gi|2529707	N/A	60722	70000	6.49	7.6	11	20	21	97	42	10673336

Table 2. continued,

Protein	Gene	Accession gi	closest RefSeq	Mass predicted	Mass measured	pI predicte	pI measur	peptide	Error (ppm)	coverage (%)	Score	spot #	PMID
*IQGAP 1	IQGAP 1	gi|4506787	3870.2	189761	N/A	6.08	N/A	N/A	N/A	N/A	N/A	+WB	8798539
Lyn B	LynB	gi|2117805	N/A	56454	55000	6.1	7	10	17	23	123	103	8125304
Lyn B	LynB	gi|2117805	N/A	56454	55000	6.1	6.4	10	52	23	80	99	8125305
Lyn	LYN	gi|37589566	N/A	56454	55000	6.1	6.8	13	51	24	82	101	8125306
Lyn B protein	N/A	gi|187271	N/A	56454	55000	6.1	6.3	9	27	23	65	98	8125307
7.Proteins involved in ubiquitin-proteasome degradation													
*Major vault protein	MVP	gi|19913410	17458.2	99551	105000	5.34	4.5	22	33	29	192	12	9331335
*Major vault protein	MVP	gi|19913410	17458.2	99551	105000	5.34	5	19	41	25	170	13	9331336
*Valosin containing protein	VCP	gi|6005942	7126.2	89950	90000	5.14	5.1	14/27	28	21	133	WB	15037236
8.Others													
eukaryotic translation initiation factor 3, subunit 2 beta	EIF3S2	gi|4503513	3757.1	36878	38000	5.38	4.9	10	48	40	92	61	10887144
Neutrophil adherence receptor alpha-M subunit	ITGAM	gi|386975	N/A	127628	200000	6.73	7	12	23	11	70	8	2454931
Neutrophil adherence receptor alpha-M subunit	ITGAM	gi|386975	N/A	127628	200000	6.73	7.3	20	63	19	178	9	2454932
Neutrophil adherence receptor alpha-M subunit	ITGAM	gi|386975	N/A	127628	200000	6.73	6.7	14	28	13	115	3	2454933
integrin alpha M precursor	ITGAM	gi|1708572	N/A	128470	180000	6.9	6.5	27	69	26	1	5	2454931
integrin alpha-IIb precursor	ITGA2B	gi|124951	N/A	114460	180000	5.21	6.7	20	10	22	136	6	3801670
PWP1 interacting protein 4	N/A	gi|14579002	N/A	40760	45000	5.81	5.8	12	20	34	124	48	15588312
Lung Cancer Related Protein 8 - like	N/A	gi:13477103	N/A	51781	46000	9.15	5.2	7	56	17	70	52	12477932

Table 2. The proteins identified from Triton X-100 insoluble membrane.

a) Only proteins identified in two out of three experiments are listed.

b) The sequence coverage represents the percentage of coverage of the whole sequence by tryptic peptides detected by MALDI-TOF MS.

c) Significance scores were obtained from Mascot.

d) Spot numbers are indicated in Fig. 14. Spots marked +WB were identified by western blot and presented on Fig. 16, while spots marked +1D were identified by one-dimensional SDS-PAGE (not shown).

e) PMID, denotes the Medline reference describing the function of each protein.

* Proteins previously not known to associate with cytoskeleton.

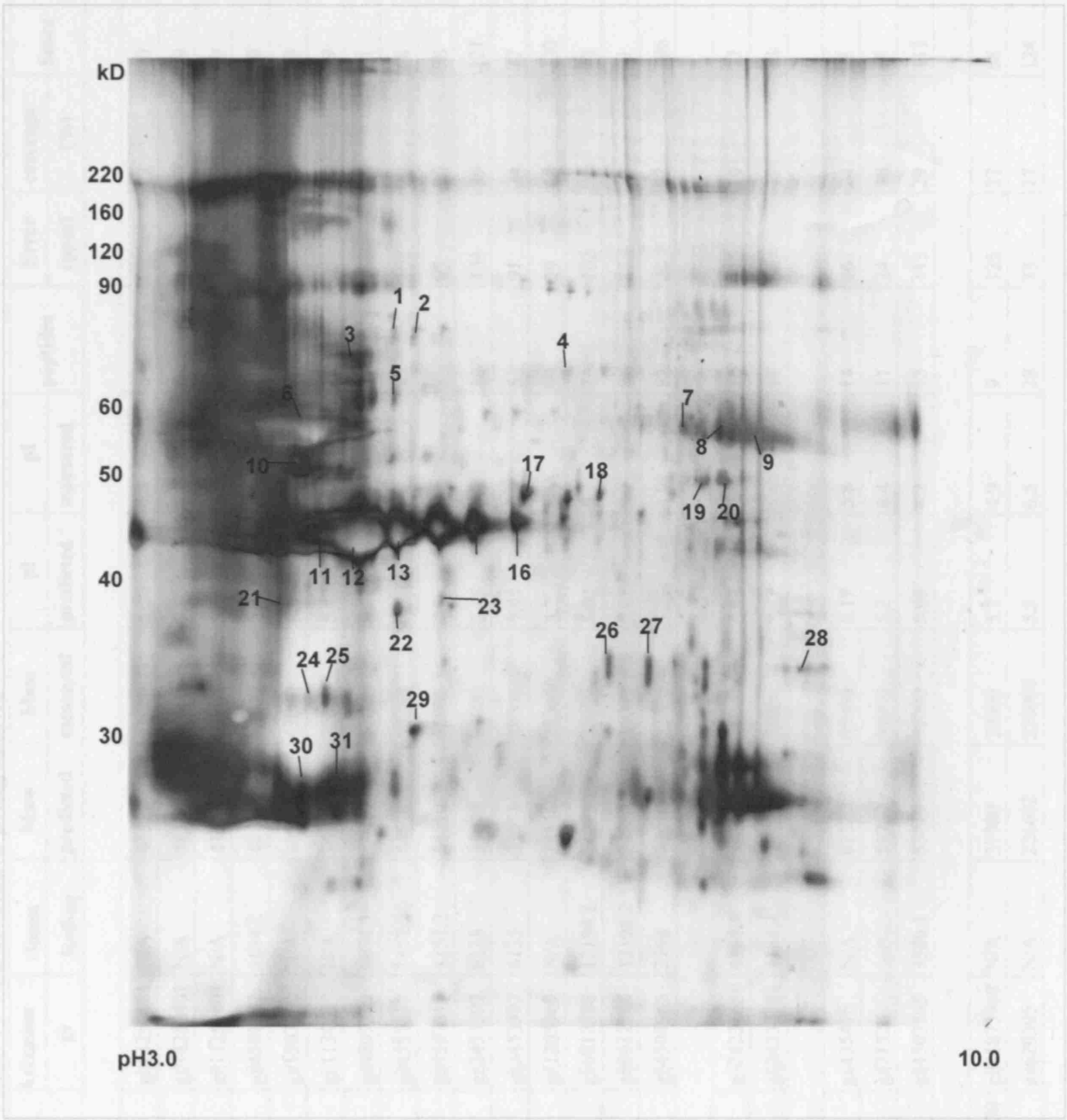

Fig 16. 2-DE map of Triton X-100 insoluble fractions of the phagocytic vacuole.
Proteins identified by MALDI-TOF mass spectrometry and are summarised in Table 3. IgG coated latex beads were phagocytosed by neutrophils for 4 mins. After homogenization of the cell, phagosomes were isolated on sucrose gradient and their proteins separated by 2-D gel electrophoresis. Proteins were separated according to their isoelectric point on immobilized pH gradients 3-10, and then by standard 8% SDS-PAGE. Proteins identified are listed in Table 3.

Table 3. Proteins identified in neutrophil Triton X-100 insoluble phagosome

Protein	Gene	Accession gi	closest RefSeq	Mass predicted	Mass measured	pI predicted	pI measured	peptides	Error (ppm)	coverage (%)	Score	spot #	PMID
1.Actin and associated proteins													
Actin b	ACTB1	gi|14250401	N/A	41321	43000	5.56	4.8	6	92	22	80	11	12663865
Actin b	*ACTB1*	*gi|14250401*	*N/A*	*41321*	*43000*	*5.56*	*5*	*6*	*18*	*20*	*69*	*12*	*12663865*
Actin b	ACTB1	gi|14250401	N/A	41321	43000	5.56	5.2	7	12	27	69	13	12663865
Actin g	ACTG1	gi|4501887	1614.2	42108	45000	5.31	6.5	7	82	26	69	17	12663865
Actin b	ACTB1	gi|15077503	N/A	40540	43000	5.6	6.2	12	93	33	69	16	12663865
Annexin VI	ANXA6	gi|113962	N/A	76168	70000	5.42	6.2	11	23	19	89	4	9230932
Annexin VII	ANXA7	gi|4809279	4034.1	53010	50000	5.5	7	7	138	17	81	18	9230932
Annexin XI	ANXA11	gi|4557317	1157.2	54710	55000	7.7	8	8	102	20	68	7	12805373
Annexin XI	ANXA11	gi|4557317	1157.2	54710	55000	7.7	8.2	8	95	20	98	9	12805374
Cap Z alpha 1	CAZ1	gi|3453597	6135	33073	37000	5.45	5.1	10	104	39	121	22	12660160
Cap Z alpha 1	CAZ1	gi|3453597	6135	33073	38000	5.45	5.8	5	91	24	77	23	12660160
Filamin	FLN	gi|1203969	N/A	283460	250000	5.7	N/A	39	29	18	230	+1D	7929100
*Grancalcin	GCA	gi|6912388	12198.2	24223	26000	5.02	5	7	102	25	78	30	N/A
*Grancalcin	GCA	gi|6912388	12198.2	24223	26000	5.02	5.2	8	88	21	81	31	N/A
L-plastin	LCP1	gi|4504965	2298	70814	72000	5.29	4.9	32	26	52	396	3	12525560
2.Molecular chaperones													
Heat shock 70kDa protein 9B precursor	HSPA9B	gi|24234688	4134.4	73920	75000	5.87	5	10	33	19	77	1	12729798
Heat shock 70kDa protein 9B precursor	HSPA9B	gi|24234688	4134.4	73920	75000	5.87	5.4	11	86	19	73	2	12729799
3.Intermediate filaments and associated proteins													
Cytokeratin 9	KRT9	gi|435476	N/A	62320	65000	5.19	5.8	14	46	24	98	5	2425683
Keratin 10, cytoskeletal	KRT10	gi|71528		59740	59000	5.2	6.4	11	24	18	88	1D	15274135
Vimentin	VIM	gi|4507895	3380.1	53710	50000	5.06	4.2	13	115	29	111	6	14676269
4.Molecular motors and associated proteins													
Myosin tail domain containing protein	DKFZp68610230	gi|31873968	N/A	37980	33000	5.7	4.9	9	125	27	68	25	N/A
Myosin heavy chain	N/A	gi|620305	N/A	226602	220000	5.5	6.5	28	33	17	124	+1D	9013678

Table 3. Continued,

Protein	Gene	Accession gi	closest RefSeq	Mass predicted	Mass measured	pI predicted	pI measured	peptides	Error (ppm)	coverage (%)	Score	spot #	PMID
5.Energy and metabolic enzymes													
ATP synthase	ATP5B	gi|32189394	1686.3	56540	52000	5.3	4.3	13	109	33	172	10	15048984
Protein disulfide-isomerase	N/A	gi|7437388	N/A	57160	50000	5.98	N/A	7	29	13	79	+1D	9826346
6.Signal transduction molecules													
Ficolin	FCN	gi|1510127	N/A	34830	35000	6.7	7.2	14	62	29	135	26	14642811
Ficolin	FCN	gi|1510127	N/A	34830	35000	6.7	7.5	12	108	28	112	27	14642812
Flotillin	FLOT	gi|5114049	N/A	47531	52000	7.04	8	11	116	31	122	19	15128873
Flotillin	FLOT	gi|5114049	N/A	47531	52000	7.04	8.1	7	82	23	89	20	15128873
*IQGAP1	IQGAP1	gi|4506787	3870.2	189761	180000	6.08	N/A	N/A	N/A	N/A	N/A	+WB	8798539
7.Proteins involved in ubiquitin-proteasome degradation													
*Valosin containing protein	VCP	gi|6005942	6005942	89950	92000	5.14	N/A	N/A	N/A	N/A	N/A	+WB	10364224
8.Others													
Adaptor protein p47phox	NCF1	gi|13345794	N/A	31484	38000	9.01	4.4	6	54	23	84	21	12716910
EF hand domain containing 2	EFHD2	gi|38196040	24329.4	26790	33000	5.2	4.8	15	118	36	142	24	10673336
Microtubule associated protein-6	N/A	gi|48375157	N/A	49130	55000	9.9	8.2	7	86	27	72	8	N/A
VDAC-1	N/A	gi|238427	N/A	30740	35000	8.8	9	8	71	38	74	28	11035728
Prohibitin	PHB	gi|4505773	2634.2	29840	29000	5.6	5.5	8	110	35	92	29	15378696

Table 3. The proteins identified from Triton X-100 insoluble phagosome.

a) Only proteins identified in two out of three experiments are listed .

b) The sequence coverage represents the percentage of coverage of the whole sequence by tryptic peptides detected by MALDI-TOF MS.

c) Significance scores were obtained from Mascot.

d) Spot numbers are indicated in Fig. 14. Spots marked +WB were identified by western blot and presented on Fig. 16, while spots marked +1D were identified by one-dimensional SDS-PAGE (not shown).

e) PMID, denotes the Medline reference describing the function of each protein.

* Proteins previously not known to associate with cytoskeleton.

include actin, the largest relative amount of protein being found in all the fractions; vimentin, the intermediate filament protein; grancalcin, a member of penta-EF-hand family protein with unknown function; protein disulfide-isomerase; IQGAP1, a protein integrates the actin microfilament and microtubule; and valosin-containing protein, which is involved in ubiquitin-proteosome degradation.

In neutrophil cytosol high-speed pellet, apart from the proteins mentioned above, we also identified actin and associated proteins 14-3-3 β, 14-3-3 ε, α-actinin, cofilin, eEF1γ, profilin 1, S 100 protein A8 and A9, cytoskeletal tropomyosin, vinculin, and tubulin and associated proteins β-tubulin, Bip, chaperonin containing TCP1, T complex protein 1. This is the first report of TCP1 in neutrophils. To our knowledge this is also the first report of association of n-acetylglucosamine kinase, phosphoglycerate mutase 1, phosphogluconate dehydrogenase, glucosidase, transketolase and aldehyde dehydrogenase with the cytoskeleton. All these enzymes were identified only in the cytosol high speed pellet fraction. This group included enzymes participating in glycolysis: phosphoglycerate mutase 1; pentose phosphate pathway: phosphogluconate dehydrogenase, transketolase; and glycoprotein processing: glucosidase. This was not surprising, as it is known that a number of metabolic processes take place in cytoplasm as opposed to membrane and phagosome. We also identified signal transduction molecules Rab GDP-dissociation inhibitor and Rac-Rho GDI complex. A number of subunits of 26S proteasome were detected in the cytosol high-speed pellet. Previously, 26S proteasome has been identified in an unperturbed cellular environment associated with the actin cytoskeletal network, by electron tomography, which confirmed their structurally related to the cytoskeleton. Electron tomography is a noninvasive three-dimensional imaging technique that shows supramolecular organization of the cytoplasm. In actin networks reconstructed without prior removal of membranes or extraction of soluble proteins, the cross-linking of individual microfilaments, their branching angles, and membrane attachment sites can be analysed (Medalia et al., 2002). Our results indicate for the

first time the association of the valosin-containing protein with the cytoskeleton. Detailed information on the proteins identified is listed in Table 1.

As expected, most of the signal transduction molecules were found exclusively in detergent-resistant membrane fraction: G protein alpha inhibiting unit (GdI-α), Gi α_2 chain, G protein β_2, Hpast, IQGAP1, lyn and lyn B. A group of uncategorized proteins like eukaryotic translation initiation factor 3, neutrophil adherence receptor α_M, integrin α_M precursor, integrin α_{IIb} precursor, PWP1 interacting protein 4 and lung cancer related protein 8 were also found located in this Triton X-100 insoluble fraction.

A number of proteins have been found specific to the Triton X-100 insoluble phagosome, such as annexin VI, VII and XI, cytokeratin 9, ATP synthase, adaptor protein p47phox, EF hand domain containing 2, microtubule associated protein-6, VDAC-1 and prohibitin.

Some of the proteins share their distribution at different locations. Actin binding protein filamin and side binding protein L-plastin, which have been identified in the neutrophil phagosome for the first time, were also found in the cytosol high-speed pellet. Some of the proteins showed apparent molecular weights indicative of alternative isoforms of the full length protein. These different subunits have been found present at different subcellular fractions, suggestive of specialised functions at the different locations. Taking molecular chaperone as an example, four molecular chaperones were found in the cytoplasm (Bip protein, heat shock cognate protein, heat shock protein 90 and TCP1), three of them in the detergent-resistant phagosome (prohibitin, heat shock 70kDa protein 8 isoform 1 and heat shock 70kDa protein 9B precursor), and one in the detergent-resistant plasma membrane (heat shock 70kDa protein 8 isoform 1). This also applies to different subunits of actin capping protein cap Z, and different types of myosin heavy chain and light chains.

A lot of proteins found in the Triton X-100 insoluble phagosome were also found in the Triton X-100 insoluble membrane, as the phagosome proteins were partly generated from

membrane and granules. Thus we found actin binding protein cap Z, cytoskeletal keratin 10, ficolin and flotilin in both membrane and phagosome fractions.

The majority of the 138 proteins identified are known to associate with the cytoskeleton thus confirming that the methods employed here for the isolation of the cytoskeleton are valid. However, our detergent-resistant plasma membrane and detergent-resistant phagosome preparations were also found to contain lipid rafts, as these structures are also insoluble in Triton X-100 under the conditions used in our experiments. Accordingly, the presence of lipid rafts was confirmed by the identification of flotillin, a marker protein of lipid rafts, in both membrane-rich fractions, the detergent-resistant plasma membrane and detergent-resistant phagosome, but not in the cytosol high-speed pellet that is devoid of membranes. Protein disulfide isomerase is generally considered as a marker protein of ER (Clementi et al., 1994). However, its finding in all analysed compartments does not indicate a contamination by ER, as it was recently demonstrated that this enzyme is also localized at the cell surface and in the cytosol (Turano et al., 2002).

Eleven of the 138 identified proteins were to our knowledge not previously known to associate with the cytoskeleton or lipid rafts: n-acetylglucosamine kinase, phosphoglycerate mutase 1, prohibitin, ficolin, phosphogluconate dehydrogenase, glucosidase, transketolase, major vault protein, valosin-containing protein, aldehyde dehydrogenase and lung cancer-related protein-8 (LCRP8). Most of these proteins were identified in cytosolic high-speed pellet fraction (8/11), ficolin was detected in the detergent-resistant phagosome and detergent-resistant plasma membrane fractions, prohibitin only in detergent-resistant phagosome, LCRP8 in the detergent-resistant plasma membrane while valosin-containing protein could be identified in all three analysed compartments. Several of the identified proteins known to associate with the cytoskeleton have not previously been reported in neutrophils: eEF1γ, T-complex protein 1 (TCP1), dynactin, Hpast, IQGAP1, VDAC-1 and rabex-5. Most

importantly, this is the first report of the characterization of grancalcin, cap Z, filamin, IQGAP1, L-plastin, vimentin, and valosin-containing protein with the neutrophil phagosome.

Among other proteins, ficolin, prohibitin and LCRP8 have not been previously reported to associate with the cytoskeleton or lipid rafts. Ficolin was detected in detergent-resistant plasma membrane and phagosome fraction, prohibitin in detergent-resistant phagosome and LCRP-8 in detergent-resistant plasma membrane. No unnamed proteins was detected in any of the analysed fractions.

3.1.3. Confirmation of the association of grancalcin, IQGAP1 and valosin-containing protein with actin cytoskeleton

In order to validate the data obtained from mass spectrometry, we examined the enrichment of several newly discovered proteins in the cytosol high-speed pellet, detergent-resistant membrane and detergent-resistant phagosome fractions in comparison with less pure subcellular preparations such as PNS, membrane and cytosol. We confirmed the enrichment of grancalcin, valosin-containing protein and IQGAP1 in the cytosol high-speed pellet (Fig 17) by western blot. These findings support our proteomic data, which indicate the association of these proteins with the cytoskeleton.

3.1.4. MALDI-TOF analysis of the phosphorylation of grancalcin in the detergent-resistant phagosome fraction

Grancalcin was identified in the cytosol high-speed pellet and in the detergent-resistant phagosome fraction by proteomic analysis and in the detergent-resistant plasma membrane fraction by western blot analysis (Fig 17). Its mass spectrometry data was analysed further to test if there was any evidence of post-translational modification. Grancalcin's molecular weight was estimated to be 30kD and pI 5.0. As described in Fig 15, spots 30 and 31 from the detergent-resistant phagosome but not the cytosol pellet, were both identified as

Fig 17. The enrichment of grancalcin, valosin-containing protein and IQGAP1 in cytoskeletal fractions.
(A) The resulting Commassie Blue stained gel shows equal amount of protein loading. (B) the corresponding western blot of IQGAP1, VCP and grancalcin. The figure demonstrates the enrichment of IQGAP1 and VCP in the cytosol high-speed pellet fraction, and the enrichment of grancalcin in the Triton X-100 insoluble phagosome.

grancalcin, with the same molecular mass of 30kD but different pI values of 5 and 5.2. MALDI-TOF analysis of spot 30 and 31 indicated phosphorylation of the residues 155-166 LSPQTLTTIVKR while the same peptide derived from spot 32 in cytosol high-speed pellet was not modified (Fig 14). The mass-spectrometric analysis of spots 30 and 31 are summarised in Fig 18. The peptide corresponding to LSPQTLTTIVKR has a theoretical mass of 1355.854 Da. However, besides this peptide a new unexpected peptide occurred with the mass of 1515.774 m/z or 1515.802 m/z in spot 30 and 31 respectively, the difference in mass being 160. Since the addition of one-phosphate results in the molecular mass change of 80, the increase of 160 suggested two phosphorylations on this peptide.

Overall, our MS analysis indicated that grancalcin was dually phosphorylated in the vacuoles and was unmodified in the cytosol. The determination of the exact phosphorylation site will demand further ion analysis by tandem mass spectrometry. Analysis of grancalcin phosphorylation is important for the understanding of its function, as post-translational modifications of this protein have not been previously reported.

A.

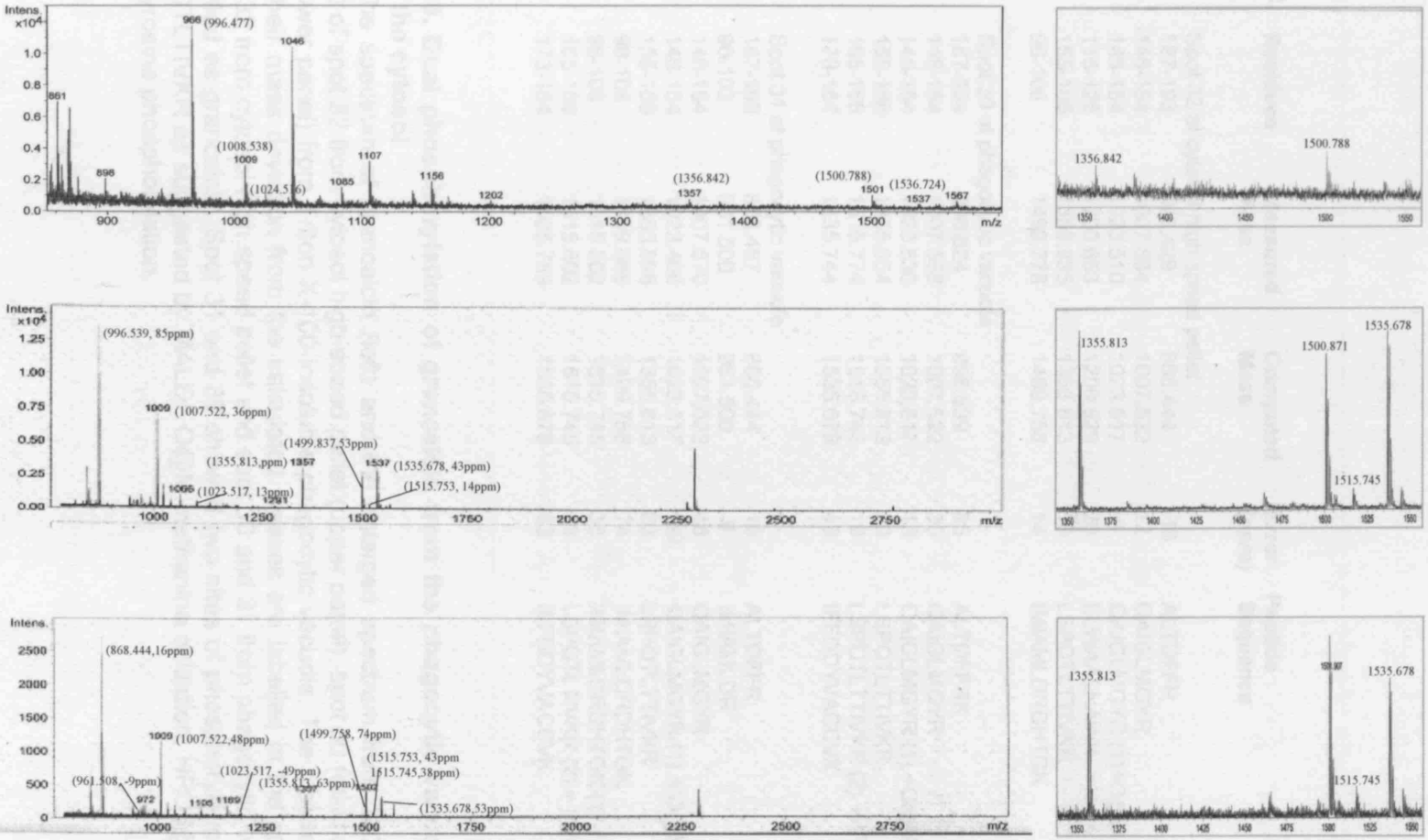
Intens.
x10^4
966 (996.477)
1046
861
(1008.538)
1009
1107
898
1085
1156
1202
(1356.842)
1357
(1500.788)
1501
(1536.724)
1537
1567
m/z
1356.842
1500.788
(996.539, 85ppm)
1009 (1007.522, 36ppm)
(1499.837,53ppm)
(1355.813,ppm) 1357
1537 (1535.678, 43ppm)
(1023.517, 13ppm)
(1515.753, 14ppm)
1355.813
1500.871
1535.678
1515.745
Intens.
(868.444,16ppm)
1009 (1007.522,48ppm)
(1499.758, 74ppm)
(1515.753, 43ppm
(1023.517, -49ppm)
1515.745,38ppm)
(961.508, -9ppm)
(1535.678,53ppm)
1355.813
1535.678
1515.745

B.

Residues	Measured Mass	Computed Mass	Error (ppm)	Peptide Sequence
Spot 32 at cytosol high speed pellet				
187-193	868.429	868.444	-18	ALTDFFR
146-154	1007.534	1007.522	12	QAIGLMGYR
146-154	1023.510	1023.517	-6	QAIGLMGYR (1)+O@M
116-125	1200.653	1200.629	20	ELWAALNAWK
155-166	1355.835	1356.813	19	LSPQTLTTIVKR
96-108	1499.778	1499.758	14	IMIAMLDRDHTGK
Spot 30 at phagocytic vacuole				
187-194	996.624	996.539	85	ALTDFFRK
146-154	1007.558	1007.522	36	QAIGLMGYR
146-154	1023.530	1023.517	13	QAIGLMGYR (1) +O@M
155-166	1355.854	1355.813	30	LSPQTLTTIVKR
155-166	1515.774	1515.745	19	LSPQTLTTIVKR (2) +HPO3@ST
173-184	1535.744	1535.678	43	IFFDDYVACCVK
Spot 31 at phagocytic vacuole				
187-193	868.457	868.444	16	ALTDFFR
96-103	961.500	961.508	-9	IMIAMLDR
146-154	1007.570	1007.522	48	QAIGLMGYR
146-154	1023.466	1023.517	-49	QAIGLMGYR (1) + O@M
155-166	1355.898	1355.813	63	LSPQTLTTIVKR
96-108	1499.869	1499.758	74	IMIAMLDRDHTGK
96-108	1515.802	1515.745	38	IMIAMLDRDHTGK (1) + O@M
155-166	1515.802	1515.745	38	LSPQTLTIVKR (2) + HPO3@ST
173-184	1535.759	1535.678	53	IFFDDYVACCVK

Fig 18. Dual phosphorylation of grancalcin from the phagocytic vacuole, but not from the cytosol

(A) The spectrum of grancalcin (left) and the enlarged spectrum from 1300-1550 m/z (right) of spot 32 from cytosol high-speed pellet (upper panel), spot 30 (middle panel) and 31 (lower panel) from Triton X-100-insoluble phagocytic vacuole. The matching peptides and their mass deviation from the calculated masses are labelled in the spectrum. (B) Spot 32 from cytosol high speed pellet and spot 30 and 31 from phagocytic vacuole were identified as grancalcin. Spot 31 and 32 showed two sites of phosphorylation of peptide LSPQTLTIVKR as suggested by MALDI. O@M:methanine oxidation; HPO3@ST : serine and tyrosine phosphorylation.

3.2. THE BINDING OF GRANCALCIN TO F-ACTIN

3.2.1. Expression, purification and characterisation of GST-grancalcin

In order to investigate its interaction with actin, recombinant GST-grancalcin was purified to high homogeneity and analysed by SDS-PAGE (Fig 19). The recombinant protein was soluble and no protease inhibitor was used during the purification procedure.

3.2.2. Binding of GST-grancalcin to F-actin in vitro

To determine whether grancalcin interacts with F-actin, full-length recombinant GST-tagged human grancalcin was expressed in BL-21 competent cells, purified from cell lysates by affinity chromatography, and incubated with human non-muscle F-actin (Fig 20). Actin filaments, along with the proteins that bind to actin, are pelleted by high centrifugation force (375,000 x g for 20min).

For stoichiometric binding curve of grancalcin and F-actin, 5μM of F-actin was incubated with increasing concentrations of grancalcin for 30 minutes at room temperature and centrifuged at 375,000x g for 20 min. Pellets and supernatants were then analysed by SDS-PAGE. The amounts of free and bound protein were determined densitometrically from Coommassie Blue-stained gels. The significant shift of grancalcin from supernatant to pellet in the presence of F-actin was observed when the concentration of grancalcin was above 5μM (Fig 21A), whilst no such shift was found for the GST and GST-grancalcin alone (Fig 21B). Binding data were then used for the Scatchard analysis. Scatchard analysis showed that in the absence of calcium the dissociation constant for binding of GST-grancalcin to F-actin is approximately 2.5×10^{-6} M with stoichiometric binding of 1.1 mole of GST-grancalcin to 1 mole of F-actin (Fig 21C). Thus, full-length recombinant grancalcin interacts directly with F-actin.

We also tested whether the binding of grancalcin to F-actin was influenced by calcium. Therefore 5μM grancalcin was incubated with F-actin both in the absence and the

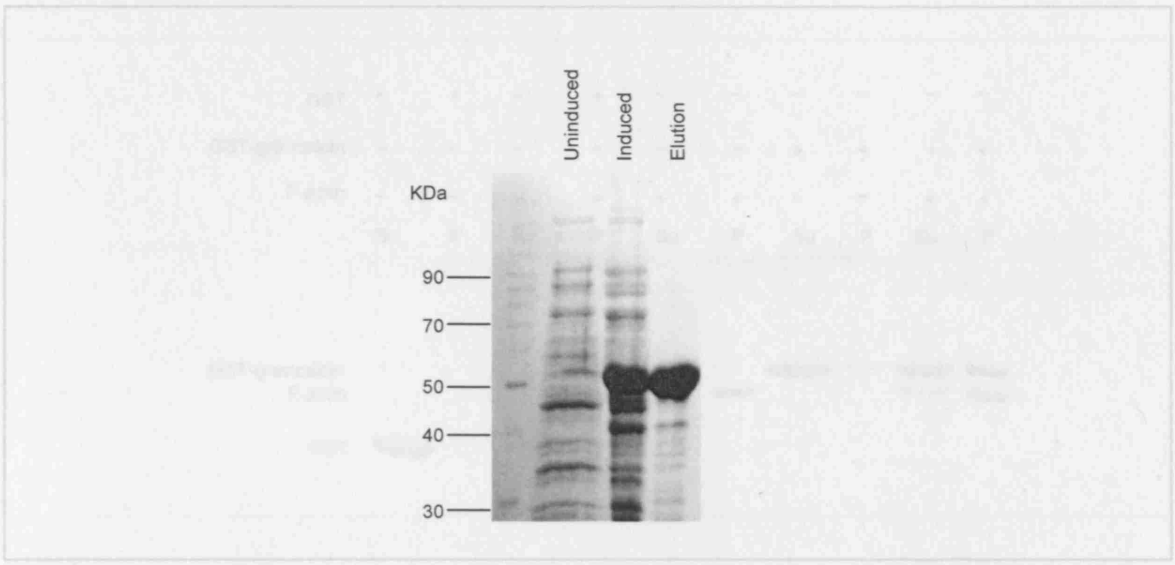

Fig 19. Expression of GST tag full-length human grancalcin in XL1-blue competent *E.coli.*

Single colonies were picked from LB Agar plates containing ampicillin and bacteria grown as described in the methods section. Bacteria were lysed in lysis buffer and GST-grancalcin was eluted from the Sepharose beads with the reduced form of glutathione. Samples from each step were taken and mixed with SDS sample buffer. 10µl of each sample were analysed by SDS-PAGE and stained with Coommassie Blue R-250.

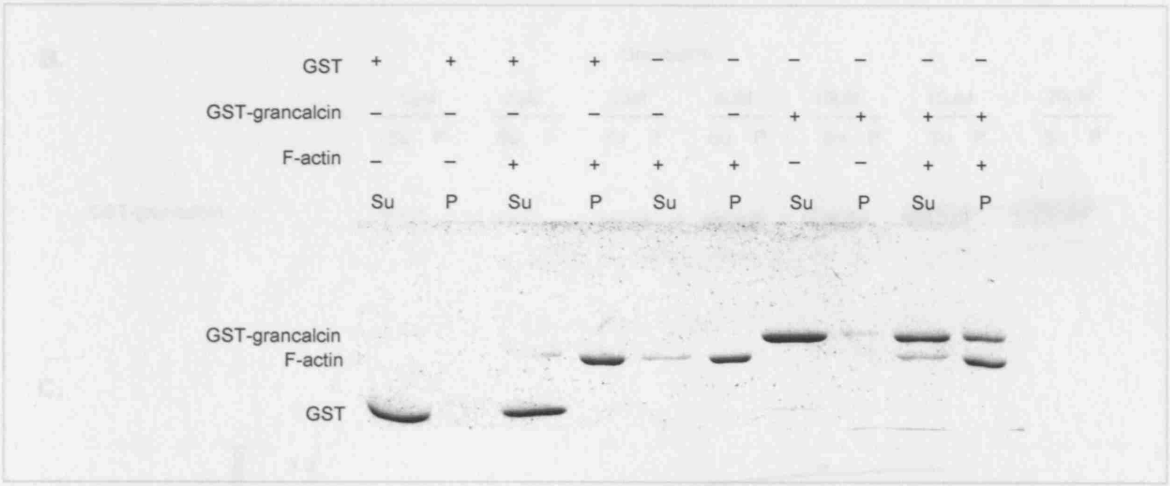

Fig 20. Direct binding of grancalcin to actin.
Mixtures of proteins as indicated were centrifuged at high-speed. Supernatant (Su) and pellet (P) were then analysed by SDS-PAGE and stained with Coommassie. Most of the actin was found in the pellet under these conditions and so were the actin associated proteins. GST and GST-grancalcin alone were not observed in the pellet. GST-grancalcin was cosedimented when incubated with F-actin, thus suggesting it was an actin binding protein. Data are representative of three independent experiments.

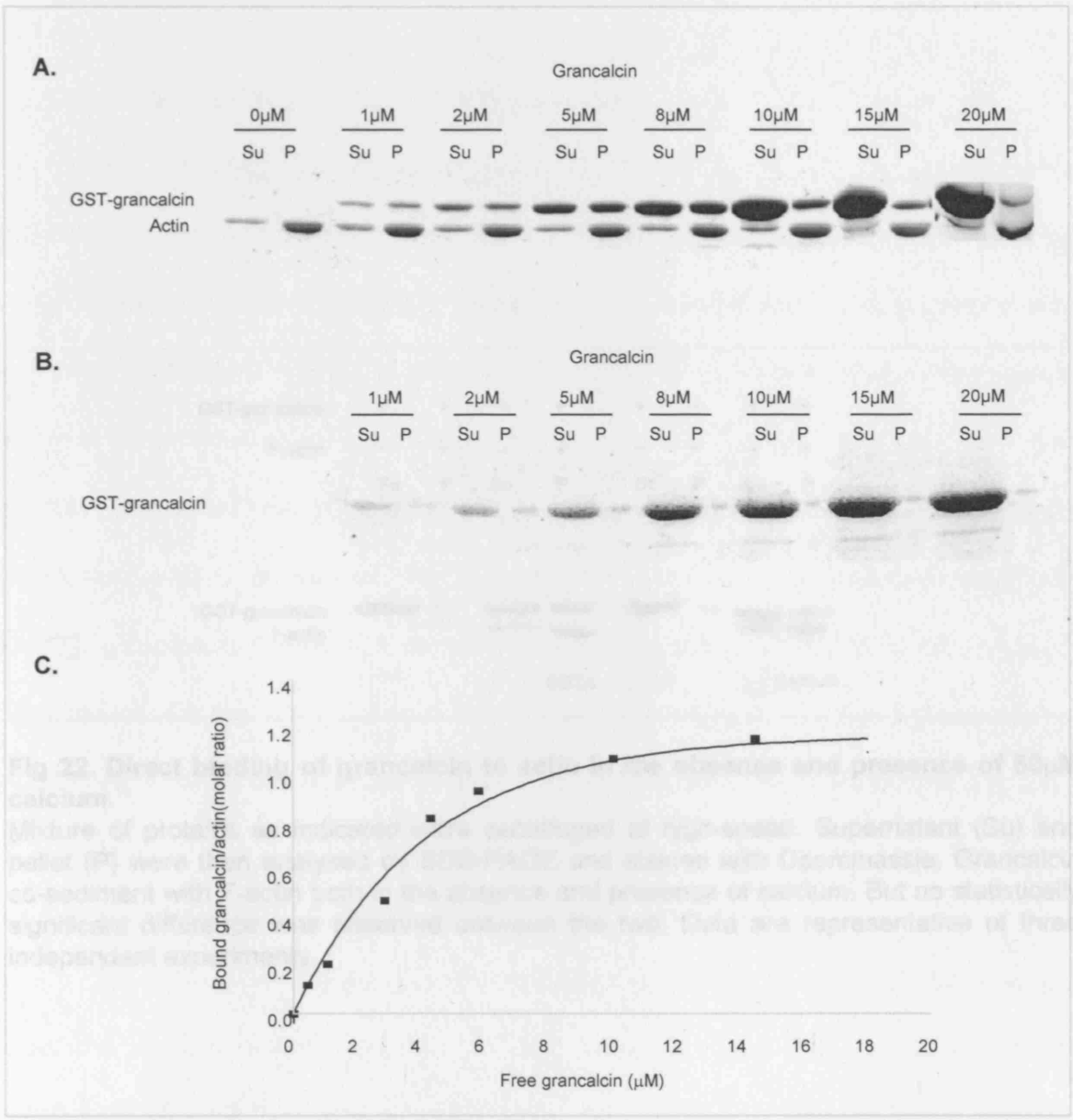

Fig 21. Stoichiometric binding of grancalcin and F-actin.
(A) Co-sedimentation assay of grancalcin with F-actin. Increased amounts of grancalcin were mixed with a fixed amount of F-actin, incubated for 30 mins, and then centrifuged at high speed to pellet cytoskeletal polymer and associated protein. Pellets (P) and supernatants (Su) were analysed on a 10% SDS-PAGE and stained with Coomassie. (B) Sedimentation of grancalcin alone as a control. The centrifugation was at the same condition as under (A). (C) The gels were then dried and scanned using Sicon Image software to generate the stoichiometric binding curve. Grancalcin binds to F-actin in a 1.1 to 1 ratio and kd=2.5×10^{-6} M. Data are representative of three experiments.

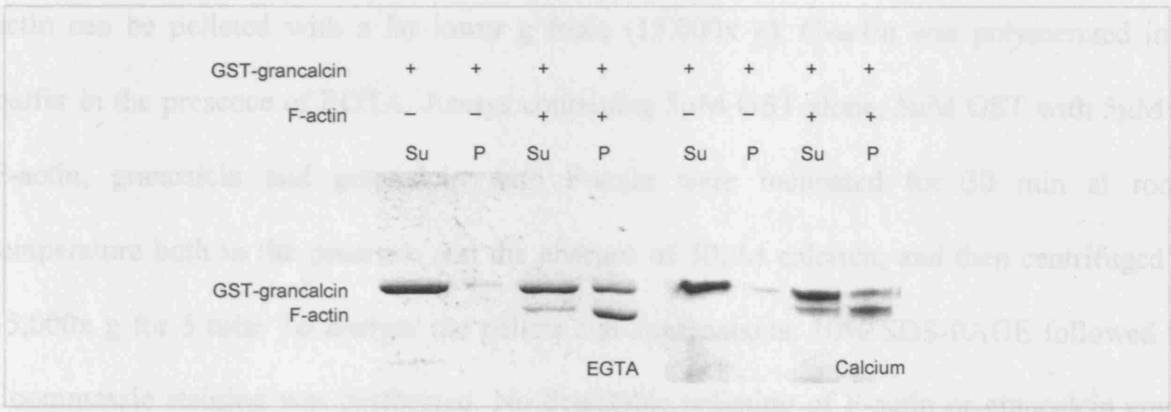

Fig 22. Direct binding of grancalcin to actin in the absence and presence of 50μM calcium.

Mixture of proteins as indicated were centrifuged at high-speed. Supernatant (Su) and pellet (P) were then analysed by SDS-PAGE and stained with Coommassie. Grancalcin co-sediment with F-actin both in the absence and presence of calcium. But no statistically significant difference was observed between the two. Data are representative of three independent experiments.

presence of calcium, and then centrifuged at high-speed. No statistically significant difference was observed in terms of the binding of grancalcin to F-actin in both conditions (Fig 22).

3.2.3. Actin-bundling activity of GST-grancalcin

As grancalcin forms dimers (Jia et al., 2000), we set out to examine whether grancalcin is able to bundle the F-actin fibres. Sedimentation of single F-actin filaments needs a high centrifugation force (375,000x g), but the cross-linked (bundled) large complexes of F-actin can be pelleted with a far lower g force (15,000x g). G-actin was polymerized in F buffer in the presence of EGTA. Assays containing 5μM GST alone, 5μM GST with 5μM of F-actin, grancalcin and grancalcin with F-actin were incubated for 30 min at room temperature both in the presence and the absence of 50μM calcium, and then centrifuged at 15,000x g for 5 min. To analyse the pellets and supernatants, 10% SDS-PAGE followed by Coommassie staining was performed. No detectable pelleting of F-actin or grancalcin could be observed in both conditions, indicating that grancalcin does not bundle F-actin (Fig 23).

3.2.4. Co-localization of Myc-grancalcin with F-actin *in vivo*

In order to investigate the co-localization of grancalcin and F-actin *in vivo*, we selected a monkey kidney cell line (COS-7) as the host cell for transfection. The co-localization of a MyC-grancalcin and F-actin was analysed by transfection of grancalcin-containing pRKMyC vector into these cells. The plasmid map of pRKMyC is illustrated in Fig 24A. Grancalcin was fused in frame with a MyC tag so that it could be detected by an anti-MyC antibody. Grancalcin was subcloned into pRKMyC and positive clones were identified by digestion with restriction enzymes BamHI and EcoRI. Clones 1,2,3,5,6,8,9, and 10 were identified as positive (Fig 24B). There were one PstI sites in pRKMyC plasmid as illustrated and one in grancalcin. Fig 24C shows the confirmation of the identification of the positive clone 1.

After transfection, COS-7 cells were fixed with paraformaldehyde, permeabilised with Triton X-100 and double labelled with rhodamine-phalloidin for F-actin and anti-Myc antibody followed by FITC-conjugated secondary antibody to identify expressed pRKMyC-grancalcin. No obvious labelling of FITC of non-transfected cells, which served as negative control, was observed. The colocalization of F-actin with MyC-grancalcin at the membrane ruffle of the COS-7 cells was apparent (Fig 25). Therefore, this result was suggestive of the co-localization of grancalcin and F-actin *in vivo*.

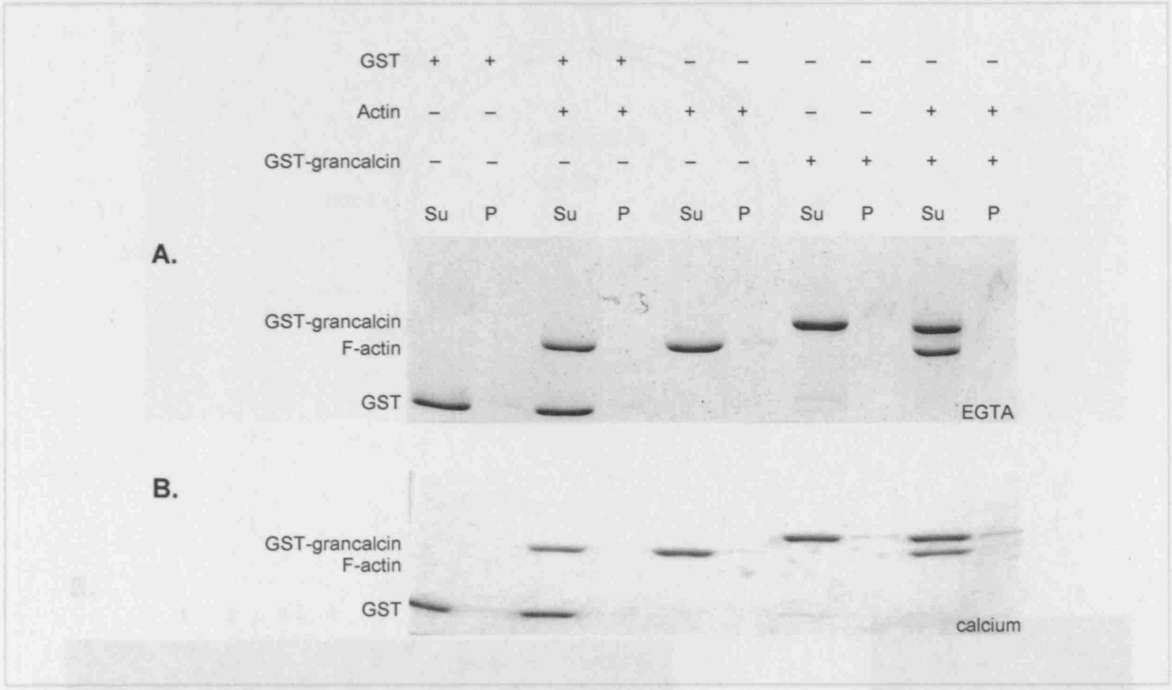

Fig 23. Actin bundling activity of grancalcin as analysed by low speed cosedimentation of GST-grancalcin and F-actin in the presence and absence of calcium.

Mixture of proteins as indicated were centrifuged at low speed, and visualized by Coomassie staining of supernatant (S) and pellet (P) fractions. F-actin was found in the supernatant under these conditions. When GST or GST-grancalcin was added, the amount of F-actin in the pellet was unchanged suggesting that GST-grancalcin does not have F-actin bundling activity. Data are shown in the absence (A) and presence (B) of calcium.

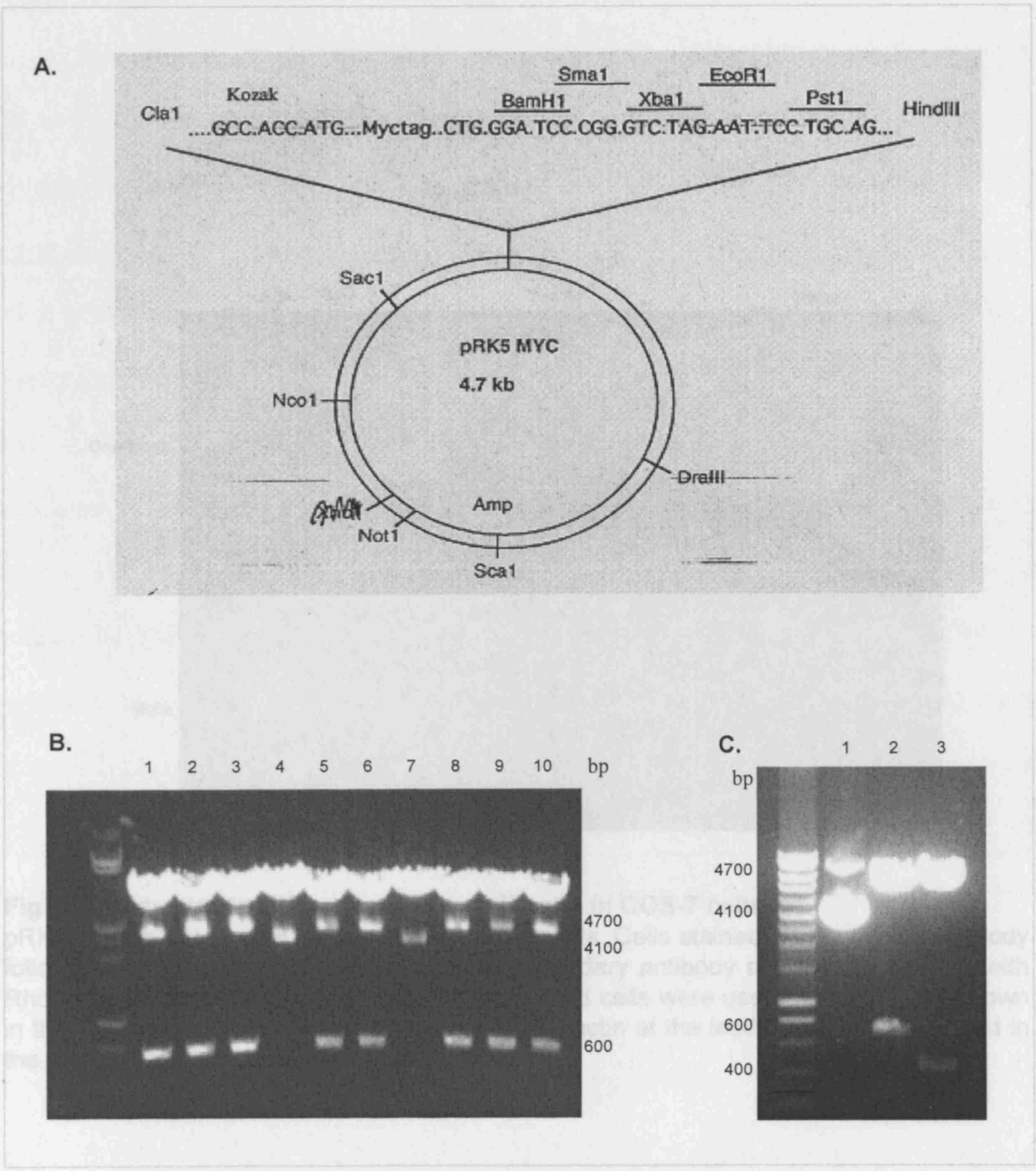

Fig 24. The identification the positive clone of pRKMyC grancalcin.
(A) The illustration of the pRKMyC plasmid map. (B) Grancalcin was subcloned into pRKMyC and positive clones were identified by digestion with restrictive enzymes BamH1 and EcorR1. Clones 1,2,3,5,6,8,9 and 10 were identified as positive. (C) The confirmation of the identification of the positive clone 1. Lane 1: the uncut plasmid, lane 2: the plasmid digested with BamH1 and EcoR1 and lane 3: after the digestion with Pst 1, resulting in a DNA fragment of 400bp.

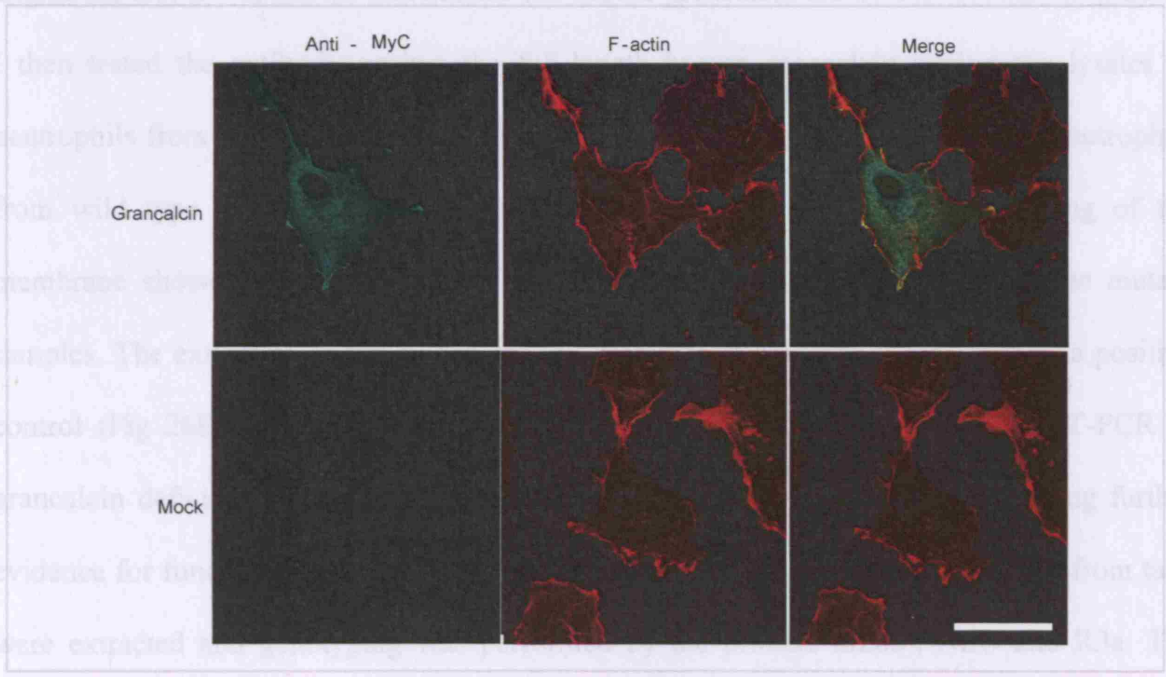

Fig 25. Colocalization of grancalcin and F-actin in COS-7 cells.
pRKMyC-grancalcin was transfected in COS-7 cells. Cells stained with anti-MyC antibody followed by FITC labelled goat anti-mouse secondary antibody and F-actin staining with Rhodamine-phalloidin (upper panel). Untransfected cells were used as control and shown in the lower panel. Grancalcin colocalised with F-actin at the leading edge as indicated in the merge panel. Scale bar equals to 5μm.

3.3 INVESTIGATION OF THE FUNCTION OF GRANCALCIN

3.3.1. Characterization of grancalcin-deficient mice

Grancalcin-deficient mice were characterized by western blotting and genotyping. The antibody against the SYSPADDSMWTYFTAB peptide from the mouse grancalcin sequence in the first EF hand produced weak staining in the wild type. By using the NCBI alignment tool it was shown that human and mouse grancalcin are 81.4% identical (Fig 26A). I then tested the antibody against the full-length human grancalcin against the lysates of neutrophils from both human and mouse. This antibody recognised grancalcin in neutrophils from wild type mice and no signal was found in $Gca^{-/-}$ mice. Ponceau staining of the membrane showed the equal loading of the proteins from the wild type and the mutant samples. The extract from the human granule fractions in neutrophils was used as a positive control (Fig 26B). Neither full-length nor truncated mRNA were detected by RT-PCR in grancalcin deficient mice using primers flanking the insertion in exon 4, providing further evidence for functional inactivation of the Gca gene (Roes et al., 2003). The DNA from tails were extracted and genotyping was performed by the primers m285', NEO and R3a. The resulting 1000bp or 600bp products reflected the differences between grancalcin deficient mice and wild type respectively (Fig 27).

3.3.2. Normal respiratory burst in grancalcin$^{-/-}$ PMN

As grancalcin is a Ca^{2+} -binding protein and regional increases in $[Ca^{2+}]i$ are strategically located to modulate such cellular functions as oxidative activity and degranulation (Sawyer et al., 1985), we therefore examined whether the absence of grancalcin affects NADPH oxidase activation. Neutrophils from wild type or grancalcin-deficient mice were stimulated with phorbol-12-myristate-13-acetate or heat-killed *S.aureus*. When treated with PMA, the maximal rate of superoxide production, was 4.51±0.15 nmol/10^7 cells/min in

A.

```
81.4% identity in 220 aa overlap; score: 1230 E(10,000): 4.7e-103

               10         20          30         40         50
human   MAYPGYGGGFGNFS IQVPGMQM--GQPVP ETGPAILLDGYSGP-AYSDTYSSAGDSVYTY
mouse   MAYPGYGGAFGNFS GQIPGMQMQMGQPMP GAGPNMFSGGYPGYLGYSDSYSPADDSMWTY
               10         20          30         40         50         60
         60         70         80         90         100        110
human   FSAVAGQDGEVDAEELQRCLTQSGI  NGTYSPFSLETCRIMIAMLDRD HTGKMGFN AFKEL
mouse   FTAVAGQDGEVDAEELQRCLTQSGI  SGTYAPFSLETCRIMIAMLDRD YTGKMGFN EFKEL
               70         80          90         100        110        120
        120        130        140         150        160        170
human   WAALNAWK ENFMT VDQDGSGTVEHHEL RQAI GLMGYRLSPQTL TTIVKRYSKNGRIFFDD
mouse   WAALNAWK QNFMT IDQDQSGTVEHHEL SQAI ALMGYRLSPQTL AAIVRRYSKNGRIFFDD
               130        140         150        160        170        180
        180        190        200         210
human   YVACCVKLRALTDFFR KRDHLQQG SANFIYDDFLQGTM AI
mouse   YVACCVKLRALTDFFR RRDHLQQG IVNFMYEDFLQGTM TI
               190        200         210        220
```

B.

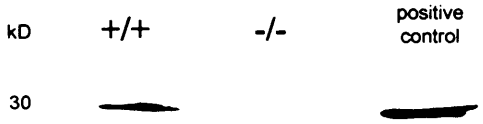

Fig 26. Identification of murine grancalcin by antibody raised against human grancalcin.

(A) Alignment of human and mouse grancalcin using NCBI alignment tool. The identical amino acids are shown in red and the non-consensus amino acids are shown in blue. (B) Western blot of murine neutrophils was performed with antibody to human grancalcin. It shows the band of grancalcin protein with a molecular mass of 28kD detected in neutrophil lysate from wild type mice but no signal was detected in the grancalcin$^{-/-}$ mice. Granule fraction from human neutrophils was employed as a positive control.

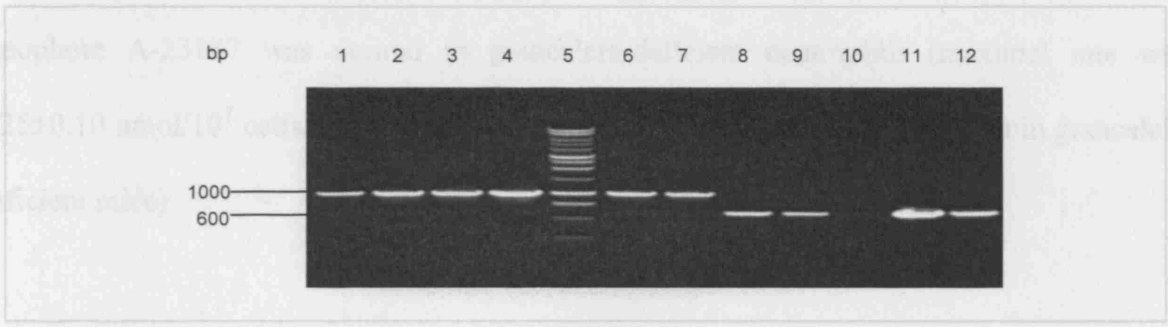

Fig 27. Genotyping of the grancalcin-deficient mice.
DNAs from tails of both the $Gca^{-/-}$ mice and wild type mice were extracted and PCR was performed. The wild-type showed a band at 600bp (lane 8-12). DNA isolated from grancalcin deficient mice produced a band of 1000bp (1-7).

wild type and 3.66±0.056 nmol/10^7 cells/min in grancalcin-deficient neutrophils (Fig 28). This difference was not statistically significant. The lag phase time to maximal rate which reflects the activation of NADPH oxidase was also not significantly changed, being 45.17±2.35 seconds in the normal and 49.5±1.5 seconds in the mutants. The respiratory burst after stimulation with IgG coated *S.aureus* in the wild type and grancalcin-deficient neutrophils was also not changed significantly. The maximal rate was 2.26±0.77 nmol/10^7 cells/min in the wild type and 1.99±0.61 nmol/10^7 cells/min in the grancalcin-deficient neutrophils. Furthermore, activity of NADPH oxidase induced by Ca^{2+} influx by calcium ionophore A-23187 was normal in grancalcin-deficient neutrophils (maximal rate was 0.25±0.10 nmol/10^7 cells/min in wild type versus 0.25±0.07 nmol/10^7 cells/min in grancalcin deficient mice).

3.3.3. Degranulation of grancalcin-deficient neutrophils

Grancalcin was enriched around the phagocytic vacuole as previously shown by immunoblotting and immunohistochemistry, and grancalcin deficient mice were less susceptible to LPS-induced shock (Roes et al., 2003). Taken together, this phenomenon could be explained by the involvement of grancalcin in degranulation, as the release of granule contents may enhance the damaging effects of septic shock. In order to examine this hypothesis, degranulation was analysed by extracellular release of marker proteins for the secondary granule marker lactoferrin. Degranulation measured in this way was normal in response to PMA in neutrophils from grancalcin–deficient mice (Roes et al., 2003). However, this assay measures only the extracellular degranulation but not the release into the phagocytic vacuole. To further determine the effects of grancalcin on degranulation, we sought to assess degranulation parameters at the ultrastructural level. Ideally, the three dimensional stack should be analyzed. But in this case, we measure the degranulation in two-dimension. We first

		Wild type	grancalcin$^{-/-}$
A.	Maximal rate (nmol/10^{7}cells/min)	4.51±0.15	3.66±0.056
	Time to maximal rate (seconds)	45.17±2.35	49.5±1.5
B.	Maximal rate (nmol/10^{7}cells/min)	2.26±0.77	1.99±0.61
	Time to maximal rate (seconds)	106.4±17.65	111.2±26.46

Fig 28. The superoxide production of neutrophils from wild type and grancalcin-deficient mice.
(A) Stimulation of neutrophils from wild type and grancalcin-deficient mice with PMA induced similar in maximal rate of superoxide production and time to maximal rate. (B) Stimulation with heat killed *S.aureus* induced a normal respiratory burst. Analysis of the data were given as mean ± SE (n=3).

measured the surface area of the neutrophils vs. the granule numbers on EM sections of resting neutrophils, and we found that there was no significant difference in numbers of granules in bone marrow neutrophils from grancalcin-deficient mice (Fig 29). We then stimulated neutrophils with IgG-opsonised *S. aureus* and analysed degranulation at various time points. The numbers of granules in grancalcin-deficient neutrophils at unstimulated state was significantly lower than that in the wild type ($P<0.05$), but no difference was observed after IgG-coated *S.aureus* stimulation, indicating that either the degranulation was significantly increased during the transmigration in grancalcin-deficient mice, or the degranulation in grancalcin deficient mice was impaired during the phagocytosis process (Fig 30).

3.3.4. Recruitment of neutrophils to the inflammatory site of $Gca^{-/-}$ mice was not changed.

The recruitment of granulocytes into the peritoneal cavity requires rolling, adhesion and transmigration. These processes are dependent on β_2 integrin (Lindbom et al., 2002). We tested whether the recruitment of neutrophils to the inflammatory site of mutant and normal mice is different. Cells from peritoneal lavages were stained with the macrophage surface marker F4/80 antibody and neutrophil surface marker Gr-1 antibody in order to analyse the two populations in the peritoneal cavity. Fig 31 shows neutrophils and macrophages to be separated by the forward scatter, side scatter and fluorescence channels. The results show that in grancalcin-deficient mice, the recruitment neutrophils and macrophages to this inflammed site was normal.

3.3.5. Requirement of grancalcin for fibronectin mediated adhesion

Two previous reports suggested that grancalcin might have a role in neutrophil adhesion (Chen, et al., 2003; Correia, et al., 1999). Firstly, grancalcin belongs to the same

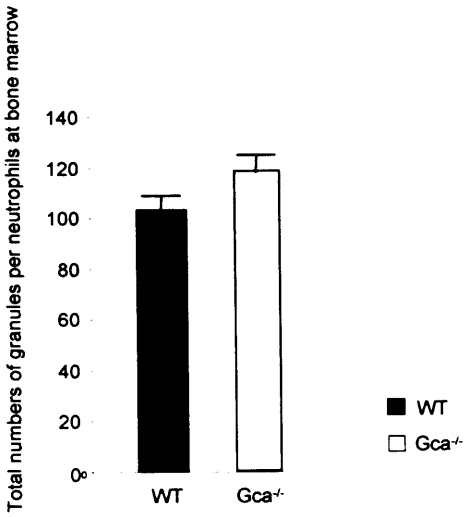

Fig 29. Quantification of total numbers of granules in unstimulated neutrophils isolated from bone marrow.
The EMs show no significant difference in appearance and numbers of granules in neutrophils from bone marrow between wild type and $Gca^{-/-}$ mice. Data are mean ± S.E. from the analysis of at least eight EM sections analysed.

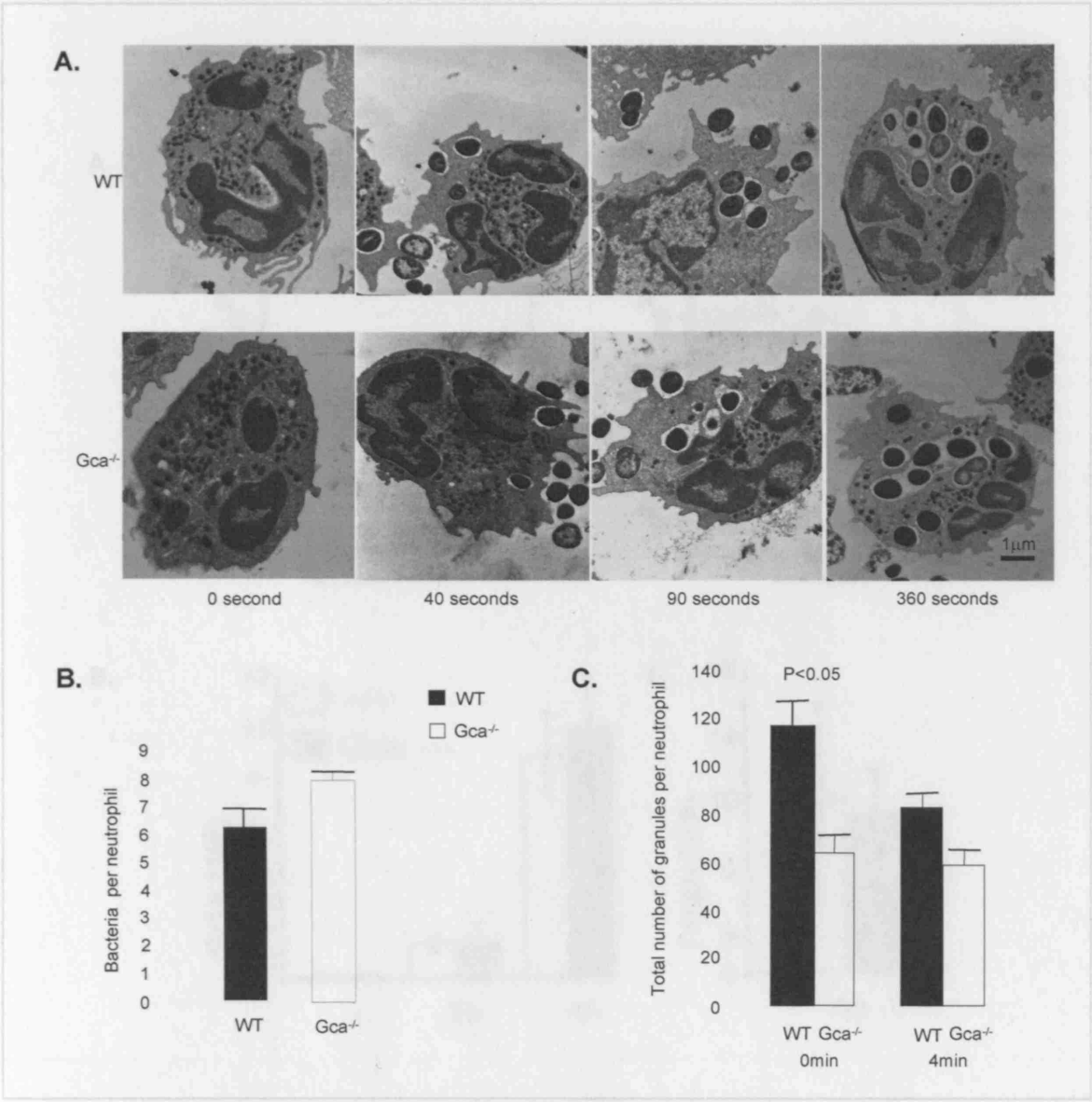

Fig 30. Degranulation of grancalcin-deficient neutrophils.
(A) Transmission electron micrographs of neutrophils stimulated with IgG-coated *S.aureus* at time points 0, 40, 90 and 360 seconds. (B) The numbers of bacteria phagocytosed by the neutrophils from wild type and mutant were similar. (C) Total number of granules per neutrophil isolated from peritoneal cavity of mice with sterile peritonitis induced by thioglycollate. There was a significant decrease of granules in the grancalcin-deficient mice compared to the wild type at unstimulated state, but no difference was observed after phagocytosis of IgG-coated *S.aureus*, indicating that the degranulation in grancalcin-deficient mice is impaired ($P<0.05$). Data are mean ± S.E. from the analysis of at least eight EM sections.

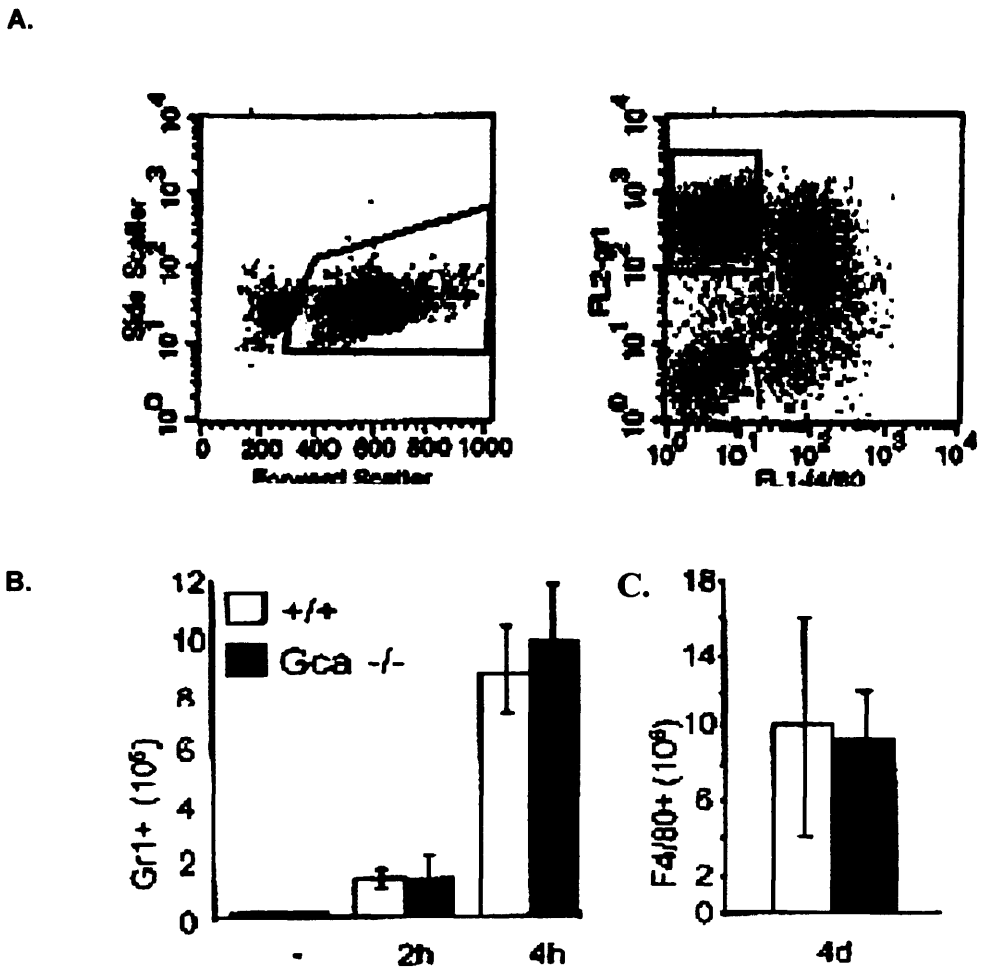

Fig 31. Leukocyte recruitment in grancalcin-deficient mice.
(A) PMN granulocytes and macrophages were obtained by peritoneal lavage and identified by flow cytometry as Ly-6G- (Gr-1) or F4/80-positive cells respectively. (B and C) Neutrophil (B) and macrophage (C) recruitment in sterile peritonitis. PMN granulocytes and macrophages were obtained by peritoneal lavage at the time points indicated after injection of thioglycolate and identified by flow cytometry as indicated in (A).

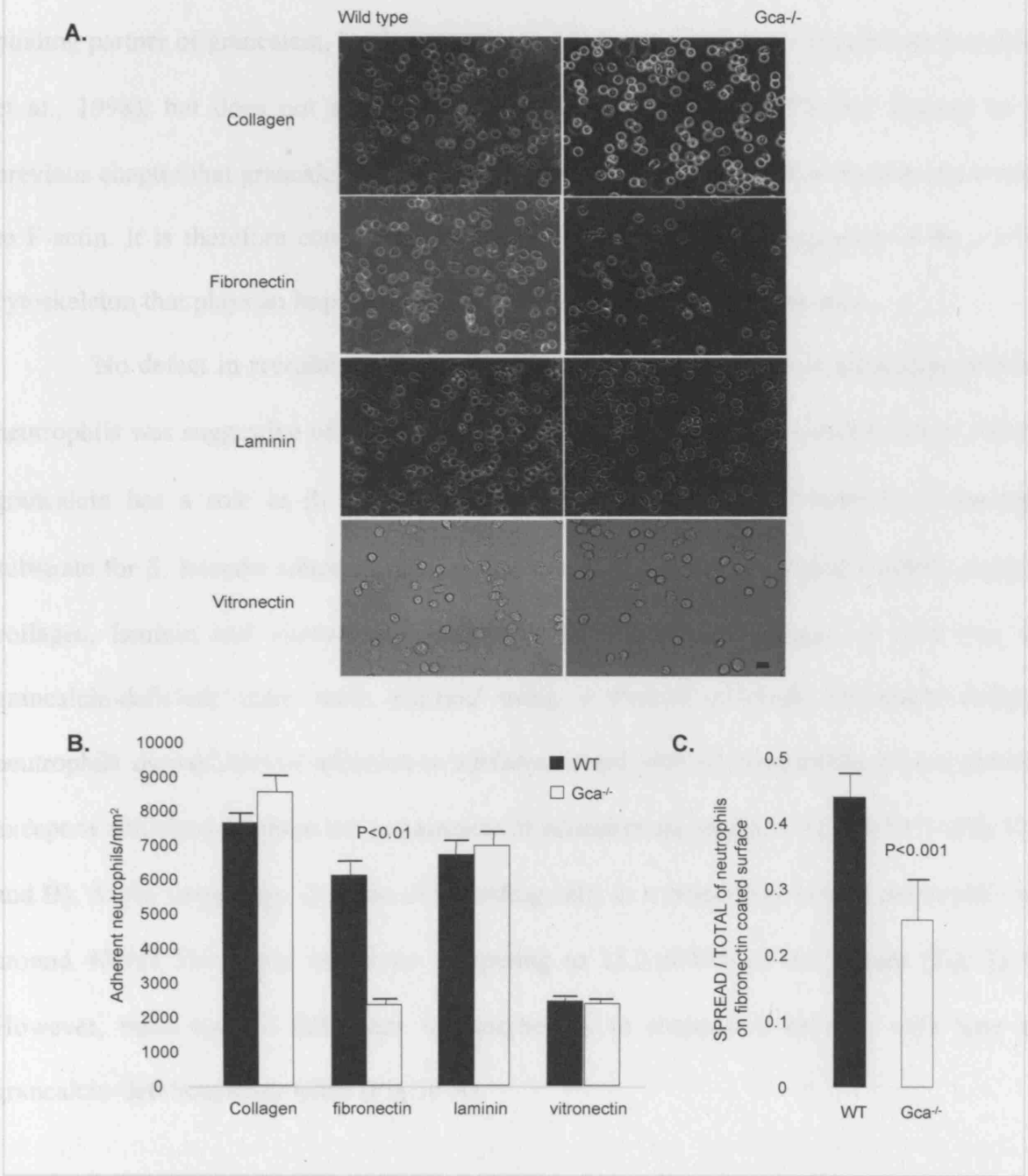

Fig 32. The adhesion of neutrophils from peritoneal lavages on collagen, fibronectin, laminin and vitronectin coated surfaces and spreading of neutrophils on fibronectin coated surface.

(A) The phase images of neutrophil adhesion to different substrates. One of ten random images is shown. (B) Adhesion of neutrophils per mm^2 to surfaces coated with different substrates as obtained under figure A. (C) The ratio of spreading neutrophils to total adherent neutrophils on fibronectin coated coverslips. Data given as mean ±SE. Cells were counted in at least ten randomly selected fields. Scale bar equals to 10 μm.

family of proteins as calpain, which has recently been found to be involved in integrin mediated adhesion (Goll et al., 2003; Han et al., 2000; Jia et al., 2000). Secondly, L-plastin, a binding partner of grancalcin, has been implicated in the regulation of integrin function (Jones et al., 1998), but does not affect β_2 integrin-mediated adhesion. We also showed in the previous chapter that grancalcin is predominantly found in the membrane fraction and it binds to F-actin. It is therefore conceivable that grancalcin might be a component of the cortical cytoskeleton that plays an important role in the regulation of integrin function.

No defect in recruitment to the site of a sterile inflammation in grancalcin-deficient neutrophils was suggestive of normal β_2 integrin levels. We therefore decided to test whether grancalcin has a role in β_1 and β_3 integrin-mediated adhesion. Fibronectin is the main substrate for β_1 integrin adhesion, but we also tested additional extracellular matrix proteins: collagen, laminin and vitronectin. Neutrophils from peritoneal lavages of wild type and grancalcin-deficient mice were purified using a Percoll gradient. Grancalcin-deficient neutrophils showed normal adhesion to surfaces coated with all extracellular matrix proteins, except to fibronectin, where the impairment of adhesion amounted to 61.8±2.93% (Fig 32 A and B). At the same time, the ratio of spreading cells as a proportion of total neutrophils was around 43.9±3.5% in the wild type comparing to 25.2±6.00% in the mutant (Fig 32 C). However, there was no difference in morphology in suspension between wild type and grancalcin-deficient neutrophils (Fig 30 A).

3.3.6. Requirement for grancalcin in cytoskeletal rearrangement

Since grancalcin-deficient leukocytes spread and adhere less on a fibronectin coated surface, and grancalcin was found in all three cytoskeletal compartments in neutrophils, we tested whether the absence of grancalcin also affects cytoskeleton rearrangement during neutrophil adhesion and spreading. We therefore stained F-actin in granulocytes adhered to a

FN-coated surface. F-actin in both wild type and grancalcin-deficient neutrophils was mostly present as cortical actin. In contrast to around 1.64±0.35 focal adhesion counts per neutrophil from the neutrophils of grancalcin-deficient mice, large punctuate structures at the adhesion site of the cell were mainly observed in the neutrophils from the wild type at 12.38±1.51 per cell, as well as dominant F-actin ruffles at the membrane (Fig 33).

3.3.7. The fibronectin-mediated phagocytosis is impaired in grancalcin-deficient mice

As fibronectin acts as opsonin, we tested the efficiency of grancalcin-deficient neutrophils in phagocytosis of fibronectin-opsonized bacteria (Blystone et al., 1994 and 1999). We then chose to test whether grancalcin is involved in this process. Fig 34 shows that phagocytosis was impaired in the mutants comparing to the wild type after 8 minutes. Some bacterial strains express a host of fibronectin binding proteins such as shdA and invasin to infect host cells (Kingsley et al., 2004). As $\alpha_5\beta_1$ integrin is the main fibronectin receptor in neutrophils, a defect in interaction of fibronectin and $\alpha_5\beta_1$ integrin could affect killing of fibronectin opsonised bacteria by neutrophils. These observations support our original hypothesis that grancalcin has a role in the antimicrobial response.

3.3.8. Expression of integrins at the surface of grancalcin-deficient neutrophils

Reduced adhesion of neutrophils from grancalcin-deficient mice may be due to the reduced expression of the surface integrins. To test this possibility, we investigated the surface expression of the β_1, β_2, α_4 and α_5 integrins on neutrophils, using IgG_{2b} antibody as isotype control (Fig 35). The expression of α_4 integrin defined by the parameter of percentage gated cells, was significantly reduced (25.37% in grancalcin-deficient compared to 34.68% in the wild type mice). However, the comparison of values measuring fluorescence intensity (Geomean) showed no difference in either α_4 or α_5 (data not shown). The expression of α_5

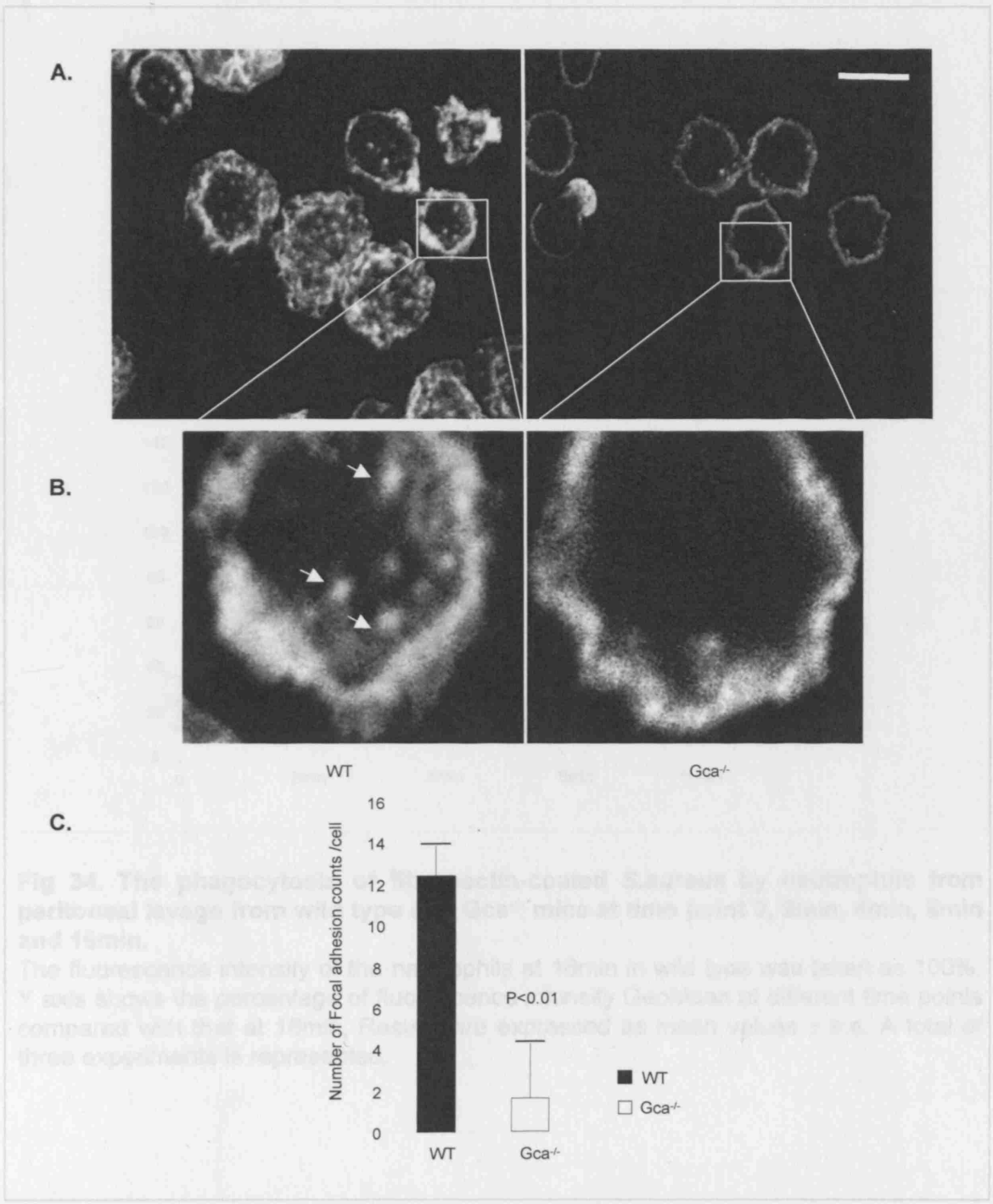

Fig 33. Actin staining of neutrophils adhered to fibronectin.
(A) Neutrophils from wild type and $Gca^{-/-}$ mice from peritoneal lavage were stained for actin with phalloidin and visulized by fluorescence microscopy. Wild type neutrophils were well spread with well demonstrated membrane ruffling. (B) The enlarged images of individual cells. The arrow marks F-actin staining. Images were taken with 100 x magnification. Representative of at least 20 images. (C) The statistic analysis of the adhesion structures of peritoneal neutrophils from wild type and grancalcin-deficient mice on fibronectin coated surface. Scale bar equals to 5μm.

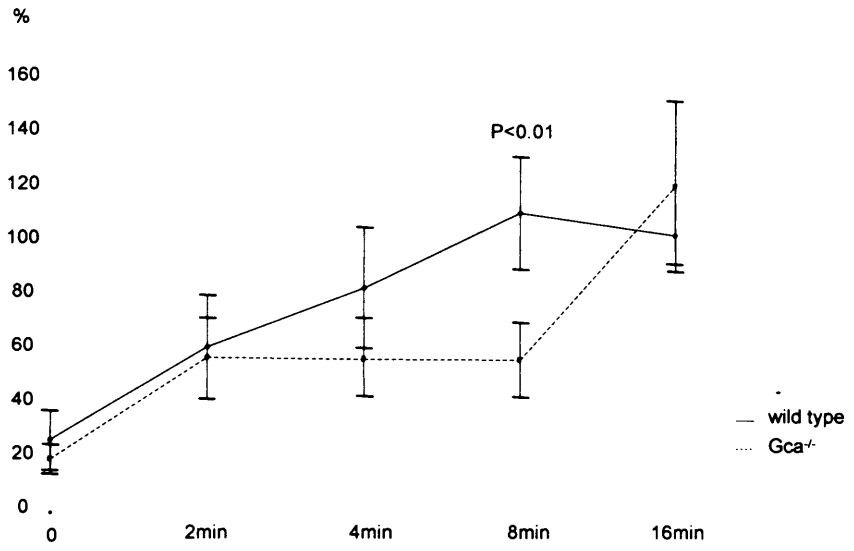

Fig 34. The phagocytosis of fibronectin-coated *S.aureus* by neutrophils from peritoneal lavage from wild type and $Gca^{-/-}$ mice at time point 0, 2min, 4min, 8min and 16min.

The fluorescence intensity of the neutrophils at 16min in wild type was taken as 100%. Y axis shows the percentage of fluorescence intensity GeoMean at different time points compared with that at 16min. Results are expressed as mean values ± s.e. A total of three experiments is represented.

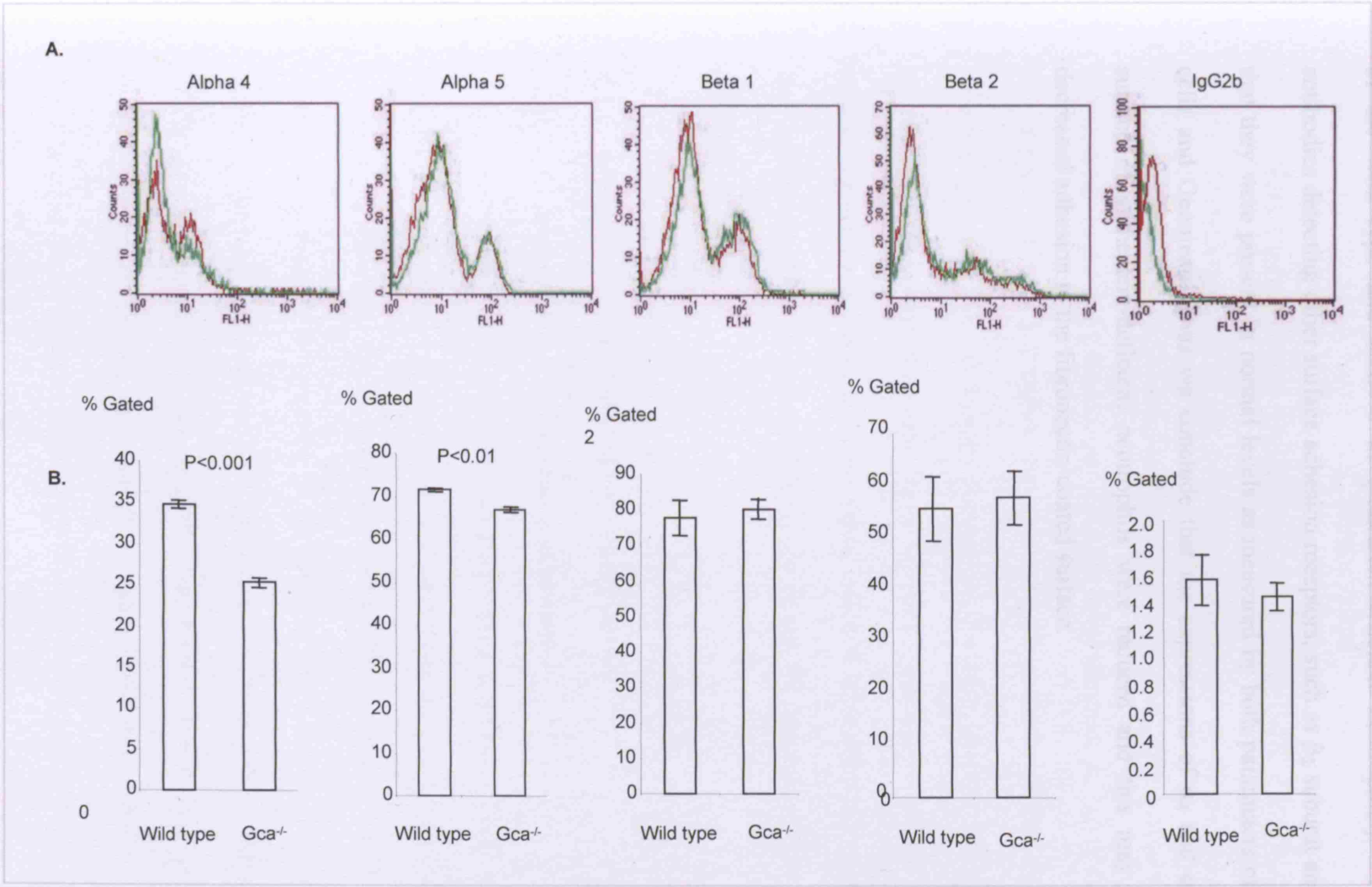

Fig 35. Integrin expression on neutrophils from wild type (red line) and grancalcin$^{-/-}$ mice (green line).
(A) Binding of FITC-conjugated anti α_4, α_5, β_1, β_2 and IgG_{2b} antibodies to neutrophils from peritoneal cavity from wild type and grancalcin deficient mice. (B) The statistic analysis of % gated positively fluorescent cells. Representative of three independent experiments (n=3).

integrin was also significantly reduced by approximately 5% in grancalcin-deficient (71.63% in the wild type and 66.64% in grancalcin-deficient neutrophils). Also, monoclonal antibodies detecting other surface adhesion receptors, such as β_2 subunit and IgG_{2b}, indicated that they were present in normal levels as measured by both parameters of percentage gated cells and Geomean. Thus we conclude that the expressions of α_4 and α_5 integrins at the surface of grancalcin-deficient neutrophils were reduced and this may contribute to the decreased adhesion to the fibronectin-coated surface.

Chapter 4

Discussion

4.1. THE PROTEOMIC ANALYSIS OF NEUTROPHIL CYTOSKELETON

In this study, we set out to perform a proteome analysis on cytoskeleton-associated proteins in several cellular compartments, a first inventory of the cytoskeleton proteome in human neutrophils. The present experiments do not distinguish the up- or down- regulation of the proteins, but are appropriate for obtaining an overview of the distribution of these proteins. The following discussion focuses on the new proteins found in these groups, summarizes the known functional roles of these proteins, considers whether they may involved in the cytoskeletal rearrangements, indicates what functional relevances relay, and how this set of proteins might be related to the neutrophil functions of cytosol, membrane and phagocytic vacuole.

4.1.1. Neutrophil cytosol high-speed pellet proteins

4.1.1.1. Cytosolic polymerised cytoskeletal proteins

As we observed differences between proteins in the cytosol high-speed pellet and the remaining supernatant, it is concluded that the high-speed pellet fractionated the cytosol in some way, assumed the polymerised cytoskeletal structure. By MALDI-TOF mass spectrometry analysis, the majority of the proteins found in this fraction were cytoskeletal proteins, which are in consistent with those found in the neutrophil cytosol (Piubelli et al., 2002). Table 1 includes proteins detected in all types of cytoskeletal subclasses. However, using our global MS-protein identification approach, we were able to add new members to the list of proteins found in the neutrophil cytosolic cytoskeleton, such as eEF1Bγ, TCP1, proteins involved in ubiquitin-proteasome degradation, and proteins involved in energy and metabolism.

eEF1 is a GTP-binding protein that plays a role in protein synthesis by mediating the transfer of aminoacyl-tRNA to 80S ribosomes (Munshi et al., 2001). It is formed by four subunits A, Bα, Bβ, and Bγ. Both eEF1Bα and eEF1Bβ have ganunine nucleotide exchange activities. eEF1A has conserved actin-binding activity (Demma et al., 1990), and has also been shown to associate with tubulin and microtubules in some cell types (Marchesi et al., 1993; Durso et al., 1994; Shiina et al., 1994). In quiescent cells, around half of the cellular eEF1A is associated with the cytoskeleton and it displays a diffuse distribution throughout the cytoplasm. Upon stimulation with cytokines that stimulate cell motility, the distribution of eEF1A concentrates into *de novo* actin-containing surface projections (Dharmawardhane et al., 1991). The biological function of this association is suggested to influence the efficiency of mRNA translation (Kreis et al., 1999). eEF1Bγ tightly forms a complex with the β unit, and the complex shows functions in protein synthesis or cellular proliferation (Cho et al., 2003; Jonusiene et al., 2005). Our results suggest that eEF1Bγ may also have actin binding property.

TCP1 is a cytosolic molecular chaperone known to associate with the cytoskeleton. It was implicated in the biogenesis of cytoskeletal proteins by promoting the correct folding of the major ubiquitous cytoskeletal components actin and tubulin (Chen et al., 1994). It has been previously demonstrated to associate with erythrocyte actin fibres only following their exposure to elevated temperature (Wagner et al., 2004). Interestingly, in neutrophils, as shown here, TCP1 is associated with the cytoskeleton even without prior heat shock, thus indicating a different role of this protein in neutrophils.

4.1.1.2. Proteins involved in ubiquitin and proteasome degradation

We also identified a group of proteins involved in the ubiquitin and proteasome pathways. Intracellular proteolytic systems recognise and destroy misfolded damaged proteins, unassembled polypeptide chains and short-lived regulatory proteins. The ubiquitin-

proteasome pathway is one of the mechanisms for protein degradation within cells. It functions widely in intracellular protein turnover (Hartmann-Petersen et al., 2004). The pathway employs an enzymatic cascade by which multiple ubiquitin molecules are covalently attached to the protein substrate. The polyubiquitin modification marks the protein for destruction and directs it to the 26s proteasome complex for degradation.

Two possibilities are suggested to account for the presence of these proteins involved in ubiquitin and proteasome degradation into the cytosol high-speed pellet, One is that because the molecular weight of this macrocomplex is around 2500kDa, it is easily to be pelleted at high centrifuge force. Another explanation is that its presence is due to its association with the cytoskeletal proteins. Previously, the involvement of proteasome proteins with actin microfilaments, microtubules, and intermediate filaments has been established. When the capacity of the proteasome is exceeded by the production of misfolded proteins, the formation of intracellular protein aggregates occurs (Bassaglia et al., 2005; Johnston et al., 1998). These structures are designated as aggresomes, and are associated with IFs and ubiquitin. Microtubules are also required for aggresome formation, but not in its long-term maintainance (Johnston et al., 1998). Aggresomes are pericentriolar, membrane-free cytoplasmic inclusions containing misfolded and ubiquitinated protein ensheathed in cages composed of IFs (Johnston et al., 1998). This could explain why these proteins have solely been observed in the cytosolic cytoskeletal structures.

Furthermore, aggresomes are structurally associated with cytoskeletal proteins microtubules and intermediate filaments, rather than they function as cytoskeletal proteins themselves. Retrograde transport on microtubule is used to deliver misfolded protein aggregates from the peripheral sites where they are generated to a central location at the microtubule-organizing center (MTOC), while the dense network of intermediate filaments that encircle and enmesh the aggresome serves to stabilize this structure by restricting the diffusion of aggregated protein particles (Johnston et al., 1998). This macromolecular

structure has also been suggested in the association with the actin cytoskeleton by cryoelectron tomography (Medalia et al., 2002). By examining the molecular organization of the cytoplasm through this non-invasive three-dimensional imaging technique, the 26S proteasome has been shown to physically associate with microfilaments in an unperturbed cellular enviroment (Medalia et al., 2002). Although proteasomes have been considered as true components of the myofibrils, due to their binding to actin, gelsolin and other binding partners in myofibrils in mature skeletal muscle, the physiological significance of the association remains unclear (Bassaglia et al., 2005).

4.1.1.3. Energy and metabolic enzymes:

Among the proteins not previously reported to associate with cytosolic skeleton compartment, the majority could be functionally classified as energy and metabolic enzymes: phosphoglycerate mutase 1, transketolase, phosphogluconate dehydrogenase, N-acetylglucosamine kinase and aldehyde dehydrogenase. Consistently, these proteins were previously localized in cytoplasm (Urena et al., 1990; Schenk et al., 1998; Ninfali et al., 2001; Hinderlich et al., 2000; Mossink et al., 2003). Accordingly, several metabolic enzymes identified here were already known to associate with actin microfilaments: glutamate dehydrogenase (Akutsu et al., 2002), glyceraldehyde-3-phosphate dehydrogenase (GAPDH) (Cao et al., 1999; Schmitz et al., 2002), pyruvate kinase (Clarke et al., 1975) and enolase (Gitlits et al., 2000). The association of metabolic enzymes with the cytoskeleton highlights the importance of these enzymes for the following cellular functions.

Polymerisation of actin

The microfilament structure and location are dependent of the energy from nucleotide triphosphate hydrolysis (Carlier et al., 1992; Korn et al., 1987). Numerous studies have demonstrated the interaction between glycolytic enzymes and cytoskeleton. Substantial

association between such structures and individual glycolytic enzymes, such as aldolase, glyceraldehyde-3-phosphate dehydrogenase, have been described both *in vivo* and *in vitro* (Clegg et al., 1984; Walsh et al., 1981; Masters et al., 1991 and 1992; Mejean et al., 1989). The function of the binding between cytoskeletal proteins and metabolic enzyme may be to initiate energy production, or to transport the necessary substrates for the increased cooperative binding of other components (Master et al., 1981 and Stephen et al., 1983). The metabolic elements appear to have evolved a parallel system that provides for the appropriate positioning of an energy-producing sequence in relation to the specific dynamic requirements of the cytoskeleton (Masters et al., 1984).

Apart from the proteins mentioned above, our experiments result in the identification of other proteins in this compartment, which are suggestive of their functional relevance to the cytoskeleton. The pentose phosphate pathway (transketolase and phosphogluconate dehydrogenase) (Schenk et al., 1998), and amino acid activation (N-acetylglucosamine kinase) are some of the other processes occurring in this compartment, and evidence is accumulating that the coordination of structure and function of the cytoskeleton-glycolytic associations may also extend to other 'soluble' pathways (Master et al., 1984), such as starch and sucrose metabolism (glucosidase), and butanoate metabolism (aldehyde dehydrogenase), which potentially related to pyruvate metabolism (KEGG pathway).

Activation of ionic pump activities

Metabolic pathways form multi-enzyme complexes, which channel substrates and connect membranes and nucleic acids to create the extensive, cross-linked, intracellular structure (Norris et al., 1996). For example, ATP-sensitive potassium (K_{ATP}) channels are regulated by adenine nucleotides to convert changes in cellular metabolic levels into membrane excitability (Matsuo et al., 2005), and thus link the metabolism of the cell to the membrane potential. The processes of rundown and reactivation of K_{ATP} channels can be

influenced by the assembly and disassembly of the actin cytoskeletal network, which provides a novel regulatory mechanism of this channel. Actin filament disrupters can attenuate the ATP-dependent inhibitory gating of K_{ATP} channels (Furukawa et al., 1996).

Cytoskeletal organization induces coherent behavior in a metabolic network at the level of control of the flux partition between glycolysis and the pentose phosphate pathway. Additionally, high levels of polymerized microtubule protein increase the robustness of the metabolic network's steady state dynamics. These properties add to the plasticity of mass-energy transforming networks to adapt to changing environmental conditions without losing stability while retaining biological function (Aon et al., 2002).

4.1.2. Detergent-resistant plasma membrane.

Membrane-associated cytoskeletal protein networks are involved in the control of cell shape, attachment to other cells and to the substrate, and organization of specialized membrane domains. In consistent with the literature, proteins that can influence membrane skeleton dynamics, such as moesin, vinlin and coronin, were found in this fraction (Goode et al., 1999).

A protein newly identified is hpast (EHD1). It is a member of the EHD family that contains four mammalian homologs. Three domains of this protein have been suggested, an ATP/GTP-binding site motif, suggestive of enzymatic function (Carson and Welsh. 1995; Deyrup et al., 1998), a bipartite nuclear localization signal, indicative of nuclear targeting (Koike et al., 1999), and an EH domain including an EF-hand calcium-binding motif, which are often associated with protein transport, trafficking and endocytosis (Salcini et al., 1997; Carbone et al., 1997). EHD1 plays a central role in regulating the recycling of various receptors from the perinuclear recycling compartment to the plasma membrane. EHD1 has also been implicated at earlier stages of the endocytic pathway, including the internalization of insulin-like growth factor 1 receptor (IGF-1R). EHD1 is itself regulated by the small

GTPase Arf6 (Caplan et al., 2002), a protein dynamicly cycling between GDP- and GTP-bound states. Arf6 is thought to regulate membrane trafficking and recycling, and to control transport of receptors internalized in a clathrin-independent manner. But if this protein also has an actin regulation role as some related EHD proteins, will require further investigation (Duncan et al., 2001; Wendland et al., 1996).

4.1.3. Detergent-resistant phagosome

The function of the phagosome skeleton proteins such as actin and tubulin is to give structure to the phagosome and to facilitate fusion between phagosomes and late endosomes (Kjeken et al., 2004). We have focused on the analysis of the detergent-resistant phagosome a fraction not analysed in previous proteomics studies (Gagnon et al., 2002; Garin et al., 2001). This is also the first proteomics analysis of neutrophil phagosomes, as previous studies were mainly done on macrophages (Gagnon et al., 2002; Garin et al., 2001). Detection of flotilin (a marker protein of lipid rafts) in detergent-resistant phagosome fraction was consistent with the recent report demonstrating the presence of lipid rafts on phagosomes (Dermine et al., 2001). Three proteins not previously reported to associate with cytoskeleton were found in detergent-resistant phagosome: prohibitin, ficolin and valosin-containing protein.

Prohibitin was previously identified in the proteomic study of the macrophage phagosome proteome (Garin et al., 2001). Although this protein is mainly found in mitochondria, reports indicate that it may associate with certain receptors present at the cell surface (Mishra et al., 2005), a phenomenon that could explain its occurrence on phagosomes, as it is known that plasma membrane is the major source of membrane for phagosome formation (Gagnon et al., 2002). The mitochondrial prohibitin complex consists of two subunits (PHB1 of 32kD and PHB2 of 34kD), assembled into a membrane-associated supercomplex of approximately 1 MD (Back et al., 2002). Overall, as association of prohibitin with lipid rafts has been established (Mielenz et al., 2005). It is plausible that its

presence in our Triton X-100 insoluble phagosome fraction does not derive from its association with cytoskeleton, but is rather due to its integration in lipid rafts. The potential involvement of prohibitin in the regulation of mitochondrial membrane protein degradation (Steglich et al., 1999) may be relevant to some of the phagolysosome degradative functions. Furthermore, it was recently discovered that prohibitin is indispensable for the activation of Raf-MEK-ERK pathway by Ras (Rajalingam et al., 2005). As the phosphorylation of ERK is a key signalling event during IgG-dependent phagocytosis in human neutrophils, it may be speculated that prohibitin is also involved in signalling leading to the initiation of phagocytosis and maturation of phagosomes.

The association of ficolin-1 (M-ficolin, ficolin A) with cytoskeleton, phagosome, or lipid rafts has not been yet reported. It was previously detected in the plasma membrane and cytoplasmic fraction of non-activated neutrophils (Brooks et al., 2003). Ficolins are lectins with collagen- and fibrinogen- like domains that function as opsonins by binding to the N-acetylglucosamine moiety present on bacterial cell walls, thereby promoting phagocytosis and activating the lectin pathway of complement. Ficolins may therefore have important roles in innate immunity to bacterial infections. The majority of ficolin is secreted by neutrophils upon activation. Human M-ficolin does not contain transmembrane domains but is present on the cell surface and is indirectly implicated as a phagocytic receptor in the phagocytosis of *E.coli* (Steglich et al., 1999). It was suggested that M-ficolin might be anchored to the cell surface by protein-protein interactions with a membrane protein that has yet to be characterized. The role of ficolin in the detergent-resistant phagosome fraction remains to be determined.

Valosin-containing protein is required for the degradation of ubiquitinated-proteasome substrates and it co-purifies with the 26S proteasome (Dai et al., 1998). It has been previously localized in ER membranes (Waugh et al., 2003) and is associated with the unusually large number of functions (Wang et al., 2004). Apart from its role in the removal of

misfolded membrane proteins from the ER, valosin-containing protein regulates cellular signalling pathways by physical association with ubiquitinated IkappaBα (IkBα) and the 26S proteasome, and is targeting IKBa to the proteasome for degradation (Dai et al., 1998). In phagosomes, it may be involved in the process of degradation of ingested foreign particles and antigen presentation (Kloetzel et al., 2004), as well as phagosome maturation due to its known function as a chaperone in membrane fusion (Woodman et al., 2003). Although previously localized only to the endoplasmic reticulum membrane (Waugh et al., 2003), we could detect this protein in all three analysed compartments in neutrophils. Its detection in the detergent-resistant phagosome fraction was not surprising as it is known that endoplasmic reticulum is a source of membrane for phagosome formation (Gagnon et al., 2002).

Although the previous proteomic study of macrophage phagosomes has identified VDAC-1 in the membrane fraction of phagosomes, its identification in Triton insoluble phagosomes was surprising. Previous evidence has suggested that this protein is exclusively localized in the outer mitochondrial membrane (Baker et al., 2004), but its localization and function in extramitochondrial sites such as the plasma membrane (Buettner et al., 2000; Okada et al., 2004) has been reported recently. However, it is improbable that this finding is due to a contamination for several reasons. First, aprevious morphological and biochemical analysis of latex bead phagosome preparations indicated the virtual absence of contamination by mitochondria, Golgi vesicles, endosomes, and the plasma membrane (Garin et al., 2001). Second, VADC-1 and prohibitin were not identified as major mitochondrial components in a recent proteomics study (Rabilloud et al., 2002). Therefore, this controversy may be due to cell-type differences in intracellular distribution of VDAC-1. Taken together, on the basis of our finding of VDAC-1 in detergent-resistant phagosomes, and the fact that it is a transmembrane protein, we assume that VDAC-1 associates with phagosome membrane lipid rafts rather than with the phagosome skeleton. The association of VDAC-1 with plasma membrane lipid rafts has been shown previously (Bahamonde et al., 2003), but this is the first

report suggesting the association of VDAC-1 with the phagosome membrane lipid rafts. The main function of VDACs in the outer mitochondrial membrane is the mediation of the flow of ATP and ADP between cytosol and the mitochondrial spaces (Rostovtseva et al., 1997). It is also involved in the activation of the mitochondrial apoptotic pathway. Whether VDAC-1 on phagosomes also takes part in the initiation of the apoptotic process or/and regulates ATP/ADP ratio, remains to be investigated.

The macrophage and neutrophil proteomes share similarities due to the common phagocytic function of these cells (Garin et al., 2001). But we also identified for the first time several proteins not known to associate with phagosomes in macrophages, in our Triton X-100 insoluble neutrophil phagosome preparation. This is the first report that cytoskeletal proteins filamin, IQGAP1 and grancalcin, are associated with the phagocytic vacuole in neutrophils.

Besides its cross-linking function, filamin serves as a linker protein between membrane integrins and actin filaments. This linkage may be necessary for the stability of membrane ruffles during their retraction (Pfaff et al., 1998). Filamin has been shown to integrate in cellular signaling pathways downstream of Rho GTPases. These enzymes modulate the bundling and stabilizing activity of filamin on actin filaments (Bellanger et al., 2000; Borm et al., 2005). RhoGTPases are actively involved in neutrophil phagocytosis, however, whether filamin is in any way involved in this process through RhoGTPase is not clear.

IQGAP1 contains a region with extensive similarity with the catalytic domains of Ras GTPase activation proteins. Members of the Ras superfamily of GTPases act as molecular switches by cycling between inactive GDP- and active GTP-bound states. This cycling is controlled by guanine nucleotide exchange factors, which activate Ras family members, and RasGAPs, which increase the intrinsic GTPase activity of Ras proteins, thereby inactivating them. IQGAP1 has been shown bind to actin, cdc42, Rac1, and calmodulin

(Kuroda et al., 1999). It has been shown recently that IQGAP1 and CLIP-170 target to the cortical membrane, leading to cell polarization (Fukata et al., 2002). Here, we suggest that this protein may also have a role in signalling leading to phagocytosis.

The finding that grancalcin was associated with the cytosol high-speed pellet, Triton X-100 -insoluble membrane, and detergent insoluble phagocytic vacuole was consistent in several ways with the biochemical hallmarks and established subcellular distribution of grancalcin. This finding demonstrates the association of grancalcin with the phagosome, and confirms its association of grancalcin with cytoskeleton. We previously identified grancalcin as a highly enriched cytoskeletal protein that translocates from cytosol to the granule and plasma membrane upon neutrophil activation (Boyhan et al., 1992). Grancalcin belongs to a group of EF-hand Ca^{2+} binding proteins comprising calpain, Alg-2 and sorcin, which have structural rather than functional similarity (Nebl et al., 2002) and is most abundant in neutrophils and macrophages (Boyhan et al., 1992). Its abundance is increased in leukocytes within infected sites (Liu et al., 2004). Binding of grancalcin to sorcin (Hansen et al., 2003) and L-plastin (Lollike et al., 2001) has recently been reported. Its binding to L-plastin can explain its association with the cytoskeleton, as L-plastin is an actin-binding protein. The function of grancalcin, as well as sorcin is unknown, while L-plastin was demonstrated to contribute to the regulation of integrin-mediated leukocyte adhesion and activation (Jones et al., 1998). The only positive experimental result regarding the function of grancalcin so far is that grancalcin-deficient mice show low responsiveness to bacterial LPS (Roes et al., 2003). On the basis of the known interaction between L-plastin and grancalcin it may be speculated that the role of grancalcin at the cellular level is to modulate the above-mentioned effects of L-plastin. Whether grancalcin is associated with F-actin directly will be discussed in the following chapters.

The sequence of grancalcin was found to be 57.8% identical to sorcin, an EF-hand calcium binding protein overexpressed in multi-drug resistance Chinese hamster ovary cell

lines. The phosphorylation of grancalcin has been shown previously (Boyhan et al., 1992), however, at a site different than that shown in this study. The sequences of both sorcin and grancalcin indicate potential phosphorylation site on a serine residue in the third calcium-binding region. This sequence (KRXS) is a low affinity target site for cAMP-dependent protein kinase II, which is involved in a number of signalling pathways (Bhalla et al., 2001). The higher affinity recognition site RRRXS in the fourth Ca^{2+} binding domain of sorcin is not conserved in grancalacin where the serine residue is replaced by histidine (Boyhan et al., 1992).

Mass spectrometry is the tool of choice for the identification of phosphorylation sites *in vivo*. Interestingly, although post-translational modifications of grancalcin have not been described before, our results are suggestive of its dual phosphorylation in the detergent-resistant phagosome fraction. This modification could not be detected in detergent-resistant membrane and cytosolic skeleton preparations. The major regulatory modification of cell-signalling proteins is phosphorylation, therefore the finding that grancalcin is phosphorylated at the phagocytic vacuole is highly significant.

NADPH oxidase is a superoxide-generating enzyme expressed in phagocytic leukocytes and is essential for host defense (Segal et al., 2005). This enzyme is multicomponent, comprising several cytosolic proteins such as $p40^{phox}$, $p47^{phox}$ and $p67^{phox}$ and membrane components as $gp91^{phox}$ and $p22^{phox}$. It has recently been shown that the cytoskeleton is required for the full activity of this enzyme. It is therefore conceivable that leukocyte-specific proteins such as grancalcin and $p67^{phox}$ function in a collaborative manner in the actin cytoskeleton to acquire the full activity of the NADPH oxidase. Membrane-proximal cytoskeletal structure is critically involved in multiple signal transduction events (Fuller et al., 2003; Juliano et al., 1972). We hypothesis that grancalcin may have a role in signalling leading to the neutrophil phagocytosis function.

This is the first systematic examination of the neutrophil cytoskeleton in the different subcellular compartments with particular reference to the cytoskeletal proteins surrounding the phagocytic vacuole. Although many of the proteins were found in all the three locations examined, some of them showed differential distribution suggestive of a specialised function in that particular location. Thus this study provides the first inventory of the composition of neutrophil cytoskeleton and also contributes additional clues regarding the functions and localizations of individual proteins.

4.2. GRANCALCIN BINDS TO POLYMERIC F-ACTIN

In the previous chapter, we show that the presence at low abundance of grancalcin in the cytosol high-speed pellet, and its enrichment in Triton-insoluble membrane and Triton-insoluble phagocytic vacuoles. MALDI-TOF MS analysis demonstrated the phosphorylation of grancalcin in the phagocytic vacuole but not in the cytosol. Grancalcin is a protein with unknown function, which was first identified in the Professor Segal's laboratory in 1992 (Teahan et al., 1992). Grancalcin-deficient mice were generated, but only the phenotype displaying reduced susceptibility to LPS induced shock was observed. Thus, the function of this penta-EF-hand protein was analysed further. The possibility of this protein binding to F-actin was analysed by standard biochemical methods.

We have demonstrated for the first time that grancalcin binds to F-actin in a stoichiometric ratio of 1.1 mol grancalcin to 1 mol F-actin. With a Kd value of ~2.5 μM, this interaction exhibits a moderate affinity. Although grancalcin forms a dimer through the interaction of the EF5 domains (Jia et al., 2000), it does not cross-link F-actin *in vitro* since it does not form F-actin bundles which sediment at low centrifugal forces. Considering the stoichimetric ratio of this binding, we suggest that grancalcin is a side binding protein rather than a capping protein to F-actin filaments.

Grancalcin has previously been shown to bind to L-plastin. It is thought that the cytoskeletal co-localization of grancalcin is entirely a result of this interaction (Lollike et al., 2001). Grancalcin binds to F-actin in the absence of calcium, and also binds to L-plastin in a calcium independent manner. But it is not known whether the dual binding of L-plastin and F-actin is synergistic or competitive, Raising several questions. Firstly, L-plastin was found to interact with grancalcin in the absence of calcium by affinity chromatography, whereas in the presence of calcium, no such interaction was observed. This binding occured when the calcium concentration was 0.5 mM (Lollike et al., 2001), which is well above the calcium concentration that causes grancalcin to precipitate (Liu et al., 2004). Secondly, no direct

binding assay of grancalcin and L-plastin was performed (Lollike et al., 2001). Moreover, X-ray scattering experiments were unable to detect the formation of the complex of grancalcin with p65/L-plastin (Shinomiya et al., 2003). Our results indicated that COS-7 cells do not express L-plastin, but grancalcin still co-localised with actin. Further experiments are needed to clarify the functional role of grancalcin and the importance of its interaction with actin as well as the structural aspects of this interaction.

L-plastin, as well as other plastin isoforms such as T-plastin and I-plastin, is a mosaic protein containing 2EF-hands, a calmodulin-binding domain and two actin-binding domains (Zu et al., 1990). In resting cells, the Ca^{2+} binding sites are unoccupied, and L-plastin is mostly involved in cross-linking of F-actin fibers. Following stimulation of leukocytes with inflammatory stimuli such as formyl-methionine-leucine-phenylalanine or immune complexes that bind to Fcγ receptors, L-plastin is phosphorylated at Ser5, and this in turn leads to integrin activation and subsequent increased adhesion (Jones et al., 1996 and 1998). At present, it is not known whether L-plastin-grancalcin complexes in the absence of Ca^{2+} still have actin-bundling activity and whether, in this complex, Ser5 can still be phosphorylated. Cell stimulation leads to a rise of cytoplasmic Ca^{2+} leading to inhibition of its actin-bundling activity *in vitro* (Jones et al., 1996) and dissociation of the L-plastin-grancalcin complex (Lollike et al., 2001). Thus, calcium regulates the activity of L-plastin in a complex way, via endogenous EF-hand motifs and/or grancalcin (Lollike et al., 2001).

We also show that in COS-7 cells, grancalcin colocalised with F-actin at the leading edge. This observation is in line with the finding that grancalcin translocates to lamellipodia in macrophages upon stimulation with bacterial lipopolysaccharide. On the basis of this result it is proposed that this protein may have a function in host defence *in vivo*. It is therefore plausible that grancalcin, p65/L-plastin, and actin are closely and dynamically coupled in phagocytic leukocytes upon exposure to bacteria in order to organize the cytoskeltal scaffold that optimises the anti-microbial functions of the cell (Liu et al., 2004).

There are no reports regarding the expression of L-plastin in COS-7 cells (Lin et al., 1994), although I-plastin may be present because it is specifically expressed in the small intestine, colon and kidney. L-plastin and I-plastin share the same actin binding domains, whilst their N-termini differ. Human L-plastin contains one nuclear export signal (NES) domain while I-plastin contains two EF-hand domains (Delanote et al., 2005). The presence of the EF-hands, suggest that calcium could regulate actin-binding or other functions of plastins. Like L-plastin, I-plastin's bundling activity is also inhibited by calcium (Delanote et al., 2005). Under certain conditions, a number of residues in the actin binding proteins were buried within the protein core and therefore could not be involved in the binding. Without experimental evidence of interaction between I-plastin and grancalcin, it would not be clear whether the observed co-localization of actin and grancalcin in COS-7 cells is only due to their direct interaction, or whether I-plastin is also involved.

Interaction of other members of this penta-EF-hand family protein with the cytoskeleton has been reported. Calpain has been implicated in cytoskeletal remodeling, including disruption of cell-matrix interactions at the rear of the cell during crawling and lamellipodial and protrusion formation during spreading, by cleavage of these proteins thereby modulating integrin-cytoskeletal interactions, such as talin, pp60c-src, and integrin $\alpha_{IIb}\beta_3$ (Huttenlocher et al., 1997; Schoenwaelder et al., 1997). Thus calpain itself has been suggested as the connection between molecules that comprise the integrin-cytoskeletal linkage at the cell's rear (Cooray et al., 1996; Beckerle et al., 1987).

In conclusion, the interaction of grancalcin with actin at the leading edge upon LPS stimulation, its phosphorylation at the phagosome membrane after IgG-coated latex stimulation, its interaction with plague virulence protein YopM (personal communication with Prof. Sue Straley), all suggested it may be involved in a spectrum of biological responses such as cell motility, phagocytosis, and therefore the microbe killing. We therefore

investigated the precise role of this protein *in vivo* using grancalcin-deficient mice as a model system.

4.3. THE FUNCTION OF GRANCALCIN *IN VIVO*

The aim of these experiments was to explore the function of grancalcin in neutrophils using grancalcin-deficient mice as a model system. Grancalcin was discovered in 1992 (Boyhan et al., 1992), but its function remained unknown. This work for the first time describes a possible function for grancalcin.

Grancalcin-deficient neutrophils were examined for a number of neutrophil functions. Stimulation of murine neutrophils with PMA and IgG opsonised particles resulted in normal NADPH oxidase activation in grancalcin-deficient mice. Grancalcin-deficient PMN migrated to the site of infection at rates indistinguishable from wild-type, which was also observed by the previous study using the same model (Roes et al., 2003). This result indicated the normal function of β_2 integrin, as it is the major factor involved in transmigration.

Degranulation in grancalcin-deficient mice was measured at an ultrastructural level using electron microscopy. The numbers of the granules of neutrophils from bone marrow were similar. The number of granules of the neutrophils from peritoneal lavage of grancalcin-deficient mice at unstimulated state was significantly lower. However, after stimulation with IgG-opsonized *S.aureus*, the number of granules in both groups was not significantly different. This result suggested an increase of degranulation in grancalcin-deficient neutrophils as they migrated from bone marrow to peritoneum. This indicated that either the degranulation was significantly increased during transmigration in grancalcin-deficient mice, or some of the granules involved in the phagocytosis were already exocytosed during the transmigration from bone marrow to the peritoneum, thus the degranulation in grancalcin-deficient neutrophils was impaired during the IgG-receptor-dependent phagocytosis was purely because the previous procedure. This novel finding confirmed our hypothesis that grancalcin has a role in degranulation of neutrophils.

This novel finding is in contrast with the previous report, which found no evidence for a role of grancalcin in degranulation as judged by flow cytometry and measuring the release of lactoferrin (Roes et al., 2003). The measurement of the release of lactoferrin to the extracellular space has limited the scope of the assay to secondary granules. Therefore, degranulation of primary and tertiary granules was unaccounted for. Measuring degranulation by electron microscopy is advantageous over measurement of released granular enzymes because a total number of granules can be determined, which includes the extracellular release of all types of granules and also the loss of granules due to their fusion with the phagosome. Neutrophil granules contain an array of proteolytic and microbicidal enzymes, which are released into the phagocytic vacuole. The release of the granule contents, including elastase and cathepsin G, is essential for the killing of bacteria and fungi (Reeves et al., 2002). The calcium-dependent association of grancalcin with the membrane and granules (Boyhan et al., 1992) suggests its possible involvement in the fusion of granules with the phagosome and degranulation. Neutrophil degranulation can lead to injury in many inflammatory disorders. Lipopolysaccharides (LPS) from gram-negative bacteria are the most potent agonists for release of granules by PMNs (Gill et al., 1998). Overexuberant activation of neutrophils can lead to extensive degranulation in septic shock, acute lung injury and other serious inflammatory disorders (Abdel-Latif et al., 2004). Grancalcin-deficient mice are less susceptibe to LPS induced shock, which suggested the role of grancalcin in degranulation. Consequently, in the absence of grancalcin, degranulation could be reduced and the release of the proteases from neutrophils to surrounding tissue would also be decreased. So the damage by the endotoxic shock, largely induced by the release of the proteases, would also be decreased, in agreement with increased resistance of grancalcin-deficient mice to endotoxic shock.

Earlier studies using permeabilized or patch-clamped neutrophils have shown that the final steps of granule fusion with the plasma membrane, leading to release of granule contents,

are dependent on guanosine triphosphate (GTP) and Ca^{2+} (Abdel-Latif, et al., 2004). Elevation of intracellular Ca^{2+} is known to elicit exocytosis of storage granules in a variety of cells (Wright et al., 1979; Cromwell et al., 1991; Regazzi et al., 1995; and Hay et al., 1995), but the molecular mechanism by which this occurs is unknown. It has been shown that several cytosolic proteins translocate to granules in a Ca^{2+}-dependent manner (annexins I, II, III, IV, VI, and XI) (Borregaard et al., 1992; Sjölin et al., 1994 and 1996; Le Cabec et al., 1994; Ernst et al., 1991; Kaufman et al., 1996; Hayes et al., 2004; Gerke et al., 2005). Grancalcin has been previously reported to translocate selectively to secretory vesicles (Borregaard, et al., 1992) and granules (Lollike et al., 1995). However, the role, if any, of these proteins in the regulation of exocytosis is unclear. It has previously been shown that although morphologically mature neutrophils can be identified in human bone marrow, they are in a functionally immature state, whereas murine bone marrow contains a large reservoir of functionally competent neutrophils. Secretory vesicles are a specialized form of endocytotic residues that are formed during neutrophil maturation in the bone marrow. During exudation, secretory vesicles are fully mobilized. Exocytosis of gelatinase granules play a significant role in the neutrophil extravasation (Delclaux et al., 1996). During the subsequent migration of neutrophils through interstitial tissues, specific granules and azurophil granules undergo partial exocytosis (Sengelov et al., 1993). The specific and azurophil granules are also actively involved in the phagocytosis of the bacteria (Faurschou et al., 2003).

Our results shed light on different functions of this protein in degranulation at two separate stages: during migration from bone marrow to peritoneum after thioglycollate induced sterile inflammation, in which the degranulation of secretory vesicles or specific granules were increased, and/or by activation with IgG-coated particles, in which the degranulation of specific granules and azurophil granules were impaired.

This work has also resulted in first identification of grancalcin function, as we tested grancalcin-deficient neutrophils for adhesion and spreading. Interestingly, several of the extracellular matrix proteins tested, defective adhesion of grancalcin-deficient neutrophils was specific for the fibronectin-coated surface.

Impaired adherence of grancalcin-deficient neutrophils is consistent with the function of calpain, another penta-EF-hand protein, which also has a role in β_2 integrin-mediated adhesion. Fibronectin is a high-molecular-weight glycoprotein found as a soluble dimer in plasma and as an insoluble multimer in tissues. It binds to several members of the integrin receptor family mediating adhesion and migration (Ruoslahti et al., 1996). The integrins are heterodimeric, transmembrane receptors: 19 α subunits and 8 β subunits combine to form 25 different integrins (Quinn et al., 2003). Integrins bind to insoluble ligands and link them to the intracellular cytoskeleton (Yan et al., 2001). The ability of many integrins to bind ligands is regulated by cellular signaling mechanisms. This process, often called integrin "activation" or "inside-out signaling," can arise through conformational changes in the integrin extracellular domain between a constitutive low affinity (inactive) state and a high affinity (primed) state (Bennett et al., 1999; Elemer et al., 1994). The molecular basis of the conformational changes involved is currently uncertain. Regulation of ligand binding can also be influenced by changes in the physical distribution of these receptors at the cell surface (Yan et al., 2001; Yauch et al., 1997). Taken together with properties of integrins described above, it is possible that grancalcin plays a role in the affinity maturation or surface distribution of fibronectin-specific integrins. Alternatively, the effect of grancalcin on neutrophil adhesion may be mediated through its interaction with L-plastin as this protein has been implicated in the regulation of integrin function (Chen, et al., 2003; Correia, et al., 1999; Jones et al., 1998). However, this is unlikely as L-plastin-deficient neutrophils adhere and spread normally on different extracellular matrix coated surface (Chen et al., 2003).

Spreading is an interesting model for understanding the mechanism of the relationship between cells and the extracellular matrix (Carter, et al., 1990; Chen, et al., 1979). The rounding of cells, may be accompanied by a loss of the normal cytoskeletal organization (Bissell et al. 1982; Bissell and Aggeler, 1987; Werb et al. 1986), therefore resulted from the detachment of the plasma. Depolymerization of actin seems to be evoked by calcium influx. As a penta-EF-hand calcium binding protein, the differences between the spreading of neutrophils from grancalcin-deficient mice and wild type in fibronectin-coated surface, raises the possibility that grancalcin may influence the spreading through the regulation of calcium, detachment to the substratum and therefore the inability to form the extension of lamella.

To understand the impairment of adhesion to fibronectin of grancalcin-deficient mice better, we examined the adhesive structures formed by neutrophils adherent to a substrate coated with fibronectin. Actin staining of adherent neutrophils has demonstrated punctate structures resembling focal adhesion complexes in neutrophils (Lawrence et al., 2001). These structures are anchor points linking cells to the extracellular matrix proteins. They consist mainly of actin fibres, integrins and Syk non-receptor tyrosine kinase. Larger numbers of F-actin foci were seen in wild-type neutrophils, while cortical actin staining predominated in grancalcin deficient neutrophils. The mechanism of the involvement of grancalcin in adhesion remains to be investigated.

In view of the potential defect in fibronectin-mediated phagocytosis and 40% reduced susceptibility to endotoxic shock in the mutants, a subtle role of grancalcin in the control of leukocyte activation or protection against specific microbial pathogens was suggested. Many pathogenic microorganisms express proteins that mimic the activity of extracellular matrix proteins in order to influence cellular functions to the advantage of the microbe (reviewed in Stebbins and Galan, 2001). Either being the homology to the host protein that is being mimicked, or the ligand of the host protein can achieve it. *S.Typhimurium*

may have taken the convergent evolution strategy further by expressing an outer-surface adhesion *ShdA* that mimics the binding activity of host polysaccharide heparin to gain access to a binding site in the extracellular matrix. *ShdA* is a fibronectin binding protein required for persistent intestinal carriage of salmonellosis. It is specific to *S.enterica* subspecies I serotypes. *ShdA*-mediated binding of one or more receptors in the extracellular matrix has a role in decreasing the clearance rate, thereby resulting in an increase in the reproduce of *Serotype Typhimurium* (Kinsley et al., 2000). We speculate that since grancalcin mutant has a defect in binding to fibronectin, that might influence the recognising of *S.Typhimurium* which binds to this ligand and thus impair its phagocytose of this microbe. We hypothesis that grancalcin-deficient mice might show defective in killing *S.Typhimurium*.

Our results imply that the observed impairment of grancalcin-deficient neutrophils to adhere, spread, form focal adhesion complexes on fibronectin surfaces, and impair in fibronectin mediated phagocytosis, may be a result of decreased surface expression of major neutrophil fibronectin receptors $\alpha_4\beta_1$ and $\alpha_5\beta_1$. This may be due to the effect of grancalcin on transcription of these receptors. Involvement of grancalcin in regulation of transcription is also suggested by its increase during relapse of T cell dysfunction among 84 transcripts identified during this process (Sahali et al., 2002). Multiple fibronectin receptors, including β_1 integrins, need to work co-operatively to regulate macrophage phagocytic responses (McCutcheon et al., 1998). Ligation of one integrin may influence the behavior of others in the cell, a phenomenon called integrin cross-talk. In macrophages, fibronectin-mediated phagocytosis is mediated by the integrin cross-talk of $\alpha_v\beta_3$ and $\alpha_5\beta_1$ (Blystone et al., 1994 and 1999), or through $\alpha_4\beta_1$ (McCutcheon et al., 1998). Antibody to $\alpha_v\beta_3$ can block phagocytosis of fibronectin-opsonised beads completely (Blystone et al., 1994). Ligation of the integrin $\alpha_v\beta_3$ inhibits both phagocytosis and migration mediated by $\alpha_5\beta_1$. This effect is mediated by the β_3 cytoplasmic tail through the activation of calcium- and calmodulin-dependent protein

kinase II (CamKII) (Blystone et al., 1999). Whether the same process occurs in neutrophils is not clear.

4.4. CONCLUSIONS AND FUTURE PERSPECTIVES

In conclusion, this study provides the first inventory of the analysis of neutrophil cytoskeletal proteome, therefore provides the novel functional suggestions of the newly identified proteins in specific locations. The high-speed co-sedimentation assay demonstrated that grancalcin is a F-actin binding protein. Murine neutrophils lacking grancalcin appear to have defect in fibronectin-mediated adhesion and spreading, reduced focal adhesion, and decreased phagocytosis after 8 minutes. Thus we suggest that grancalcin is a linking protein between cytoskeleton and integrin. The challenge now is to understand what role grancalcin proforms at a mechanistic level. In this case, the mutagenesis and functional protein interaction assays can be performed.

There are several aspects of grancalcin biology, which would be interesting to investigate further, based on our findings so far.

Enzymes and other factors secreted by degranulating neutrophils contribute significantly in endothelial injury, thrombosis, and vascular remodelling. Release of granular enzymes by LPS stimulated neutrophils is also a key mechanism of alveolar capillary injury in the acute respiratory distress symdrome, usually followed by endotoxemia and gram negative bacterial shock (Rocker et al., 1989; Donnelly et al., 1995; Delclaux et al., 1997; Moreland et al., 2006). The PMN degranulation also has severe implications in the development of multiple organ failure and correlates with the patient outcome after trauma and infection (Jochum et al., 1994; Moreland et al., 2006). So it will be interesting to explore the mechanism and implication of grancalcin in degranulation further, thus to understand the clinical implication of its resistance to LPS induced shock in grancalcin-deficient mice.

The role of grancalcin in killing of *S.Typhimurium* can be examined by the *in vitro* studies. *ShdA* is a fibronectin binding protein required for persistent intestinal carriage of salmonellosis. It is specific to *S.enterica* subspecies I serotypes. By comparing the bacteria loading experiments with *ShdA* positive and negative *S.enteria*, if grancalcin has a role in

their *in vivo* killing can also be identified. Our data may therefore leads to the analysis of the involvement of this protein in immune defence against specific microbes, thus provide new strategies for therapeutic intervention.

ACKNOWLEDGEMENTS

To my supervisors.

I would like to thank my primary supervisor, Professor Anthony Segal for his support, inspiration and encouragement before and during my PhD project, at his laboratory at the Rayne Institute.
Dr. Michael Way, my secondary supervisor, for the genius scientific inspiration and advices.
Dr. Marko Radulovic, my third supervisor, for the immense amount of helps and support, especially for 2D gel electrophoresis and thesis correction.

To my collaborators.

Professor Jasminka Godovac-Zimmermann, for the advices on proteomics and discussion of the manuscript of the proteomics paper.
Dr. Jurgen Roes who generated and supplied the grancalcin knock out mice, for the discussions about the manuscript of the first grancalcin paper.
Professor Giorgio Gabella and Christine Davis, Department of Anatomy, UCL, for which the electron microscopic experiments were depended.
Dr. Emmanuelle Caron for the advice on the actin cytoskeleton and the upgrade.
Dr. Dongmin Shao, for helpful discussions and performing the 'podosome' experiment.
Mr. Mark Crawford, for the endless help in proteomics and manuscript correction.
Dr. Reeves, Dr. Messina, Dr. Nagl and Dr. Dekker for friendship and help.

To Chronic Granulomatous Disease Research Trust, who partly supported my study.

I thank my friend Lei, and my family, especially Dongmin and Yiyun.

Finally, I dedicate this work to my parents.

REFERENCE LIST

Abdel-Latif,D., Steward,M., Macdonald,D.L., Francis,G.A., Dinauer,M.C., and Lacy,P., Rac2 is critical for neutrophil primary granule exocytosis, Blood, 104 (2004) 832-839.

Abo,A., Pick,E., Hall,A., Totty,N., Teahan,C.G., and Segal,A.W., Activation of the NADPH oxidase involves the small GTP-binding protein p21rac1, Nature, 353 (1991) 668-670.

Abo,A. and Pick,E., Purification and characterization of a third cytosolic component of the superoxide-generating NADPH oxidase of macrophages, J. Biol. Chem., 266 (1991) 23577-23585.

Ahluwalia,J., Tinker,A., Clapp,L.H., Duchen,M.R., Abramov,A.Y., Pope,S., Nobles,M., and Segal,A.W., The large-conductance Ca2+-activated K+ channel is essential for innate immunity, Nature, 427 (2004) 853-858.

Akutsu,S. and Miyazaki,J., Biochemical and immunohistochemical studies on tropomyosin and glutamate dehydrogenase in the chicken liver, Zoolog. Sci., 19 (2002) 275-286.

Albrethsen,J., Bogebo,R., Gammeltoft,S., Olsen,J., Winther,B., and Raskov,H., Upregulated expression of human neutrophil peptides 1, 2 and 3 (HNP 1-3) in colon cancer serum and tumours: a biomarker study, BMC. Cancer, 5 (2005) 8.

Allen,L.A. and Aderem,A., Molecular definition of distinct cytoskeletal structures involved in complement- and Fc receptor-mediated phagocytosis in macrophages, J. Exp. Med., 184 (1996) 627-637.

Allen,L.A., DeLeo,F.R., Gallois,A., Toyoshima,S., Suzuki,K., and Nauseef,W.M., Transient association of the nicotinamide adenine dinucleotide phosphate oxidase subunits p47phox and p67phox with phagosomes in neutrophils from patients with X-linked chronic granulomatous disease, Blood, 93 (1999) 3521-3530.

Ameen,N.A., Figueroa,Y., and Salas,P.J., Anomalous apical plasma membrane phenotype in CK8-deficient mice indicates a novel role for intermediate filaments in the polarization of simple epithelia, J. Cell Sci., 114 (2001) 563-575.

Anderson,K.L. and Ferreira,A., alpha1 Integrin activation: a link between beta-amyloid deposition and neuronal death in aging hippocampal neurons, J. Neurosci. Res., 75 (2004) 688-697.

Aon,M.A. and Cortassa,S., Coherent and robust modulation of a metabolic network by cytoskeletal organization and dynamics, Biophys. Chem., 97 (2002) 213-231.

Arcaro,A., The small GTP-binding protein Rac promotes the dissociation of gelsolin from actin filaments in neutrophils, J. Biol. Chem., 273 (1998) 805-813.

Azuma,T., Witke,W., Stossel,T.P., Hartwig,J.H., and Kwiatkowski,D.J., Gelsolin is a downstream effector of rac for fibroblast motility, EMBO J., 17 (1998) 1362-1370.

Babior, B.M., Curnutte, J.T., Chronic granulomatous disease-pieces of a cellular and molecular puzzle, Blood Rev, 1 (1987) 215-218.

Back,J.W., Sanz,M.A., De Jong,L., De Koning,L.J., Nijtmans,L.G., de Koster,C.G., Grivell,L.A., Van Der,S.H., and Muijsers,A.O., A structure for the yeast prohibitin complex: Structure prediction and evidence from chemical crosslinking and mass spectrometry, Protein Sci., 11 (2002) 2471-2478.

Baggiolini,M., Bretz,U., Dewald,B., and Feigenson,M.E., The polymorphonuclear leukocyte, Agents Actions, 8 (1978) 3-10.

Bahamonde,M.I., Fernandez-Fernandez,J.M., Guix,F.X., Vazquez,E., and Valverde,M.A., Plasma membrane voltage-dependent anion channel mediates antiestrogen-activated maxi Cl- currents in C1300 neuroblastoma cells, J. Biol. Chem., 278 (2003) 33284-33289.

Baker,M.A., Lane,D.J., Ly,J.D., De,P., V, and Lawen,A., VDAC1 is a transplasma membrane NADH-ferricyanide reductase, J. Biol. Chem., 279 (2004) 4811-4819.

Baldridge,C.W., The extra respiration of phagocytosis, Am. J. Physiol, 103 (1933) 235-236.

Bannenberg,G.L., Chiang,N., Ariel,A., Arita,M., Tjonahen,E., Gotlinger,K.H., Hong,S., and Serhan,C.N., Molecular circuits of resolution: formation and actions of resolvins and protectins, J. Immunol., 174 (2005) 4345-4355.

Barak,Y. and Nir,E., Chediak-Higashi syndrome, Am. J. Pediatr. Hematol. Oncol., 9 (1987) 42-55.

Bassaglia Y, Cebrian J, Covan s, Garcia M, and Foucrier J, proteasomes are tightly associated to myofibrils in mature skeletal muscle, Exp Cell Res, 302 (5 A.D.) 221-232.

Beckerle,M.C., Burridge,K., DeMartino,G.N., and Croall,D.E., Colocalization of calcium-dependent protease II and one of its substrates at sites of cell adhesion, Cell, 51 (1987) 569-577.

Belaaouaj,A., McCarthy,R., Baumann,M., Gao,Z., Ley,T.J., Abraham,S.N., and Shapiro,S.D., Mice lacking neutrophil elastase reveal impaired host defense against gram negative bacterial sepsis, Nat. Med., 4 (1998) 615-618.

Belaaouaj,A., Kim,K.S., and Shapiro,S.D., Degradation of outer membrane protein A in Escherichia coli killing by neutrophil elastase, Science, 289 (2000) 1185-1188.

Bellanger JM, Astier C, Sardet C, Ohta Y, Stossel TP, and Debant A, The Rac1- and RhoG-specific GEF domain of Trio targets filamin to remodel cytoskeletal actin, Nat Cell Biol, 2 (2000) 888-892.

Bennett,J.S., Zigmond,S., Vilaire,G., Cunningham,M.E., and Bednar,B., The platelet cytoskeleton regulates the affinity of the integrin alpha(IIb)beta(3) for fibrinogen, J. Biol. Chem., 274 (1999) 25301-25307.

Bereiter-Hahn,J., Luck,M., Miebach,T., Stelzer,H.K., and Voth,M., Spreading of trypsinized cells: cytoskeletal dynamics and energy requirements, J. Cell Sci., 96 (Pt 1) (1990) 171-188.

Bey,E.A., Xu,B., Bhattacharjee, A., Oldfield, C.M., Zhao, X., Li,Q., Subbulakshmi, V., Feldman, G.M., Wientjes, F.B., Cathcart, M.K., Protein kinase C delta is required for p47phox phosphoryation and translocation in activated human monocytes, J. Immunol,173 (2004):5730-5738.

Bhalla,U.S. and Iyengar,R., Functional modules in biological signalling networks, Novartis. Found. Symp., 239 (2001) 4-13.

Bienvenu,K., Harris,N., and Granger,D.N., Modulation of leukocyte migration in mesenteric interstitium, Am. J. Physiol, 267 (1994) H1573-H1577.

Bissell,M.J., Hall,H.G., and Parry,G., How does the extracellular matrix direct gene expression?, J Theor. Biol, 99 (1982) 31-68.

Bissell,M.J. and Aggeler,J., Dynamic reciprocity: how do extracellular matrix and hormones direct gene expression?, Prog. Clin Biol Res, 249 (1987) 251-262.

Blagoev,B., Kratchmarova,I., Ong,S.E., Nielsen,M., Foster,L.J., and Mann,M., A proteomics strategy to elucidate functional protein-protein interactions applied to EGF signaling, Nat. Biotechnol., 21 (2003) 315-318.

Blanchoin,L., Amann,K.J., Higgs,H.N., Marchand,J.B., Kaiser,D.A., and Pollard,T.D., Direct observation of dendritic actin filament networks nucleated by Arp2/3 complex and WASP/Scar proteins, Nature, 404 (2000) 1007-1011.

Blystone,S.D., Graham,I.L., Lindberg,F.P., and Brown,E.J., Integrin alpha v beta 3 differentially regulates adhesive and phagocytic functions of the fibronectin receptor alpha 5 beta 1, J. Cell Biol, 127 (1994) 1129-1137.

Blystone,S.D., Slater,S.E., Williams,M.P., Crow,M.T., and Brown,E.J., A molecular mechanism of integrin crosstalk: alphavbeta3 suppression of calcium/calmodulin-dependent protein kinase II regulates alpha5beta1 function, J. Cell Biol., 145 (1999) 889-897.

Boggs,D.R., Neutrophils in the blood bank, N. Engl. J. Med., 296 (1977) 748-750.

Borm B, Requardt RP, Herzog V, and Kirfel G, Membrane ruffles in cell migration:indicators of inefficient lamellipodia adhesion and compartments of actin filament reorganization, Exp Cell Res, 302 (2005) 83-95.

Borregaard,N., Kjeldsen,L., Lollike,K., and Sengelov,H., Ca(2+)-dependent translocation of cytosolic proteins to isolated granule subpopulations and plasma membrane from human neutrophils, FEBS Lett., 304 (1992) 195-197.

Bouin,A.P., Grandvaux,N., Vignais,P.V., and Fuchs,A., p40(phox) is phosphorylated on threonine 154 and serine 315 during activation of the phagocyte NADPH oxidase. Implication of a protein kinase c-type kinase in the phosphorylation process, J. Biol. Chem., 273 (1998) 30097-30103.

Boussa, calcium-dependent secretion in human neutrophils: a proteomic approach, Electrophoresis, 21 (2000) 665-672.

Boyhan, molecular cloning and characterization of grancalcin, a novel EF-hand calcium-binding protein abundant in neutrophils and monocytes, J. Biol. Chem., 267 (1992) 2928-2933.

Bretscher,M.S., Getting membrane flow and the cytoskeleton to cooperate in moving cells, Cell, 87 (1996) 601-606.

Briggs,M.W. and Sacks,D.B., IQGAP1 as signal integrator: Ca2+, calmodulin, Cdc42 and the cytoskeleton, FEBS Lett., 542 (2003) 7-11.

Brooks,A.S., DeLay,J.P., and Hayes,M.A., Purification and binding properties of porcine plasma ficolin that binds Actinobacillus pleuropneumoniae, Dev. Comp Immunol., 27 (2003) 835-844.

Brunner,D. and Nurse,P., CLIP170-like tip1p spatially organizes microtubular dynamics in fission yeast, Cell, 102 (2000) 695-704.

Buettner,R., Papoutsoglou,G., Scemes,E., Spray,D.C., and Dermietzel,R., Evidence for secretory pathway localization of a voltage-dependent anion channel isoform, Proc. Natl. Acad. Sci. U. S. A, 97 (2000) 3201-3206.

Buhimschi,I.A., Buhimschi,C.S., Weiner,C.P., Kimura,T., Hamar,B.D., Sfakianaki,A.K., Norwitz,E.R., Funai,E.F., and Ratner,E., Proteomic but not enzyme-linked immunosorbent assay technology detects amniotic fluid monomeric calgranulins from their complexed calprotectin form, Clin. Diagn. Lab Immunol., 12 (2005) 837-844.

Burns,S., Cory,G.O., Vainchenker,W., and Thrasher,A.J., Mechanisms of WASp-mediated hematologic and immunologic disease, Blood, 104 (2004) 3454-3462.

Cairns,N.J., Lee,V.M., and Trojanowski,J.Q., The cytoskeleton in neurodegenerative diseases, J. Pathol., 204 (2004) 438-449.

Cao,F., Yanagihara,N., and Burke,J.M., Progressive association of a "soluble" glycolytic enzyme with the detergent-insoluble cytoskeleton during in vitro morphogenesis of MDCK epithelial cells, Cell Motil. Cytoskeleton, 44 (1999) 133-142.

Caplan,S., Naslavsky,N., Hartnell,L.M., Lodge,R., Polishchuk,R.S., Donaldson,J.G., and Bonifacino,J.S., A tubular EHD1-containing compartment involved in the recycling of major histocompatibility complex class I molecules to the plasma membrane, EMBO J., 21 (2002) 2557-2567.

Capsoni,F., Acerbi,L., Bonora,G., Perletti,L., Ongari,A.M., Vanoli,M., and Zanussi,C., Phagocyte function and immunological findings in a Wiskott-Aldrich syndrome long-term survivor, J. Clin. Lab Immunol., 19 (1986) 91-97.

Carbone R, Fre S, Iannolo G, Belleudi F, Mancini P, Pelicci PG, Torrisi MR, and Di Fiore PP, eps15and eps15R are essential components of the endocytic pathway, Cancer Res, 57 (1997) 5498-5504.

Carlier,M.F., Pantaloni,D., Evans,J.A., Lambooy,P.K., Korn,E.D., and Webb,M.R., The hydrolysis of ATP that accompanies actin polymerization is essentially irreversible, FEBS Lett., 235 (1988) 211-214.

Carlier,M.F., Nucleotide hydrolysis regulates the dynamics of actin filaments and microtubules, Philos. Trans. R. Soc. Lond B Biol. Sci., 336 (1992) 93-97.

Caron,E., Regulation of Wiskott-Aldrich syndrome protein and related molecules, Curr Opin Cell Biol., 14 (2002):82-87.

Caron,E. and Hall,A., Identification of two distinct mechanisms of phagocytosis controlled by different Rho GTPases, Science, 282 (1998) 1717-1721.

Carraway KL. The cytoskeleton (Practical approach S.). 1. 1992. Oxford university press. Ref Type: Serial (Book,Monograph)

Carson,M.R. and Welsh,M.J., Structural and functional similarities between the nucleotide-binding domains of CFTR and GTP-binding proteins, Biophys. J., 69 (1995) 2443-2448.

Carter,W.G., Kaur,P., Gil,S.G., Gahr,P.J., and Wayner,E.A., Distinct functions for integrins alpha 3 beta 1 in focal adhesions and alpha 6 beta 4/bullous pemphigoid antigen in a new stable anchoring contact (SAC) of keratinocytes: relation to hemidesmosomes, J. Cell Biol., 111 (1990) 3141-3154.

Casimir,C., Chetty,M., Bohler,M.C., Garcia,R., Fischer,A., Griscelli,C., Johnson,B., and Segal,A.W., Identification of the defective NADPH-oxidase component in chronic granulomatous disease: a study of 57 European families, Eur. J. Clin. Invest, 22 (1992) 403-406.

Castegna,A., Aksenov,M., Aksenova,M., Thongboonkerd,V., Klein,J.B., Pierce,W.M., Booze,R., Markesbery,W.R., and Butterfield,D.A., Proteomic identification of oxidatively modified proteins in Alzheimer's disease brain. Part I: creatine kinase BB, glutamine synthase, and ubiquitin carboxy-terminal hydrolase L-1, Free Radic. Biol. Med., 33 (2002) 562-571.

Castellano,F., Chavrier,P., and Caron,E., Actin dynamics during phagocytosis, Semin. Immunol., 13 (2001) 347-355.

Chaponnier,C. and Gabbiani,G., Pathological situations characterized by altered actin isoform expression, J. Pathol., 204 (2004) 386-395.

Chen,A.K., Liu,C.C., and Schiller,J.G., Potentiometric method for substrate analysis using immobilized NAD + -dependent oxidoreductase enzymes, Biotechnol. Bioeng., 21 (1979) 1905-1915.

Chen,H., Mocsai,A., Zhang,H., Ding,R.X., Morisaki,J.H., White,M., Rothfork,J.M., Heiser,P., Colucci-Guyon,E., Lowell,C.A., Gresham,H.D., Allen,P.M., and Brown,E.J., Role for plastin in host defense distinguishes integrin signaling from cell adhesion and spreading, Immunity., 19 (2003) 95-104.

Chen,X., Sullivan,D.S., and Huffaker,T.C., Two yeast genes with similarity to TCP-1 are required for microtubule and actin function in vivo, Proc. Natl. Acad. Sci. U. S. A, 91 (1994) 9111-9115.

Chikkappa,G., Borner,G., Burlington,H., Chanana,A.D., Cronkite,E.P., Ohl,S., Pavelec,M., and Robertson,J.S., Periodic oscillation of blood leukocytes, platelets, and reticulocytes in a patient with chronic myelocytic leukemia, Blood, 47 (1976) 1023-1030.

Cho,D.I., Oak,M.H., Yang,H.J., Choi,H.K., Janssen,G.M., and Kim,K.M., Direct and biochemical interaction between dopamine D3 receptor and elongation factor-1Bbetagamma, Life Sci., 73 (2003) 2991-3004.

Cicchetti,G., Allen,P.G., and Glogauer,M., Chemotactic signaling pathways in neutrophils: from receptor to actin assembly, Crit Rev. Oral Biol. Med., 13 (2002) 220-228.

Clarke,F.M. and Masters,C.J., On the association of glycolytic enzymes with structural proteins of skeletal muscle, Biochim. Biophys. Acta, 381 (1975) 37-46.

Clegg,J.S., Properties and metabolism of the aqueous cytoplasm and its boundaries, Am. J. Physiol, 246 (1984) R133-R151.

Clementi,E., Martino,G., Grimaldi,L.M., Brambilla,E., and Meldolesi,J., Intracellular Ca2+ stores of T lymphocytes: changes induced by in vitro and in vivo activation, Eur. J. Immunol., 24 (1994) 1365-1371.

Collins,F.M., Cellular antimicrobial immunity, CRC Crit Rev. Microbiol., 7 (1978) 27-91.

Cooray,P., Yuan,Y., Schoenwaelder,S.M., Mitchell,C.A., Salem,H.H., and Jackson,S.P., Focal adhesion kinase (pp125FAK) cleavage and regulation by calpain, Biochem. J, 318 (Pt 1) (1996) 41-47.

Correia, Integrating the actin and vimentin cytoskeletons. adhesion-dependent formation of fimbrin-vimentin complexes in macrophages, J. Cell Biol., 146 (1999) 831-842.

Critchley,D.R., Focal adhesions - the cytoskeletal connection, Curr. Opin. Cell Biol., 12 (2000) 133-139.

Cromwell,O., Bennett,J.P., Hide,I., Kay,A.B., and Gomperts,B.D., Mechanisms of granule enzyme secretion from permeabilized guinea pig eosinophils. Dependence on Ca2+ and guanine nucleotides, J. Immunol., 147 (1991) 1905-1911.

Curnutte,J.T., Chronic granulomatous disease: the solving of a clinical riddle at the molecular level, Clin. Immunol. Immunopathol., 67 (1993) S2-15.

Dai,R.M., Chen,E., Longo,D.L., Gorbea,C.M., and Li,C.C., Involvement of valosin-containing protein, an ATPase Co-purified with IkappaBalpha and 26 S proteasome, in ubiquitin-proteasome-mediated degradation of IkappaBalpha, J. Biol. Chem., 273 (1998) 3562-3573.

Deinard,A.S. and Page,A.R., Letter: Determination of neutrophil half-life, N. Engl. J. Med., 292 (1975) 533-534.

Delanote,V., Vandekerckhove,J., and Gettemans,J., Plastins: versatile modulators of actin organization in (patho)physiological cellular processes, Acta Pharmacol. Sin., 26 (2005) 769-779.

Delclaux,C., Delacourt,C., d'Ortho,M.P., Boyer,V., Lafuma,C., and Harf,A., Role of gelatinase B and elastase in human polymorphonuclear neutrophil migration across basement membrane, Am. J. Respir. Cell Mol. Biol., 14 (1996) 288-295.

Delclaux,C., d'Ortho,M.P., Delacourt,C., Lebargy,F., Brun-Buisson,C., Brochard,L., Lemaire,F., Lafuma,C., and Harf,A., Gelatinases in epithelial lining fluid of patients with adult respiratory distress syndrome, Am. J. Physiol, 272 (1997) L442-L451.

DeLeo,F.R. and Quinn,M.T., Assembly of the phagocyte NADPH oxidase: molecular interaction of oxidase proteins, J. Leukoc. Biol, 60 (1996) 677-691.

Demma,M., Warren,V., Hock,R., Dharmawardhane,S., and Condeelis,J., Isolation of an abundant 50,000-dalton actin filament bundling protein from Dictyostelium amoebae, J. Biol. Chem., 265 (1990) 2286-2291.

Dermine,J.F., Duclos,S., Garin,J., St Louis,F., Rea,S., Parton,R.G., and Desjardins,M., Flotillin-1-enriched lipid raft domains accumulate on maturing phagosomes, J. Biol. Chem., 276 (2001) 18507-18512.

Dewitt,S. and Hallett,M.B., Cytosolic free Ca(2+) changes and calpain activation are required for beta integrin-accelerated phagocytosis by human neutrophils, J. Cell Biol., 159 (2002) 181-189.

Deyrup,A.T., Krishnan,S., Cockburn,B.N., and Schwartz,N.B., Deletion and site-directed mutagenesis of the ATP-binding motif (P-loop) in the bifunctional murine ATP-sulfurylase/adenosine 5'-phosphosulfate kinase enzyme, J. Biol. Chem., 273 (1998) 9450-9456.

Dharmawardhane,S., Demma,M., Yang,F., and Condeelis,J., Compartmentalization and actin binding properties of ABP-50: the elongation factor-1 alpha of Dictyostelium, Cell Motil. Cytoskeleton, 20 (1991) 279-288.

Dinauer,M.C., Pierce,E.A., Bruns,G.A., Curnutte,J.T., and Orkin,S.H., Human neutrophil cytochrome b light chain (p22-phox). Gene structure, chromosomal location, and mutations in cytochrome-negative autosomal recessive chronic granulomatous disease, J. Clin. Invest, 86 (1990) 1729-1737.

Ding,J., Vlahos,C.J., Liu,R., Brown,R.F., and Badwey,J.A., Antagonists of phosphatidylinositol 3-kinase block activation of several novel protein kinases in neutrophils, J. Biol. Chem., 270 (1995) 11684-11691.

Ding,J., Knaus,U.G., Lian,J.P., Bokoch,G.M., and Badwey,J.A., The renaturable 69- and 63-kDa protein kinases that undergo rapid activation in chemoattractant-stimulated guinea pig neutrophils are p21-activated kinases, J. Biol. Chem., 271 (1996) 24869-24873.

Donnelly,S.C., MacGregor,I., Zamani,A., Gordon,M.W., Robertson,C.E., Steedman,D.J., Little,K., and Haslett,C., Plasma elastase levels and the development of the adult respiratory distress syndrome, Am. J. Respir. Crit Care Med., 151 (1995) 1428-1433.

dos Remedios,C.G., Chhabra,D., Kekic,M., Dedova,I.V., Tsubakihara,M., Berry,D.A., and Nosworthy,N.J., Actin binding proteins: regulation of cytoskeletal microfilaments, Physiol Rev., 83 (2003) 433-473.

Drubin,D.G., Mulholland,J., Zhu,Z.M., and Botstein,D., Homology of a yeast actin-binding protein to signal transduction proteins and myosin-I, Nature, 343 (1990) 288-290.

Duncan,M.C., Cope,M.J., Goode,B.L., Wendland,B., and Drubin,D.G., Yeast Eps15-like endocytic protein, Pan1p, activates the Arp2/3 complex, Nat. Cell Biol., 3 (2001) 687-690.

Dupuis-Girod,S., Medioni,J., Haddad,E., Quartier,P., Cavazzana-Calvo,M., Le Deist,F., de Saint,B.G., Delaunay,J., Schwarz,K., Casanova,J.L., Blanche,S., and Fischer,A.,

Autoimmunity in Wiskott-Aldrich syndrome: risk factors, clinical features, and outcome in a single-center cohort of 55 patients, Pediatrics, 111 (2003) e622-e627.

Durso,N.A. and Cyr,R.J., A calmodulin-sensitive interaction between microtubules and a higher plant homolog of elongation factor-1 alpha, Plant Cell, 6 (1994) 893-905.

Eden, S., Rohatgi, R., Podtelejnikov, A.V., Mann, M., Kirschner, M.W., Mechanism of regulation of WAVE-induced actin nucleation by Rac1 and Nck, Nature, 418 (2002) 732-733.

Edwards SW, Biochemistry and physiology of the neutrophil, Cambridge University Press, Cambridge, 1994.

el Benna,J., Ruedi,J.M., and Babior,B.M., Cytosolic guanine nucleotide-binding protein Rac2 operates in vivo as a component of the neutrophil respiratory burst oxidase. Transfer of Rac2 and the cytosolic oxidase components p47phox and p67phox to the submembranous actin cytoskeleton during oxidase activation, J. Biol Chem., 269 (1994) 6729-6734.

el Benna,J., Labro,M.T., and Hakim,J., Resolution of major protein kinase substrates in neutrophil cytosol in response to DAG/PS and arachidonic acid stimulation and the selective action of various protein kinase inhibitors, Cell Signal., 6 (1994) 167-171.

el Benna,J., Faust,L.P., and Babior,B.M., The phosphorylation of the respiratory burst oxidase component p47phox during neutrophil activation. Phosphorylation of sites recognized by protein kinase C and by proline-directed kinases, J. Biol. Chem., 269 (1994) 23431-23436.

el Benna,J., Faust,R.P., Johnson,J.L., and Babior,B.M., Phosphorylation of the respiratory burst oxidase subunit p47phox as determined by two-dimensional phosphopeptide mapping. Phosphorylation by protein kinase C, protein kinase A, and a mitogen-activated protein kinase, J. Biol. Chem., 271 (1996) 6374-6378.

el Benna,J., Dang,P.M., Andrieu,V., Vergnaud,S., Dewas,C., Cachia,O., Fay,M., Morel,F., Chollet-Martin,S., Hakim,J., and Gougerot-Pocidalo,M.A., P40phox associates with the neutrophil Triton X-100-insoluble cytoskeletal fraction and PMA-activated membrane skeleton: a comparative study with P67phox and P47phox, J. Leukoc. Biol., 66 (1999) 1014-1020.

Elemer,G.S. and Edgington,T.S., Microfilament reorganization is associated with functional activation of alpha M beta 2 on monocytic cells, J. Biol. Chem., 269 (1994) 3159-3166.

Elferink,J.G. and VanUffelen,B.E., The role of cyclic nucleotides in neutrophil migration, Gen. Pharmacol., 27 (1996) 387-393.

Ernst,J.D., Annexin III translocates to the periphagosomal region when neutrophils ingest opsonized yeast, J. Immunol., 146 (1991) 3110-3114.

Etienne-Manneville,S. and Hall,A., Rho GTPases in cell biology, Nature, 420 (2002) 629-635.

Etzioni A and Alon R, Leukocyte adhesion deficiency III: a group of integrin activation defects in hematopoietic lineage cells, Curr Opin Allergy Clin Immunol, 4 (2004) 485-490.

Evangelista,M., Zigmond,S., and Boone,C., Formins: signaling effectors for assembly and polarization of actin filaments, J. Cell Sci., 116 (2003) 2603-2611.

Faist,E. and Kim,C., Therapeutic immunomodulatory approaches for the control of systemic inflammatory response syndrome and the prevention of sepsis, New Horiz., 6 (1998) S97-102.

Faurschou,M. and Borregaard,N., Neutrophil granules and secretory vesicles in inflammation, Microbes. Infect., 5 (2003) 1317-1327.

Fessler,M.B., Malcolm,K.C., Duncan,M.W., and Worthen,G.S., A genomic and proteomic analysis of activation of the human neutrophil by lipopolysaccharide and its mediation by p38 mitogen-activated protein kinase, J. Biol. Chem., 277 (2002) 31291-31302.

Fossati,G., Bucknall,R.C., and Edwards,S.W., Fcgamma receptors in autoimmune diseases, Eur. J. Clin. Invest, 31 (2001) 821-831.

Fuchs,E. and Cleveland,D.W., A structural scaffolding of intermediate filaments in health and disease, Science, 279 (1998) 514-519.

Fujita,Y., Hogan,C., and Braga,V.M., Regulation of cell-cell adhesion by rap1, Methods Enzymol., 407 (2005) 359-372.

Fukata,M., Watanabe,T., Noritake,J., Nakagawa,M., Yamaga,M., Kuroda,S., Matsuura,Y., Iwamatsu,A., Perez,F., and Kaibuchi,K., Rac1 and Cdc42 capture microtubules through IQGAP1 and CLIP-170, Cell, 109 (2002) 873-885.

Fuller,C.L., Braciale,V.L., and Samelson,L.E., All roads lead to actin: the intimate relationship between TCR signaling and the cytoskeleton, Immunol. Rev., 191 (2003) 220-236.

Furukawa,T., Yamane,T., Terai,T., Katayama,Y., and Hiraoka,M., Functional linkage of the cardiac ATP-sensitive K+ channel to the actin cytoskeleton, Pflugers Arch., 431 (1996) 504-512.

Gagnon,E., Duclos,S., Rondeau,C., Chevet,E., Cameron,P.H., Steele-Mortimer,O., Paiement,J., Bergeron,J.J., and Desjardins,M., Endoplasmic reticulum-mediated phagocytosis is a mechanism of entry into macrophages, Cell, 110 (2002) 119-131.

Gale,R.P. and Zighelboim,J., Polymorphonuclear leukocytes in antibody-dependent cellular cytotoxicity, J. Immunol., 114 (1975) 1047-1051.

Garin,J., Diez,R., Kieffer,S., Dermine,J.F., Duclos,S., Gagnon,E., Sadoul,R., Rondeau,C., and Desjardins,M., The phagosome proteome: insight into phagosome functions, J. Cell Biol., 152 (2001) 165-180.

Gerke,V., Creutz,C.E., and Moss,S.E., Annexins: linking Ca2+ signalling to membrane dynamics, Nat. Rev. Mol. Cell Biol., 6 (2005) 449-461.

Gevaert K, Chromatographic isolation of methionine-containing peptides for gel-free proteome analysis, Molecular cell proteomics, 1 (2002) 896-903.

Gevaert,K., Goethals,M., Martens,L., Van Damme,J., Staes,A., Thomas,G.R., and Vandekerckhove,J., Exploring proteomes and analyzing protein processing by mass spectrometric identification of sorted N-terminal peptides, Nat. Biotechnol., 21 (2003) 566-569.

Gill,E.A., Imaizumi,T., Carveth,H., Topham,M.K., Tarbet,E.B., McIntyre,T.M., Prescott,S.M., and Zimmerman,G.A., Bacterial lipopolysaccharide induces endothelial cells to synthesize a degranulating factor for neutrophils, FASEB J., 12 (1998) 673-684.

Gitlits,V.M., Toh,B.H., Loveland,K.L., and Sentry,J.W., The glycolytic enzyme enolase is present in sperm tail and displays nucleotide-dependent association with microtubules, Eur. J. Cell Biol., 79 (2000) 104-111.

Glogauer,M., Hartwig,J., and Stossel,T., Two pathways through Cdc42 couple the N-formyl receptor to actin nucleation in permeabilized human neutrophils, J. Cell Biol., 150 (2000) 785-796.

Goll,D.E., Thompson,V.F., Li,H., Wei,W., and Cong,J., The calpain system, Physiol Rev., 83 (2003) 731-801.

Gombart,A.F., Shiohara,M., Kwok,S.H., Agematsu,K., Komiyama,A., and Koeffler,H.P., Neutrophil-specific granule deficiency: homozygous recessive inheritance of a frameshift mutation in the gene encoding transcription factor CCAAT/enhancer binding protein--epsilon, Blood, 97 (2001) 2561-2567.

Gombart, A.F., Krug, U., O'Kelly, J., An, E., Vegesna, V., Koeffler, H.P., Aberrant expression of neutrophil and macrophage-related genes in a murine model for human neutrophil-specific granule deficiency, J.Leukoc Biol, 78 (2005) 1153-1165.

Goode,B.L., Wong,J.J., Butty,A.C., Peter,M., McCormack,A.L., Yates,J.R., Drubin,D.G., and Barnes,G., Coronin promotes the rapid assembly and cross-linking of actin filaments and may link the actin and microtubule cytoskeletons in yeast, J. Cell Biol., 144 (1999) 83-98.

Grogan,A., Reeves,E., Keep,N., Wientjes,F., Totty,N.F., Burlingame,A.L., Hsuan,J.J., and Segal,A.W., Cytosolic phox proteins interact with and regulate the assembly of coronin in neutrophils, J. Cell Sci., 110 (Pt 24) (1997) 3071-3081.

Gronborg,M., Bunkenborg,J., Kristiansen,T.Z., Jensen,O.N., Yeo,C.J., Hruban,R.H., Maitra,A., Goggins,M.G., and Pandey,A., Comprehensive proteomic analysis of human pancreatic juice, J. Proteome. Res., 3 (2004) 1042-1055.

Guerrera,I.C. and Kleiner,O., Application of mass spectrometry in proteomics, Biosci. Rep., 25 (2005) 71-93.

Gullberg,U., Bengtsson,N., Bulow,E., Garwicz,D., Lindmark,A., and Olsson,I., Processing and targeting of granule proteins in human neutrophils, J. Immunol. Methods, 232 (1999) 201-210.

Gustavsson,A., Yuan,M., and Fallman,M., Temporal dissection of beta1-integrin signaling indicates a role for p130Cas-Crk in filopodia formation, J. Biol. Chem., 279 (2004) 22893-22901.

Hall,A., Ras-related GTPases and the cytoskeleton, Mol. Biol Cell, 3 (1992) 475-479.

Han,Q., Jia,J., Li,Y., Lollike,K., and Cygler,M., Crystallization and preliminary X-ray analysis of human grancalcin, a novel cytosolic Ca2+-binding protein present in leukocytes, Acta Crystallogr. D. Biol. Crystallogr., 56 (Pt 6) (2000) 772-774.

Hansen,C., Tarabykina,S., la Cour,J.M., Lollike,K., and Berchtold,M.W., The PEF family proteins sorcin and grancalcin interact in vivo and in vitro, FEBS Lett., 545 (2003) 151-154.

Harper,A.M., Chaplin,M.F., and Segal,A.W., Cytochrome b-245 from human neutrophils is a glycoprotein, Biochem. J., 227 (1985) 783-788.

Hartmann-Petersen,R. and Gordon,C., Protein degradation: recognition of ubiquitinylated substrates, Curr. Biol., 14 (2004) R754-R756.

Hattori,H., Studies on the labile, stable Nadi oxidase and peroxidase staining reactions in the isolated particles of horse granulocyte, Nagoya J. Med. Sci., 23 (1961) 362-378.

Hay,J.C., Fisette,P.L., Jenkins,G.H., Fukami,K., Takenawa,T., Anderson,R.A., and Martin,T.F., ATP-dependent inositide phosphorylation required for Ca(2+)-activated secretion, Nature, 374 (1995) 173-177.

Hayes,M.J., Rescher,U., Gerke,V., and Moss,S.E., Annexin-actin interactions, Traffic., 5 (2004) 571-576.

Heyworth,P.G., Robinson,J.M., Ding,J., Ellis,B.A., and Badwey,J.A., Cofilin undergoes rapid dephosphorylation in stimulated neutrophils and translocates to ruffled membranes enriched in products of the NADPH oxidase complex. Evidence for a novel cycle of phosphorylation and dephosphorylation, Histochem. Cell Biol., 108 (1997) 221-233.

Higgs, H.N., and Pollar, T.D., Regulation of actin filament network formation through ARP2/3 complex: activation by a diverse array of proteins, Annu Rev Biochem, 70 (2001) 649-676.

Hinderlich,S., Berger,M., Schwarzkopf,M., Effertz,K., and Reutter,W., Molecular cloning and characterization of murine and human N-acetylglucosamine kinase, Eur. J. Biochem., 267 (2000) 3301-3308.

Hinshaw,D.B., Burger,J.M., Miller,M.T., Adams,J.A., Beals,T.F., and Omann,G.M., ATP depletion induces an increase in the assembly of a labile pool of polymerized actin in endothelial cells, Am. J. Physiol, 264 (1993) C1171-C1179.

Holmes,P.K. and Levinson,H.S., Metabolic requirements for microcycle sporogenesis of Bacillus megaterium, J. Bacteriol., 94 (1967) 434-440.

Howard,J., Molecular motors: structural adaptations to cellular functions, Nature, 389 (1997) 561-567.

Howard,J. and Hyman,A.A., Dynamics and mechanics of the microtubule plus end, Nature, 422 (2003) 753-758.

Howard,T.H. and Watts,R.G., Actin polymerization and leukocyte function, Curr. Opin. Hematol., 1 (1994) 61-68.

Huttenlocher,A., Palecek,S.P., Lu,Q., Zhang,W., Mellgren,R.L., Lauffenburger,D.A., Ginsberg,M.H., and Horwitz,A.F., Regulation of cell migration by the calcium-dependent protease calpain, J. Biol. Chem., 272 (1997) 32719-32722.

Jamal,T., Barbouche,M.R., Ben Hariz,M., Bejaoui,M., Fathallah,M.D., and Dellagi,K., Genetic and immunological assessment of a bone marrow transplantation in a patient with a primary immune defect: leukocyte adhesion deficiency, Arch. Inst. Pasteur Tunis, 75 (1998) 177-183.

Janeway,C.A., S. Burt Wolbach, 1880-1954, Trans. Assoc. Am. Physicians, 67 (1954) 30-35.

Jayaraman,A., Yarmush,M.L., and Roth,C.M., Evaluation of an in vitro model of hepatic inflammatory response by gene expression profiling, Tissue Eng, 11 (2005) 50-63.

Jensen,O.N., Mortensen,P., Vorm,O., and Mann,M., Automation of matrix-assisted laser desorption/ionization mass spectrometry using fuzzy logic feedback control, Anal. Chem., 69 (1997) 1706-1714.

Jia,J., Han,Q., Borregaard,N., Lollike,K., and Cygler,M., Crystal structure of human grancalcin, a member of the penta-EF-hand protein family, J. Mol. Biol., 300 (2000) 1271-1281.

Jiang,H. and Wang,Y.C., [Cyclin-dependent kinase inhibitors in mammal cells], Sheng Li Ke. Xue. Jin. Zhan., 27 (1996) 107-112.

Jochum,M., Gippner-Steppert,C., Machleidt,W., and Fritz,H., The role of phagocyte proteinases and proteinase inhibitors in multiple organ failure, Am. J. Respir. Crit Care Med., 150 (1994) S123-S130.

Johnston,J.A., Ward,C.L., and Kopito,R.R., Aggresomes: a cellular response to misfolded proteins, J. Cell Biol., 143 (1998) 1883-1898.

Jones,S.L. and Brown,E.J., FcgammaRII-mediated adhesion and phagocytosis induce L-plastin phosphorylation in human neutrophils, J. Biol. Chem., 271 (1996) 14623-14630.

Jones,S.L., Wang,J., Turck,C.W., and Brown,E.J., A role for the actin-bundling protein L-plastin in the regulation of leukocyte integrin function, Proc. Natl. Acad. Sci. U. S. A, 95 (1998) 9331-9336.

Jonusiene,V., Sasnauskiene,S., and Juodka,B., The cloning and characterization of Tetrahymena pyriformis translation elongation factor 1b alpha and gamma subunits, Cell Mol. Biol. Lett., 10 (2005) 689-696.

Juliano,R., Ciszkowski,J., Waite,D., and Mayhew,E., RNA Associated with plasma membranes of ehrlich ascites carcinoma cells, FEBS Lett., 22 (1972) 27-30.

Kanai,F., Liu,H., Field,S.J., Akbary,H., Matsuo,T., Brown,G.E., Cantley,L.C., and Yaffe,M.B., The PX domains of p47phox and p40phox bind to lipid products of PI(3)K, Nat. Cell Biol., 3 (2001) 675-678.

Kaplan,G., Differences in the mode of phagocytosis with Fc and C3 receptors in macrophages, Scand. J. Immunol., 6 (1977) 797-807.

Katz,A., Wu,D., and Simon,M.I., Subunits beta gamma of heterotrimeric G protein activate beta 2 isoform of phospholipase C, Nature, 360 (1992) 686-689.

Kaufman,M., Leto,T., and Levy,R., Translocation of annexin I to plasma membranes and phagosomes in human neutrophils upon stimulation with opsonized zymosan: possible role in phagosome function, Biochem. J., 316 (Pt 1) (1996) 35-42.

Kim,J.S., Kim,J.M., Jung,H.C., and Song,I.S., Caspase-3 activity and expression of Bcl-2 family in human neutrophils by Helicobacter pylori water-soluble proteins, Helicobacter., 6 (2001) 207-215.

Kingsley, R.A., van Amsterdam, K., Kramer, N.B., Baumler, A.J., The shdA gene is restricted to serotypes of Salmonella enterica subspecies I and contributes to efficient and prolonged fecal shedding, Infect Immun., 68 (2000) 2720-2727.

Kingsley,R.A., Keestra,A.M., de Zoete,M.R., and Baumler,A.J., The ShdA adhesin binds to the cationic cradle of the fibronectin 13FnIII repeat module: evidence for molecular mimicry of heparin binding, Mol. Microbiol., 52 (2004) 345-355.

Kinoshita,K., Habermann,B., and Hyman,A.A., XMAP215: a key component of the dynamic microtubule cytoskeleton, Trends Cell Biol., 12 (2002) 267-273.

Kitaura,Y., Matsumoto,S., Satoh,H., Hitomi,K., and Maki,M., Peflin and ALG-2, members of the penta-EF-hand protein family, form a heterodimer that dissociates in a Ca2+-dependent manner, J. Biol. Chem., 276 (2001) 14053-14058.

Kjeken,R., Egeberg,M., Habermann,A., Kuehnel,M., Peyron,P., Floetenmeyer,M., Walther,P., Jahraus,A., Defacque,H., Kuznetsov,S.A., and Griffiths,G., Fusion between phagosomes, early and late endosomes: a role for actin in fusion between late, but not early endocytic organelles, Mol. Biol. Cell, 15 (2004) 345-358.

Klarlund,J.K., Guilherme,A., Holik,J.J., Virbasius,J.V., Chawla,A., and Czech,M.P., Signaling by phosphoinositide-3,4,5-trisphosphate through proteins containing pleckstrin and Sec7 homology domains, Science, 275 (1997) 1927-1930.

Klebanoff,S.J., Antimicrobial mechanisms in neutrophilic polymorphonuclear leukocytes, Semin. Hematol., 12 (1975) 117-142.

Kloetzel,P.M., The proteasome and MHC class I antigen processing, Biochim. Biophys. Acta, 1695 (2004) 225-233.

Knaus,U.G., Heyworth,P.G., Evans,T., Curnutte,J.T., and Bokoch,G.M., Regulation of phagocyte oxygen radical production by the GTP-binding protein Rac 2, Science, 254 (1991) 1512-1515.

Knaus,U.G., Heyworth,P.G., Kinsella,B.T., Curnutte,J.T., and Bokoch,G.M., Purification and characterization of Rac 2. A cytosolic GTP-binding protein that regulates human neutrophil NADPH oxidase, J. Biol Chem., 267 (1992) 23575-23582.

Knaus,U.G., Morris,S., Dong,H.J., Chernoff,J., and Bokoch,G.M., Regulation of human leukocyte p21-activated kinases through G protein--coupled receptors, Science, 269 (1995) 221-223.

Koike,M., Awaji,T., Kataoka,M., Tsujimoto,G., Kartasova,T., Koike,A., and Shiomi,T., Differential subcellular localization of DNA-dependent protein kinase components Ku and DNA-PKcs during mitosis, J. Cell Sci., 112 (Pt 22) (1999) 4031-4039.

Komarova,Y.A., Akhmanova,A.S., Kojima,S., Galjart,N., and Borisy,G.G., Cytoplasmic linker proteins promote microtubule rescue in vivo, J. Cell Biol., 159 (2002) 589-599.

Korn,E.D., Carlier,M.F., and Pantaloni,D., Actin polymerization and ATP hydrolysis, Science, 238 (1987) 638-644.

Krebs,J., Saremaslani,P., and Caduff,R., ALG-2: a Ca2+ -binding modulator protein involved in cell proliferation and in cell death, Biochim. Biophys. Acta, 1600 (2002) 68-73.

Kreplak,L., Aebi,U., and Herrmann,H., Molecular mechanisms underlying the assembly of intermediate filaments, Exp. Cell Res., 301 (2004) 77-83.

Kuroda,S., Fukata,M., Nakagawa,M., and Kaibuchi,K., Cdc42, Rac1, and their effector IQGAP1 as molecular switches for cadherin-mediated cell-cell adhesion, Biochem. Biophys. Res. Commun., 262 (1999) 1-6.

Landing, B.H., and SHIRKEY,H.S., A syndrome of recurrent infection and infiltration of viscera by pigmented lipid histiocytes, Pediatrics, 20 (1957) 431-438.

Lane,E.B., and McLean,W.H., Keratins and skin disorders, J. Pathol., 204 (2004) 355-366.

Lauffenburger,D.A., and Horwitz,A.F., Cell migration: a physically integrated molecular process, Cell, 84 (1996) 359-369.

Lawrence,D.W., and Pryzwansky,K.B., The vasodilator-stimulated phosphoprotein is regulated by cyclic GMP-dependent protein kinase during neutrophil spreading, J. Immunol., 166 (2001) 5550-5556.

Lawson,N.D., Krause,D.S., and Berliner,N., Normal neutrophil differentiation and secondary granule gene expression in the EML and MPRO cell lines, Exp. Hematol., 26 (1998) 1178-1185.

Le,Cabec., V and Maridonneau-Parini,I., Annexin 3 is associated with cytoplasmic granules in neutrophils and monocytes and translocates to the plasma membrane in activated cells, Biochem. J., 303 (Pt 2) (1994) 481-487.

Lechler,T., Shevchenko,A., and Li,R., Direct involvement of yeast type I myosins in Cdc42-dependent actin polymerization, J. Cell Biol., 148 (2000) 363-373.

Lee,C.H., Park,D., Wu,D., Rhee,S.G., and Simon,M.I., Members of the Gq alpha subunit gene family activate phospholipase C beta isozymes, J. Biol. Chem., 267 (1992) 16044-16047.

Lesma,E., Riva,E., Giovannini,M., Di Giulio,A.M., and Gorio,A., Amelioration of neutrophil membrane function underlies granulocyte-colony stimulating factor action in glycogen storage disease 1b, Int. J. Immunopathol. Pharmacol., 18 (2005) 297-307.

Leto,T.L., Lomax,K.J., Volpp,B.D., Nunoi,H., Sechler,J.M., Nauseef,W.M., Clark,R.A., Gallin,J.I., and Malech,H.L., Cloning of a 67-kD neutrophil oxidase factor with similarity to a noncatalytic region of p60c-src, Science, 248 (1990) 727-730.

Leung,K.Y., Reisner,B.S., and Straley,S.C., YopM inhibits platelet aggregation and is necessary for virulence of Yersinia pestis in mice, Infect. Immun., 58 (1990) 3262-3271.

Leusen,J.H., de Klein,A., Hilarius,P.M., Ahlin,A., Palmblad,J., Smith,C.I., Diekmann,D., Hall,A., Verhoeven,A.J., and Roos,D., Disturbed interaction of p21-rac with mutated p67-phox causes chronic granulomatous disease, J. Exp. Med., 184 (1996) 1243-1249.

Li,N., Mak,A., Richards,D.P., Naber,C., Keller,B.O., Li,L., and Shaw,A.R., Monocyte lipid rafts contain proteins implicated in vesicular trafficking and phagosome formation, Proteomics., 3 (2003) 536-548.

Li,Z., Hannigan,M., Mo,Z., Liu,B., Lu,W., Wu,Y., Smrcka,A.V., Wu,G., Li,L., Liu,M., Huang,C.K., and Wu,D., Directional sensing requires G beta gamma-mediated PAK1 and PIX alpha-dependent activation of Cdc42, Cell, 114 (2003) 215-227.

Lian,Z., Wang,L., Yamaga,S., Bonds,W., Beazer-Barclay,Y., Kluger,Y., Gerstein,M., Newburger,P.E., Berliner,N., and Weissman,S.M., Genomic and proteomic analysis of the myeloid differentiation program, Blood, 98 (2001) 513-524.

Lian,Z., Kluger,Y., Greenbaum,D.S., Tuck,D., Gerstein,M., Berliner,N., Weissman,S.M., and Newburger,P.E., Genomic and proteomic analysis of the myeloid differentiation program: global analysis of gene expression during induced differentiation in the MPRO cell line, Blood, 100 (2002) 3209-3220.

Lin,C.S., Shen,W., Chen,Z.P., Tu,Y.H., and Matsudaira,P., Identification of I-plastin, a human fimbrin isoform expressed in intestine and kidney, Mol. Cell Biol., 14 (1994) 2457-2467.

Lippolis,J.D. and Reinhardt,T.A., Proteomic survey of bovine neutrophils, Vet. Immunol. Immunopathol., 103 (2005) 53-65.

Liu,F. and Wen,Z., Cloning and expression pattern of the lysozyme C gene in zebrafish, Mech. Dev., 113 (2002) 69-72.

Lokuta,A.J., Meyers,M.B., Sander,P.R., Fishman,G.I., and Valdivia,H.H., Modulation of cardiac ryanodine receptors by sorcin, J. Biol. Chem., 272 (1997) 25333-25338.

Lollike,K., Sorensen,O., Bundgaard,J.R., Segal,A.W., Boyhan,A., and Borregaard,N., An ELISA for grancalcin, a novel cytosolic calcium-binding protein present in leukocytes, J. Immunol. Methods, 185 (1995) 1-8.

Lollike,K., Johnsen,A.H., Durussel,I., Borregaard,N., and Cox,J.A., Biochemical characterization of the penta-EF-hand protein grancalcin and identification of L-plastin as a binding partner, J. Biol. Chem., 276 (2001) 17762-17769.

Lominadze,G., Powell,D.W., Luerman,G.C., Link,A.J., Ward,R.A., and McLeish,K.R., Proteomic Analysis of Human Neutrophil Granules, Mol. Cell Proteomics., 4 (2005) 1503-1521.

Lowell,C.A., Fumagalli,L., and Berton,G., Deficiency of Src family kinases p59/61hck and p58c-fgr results in defective adhesion-dependent neutrophil functions, J. Cell Biol., 133 (1996) 895-910.

Machesky,L.M., Cell motility: complex dynamics at the leading edge, Curr. Biol, 7 (1997) R164-R167.

Maki and kitaura, structures, functions and molecular evolution of the penta-EF-hand Ca2+ binding proteins, Biochem. Biophys. Res. Commun., 1600 (2004) 51-60.

Maki,M., Kitaura,Y., Satoh,H., Ohkouchi,S., and Shibata,H., Structures, functions and molecular evolution of the penta-EF-hand Ca2+-binding proteins, Biochim. Biophys. Acta, 1600 (2002) 51-60.

Maly,I.V. and Borisy,G.G., Self-organization of a propulsive actin network as an evolutionary process, Proc. Natl. Acad. Sci. U. S. A, 98 (2001) 11324-11329.

Mandell,G.L., Bactericidal activity of aerobic and anaerobic polymorphonuclear neutrophils, Infect. Immun., 9 (1974) 337-341.

Mann,M., Hojrup,P., and Roepstorff,P., Use of mass spectrometric molecular weight information to identify proteins in sequence databases, Biol Mass Spectrom., 22 (1993) 338-345.

Mann,M. and Wilm,M., Error-tolerant identification of peptides in sequence databases by peptide sequence tags, Anal. Chem., 66 (1994) 4390-4399.

Mann,M., Hendrickson,R.C., and Pandey,A., Analysis of proteins and proteomes by mass spectrometry, Annu. Rev. Biochem., 70 (2001) 437-473.

Marchesi,V.T. and Ngo,N., In vitro assembly of multiprotein complexes containing alpha, beta, and gamma tubulin, heat shock protein HSP70, and elongation factor 1 alpha, Proc. Natl. Acad. Sci. U. S. A, 90 (1993) 3028-3032.

Marsh,W.L., Marsh,N.J., Moore,A., Symmans,W.A., Johnson,C.L., and Redman,C.M., Elevated serum creatine phosphokinase in subjects with McLeod syndrome, Vox Sang., 40 (1981) 403-411.

Massenet,C., Chenavas,S., Cohen-Addad,C., Dagher,M.C., Brandolin,G., Pebay-Peyroula,E., and Fieschi,F., Effects of p47phox C terminus phosphorylations on binding interactions with p40phox and p67phox. Structural and functional comparison of p40phox and p67phox SH3 domains, J. Biol. Chem., 280 (2005) 13752-13761.

Massol,P., Montcourrier,P., Guillemot,J.C., and Chavrier,P., Fc receptor-mediated phagocytosis requires CDC42 and Rac1, EMBO J., 17 (1998) 6219-6229.

Masters,C., Cellular differentiation and the microcompartmentation of glycolysis, Mech. Ageing Dev., 61 (1991) 11-22.

Masters, C., Interactions between glycolytic enzymes and components of the cytomatrix, J.Cell.Biol., 99 (1984) 222s-225s.

Masters,C., Microenvironmental factors and the binding of glycolytic enzymes to contractile filaments, Int. J. Biochem., 24 (1992) 405-410.

Masters,P.S. and Hong,J., Reconstitution of binding protein dependent active transport of glutamine in spheroplasts of Escherichia coli, Biochemistry, 20 (1981) 4900-4904.

Matsuo,M., Kimura,Y., and Ueda,K., KATP channel interaction with adenine nucleotides, J. Mol. Cell Cardiol., 38 (2005) 907-916.

May,R.C., Caron,E., Hall,A., and Machesky,L.M., Involvement of the Arp2/3 complex in phagocytosis mediated by FcgammaR or CR3, Nat. Cell Biol, 2 (2000) 246-248.

McCutcheon,J.C., Hart,S.P., Canning,M., Ross,K., Humphries,M.J., and Dransfield,I., Regulation of macrophage phagocytosis of apoptotic neutrophils by adhesion to fibronectin, J. Leukoc. Biol., 64 (1998) 600-607.

Medalia,O., Weber,I., Frangakis,A.S., Nicastro,D., Gerisch,G., and Baumeister,W., Macromolecular architecture in eukaryotic cells visualized by cryoelectron tomography, Science, 298 (2002) 1209-1213.

Mendelsohn,H.B., Berant,M., and Merzbach,D., Antibacterial prophylaxis in chronic granulomatous disease. A case report, Isr. J. Med. Sci., 19 (1983) 1004-1005.

Merrick,B.A. and Tomer,K.B., Toxicoproteomics: a parallel approach to identifying biomarkers, Environ. Health Perspect., 111 (2003) A578-A579.

Metcalf,J.A. Laboratory manula of neutrophil function. 1986. New York, Raven Press. Ref Type: Serial (Book,Monograph)

Metchnikoff E. Lectures of comparative pathology of inflammation. 1968. New York, Daven Press (Generic).
Ref Type: Serial (Book,Monograph)

Meyers,M.B., Pickel,V.M., Sheu,S.S., Sharma,V.K., Scotto,K.W., and Fishman,G.I., Association of sorcin with the cardiac ryanodine receptor, J. Biol. Chem., 270 (1995) 26411-26418.

Mielenz,D., Vettermann,C., Hampel,M., Lang,C., Avramidou,A., Karas,M., and Jack,H.M., Lipid rafts associate with intracellular B cell receptors and exhibit a B cell stage-specific protein composition, J. Immunol., 174 (2005) 3508-3517.

Miki, H., Suetsugu, S., and Takenawa, T., WAVE, a novel WASP-family protein involved in actin reorganization induced by Rac, EMBO J., 17 (1998) 6932-6941.

Miki, H., Yamaguchi, H., Suetsugu, S., Takenawa, T., IRSp53 is an essential intermediate between Rac and WAVE in the regulation of membrane ruffling, Nature., 408 (2000) 732-735.

Miller,R.K., Khuon,S., and Goldman,R.D., Dynamics of keratin assembly: exogenous type I keratin rapidly associates with type II keratin in vivo, J. Cell Biol., 122 (1993) 123-135.

Mishra, S., Murphy L.C., Nyomba, B.L., Murphy, L.J., Prohibitin: a potential target for new therapeutics, Trends Mol Med, 11 (2005) 192-197.

Mitchison,T. and Kirschner,M., Dynamic instability of microtubule growth, Nature, 312 (1984) 237-242.

Mitchison,T.J., Localization of an exchangeable GTP binding site at the plus end of microtubules, Science, 261 (1993) 1044-1047.

Mitchison,T.J. and Cramer,L.P., Actin-based cell motility and cell locomotion, Cell, 84 (1996) 371-379.

Mogilner,A. and Oster,G., Cell motility driven by actin polymerization, Biophys. J., 71 (1996) 3030-3045.

Moreau,V., Frischknecht,F., Reckmann,I., Vincentelli,R., Rabut,G., Stewart,D., and Way,M., A complex of N-WASP and WIP integrates signalling cascades that lead to actin polymerization, Nat. Cell Biol., 2 (2000) 441-448.

Moreland,J.G. and Bailey,G., Neutrophil transendothelial migration in vitro to Streptococcus pneumoniae is pneumolysin dependent, Am. J. Physiol Lung Cell Mol. Physiol, 290 (2006) L833-L840.

Mossink,M.H., van Zon,A., Scheper,R.J., Sonneveld,P., and Wiemer,E.A., Vaults: a ribonucleoprotein particle involved in drug resistance?, Oncogene, 22 (2003) 7458-7467.

Mullins,R.D., Heuser,J.A., and Pollard,T.D., The interaction of Arp2/3 complex with actin: nucleation, high affinity pointed end capping, and formation of branching networks of filaments, Proc. Natl. Acad. Sci. U. S. A, 95 (1998) 6181-6186.

Munshi,R., Kandl,K.A., Carr-Schmid,A., Whitacre,J.L., Adams,A.E., and Kinzy,T.G., Overexpression of translation elongation factor 1A affects the organization and function of the actin cytoskeleton in yeast, Genetics, 157 (2001) 1425-1436.

Nakata,T. and Hirokawa,N., Organization of cortical cytoskeleton of cultured chromaffin cells and involvement in secretion as revealed by quick-freeze, deep-etching, and double-label immunoelectron microscopy, J. Neurosci., 12 (1992) 2186-2197.

Nauseef,W.M., Volpp,B.D., McCormick,S., Leidal,K.G., and Clark,R.A., Assembly of the neutrophil respiratory burst oxidase. Protein kinase C promotes cytoskeletal and membrane association of cytosolic oxidase components, J. Biol. Chem., 266 (1991) 5911-5917.

Nebl,T., Pestonjamasp,K.N., Leszyk,J.D., Crowley,J.L., Oh,S.W., and Luna,E.J., Proteomic analysis of a detergent-resistant membrane skeleton from neutrophil plasma membranes, J. Biol. Chem., 277 (2002) 43399-43409.

Ninfali,P., Malatesta,M., Biagiotti,E., Aluigi,G., and Gazzanelli,G., Glucose-6-phosphate dehydrogenase in small intestine of rabbit: biochemical properties and subcellular localization, Acta Histochem., 103 (2001) 287-303.

Nobes,C.D. and Hall,A., Rho, rac and cdc42 GTPases: regulators of actin structures, cell adhesion and motility, Biochem. Soc. Trans., 23 (1995) 456-459.

Norris,V., Turnock,G., and Sigee,D., The Escherichia coli enzoskeleton, Mol. Microbiol., 19 (1996) 197-204.

Offermanns,S. and Simon,M.I., Organization of transmembrane signalling by heterotrimeric G proteins, Cancer Surv., 27 (1996) 177-198.

Okada,K., Takano-Ohmuro,H., Obinata,T., and Abe,H., Dephosphorylation of cofilin in polymorphonuclear leukocytes derived from peripheral blood, Exp. Cell Res., 227 (1996) 116-122.

Okada,S.F., O'Neal,W.K., Huang,P., Nicholas,R.A., Ostrowski,L.E., Craigen,W.J., Lazarowski,E.R., and Boucher,R.C., Voltage-dependent anion channel-1 (VDAC-1)

contributes to ATP release and cell volume regulation in murine cells, J. Gen. Physiol, 124 (2004) 513-526.

Olazabal,I.M., Caron,E., May,R.C., Schilling,K., Knecht,D.A., and Machesky,L.M., Rho-kinase and myosin-II control phagocytic cup formation during CR, but not FcgammaR, phagocytosis, Curr. Biol, 12 (2002) 1413-1418.

Oort,J. and Scheper,R.J., Histopathology of acute and chronic inflammation, Agents Actions Suppl, (1977) 25-30.

Owens,D.W. and Lane,E.B., Keratin mutations and intestinal pathology, J. Pathol., 204 (2004) 377-385.

Palazzo,A.F., Eng,C.H., Schlaepfer,D.D., Marcantonio,E.E., and Gundersen,G.G., Localized stabilization of microtubules by integrin- and FAK-facilitated Rho signaling, Science, 303 (2004) 836-839.

Pandey,A. and Mann,M., Proteomics to study genes and genomes, Nature, 405 (2000) 837-846.

Parker,P.J., Intracellular signalling. PI 3-kinase puts GTP on the Rac, Curr. Biol., 5 (1995) 577-579.

Parkos,C.A., Allen,R.A., Cochrane,C.G., and Jesaitis,A.J., Purified cytochrome b from human granulocyte plasma membrane is comprised of two polypeptides with relative molecular weights of 91,000 and 22,000, J. Clin. Invest, 80 (1987) 732-742.

Parry,A.L., Nixon,A.J., Craven,A.J., and Pearson,A.J., The microanatomy, cell replication, and keratin gene expression of hair follicles during a photoperiod-induced growth cycle in sheep, Acta Anat. (Basel), 154 (1995) 283-299.

Perez,F., Diamantopoulos,G.S., Stalder,R., and Kreis,T.E., CLIP-170 highlights growing microtubule ends in vivo, Cell, 96 (1999) 517-527.

Perou,C.M. and Kaplan,J., Chediak-Higashi syndrome is not due to a defect in microtubule-based lysosomal mobility, J. Cell Sci., 106 (Pt 1) (1993) 99-107.

Pfaff,M., Liu,S., Erle,D.J., and Ginsberg,M.H., Integrin beta cytoplasmic domains differentially bind to cytoskeletal proteins, J. Biol. Chem., 273 (1998) 6104-6109.

Pilloud-Dagher,M.C. and Vignais,P.V., Purification and characterization of an oxidase activating factor of 63 kilodaltons from bovine neutrophils, Biochemistry, 30 (1991) 2753-2760.

Piubelli,C., Galvani,M., Hamdan,M., Domenici,E., and Righetti,P.G., Proteome analysis of rat polymorphonuclear leukocytes: a two-dimensional electrophoresis/mass spectrometry approach, Electrophoresis, 23 (2002) 298-310.

Pollard,T.D., The cytoskeleton, cellular motility and the reductionist agenda, Nature, 422 (2003) 741-745.

Pollard,T.D. and Borisy,G.G., Cellular motility driven by assembly and disassembly of actin filaments, Cell, 112 (2003) 453-465.

Prigmore,E., Ahmed,S., Best,A., Kozma,R., Manser,E., Segal,A.W., and Lim,L., A 68-kDa kinase and NADPH oxidase component p67phox are targets for Cdc42Hs and Rac1 in neutrophils, J. Biol. Chem., 270 (1995) 10717-10722.

Quadroni,M. and James,P., Proteomics and automation, Electrophoresis, 20 (1999) 664-677.

Quie,P.G., Chronic granulomatous disease of childhood: a saga of discovery and understanding, Pediatr. Infect. Dis. J., 12 (1993) 395-398.

Quinn,M.J., Byzova,T.V., Qin,J., Topol,E.J., and Plow,E.F., Integrin alphaIIbbeta3 and its antagonism, Arterioscler. Thromb. Vasc. Biol., 23 (2003) 945-952.

Quintero-Monzon,O., Rodal,A.A., Strokopytov,B., Almo,S.C., and Goode,B.L., Structural and functional dissection of the Abp1 ADFH actin-binding domain reveals versatile in vivo adapter functions, Mol. Biol. Cell, 16 (2005) 3128-3139.

Rabbani, H., de Boer, M., Ahlin, A., Sundin, U., Elinder, G., Hammarstrom, L., Palmblad, J., Smith, C.I., and Roos, D., A 40-base-pair duplication in the gp91-phox gene leading to X-linked chronic granulomatous disease, Eur. J. Haematol, 51 (1993) 218-222.

Rabilloud,T., Strub,J.M., Carte,N., Luche,S., Van Dorsselaer,A., Lunardi,J., Giege,R., and Florentz,C., Comparative proteomics as a new tool for exploring human mitochondrial tRNA disorders, Biochemistry, 41 (2002) 144-150.

Rajalingam,K., Wunder,C., Brinkmann,V., Churin,Y., Hekman,M., Sievers,C., Rapp,U.R., and Rudel,T., Prohibitin is required for Ras-induced Raf-MEK-ERK activation and epithelial cell migration, Nat. Cell Biol., 7 (2005) 837-843.

Ramaekers,F.C. and Bosman,F.T., The cytoskeleton and disease, J. Pathol., 204 (2004) 351-354.

Reeves,E.P., Lu,H., Jacobs,H.L., Messina,C.G., Bolsover,S., Gabella,G., Potma,E.O., Warley,A., Roes,J., and Segal,A.W., Killing activity of neutrophils is mediated through activation of proteases by K+ flux, Nature, 416 (2002) 291-297.

Regazzi,R., Sasaki,T., Takahashi,K., Jonas,J.C., Volker,C., Stock,J.B., Takai,Y., and Wollheim,C.B., Prenylcysteine analogs mimicking the C-terminus of GTP-binding proteins stimulate exocytosis from permeabilized HIT-T15 cells: comparison with the effect of Rab3AL peptide, Biochim. Biophys. Acta, 1268 (1995) 269-278.

Rhee,S.G. and Bae,Y.S., Regulation of phosphoinositide-specific phospholipase C isozymes, J. Biol. Chem., 272 (1997) 15045-15048.

Ridley,A.J., Paterson,H.F., Johnston,C.L., Diekmann,D., and Hall,A., The small GTP-binding protein rac regulates growth factor-induced membrane ruffling, Cell, 70 (1992) 401-410.

Righetti,P.G., Castagna,A., Antonioli,P., and Boschetti,E., Prefractionation techniques in proteome analysis: the mining tools of the third millennium, Electrophoresis, 26 (2005) 297-319.

Roberts,A.W., Kim,C., Zhen,L., Lowe,J.B., Kapur,R., Petryniak,B., Spaetti,A., Pollock,J.D., Borneo,J.B., Bradford,G.B., Atkinson,S.J., Dinauer,M.C., and Williams,D.A., Deficiency of

the hematopoietic cell-specific Rho family GTPase Rac2 is characterized by abnormalities in neutrophil function and host defense, Immunity., 10 (1999) 183-196.

Robinson,J.M. and Badwey,J.A., Rapid association of cytoskeletal remodeling proteins with the developing phagosomes of human neutrophils, Histochem. Cell Biol., 118 (2002) 117-125.

Robinson, R.C., Turbedsky, K., Kaiser, D.A., Marchand, J.B., Higgs, H.N., Choe, S., Pollard, T.D., Crystal structure of Arp2/3 complex, Science, 294 (2001) 1679-1684.

Rocker,G.M., Wiseman,M.S., Pearson,D., and Shale,D.J., Diagnostic criteria for adult respiratory distress syndrome: time for reappraisal, Lancet, 1 (1989) 120-123.

Rodaway,A.R., Teahan,C.G., Casimir,C.M., Segal,A.W., and Bentley,D.L., Characterization of the 47-kilodalton autosomal chronic granulomatous disease protein: tissue-specific expression and transcriptional control by retinoic acid, Mol. Cell Biol., 10 (1990) 5388-5396.

Roes,J., Choi,B.K., Power,D., Xu,P., and Segal,A.W., Granulocyte function in grancalcin-deficient mice, Mol. Cell Biol., 23 (2003) 826-830.

Rohatgi,R., Ma,L., Miki,H., Lopez,M., Kirchhausen,T., Takenawa,T., and Kirschner,M.W., The interaction between N-WASP and the Arp2/3 complex links Cdc42-dependent signals to actin assembly, Cell, 97 (1999) 221-231.

Rostovtseva,T. and Colombini,M., VDAC channels mediate and gate the flow of ATP: implications for the regulation of mitochondrial function, Biophys. J., 72 (1997) 1954-1962.

Rotrosen,D. and Leto,T.L., Phosphorylation of neutrophil 47-kDa cytosolic oxidase factor. Translocation to membrane is associated with distinct phosphorylation events, J. Biol. Chem., 265 (1990) 19910-19915.

Rottner,K., Lommel,S., Wehland,J., and Stradal,T.E., Pathogen-induced actin filament rearrangement in infectious diseases, J. Pathol., 204 (2004) 396-406.

Ruoslahti,E. and Obrink,B., Common principles in cell adhesion, Exp. Cell Res., 227 (1996) 1-11.

Rush,C.L. and Izard,T., Rhombohedral crystals of the human vinculin head domain in complex with a vinculin-binding site of talin, Acta Crystallogr. D. Biol. Crystallogr., 60 (2004) 945-947.

Ryder,M.I., Niederman,R., and Taggart,E.J., The cytoskeleton of human polymorphonuclear leukocytes: phagocytosis and degranulation, Anat. Rec., 203 (1982) 317-327.

Sahali,D., Pawlak,A., Valanciute,A., Grimbert,P., Lang,P., Remy,P., Bensman,A., and Guellaen,G., A novel approach to investigation of the pathogenesis of active minimal-change nephrotic syndrome using subtracted cDNA library screening, J. Am. Soc. Nephrol., 13 (2002) 1238-1247.

Salas,P.J., Rodriguez,M.L., Viciana,A.L., Vega-Salas,D.E., and Hauri,H.P., The apical submembrane cytoskeleton participates in the organization of the apical pole in epithelial cells, J. Cell Biol., 137 (1997) 359-375.

Salcini AE, Confalonieri S, Doria M, Santolini E, Tassi E, Minenkova O, Cesareni G, Pelicci PG, and Di Fiore PP, Binding specificity and in vivo targets of the EH domain, a novel protein-protein interaction module., Genes Dev, 11 (1997) 2239-2249.

Sasahara,Y., Rachid,R., Byrne,M.J., de la Fuente,M.A., Abraham,R.T., Ramesh,N., and Geha,R.S., Mechanism of recruitment of WASP to the immunological synapse and of its activation following TCR ligation, Mol. Cell, 10 (2002) 1269-1281.

Sawada,Y. and Sheetz,M.P., Force transduction by Triton cytoskeletons, J. Cell Biol., 156 (2002) 609-615.

Sawyer,D.W., Sullivan,J.A., and Mandell,G.L., Intracellular free calcium localization in neutrophils during phagocytosis, Science, 230 (1985) 663-666.

Sbarra AJ and Karnovsky ML, The biochemical basis of phagocytosis. I.Metabolic changes during the ingestion of particles by polymorphonuclear leukocytes., J. Biol. Chem., 234 (1959) 1355-1362.

Schenk,G., Duggleby,R.G., and Nixon,P.F., Properties and functions of the thiamin diphosphate dependent enzyme transketolase, Int. J. Biochem. Cell Biol., 30 (1998) 1297-1318.

Schenk,G., Duggleby,R.G., and Nixon,P.F., Heterologous expression of human transketolase, Int. J. Biochem. Cell Biol., 30 (1998) 369-378.

Schmitz,H.D. and Bereiter-Hahn,J., Glyceraldehyde-3-phosphate dehydrogenase associates with actin filaments in serum deprived NIH 3T3 cells only, Cell Biol. Int., 26 (2002) 155-164.

Schoenwaelder,S.M., Yuan,Y., Cooray,P., Salem,H.H., and Jackson,S.P., Calpain cleavage of focal adhesion proteins regulates the cytoskeletal attachment of integrin alphaIIbbeta3 (platelet glycoprotein IIb/IIIa) and the cellular retraction of fibrin clots, J Biol Chem, 272 (1997) 1694-1702.

Segal.A.W., How neutrophils kill microbes, Annu Rev Immunol., 23 (2005) 197-223.

Segal AW, Wientjes F, Stockley RW, and Dekker LV. Components and organization of the NADPH oxidase of phagocytic cells. [5], 441-483. 1999. Phagocytosis: The host. Ref Type: Serial (Book,Monograph)

Segal,A.W. and Jones,O.T., Novel cytochrome b system in phagocytic vacuoles of human granulocytes, Nature, 276 (1978) 515-517.

Segal,A.W., Dorling,J., and Coade,S., Kinetics of fusion of the cytoplasmic granules with phagocytic vacuoles in human polymorphonuclear leukocytes. Biochemical and morphological studies, J. Cell Biol., 85 (1980) 42-59.

Segal,A.W. and Jones,O.T., Rapid incorporation of the human neutrophil plasma membrane cytochrome b into phagocytic vacuoles, Biochem. Biophys. Res. Commun., 92 (1980) 710-715.

Segal,A.W., Heyworth,P.G., Cockcroft,S., and Barrowman,M.M., Stimulated neutrophils from patients with autosomal recessive chronic granulomatous disease fail to phosphorylate a Mr-44,000 protein, Nature, 316 (1985) 547-549.

Segal,A.W., The electron transport chain of the microbicidal oxidase of phagocytic cells and its involvement in the molecular pathology of chronic granulomatous disease, J. Clin. Invest, 83 (1989) 1785-1793.

Segal,A.W. and Abo,A., The biochemical basis of the NADPH oxidase of phagocytes, Trends Biochem. Sci., 18 (1993) 43-47.

Selvaraj and Sbarra,A.J., Relationship of glyclytic and oxidative metabolism to particle entry and destraction in phagocytosing cells, Nature, 211 (1966) 1272-1276.

Sengelov,H., Kjeldsen,L., and Borregaard,N., Control of exocytosis in early neutrophil activation, J. Immunol., 150 (1993) 1535-1543.

Sepper,R. and Prikk,K., Proteomics: is it an approach to understand the progression of chronic lung disorders?, J. Proteome. Res., 3 (2004) 277-281.

Serrander,L., Skarman,P., Rasmussen,B., Witke,W., Lew,D.P., Krause,K.H., Stendahl,O., and Nusse,O., Selective inhibition of IgG-mediated phagocytosis in gelsolin-deficient murine neutrophils, J. Immunol., 165 (2000) 2451-2457.

Seveau,S., Eddy,R.J., Maxfield,F.R., and Pierini,L.M., Cytoskeleton-dependent membrane domain segregation during neutrophil polarization, Mol. Biol. Cell, 12 (2001) 3550-3562.

Shiina,N., Gotoh,Y., Kubomura,N., Iwamatsu,A., and Nishida,E., Microtubule severing by elongation factor 1 alpha, Science, 266 (1994) 282-285.

Shinagawa,Y., Tanaka,C., Teraoka,A., and Shinagawa,Y., A new cytochrome in neurophilic granules of rabbit leucocyte, J. Biochem. (Tokyo), 59 (1966) 622-624.

Shinomiya,H., Nagai,K., Hirata,H., Kobayashi,N., Hasegawa,H., Liu,F., Sumita,K., and Asano,Y., Preparation and characterization of recombinant murine p65/L-plastin expressed in Escherichia coli and high-titer antibodies against the protein, Biosci. Biotechnol. Biochem., 67 (2003) 1368-1375.

Simon,M.I., Strathmann,M.P., and Gautam,N., Diversity of G proteins in signal transduction, Science, 252 (1991) 802-808.

Siuzdak G. mass spectrometry and biotechnology. 1. 1996. Academic press inc (London) Ltd. Ref Type: Serial (Book,Monograph)

Sjolin,C., Stendahl,O., and Dahlgren,C., Calcium-induced translocation of annexins to subcellular organelles of human neutrophils, Biochem. J., 300 (Pt 2) (1994) 325-330.

Sjolin,C. and Dahlgren,C., Diverse effects of different neutrophil organelles on truncation and membrane-binding characteristics of annexin I, Biochim. Biophys. Acta, 1281 (1996) 227-234.

Spritz,R.A., Genetic defects in Chediak-Higashi syndrome and the beige mouse, J. Clin. Immunol., 18 (1998) 97-105.

Stanyon,C.A. and Bernard,O., LIM-kinase1, Int. J. Biochem. Cell Biol., 31 (1999) 389-394.

Stebbins,C.E. and Galan,J.E., Structural mimicry in bacterial virulence, Nature, 412 (2001) 701-705.

Steglich,G., Neupert,W., and Langer,T., Prohibitins regulate membrane protein degradation by the m-AAA protease in mitochondria, Mol. Cell Biol., 19 (1999) 3435-3442.

Styers,M.L., Kowalczyk,A.P., and Faundez,V., Intermediate filaments and vesicular membrane traffic: the odd couple's first dance?, Traffic., 6 (2005) 359-365.

Suarez,J., Belke,D.D., Gloss,B., Dieterle,T., McDonough,P.M., Kim,Y.K., Brunton,L.L., and Dillmann,W.H., In vivo adenoviral transfer of sorcin reverses cardiac contractile abnormalities of diabetic cardiomyopathy, Am. J. Physiol Heart Circ. Physiol, 286 (2004) H68-H75.

Sullivan,K.E., Recent advances in our understanding of Wiskott-Aldrich syndrome, Curr. Opin. Hematol., 6 (1999) 8-14.

Suzuki,K., Yamaguchi,T., Oshizawa,T., Yamamoto,Y., Nishimaki-Mogami,T., Hayakawa,T., and Takahashi,A., Okadaic acid induces both augmentation and inhibition of opsonized zymosan-stimulated superoxide production by differentiated HL-60 cells. Possible involvement of dephosphorylation of a cytosolic 21K protein in respiratory burst, Biochim. Biophys. Acta, 1266 (1995) 261-267.

Svitkina, T.M., Borisy, G.G., Arp2/3 complex and actin depolymerizing factor/cofilin in dendritic organization and treadmilling of actin filament array in lamellipodia, J. Cell Biol, 145 (1999) 1009-1026.

Tamada,M., Sheetz,M.P., and Sawada,Y., Activation of a signaling cascade by cytoskeleton stretch, Dev. Cell, 7 (2004) 709-718.

Tanaka,H., Bradley,J.D., Baudendistel,L.J., and Dahms,T.E., Mechanisms of increased pulmonary microvascular permeability induced by FMLP in isolated rabbit lungs, J. Appl. Physiol, 73 (1992) 2074-2082.

Teahan,C., Rowe,P., Parker,P., Totty,N., and Segal,A.W., The X-linked chronic granulomatous disease gene codes for the beta-chain of cytochrome b-245, Nature, 327 (1987) 720-721.

Teahan,C.G., Totty,N., Casimir,C.M., and Segal,A.W., Purification of the 47 kDa phosphoprotein associated with the NADPH oxidase of human neutrophils, Biochem. J., 267 (1990) 485-489.

Teahan,C.G., Totty,N.F., and Segal,A.W., Isolation and characterization of grancalcin, a novel 28 kDa EF-hand calcium-binding protein from human neutrophils, Biochem. J., 286 (Pt 2) (1992) 549-554.

Thrasher,A.J., Keep,N.H., Wientjes,F., and Segal,A.W., Chronic granulomatous disease, Biochim. Biophys. Acta, 1227 (1994) 1-24.

Toivola,D.M., Ku,N.O., Resurreccion,E.Z., Nelson,D.R., Wright,T.L., and Omary,M.B., Keratin 8 and 18 hyperphosphorylation is a marker of progression of human liver disease, Hepatology, 40 (2004) 459-466.

Tsai,S. and Collins,S.J., A dominant negative retinoic acid receptor blocks neutrophil differentiation at the promyelocyte stage, Proc. Natl. Acad. Sci. U. S. A, 90 (1993) 7153-7157.

Tsunawaki,S. and Yoshikawa,K., Relationships of p40(phox) with p67(phox) in the activation and expression of the human respiratory burst NADPH oxidase, J. Biochem. (Tokyo), 128 (2000) 777-783.

Turano,C., Coppari,S., Altieri,F., and Ferraro,A., Proteins of the PDI family: unpredicted non-ER locations and functions, J. Cell Physiol, 193 (2002) 154-163.

Urena,J.M., Egea,G., Grana,X., Castella,J., Marsal,J., Carreras,J., and Climent,F., Location of phosphoglycerate mutase in rat skeletal muscle. An immunocytochemical and biochemical study, Eur. J. Cell Biol., 51 (1990) 151-156.

Valerius,N.H., Stendahl,O., Hartwig,J.H., and Stossel,T.P., Distribution of actin-binding protein and myosin in polymorphonuclear leukocytes during locomotion and phagocytosis, Cell, 24 (1981) 195-202.

Van Gelder,B. and Slater,E.C., The extinction coefficient of cytochrome c, Biochim. Biophys. Acta, 58 (1962) 593-595.

Verraes, S., Hornebeck, W., Polette, M., Borradori, L., Bernard, P., Respective contribution of neutrophil elastase and matrix metalloproteinase 9 in the degradation of BP180 (type XVII collagen) in human bullous pemphigoid. 117 (2001) 1091-1096.

Wagner,C.T., Lu,I.Y., Hoffman,M.H., Sun,W.Q., Trent,J.D., and Connor,J., T-complex polypeptide-1 interacts with the erythrocyte cytoskeleton in response to elevated temperatures, J. Biol. Chem., 279 (2004) 16223-16228.

Waite,K.A., Wallin,R., Qualliotine-Mann,D., and McPhail,L.C., Phosphatidic acid-mediated phosphorylation of the NADPH oxidase component p47-phox. Evidence that phosphatidic acid may activate a novel protein kinase, J. Biol. Chem., 272 (1997) 15569-15578.

Walford,R.L., Gallagher,R., and Taylor,P., Cytotoxicity of pathologic human sera for lymphocytes and neutrophils, Ann. N. Y. Acad. Sci., 124 (1965) 563-569.

Wallar,B.J. and Alberts,A.S., The formins: active scaffolds that remodel the cytoskeleton, Trends Cell Biol, 13 (2003) 435-446.

Walsh,T.P., Masters,C.J., Morton,D.J., and Clarke,F.M., The reversible binding of glycolytic enzymes in ovine skeletal muscle in response to tetanic stimulation, Biochim. Biophys. Acta, 675 (1981) 29-39.

Wang,Q., Song,C., and Li,C.C., Molecular perspectives on p97-VCP: progress in understanding its structure and diverse biological functions, J. Struct. Biol., 146 (2004) 44-57.

Waugh,M.G., Minogue,S., Anderson,J.S., Balinger,A., Blumenkrantz,D., Calnan,D.P., Cramer,R., and Hsuan,J.J., Localization of a highly active pool of type II phosphatidylinositol 4-kinase in a p97/valosin-containing-protein-rich fraction of the endoplasmic reticulum, Biochem. J., 373 (2003) 57-63.

Weaver,A.M., Karginov,A.V., Kinley,A.W., Weed,S.A., Li,Y., Parsons,J.T., and Cooper,J.A., Cortactin promotes and stabilizes Arp2/3-induced actin filament network formation, Curr. Biol., 11 (2001) 370-374.

Weed,S.A., Karginov,A.V., Schafer,D.A., Weaver,A.M., Kinley,A.W., Cooper,J.A., and Parsons,J.T., Cortactin localization to sites of actin assembly in lamellipodia requires interactions with F-actin and the Arp2/3 complex, J. Cell Biol., 151 (2000) 29-40.

Wegner,A. and Isenberg,G., 12-fold difference between the critical monomer concentrations of the two ends of actin filaments in physiological salt conditions, Proc. Natl. Acad. Sci. U. S. A, 80 (1983) 4922-4925.

Weiner,O.D., Servant,G., Welch,M.D., Mitchison,T.J., Sedat,J.W., and Bourne,H.R., Spatial control of actin polymerization during neutrophil chemotaxis, Nat. Cell Biol, 1 (1999) 75-81.

Welch,H.C., Coadwell,W.J., Ellson,C.D., Ferguson,G.J., Andrews,S.R., Erdjument-Bromage,H., Tempst,P., Hawkins,P.T., and Stephens,L.R., P-Rex1, a PtdIns(3,4,5)P3- and Gbetagamma-regulated guanine-nucleotide exchange factor for Rac, Cell, 108 (2002) 809-821.

Welch,M.D., Rosenblatt,J., Skoble,J., Portnoy,D.A., and Mitchison,T.J., Interaction of human Arp2/3 complex and the Listeria monocytogenes ActA protein in actin filament nucleation, Science, 281 (1998) 105-108.

Wendland,B., McCaffery,J.M., Xiao,Q., and Emr,S.D., A novel fluorescence-activated cell sorter-based screen for yeast endocytosis mutants identifies a yeast homologue of mammalian eps15, J. Cell Biol., 135 (1996) 1485-1500.

Werb,Z., Hembry,R.M., Murphy,G., and Aggeler,J., Commitment to expression of the metalloendopeptidases, collagenase and stromelysin: relationship of inducing events to changes in cytoskeletal architecture, J Cell Biol, 102 (1986) 697-702.

Wientjes,F.B., Hsuan,J.J., Totty,N.F., and Segal,A.W., p40phox, a third cytosolic component of the activation complex of the NADPH oxidase to contain src homology 3 domains, Biochem. J., 296 (Pt 3) (1993) 557-561.

Wientjes,F.B., Segal,A.W., and Hartwig,J.H., Immunoelectron microscopy shows a clustered distribution of NADPH oxidase components in the human neutrophil plasma membrane, J. Leukoc. Biol., 61 (1997) 303-312.

Wientjes,F.B., Reeves,E.P., Soskic,V., Furthmayr,H., and Segal,A.W., The NADPH oxidase components p47(phox) and p40(phox) bind to moesin through their PX domain, Biochem. Biophys. Res. Commun., 289 (2001) 382-388.

Wiesner, S., Helfer, E., Didry, D., Ducouret, G., Lafuma, F., Carlier, M.F., Pantaloni, D., A biomimetic motility assay provides insight into the mechanism of actin-based motility, J. Cell Biol, 160 (2003) 387-398.

Wild,M.K., Luhn,K., Marquardt,T., and Vestweber,D., Leukocyte adhesion deficiency II: therapy and genetic defect, Cells Tissues. Organs, 172 (2002) 161-173.

Wilkins MR and Gooley AA. Protein identification in proteome projects. 46-47. 1997. New York, Springer-Verlag Berlin Heidelbery. Proteome research:new frontiers in functional genomics. Ref Type: Serial (Book,Monograph)

Winter, D.C., Choe, E.Y., Li, R., Genetic dissection of the budding yeast Arp2/3 complex: a comparison of the in vivo and structural roles of individual subunits, Proc Natl Acad Sci USA, 96(1999) 7288-7293.

Woodman,P.G., p97, a protein coping with multiple identities, J. Cell Sci., 116 (2003) 4283-4290.

Wright,D.G. and Gallin,J.I., Secretory responses of human neutrophils: exocytosis of specific (secondary) granules by human neutrophils during adherence in vitro and during exudation in vivo, J. Immunol., 123 (1979) 285-294.

Wu,R.F., Gu,Y., Xu,Y.C., Nwariaku,F.E., and Terada,L.S., Vascular endothelial growth factor causes translocation of p47phox to membrane ruffles through WAVE1, J. Biol. Chem., 278 (2003) 36830-36840.

Xu,K.F., Shen,X., Li,H., Pacheco-Rodriguez,G., Moss,J., and Vaughan,M., Interaction of BIG2, a brefeldin A-inhibited guanine nucleotide-exchange protein, with exocyst protein Exo70, Proc. Natl. Acad. Sci. U. S. A, 102 (2005) 2784-2789.

Yamaguchi,H., Miki,H., Suetsugu,S., Ma,L., Kirschner,M.W., and Takenawa,T., Two tandem verprolin homology domains are necessary for a strong activation of Arp2/3 complex-induced actin polymerization and induction of microspike formation by N-WASP, Proc. Natl. Acad. Sci. U. S. A, 97 (2000) 12631-12636.

Yan,B., Calderwood,D.A., Yaspan,B., and Ginsberg,M.H., Calpain cleavage promotes talin binding to the beta 3 integrin cytoplasmic domain, J. Biol. Chem., 276 (2001) 28164-28170.

Yang,C., Huang,M., DeBiasio,J., Pring,M., Joyce,M., Miki,H., Takenawa,T., and Zigmond,S.H., Profilin enhances Cdc42-induced nucleation of actin polymerization, J. Cell Biol., 150 (2000) 1001-1012.

Yauch,R.L., Felsenfeld,D.P., Kraeft,S.K., Chen,L.B., Sheetz,M.P., and Hemler,M.E., Mutational evidence for control of cell adhesion through integrin diffusion/clustering, independent of ligand binding, J. Exp. Med., 186 (1997) 1347-1355.

Yu,L., Zhen,L., and Dinauer,M.C., Biosynthesis of the phagocyte NADPH oxidase cytochrome b558. Role of heme incorporation and heterodimer formation in maturation and stability of gp91phox and p22phox subunits, J. Biol. Chem., 272 (1997) 27288-27294.

Zalevsky,J., Grigorova,I., and Mullins,R.D., Activation of the Arp2/3 complex by the Listeria acta protein. Acta binds two actin monomers and three subunits of the Arp2/3 complex, J. Biol. Chem., 276 (2001) 3468-3475.

Zamparelli,C., Ilari,A., Verzili,D., Vecchini,P., and Chiancone,E., Calcium- and pH-linked oligomerization of sorcin causing translocation from cytosol to membranes, FEBS Lett., 409 (1997) 1-6.

Zatloukal,K., Stumptner,C., Fuchsbichler,A., Fickert,P., Lackner,C., Trauner,M., and Denk,H., The keratin cytoskeleton in liver diseases, J. Pathol., 204 (2004) 367-376.

Zebda,N., Bernard,O., Bailly,M., Welti,S., Lawrence,D.S., and Condeelis,J.S., Phosphorylation of ADF/cofilin abolishes EGF-induced actin nucleation at the leading edge and subsequent lamellipod extension, J. Cell Biol., 151 (2000) 1119-1128.

Zhan,Q., Bamburg,J.R., and Badwey,J.A., Products of phosphoinositide specific phospholipase C can trigger dephosphorylation of cofilin in chemoattractant stimulated neutrophils, Cell Motil. Cytoskeleton, 54 (2003) 1-15.

Zhelev,D.V. and Alteraifi,A., Signaling in the motility responses of the human neutrophil, Ann. Biomed. Eng, 30 (2002) 356-370.

Zor, T., and Selinger, Z., Linearization of the Bradford protein assay increases its sensitivity theoretical and experimental studies, Anal Biochem., 236 (1996) 302-308.

Zozulya,S. and Stryer,L., Calcium-myristoyl protein switch, Proc. Natl. Acad. Sci. U. S. A, 89 (1992) 11569-11573.

Zu,Y., Kohno,M., Kubota,I., Nishida,E., Hanaoka,M., and Namba,Y., Characterization of interleukin 2 stimulated 65-kilodalton phosphoprotein in human T cells, Biochemistry, 29 (1990) 1055-1062.

Zu,Y.L., Shigesada,K., Nishida,E., Kubota,I., Kohno,M., Hanaoka,M., and Namba,Y., 65-kilodalton protein phosphorylated by interleukin 2 stimulation bears two putative actin-binding sites and two calcium-binding sites, Biochemistry, 29 (1990) 8319-8324.